UNIVERSITY OF BELGRADE

TECHNICAL FACULTY BOR

52nd International October Conference on Mining and Metallurgy

PROCEEDINGS

Edited by

Saša Stojadinović

and

Dejan Petrović

November 29th – 30th 2021

Bor, Serbia

UNIVERSITY OF BELGRADE

TECHNICAL FACULTY IN BOR

52nd International October Conference on Mining and Metallurgy

PROCEEDINGS

Edited by

Saša Stojadinović

and

Dejan Petrović

November 29th – 30th 2021

Bor, Serbia

52nd International October Conference

on Mining and Metallurgy, IOC 2021

PUBLISHER:
UNIVERSITY OF BELGRADE - TECHNICAL FACULTY IN BOR, BOR, NOVEMBER 2021

FOR THE PUBLISHER:
DEAN: Prof. dr Nada Štrbac

EDITORS:
Prof. dr Saša Stojadinović
Doc. dr Dejan Petrović

TECHNICAL EDITOR
Pavle Stojković, MSc.

PRINTED BY:
»Štamparija Atlantis d.o.o.« Niš

CIRCULATION: 100 Copies

CIP – Каталогизација у публикацији –

Народна библиотека Србије, Београд

622(082)
669(082)

INTERNATIONAL October Conference on Mining and Metallurgy (52 ; 2021 ; Bor)
Proceedings / 52nd International October Conference on Mining and Metallurgy - IOC 2021, November 29th - 30th 2021 Bor, Serbia ; [organizer] University of Belgrade, Technical Faculty in Bor ; [co-organizer Institute for Mining and Metallurgy Bor] ; edited by Saša Stojadinović and Dejan Petrović. - Bor : University of Belgrade, Technical Faculty, 2021 (Niš : Atlantis). - V, 228 str. : ilustr. ; 25 cm

Tiraž 100. - Bibliografija uz svaki rad.

ISBN 978-86-6305-119-5

а) Рударство -- Зборници б) Металургија -- Зборници

COBISS.SR-ID 52072201

ORGANIZER:

UNIVERSITY OF BELGRADE – TECHNICAL FACULTY IN BOR

Co-ORGANIZER:

INSTITUTE FOR MINING AND METALLURGY BOR

Under the Auspice of:

The Ministry of Education, Science and Technological Development of the Republic of Serbia

CONFERENCE SPONSORS

COMMITTEES

52nd International October Conference on Mining and Metallurgy, IOC 2021

SCIENTIFIC COMMITTEE

Prof. dr Nada Štrbac, (UB TF Bor, Serbia)

Prof. dr Iwao Katayama, (Osaka University, Osaka, Japan)

Prof. dr Rodoljub Stanojlović, (UB TF Bor, Serbia)

Prof. dr Radoje Pantović, (UB TF Bor, Serbia)

Prof. dr Jakob Lamut, (ULj FNT Ljubljana, Slovenia)

Prof. dr Sanda Krausz, (University of Petroşani, Romania)

Prof. dr Grozdanka Bogdanović, (UB TF Bor, Serbia)

Prof. dr Jelena Penavin Škundrić, (TF Banja Luka, B&H)

Prof. dr Seshadri Seetharaman, (Royal Institute of Technology, Stockholm, Sweden)

Prof. dr Dragoslav Gusković, (UB TF Bor, Serbia)

Prof. dr Jožef Medved, (ULj FNT Ljubljana, Slovenia)

Dr Slavomir Hredzak, (SAS Kosice, Slovakia)

Prof. dr Aleksandar Dimitrov, (FTM Skopje, FYR Macedonia)

Prof. dr Karlo Raić, (UB TMF, Serbia)

Prof. dr Snežana Šerbula, (UB TF Bor, Serbia)

Dr Ana Kostov, (IRM Bor, Serbia)

Prof. dr Kemal Delijić, (MTF Podgorica, Montenegro)

Prof. dr Stoyan Groudev, (UMG "Saint Ivan Rilski" Sofia, Bulgaria)

Dr Andrei Rotaru, (Facultatea de Mecanica, Romania)

Prof. dr Krzystof Fitzner, (AGH University, Krakow, Poland)

Prof. dr Sulejman Muhamedagić, (FMM Zenica, B&H)

Prof. dr Anđelka Mihajlov, (Educons University, Serbia)

Prof. dr Luis Filipe Malheiros, (FEUP, Porto, Portugal)

Prof. dr Svetlana Ivanov, (UB TF Bor, Serbia)

Prof. dr Batrić Pešić, (Materials Science Faculty, Idaho, USA)

Prof. dr Ljubica Ivanić, (UB TF Bor, Serbia)

Dr Srećko Stopić, (RWTH Aachen, IME Aachen, Germany)

Prof. dr Boštjan Markoli, (ULj FNT Ljubljana, Slovenia)

Dr Magnus Ericsson, (Lulea Technical University, Stockholm, Sweden)

Prof. dr Tamara Holjevac Grgurić, (MF Sisak, Croatia)

Prof. dr Boyan Boyanov, (University Paisiy Hilendarski, Plovdiv, Bulgaria)

Prof. dr Milan Antonijević, (UB TF Bor, Serbia)

Prof. dr Tatjana Volkov-Husović, (UB TMF, Serbia)

Prof. dr Branka Jordović, (TF Čačak, Serbia)

Prof. dr Milan Trumić, (UB TF Bor, Serbia)

Prof. dr Tomaš Havlik, (TUKE, Slovakia)

Prof. dr Carl Heinz Spitzer, (TU Clausthal, Germany)

Dr Mile Bugarin, (IRM Bor, Serbia)

Prof. dr Velizar Stanković, (UB TF Bor, Serbia)

Prof. dr Costas Matis, (AU Thessaloniki, Greece)

Dr Milenko Ljubojev, (IRM Bor, Serbia)

Prof. dr Velimir Radmilović, (University of California at Berkeley, USA)

Prof. dr Dejan Tanikić, (UB TF Bor, Serbia)

Dr Mirjam Jan-Blažić, (Slovenian Foundryen Society, Slovenia)

Prof. dr Vitomir Milić, (UB TF Bor, Serbia)

Prof. dr Desimir Marković, (UB TF Bor, Serbia)

Prof. dr Mirjana Rajčić Vujasinović, (UB TF Bor, Serbia)

Dr Vladan Ćosović, (UB IHTM, Serbia)

Prof. dr Dimitris Panias, (NTUA, Athens, Greece)

Prof. dr Mirko Gojić, (MF Sisak, Croatia)

Prof. dr Vladimir Krstić, (Queen's University, Canada)

Prof. dr Dimitriu Sorin, (Polytechnic University of Bucharest, Romania)

Dr Miroslav Sokić, (UB ITNMS, Serbia)

Prof. dr Vladislav Kecojević, (West Virginia University, USA)

Prof. dr Dragan Manasijević, (UB TF Bor, Serbia)

Prof. dr Mirsada Oruč, (FMM Zenica, B&H)

Prof. dr Vlastimir Trujić, (IRM Bor, Serbia)

ORGANIZING COMMITTEE

Prof. dr Saša Stojadinović, vanredni profesor, UB, TF Bor

Prof. dr Ljubiša Balanović , vanredni profesor, UB, TF Bor

Doc. dr Dejan Petrović, docent, UB, TF Bor

dr Ana Kostov, naučni savetnik, Institut za rudarstvo i metalurgiju Bor

Doc. dr Aleksandra Mitovski, docent, UB, TF Bor

Doc. dr Ana Simonović, docent, UB, TF Bor

Prof. dr Jovica Sokolović, vanredni profesor, UB, TF Bor

Prof. dr Đorđe Nikolić, redovni profesor, UB, TF Bor

Doc. dr Uroš Stamenković, docent, UB, TF Bor

Prof. dr Milan Radovanović, vanredni profesor, UB, TF Bor

Doc. dr Danijela Voza, docent, UB, TF Bor

Jelena Ivaz, asistent, UB, TF Bor

Pavle Stojković , asistent, UB, TF Bor

Mladen Radovanović , asistent, UB, TF Bor

Predrag Stolić , asistent, UB, TF Bor

Kristina Božinović , asistent, UB, TF Bor

Sandra Vasković, Nastavnik engleskog jezika, UB, TF Bor

Oliver Marković, šef IKTC, UB, TF Bor

Miomir Voza, laborant, UB, TF Bor

TABLE OF CONTENTS

The 52nd International October Conference on Mining and Metallurgy
November 29th – 30th , 2021
www.ioc.tfbor.bg.ac.rs

THE COMPLEXITY OF SEM-EDS – WHAT AFFECTS THE QUALITY OF OBTAINED RESULTS?

Aleksandra Milosavljević[1]

[1]Mining and Metallurgy Institute Bor, Zelenibulevar 35, 19210 Bor, Serbia

Abstract

SEM-EDS is a powerful technique that is constantly being improved and supplemented with other material characterization techniques. However, obtained results might be interpreted in different ways as well as the possibility of poor quality of recording itself. The reasons are numerous: sample preparation, SEM operational parameters (working distance, probe current, process time…), EDS detector type, additional WDS – if it is necessary…etc. but first of all is what is the purpose of analysis and what precision do we need. Consequently, the experience of the operator itself is very important. This paper provides an overview of how individual parameters affect the quality of SEM-EDS results of different samples.

***Keywords**: SEM-EDS, techniques, operational parameters, samples.*

1. INTRODUCTION

Materials characterization is complex and consists of different types of methods and techniques. Among them is SEM-EDS which is very detailed and varied technique. We can use it for various kinds of samples – from mineral to biological, and for various purposes – industrial, scientific, educational, medicine etc. SEM-EDS nowadays is a modern, very usable and always upgradeable, which can be supported by constantly improved detectors, software and following contents.However, despite the constant progress of the device, new questions arise in the very interpretation of the results. These questions are sometimes simple, but the answers are not so because there are too many factors that influence on.

Before starting the SEM-EDS you have to know which kind of analysis you want. If you really need to know the composition of your sample with an error of the 1-2% element by element, you should use quantitative analysis with standards. If you are just interested in recognizing different phases, than a semi-quantitative analysis will be enough. Furthermore, you need to consider using WDS instead EDS if it is necessary. The WDS spectrometer can measure trace elements and it can be used as additional to EDS if there is overlapping peaks. That not means that WDS is the better solution and that you can use it rather than EDS. In practice, it's better to use EDS for unknown sample because major elements will be rapidly identified, but in all cases the final analysis depends on operator itself [1-3].

There are several differences in EDS detectors that could be important for analyses. One is energy resolution – if it is better, than it can be use for prevent overlapping peaks. Sensor size is also important – if you want high quality maps, than you have to use larger sensor (50-150 mm^2). Nowadays, SDD detectors are in practice after the Silicon Lithium once, but there are always experienced operators who will give you the best results with the less modern equipment. It doesn't mean that if you have the latest equipment that you will have the best results or quality. It only means that you will have the best opportunity to perform fast analysis, but the quality and reliability will depend of something else.

Sample preparation is also very important and can influence on the quality [4]. The sample has to be clean, dry, non-magnetic and flat if it's possible. It depends of the sample nature itself whether you will use high or low vacuum mode, but there are some facts that you have to respect. Sample preparation varies whether it is conductive or non-conductive. Non-conductive samples must be coated(with gold - the best variant). But, those samples can't be analyzed on gold composition because of accuracy of the analysis. Also, there are samples on which it is not allowed to make any changes (not even coating), such as archaeological samples, jewelry, collectibles, conservation samples, etc.In that case, it is necessary to use low vacuum. At low vacuum and low voltage, it is possible to take a picture to some extent without the occurrence of charging.

2. EXPERIMENTAL

Before recording the sample, depending on the type of sample and the desired image, the starting conditions should be set:

- vacuum mode (HV or LV);
- voltage and probe current;
- signal type (SED, BED or both types in the same time as possible).

As an example of different types of SEM-EDS analysis which are depend of samples and starting conditions, a lot of samples were recorded and analyzed in order to get the best results. These analyzes were done on JEOL JSM IT-300LV.

3. RESULTS AND DISCUSSION

The results shown in Figures 1 – 4 were obtained under different conditions, while the signal type was the same - SED. In Figure 1 SEM snapshots of paper are shown.Both snapshots are obtained at the same probe current (60) and WD≈11. Paper sample was coated as non-conducted sample, as well as powder samples given in Figures 2 - 4.

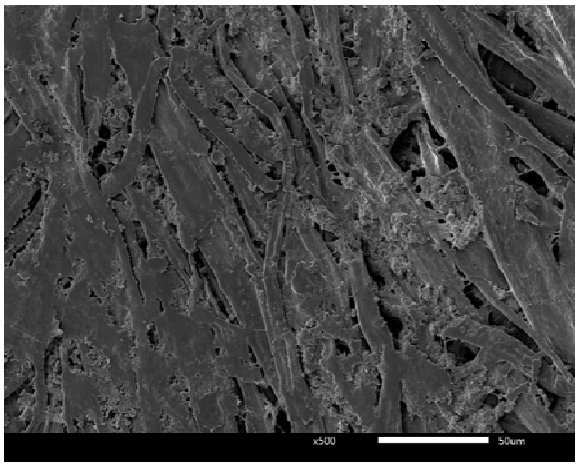

Figure 1a. SEM snapshot of paper, 5 kV

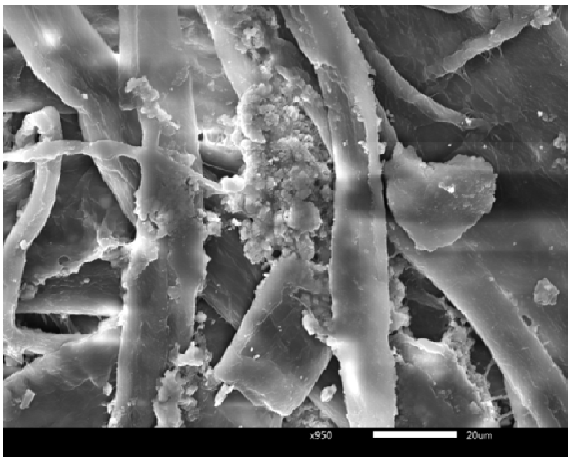

Figure 1b. SEM snapshot of paper, 20 kV

In the Figure 2 the difference between two SEM snapshots of powder, at different WD is given. With smaller WD (Figure 2a) SEM snapshot is very clear and sharp. Taking into account other factors such as kV, PC, magnification etc. (the same for Figures 2a and 2b), it might be concluded that if we want better SEM regardless of the EDS, we can decrease WD.

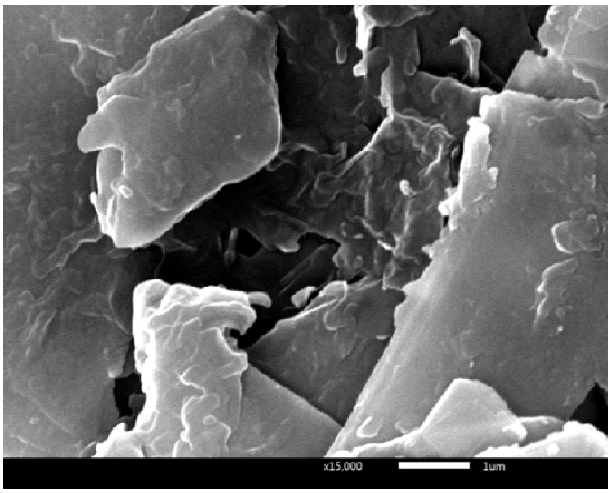

Figure 2a. SEM snapshot of powder
20 kV, PC 40, WD 7.6, M 15000

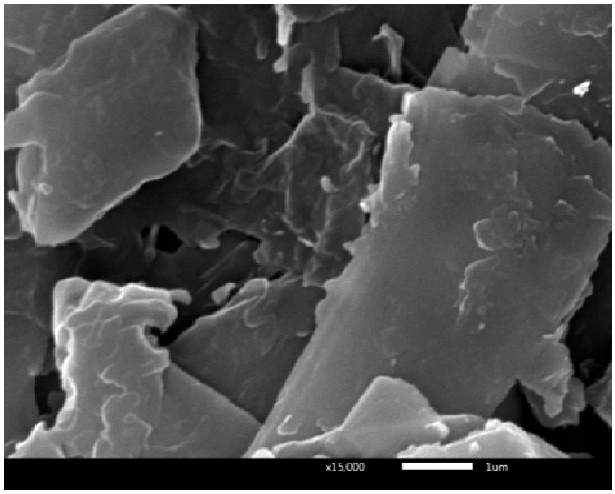

Figure 2b. SEM snapshot of powder
20 kV, PC 40, WD 11, M 15000

Unlike Figure 2, the next example shows the difference between snapshots with different probe current (Figure 3). Figure 3b in comparison with Figure 2a is with poor quality. If the voltage increased at 30 kV at the same conditions as given in Figure 2a, the details in the photo will be clearer, but the structure of the sample will be lost (Figure 4).

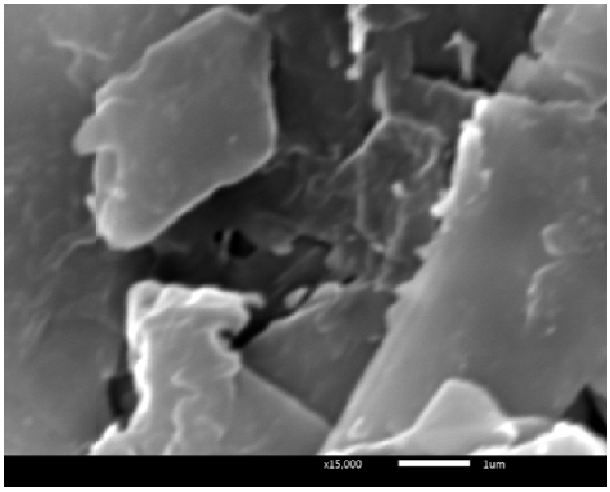

Figure 3a. SEM snapshot of powder
20 kV, PC 60, WD 11, M 15000

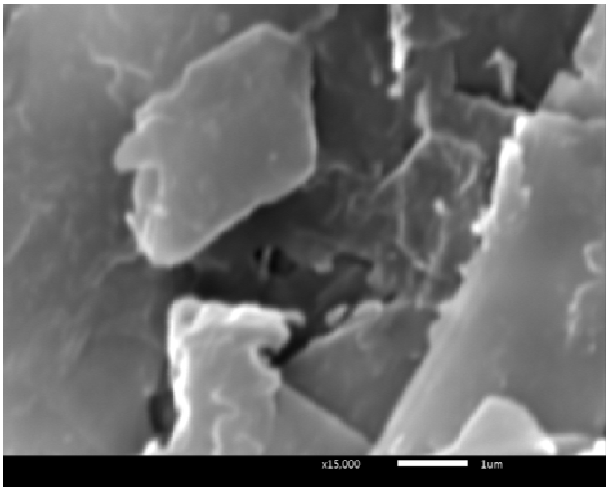

Figure 3b. SEM snapshot of powder
20 kV, PC 70, WD 11, M 15000

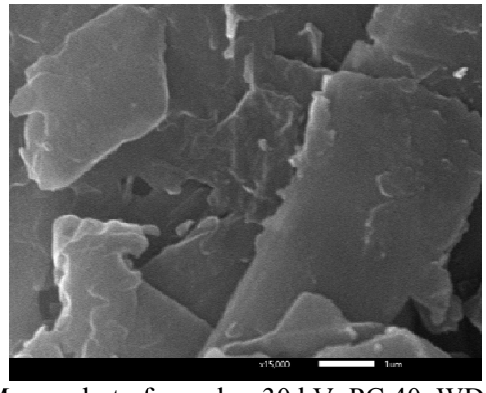

Figure 4. SEM snapshot of powder, 30 kV, PC 40, WD 7.6, M 15000

The difference between structures recorded by SED and BED type are given in Figure 5.

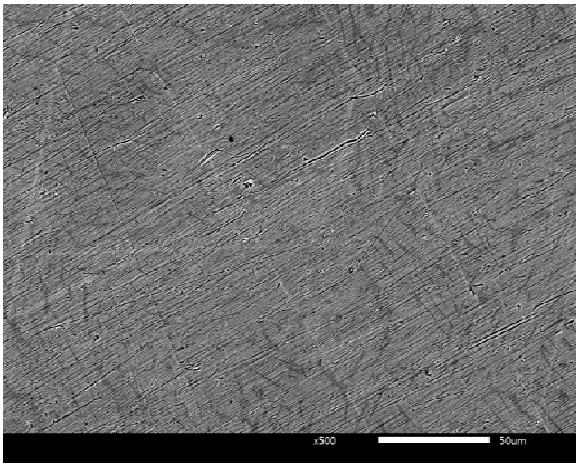

Figure 5a. SEM snapshot (BED mode) of shape memory alloy 20 kV, PC 67.2, WD 10, M 500

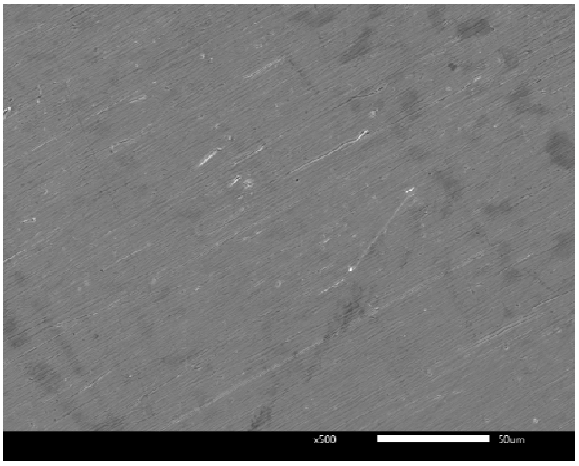

Figure 5b. SEM snapshot (SED mode) of shape memory alloy 20 kV, PC 67.2, WD 10, M 500

4. CONCLUSION

The factors which have influence on the SEM-EDS quality and reliability are numerous. In this paper, just a few examples of those factors were presented. Voltage, probe current, working distance are settings which are related with any SEM-EDS and the quality of results depends only of operator itself.

ACKNOWLEDGEMENT

The research presented in this paper was done with the financial support of the Ministry of Education, Science and Technological Development of the Republic of Serbia, within financing of scientific research work at the Mining and Metallurgy Institute Bor, according to contract no. 451-03-9/2021 – 14/200052.

REFERENCES

[1] https://www.oxford-instruments.com
[2] D. E. Newbury, N. W. M. Ritchie, Journal of Analytical Atomic Spectrometry, 28 (2013) 973-978
[3] J. I. Goldstein, D. Newbury, D. Joy, C. Lyman, P. Echlin, E. Lifshin, L. Samyer, J. Michael, Scanning Electron Microscopy and X-Ray Microanalysis, Plenum Press New York, 2007, p.273.
[4] B. D. Fahlman,Materials Chemistry, Springer Science & Business Media, 2011, p. 623

LASER QUENCHING OF CUTTING TOOL STEELS - A REVIEW

Zoran Karastojković[1], Radiša Perić[2], Milesa Srećković[3],

[1]IHIS Technoexperts, Batajnički put 23, 11080 Zemun, Serbia

[2]„Perić&Perić“ d.o.o, Dunavska 114-116, 12000 Požarevac, Serbia

[3]Faculty of Electrical Engineering, University of Belgrade, Blvd. kralja Aleksandra 76, 11000 Belgrade, Serbia

Abstract

The quenching regimes of tool steels were successfully established in past, during many years and centuries, but the laser quenching is one of the relative newest quenching methods. Laser beams may have to produce various reactions at the targeted surface, one of those here is concerned on the quenching of tool steels. Laser beams belong to high energy beams, as electron beams also. Laser heating up is extremely fast, it is enough a few μs or less. Thanks to the high energy density of those beams the surface might be even melted, but in the quenching treatment this is not allowed. During heating up for quenching by using conventional methods the surface is going to be oxidized, and such layer protects the heat conduction flow from the hot metal piece to the coolant medium. The laser heating produces pretty clear surface, without undesired oxide layers.

From the metallurgical point of view both fast heating and cooling regimes are suitable for representing into the one continuous cooling time (CCT) diagram.

The aim of laser treatment of tool surface is to obtain a harder layer in comparison to the conventionally quenched and tempered tool. After laser beams targeted the surface, such tool steels may be hardened by cooling at ordinary air conditions, it means without using water, oil or immersing into the salt bath.

Keywords*:laser, tool steels, quenching, hardness&depth profile.*

1. INTRODUCTION

Tools are generally heavy loaded, either by mechanical stresses and thermal influence [1], or frequently both of them. Heat treating is the main method for increasing the hardness & strength, and then for prolonging the service life of every tool [2-4]. The complex heat treating processes of many tools, used either for cutting or deforming, were pretty well determined, in past sometimes only on empirical way(s). Following the tendency for improving the characteristics of tool life, the significant efforts in past decades were made for treating the edge of such tools, especially in the spectrum of surface modification technologies (nitriding, boriding, PVD, CVD, ion implantation, electron beam and other elion techniques) [5-8]. One of those techniques use laser beams for improving the characteristics of previously correctly heat treated (quenched and tempered) tool.

2. WORKING CONDITIONS OF CUTTING TOOLS

No doubts that the edge is the most loaded part of every cutting tool. Beside on the existing mechanical loads during sliding of a chip over tool edge, Fig. 1a), at the same time there are formed temperature gradients, Fig. 1b), [1]. Resistance against to wear is a dominant property of a cutting edge or in other words on used tool steel. So, the tool steel must possess both high strength and thermal stability.

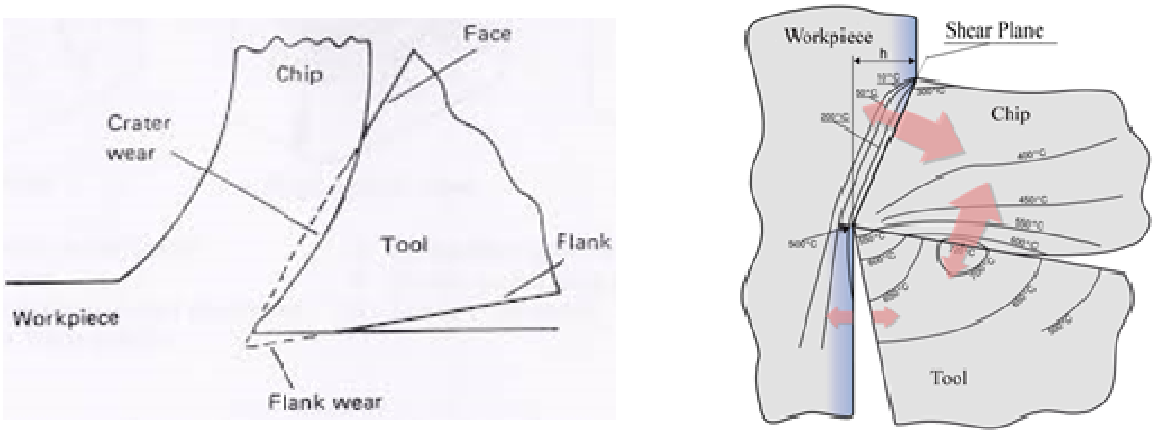

a) b)

Figure 1 Wear at tool edge during chip forming a) and temperature distribution inside tool and chip b)

Wear, further, occurs in zones as defined in Figure 2.

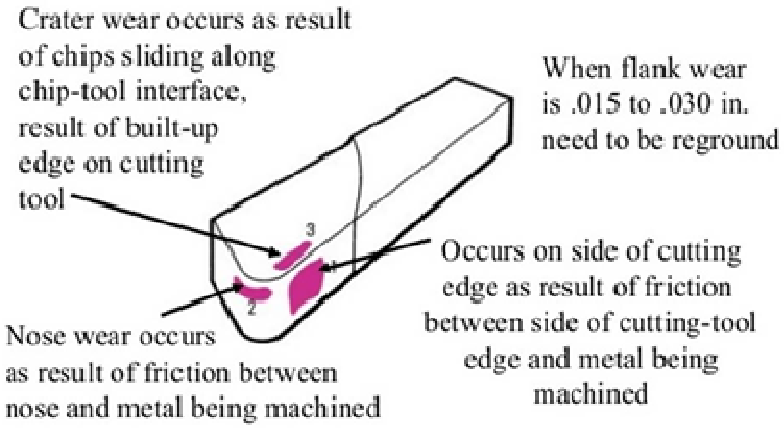

Figure 2 Geometry of tool wear

Total wear of tool is rather complex function of various mechanisms, Figure 3.

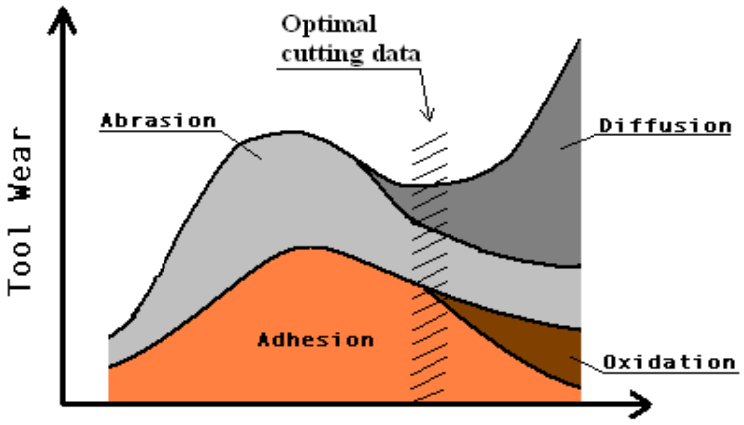

→Cutting speed
→Temperature
→Feed

Figure 3 Wear mechanisms at cutting tool [1]

Greater diversification in wear mechanisms shows the tools with complex geometry for hot forging&pressing.

3. HEAT TREATMENT OF CUTTING TOOLS

Most of tools should be made from high alloyed steels, most of them are medium or high carbon steels, but frequently for some purposes those steels must be alloyed with refractory metals, first of all with wolfram and molybdenum (HSS). The heat treatment of such steels is developed and accepted as classical route in production of tools, either for cutting or deforming purposes. An usual heat-treatment regime for cutting tool steel is presented in Figure 4.

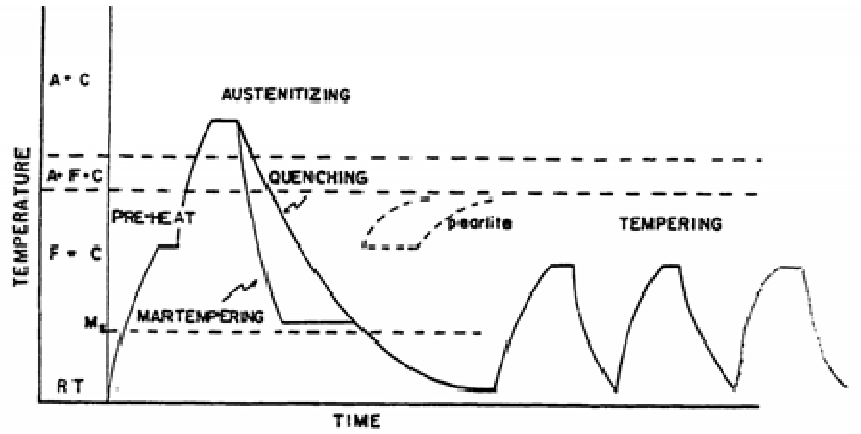

Figure 4 Ordinary quenching and tempering (t^0 – time) diagram for one cutting tool steel [3,4]

For achieving the fully austenitic structure may be applied one, as in Figure 4, two or three step pre-heatings. But, at multialloyed tool steel, the full austenitic structure was not possible to achieve before quenching, the main reason for that is a presence of carbides from alloying elements. Alloying elements in tool steels such as wolfram, vanadium, titanium and/or niobium even in small quantities play an important role by forming stable carbides and nitrides, which exhibit relatively low solubility into the austenite. During cooling and deformation (for example in rolling), these carbides/nitrides are precipitated, such controlling grain size, hardness and strength. Solubility of some carbides and nitrides on the level of (super)saturation at austenite are presented in Figure 5 [4-8].

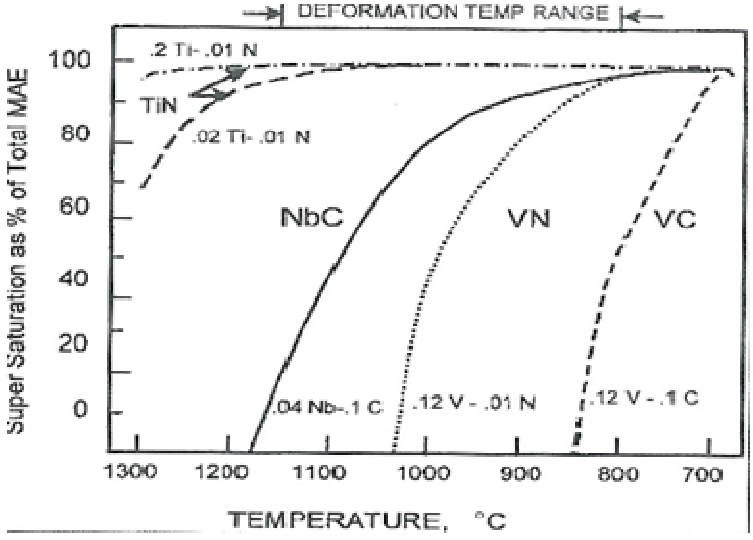

Figure 5 Solubility of common microalloying elements in austenite, MAE- Micro Alloying Element

Those carbides contribute to the control of austenitic grain size and according to their high hardness they act in decreasing the wear of tool.

4. LASER IN CONTROLING OF TOOL GEOMETRY

Lasers in machining could be used as measuring devices for controlling a final tool geometry, Figure 6a), or in automatization for control of machined piece, here in turning, Figure 6b).

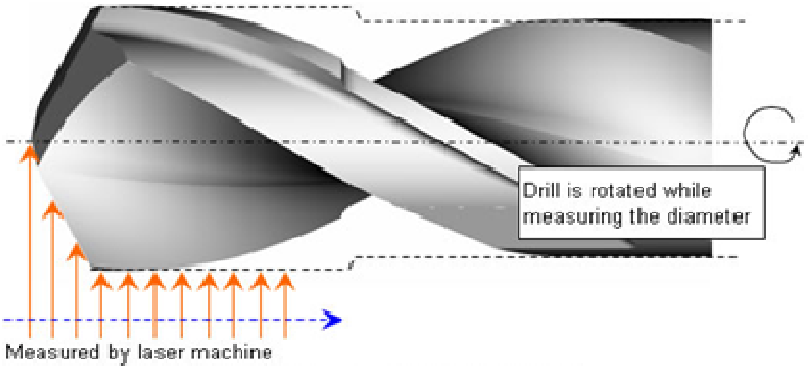

a)

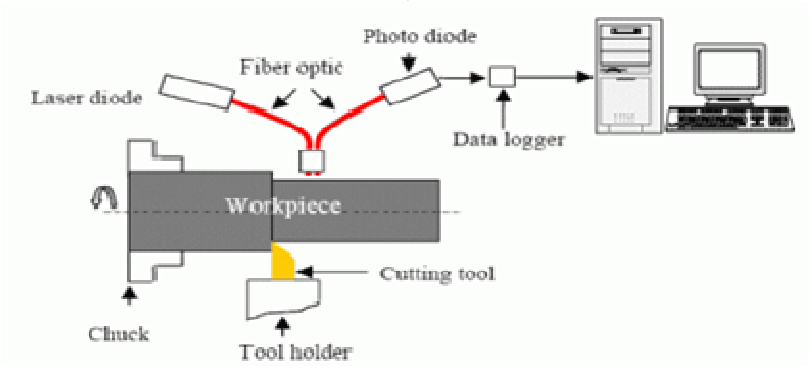

b)

Figure 6 Laser beams for geometry control of: a) drill bit and b) set-up diagram during machining

Here, the action of laser beams could be considered just as a meaning for improving the surface characteristics of tool(s).

5. PROCESSES OF LASER BEAM INTERACTIONS WITH MATERIAL SURFACE

Laser beams may interact with material surface as shown in Figure 7, roughly sketched with principal processes: transmission, reflection and absorption/adsorption in linear approach [9-12].

TRANSMISSION	REFLECTION	ABSORPTION
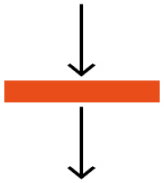		
no effect on material (e.g. glass)	no effect on material (as mirror)	many effects

Figure 7 Three principal groups of mechanisms when laser beams impact on material surface

These reactions further may have led to appearing the different heat transfer mechanisms as: conduction, convection, radiation or heat absorption, very roughly, Table 1 [7-13].

Table 1. Heat transfer mechanisms in targeted surface and their thermodynamic equations

Heat Transfer Mechanism	Governing Equation
Conduction	$Q = kA\frac{T_2 - T_1}{L}$
Convection	$Q = hA(T_2 - T_1)$
Radiation	$Q = \varepsilon\sigma A(T_2^4 - T_1^4)$
Heat Absorbed	$Q = mc_p(T_2 - T_1)$

Radiation of energy from surface during laser beam exposition, in this case represents full loss, while one of the main reaction of laser beams with surface is the heat generation. The heat absorption farther offers many practical possibilities for surface treating. This heat might be enough for melting the metal surface (further for welding - if is needed), but here will be analyzed characteristics only for heat treating, as a part of surface engineering technology. The mechanisms of reaction could be grouped into: physical, (optical, thermodynamic, fluid-mechanics, etc.), chemical and metallurgical changes. Nuclear reactions are far away from this studying.

It is established that laser beams in surface engineering are suitable for:

- increasing mechanical properties (hardness, strength, fatigue life, etc),
- reduction of friction & wear,
- corrosion resistance,
- quenching,
- alloying, etc.

Alloying, however, may significantly change the surface properties, while annealing of tool steel practically is absent in practice.

6. LASER FOR IMPROVING THE SURFACE CHARACTERISTICS OF TOOL

The using of laser beams in treating the tool surface is based on reactions which may occur after beams impact the treated surface. Important reactions in surface engineering are reflection and absorption, while scattering and transmission should be avoided. Absorption (or absorptivity A) and reflection (R-reflectance) in sum may reach values near to 1, (1,0 is 100%), Figure 8. These graphics were determined at normal incidence angle of laser beams at room temperature.

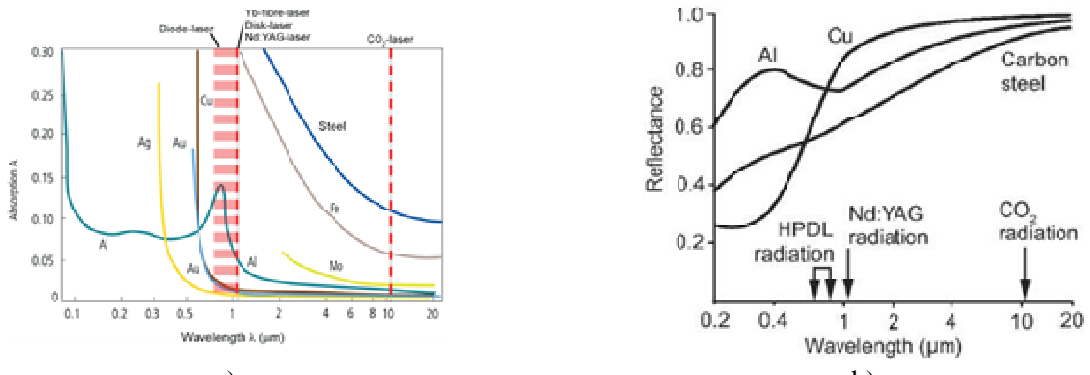

a) b)

Figure 8 Absorption a) and reflection b) for some metals as function of laser beam wavelengths [11]

The consequences of laser absorption could be rather complex, in metallurgical sense it means phase transformations, but such changes further lead to changing the principal properties of the metal surface. One of the most important fact in laser impact, the metal surface is the heat generation. Laser heating is extremely fast in comparison to conventional heating of tool. Such heating at the irradiated region may results in increasing the diffusion of many constituents from a tool material, even a melting – this behavior however is forbidden.

General metallurgical reactions&structures during heating or cooling of a steel briefly are represented in Figure 9.

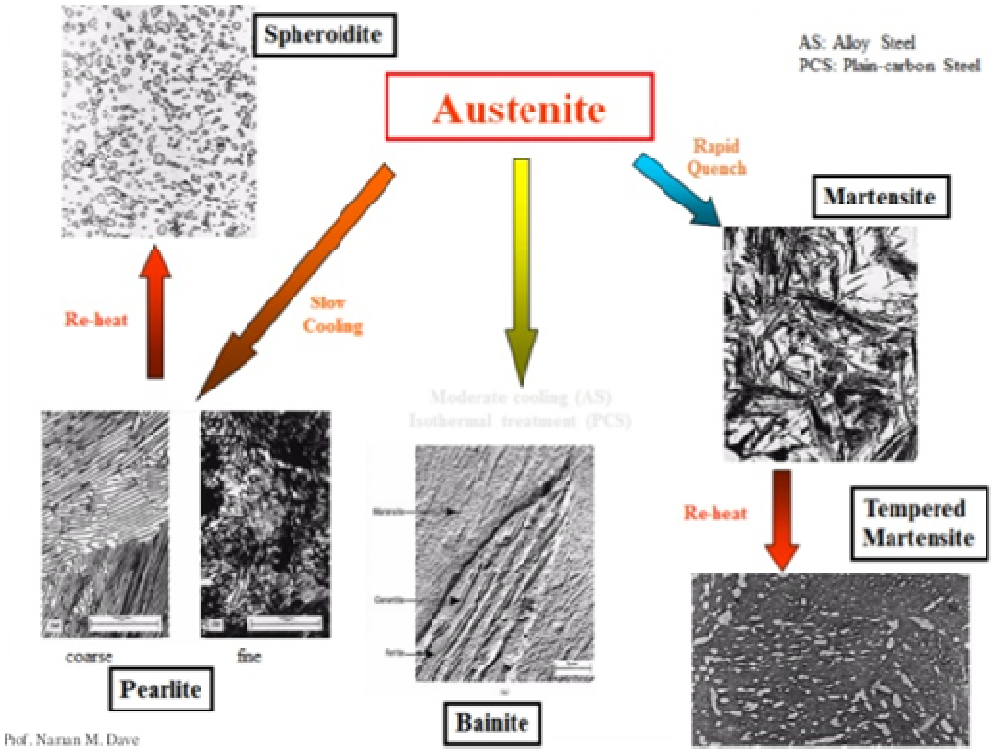

Figure 9 Structural changes in austenite during heating and cooling

The crucial influence on austenite transformation plays a cooling speed, when different structures may take place, as it was well established in heat treatment theory, also in physical metallurgy of steels.

Concept of laser surface heat treatment of a metal is based on heating the surface, Figure 10a), and then fast cooling ("self-quenching"), when is expected the martensite formation, Figure 10b).

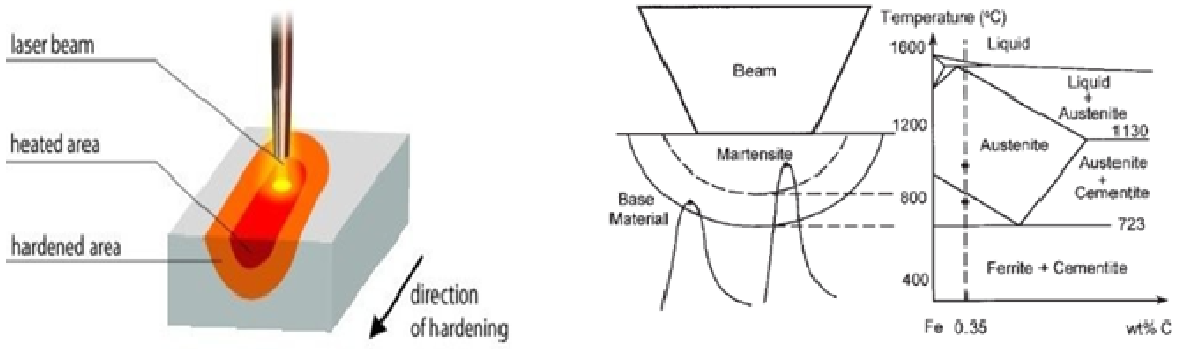

a) b)

Figure 10 Heating-up in laser processing of metal surface a) and isotherms for two temperature cycles steel after laser impacted on surface in relation to constitutional diagram Fe – C b) [9-11]

So, fast heating and then cooling lead to forming specific structures in quenched steel, for M2 steel (with pretty well wear resistance and toughness) treated with two laser powers a) 400W and b) 1800W [14]. According to such changes, generally at other steels, it is possible to illustrate different zones over base metal [10-16], Figure 11.

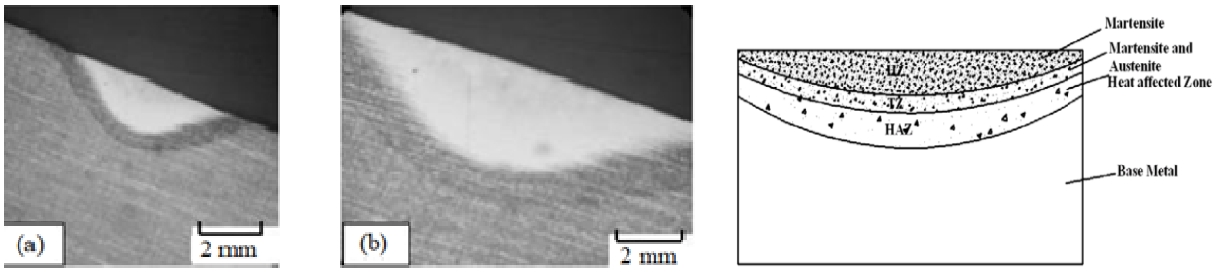

a) b) c)

Figure 11 Real microstructures of transformed structures after laser treating a), b) and sketch of zones after laser impacted surface c)

6.1 Laser scanning for quenching

Laser beams are available for treating the surface in one direction or in multipassing, sometimes producing overlapping layers, Figure 12a), or moving as in Figure 12b). At one pass will be achieved hardened layers in wide about 50mm.

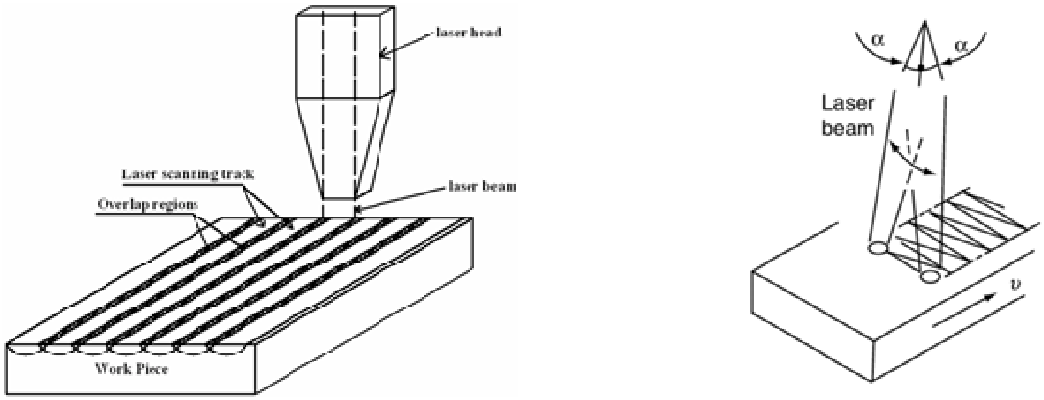

a) b)

Figure 12 Possible paths of laser beams in: a) straight directions and b) zig-zag moving

One of the main advantage in using of laser beams is the possibility for optical manipulation of these beams across the treated surface, and this ability is well illustrate in treating of the curved, hidden and irregular surfaces, Figure 13, [7].

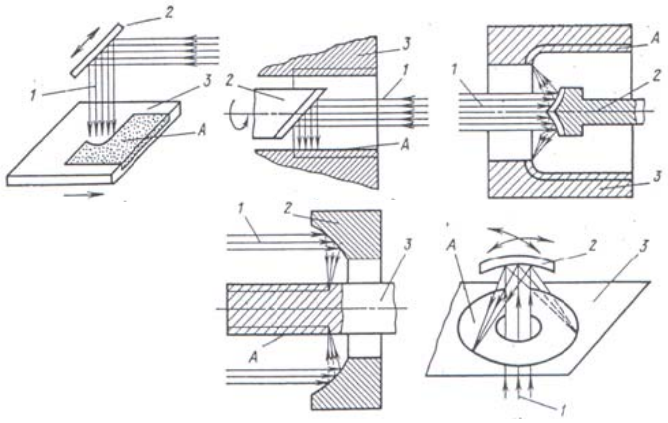

1- laser beams,
2- reflective mirror,
3- treated area and
A-quenched zone

Figure 13Possibility for laser beam manipulation by optical lenses a-e) for partial quenching

Working on such way became possible to laser quench only a cutting zone of one tool for up-setting of forgings, Figure 14a). The increasing of hardness is important, from 700HV after conventional heat treating to over 900HV units, curves 1 and 2, in Figure 14b).

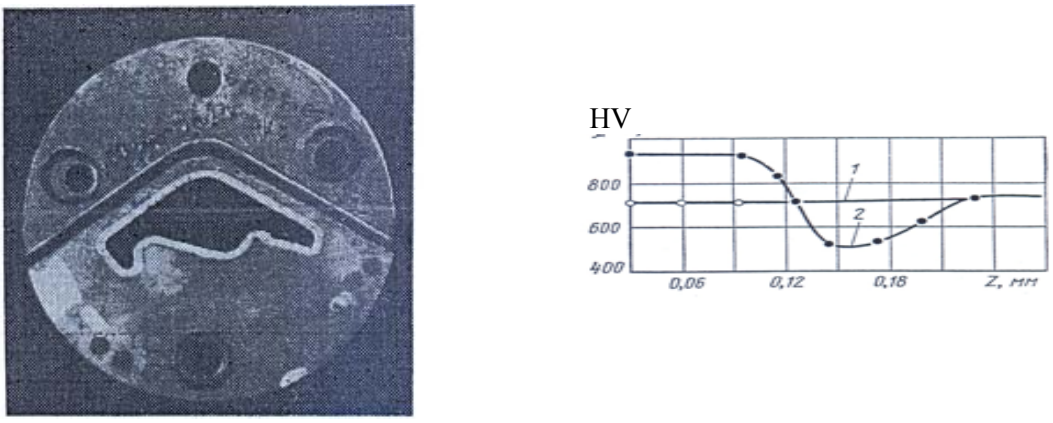

a) b)

Figure 14 Laser treated cutting zone at trimming die for flash removing a) and hardness changes b): 1-previouly quenched and tempered tool (on conventional manner) and 2-after laser treating

For achieving such results could be used both CO_2 and Nd^{3+}:YAG lasers. The depth of hardening largely depends on the technological reasons of laser treating.

7. METALLURGICAL ADVANTAGES OF LASER SURFACE HARDENING

During laser hardening the martensite participation is increased in structure while the amount of retained austenite is decreased, so all of these reactions produce greater hardness of treated tool. The best results could be achieved on previously heat treated tool on conventional manner (quenched and repeated tempering). Further hardening is provided by self-quenching without using an extra cooling medium [14] and with negligible distortion. If hardness of tool, servicing life etc, were improved, it means saving of strategic alloying metals, as refractory metals are. According to the other provided experiments [15-16], the hardness of laser treated surface is higher, about 20% or more, than conventionally quenched & tempered conditions. Such increasing of hardness is resulted in increasing the wear resistance, in a little bit greater percent.

Laser surface hardening is provided mainly for improving the tribological properties, without decreasing the bulk toughness or other properties. The depth of laser hardening layer is smaller in comparison to induction hardening. In every case, the particular attention should be considered on the temperature values during laser quenching.

For laser heat treating (quenching) are available various materials:

- low carbon steels, with contest of carbon less than 0.30%, principally may be laser quenched but with limiting effects, depth of hardening will be up to 0.5 mm;
- all cast irons with pearlitic structure could be hardened by laser beams, but beware of possible melting;
- steels with medium or high percentage of carbon (from 0.35 to 0.8%) are better choice than low carbon steels, when depth of hardening may reach about 4.0 mm. Fully annealed or spheroizided structures are not recommended for laser treating.
- alloyed steels with elements which magnifying the depth of hardening (Mn, Mo, Cr, B, and others) are pretty suitable for laser hardening. Achieved depth of hardening, in these steels up to 3.0 mm, need not further tempering;

- steels with dominant martensitic structure may be laser hardened but laser beam density and other technological parameters must be well selected, because of possible cracking in such materials, and
- tool steels which contain a greater percent of carbon and refractory metals (W, Mo, Zr and others) are available for laser hardening, similar to alloyed steels.

In any case, the surface to be laser treated must be clean, without rust or grease, for achieving the expected results. In this kind of hardening, the tools generally not require the using of coatings to enhance the absorptivity of laser beams.

7.1 Main parameters in laser hardening

Laser beams act in short time cycle, and most of working parameters are, however, independent at the laser system (laser power, beam energy and density, size and shape of beam, position of focus beam, processing speed/scanning velocity, etc.) and they are changeable while the properties of metal/tool (as like thermal properties, absorption/adsorption or reflection ability, hardening capacity, etc.) are strongly defined in advance, it means constant for a material. From the aspect of hardening, the processing parameters of laser beams acting on metal surface play an extra ordinary effect on structures that will be obtained. Laser hardening requires homogeneous structure: for a short time of laser beam acting there is no time for diffusivity of alloying elements.

Hardening demands should be carefully analyzed, so many efforts should be done for optimization the working procedure(s) in every particular case [7-16].

7.2 Disadvantages of laser hardening

There are a few disadvantages of using the laser hardening in comparison to advantages:

- optical lenses in laser systems are exposed to heavy conditions, and they require an extra maintenance costs,
- generally, the investments cost is high, and
- workers should be well trained.

8. CONCLUSION

The laser beams in their nature belong to electromagnetic radiation, and they are acting just at the optical defined area, in tools it means - where is needed. Energy from laser beams after absorption are transformed into the heat, and this heat produces metallurgical reactions which producing the increasing of hardness (over 60HRC) and wear resistance, without changing the bulk properties of a tool. Melting of the impacted surface simply is not allowed.

It is evident that laser quenching of the cutting tool is one of the newest technology at the tool which is previously well quenched and tempered. Quenching by using laser beams offers many advantages, it is time efficient process and farther the distortion after laser surface treating is negligible, while an extra medium for quenching is not needed. Disadvantages of using the laser beams for improving the cutting tool edge are minor in comparison to conventional techniques for quenching. Repeatability of obtained results is, however, on a high level.

REFERENCES

[1] Т. Н. Лоладзе: Прочност и изностојкострежушчевоинструмента, Москва 1982, Машино-строение, стр. 69-205.
[2] Yu. Geller: Tool steels, Moscow 1978, MIR Publ, p. 358-485.

[3] Ју.А. Башнин, Б.К. Ушаков, Г. Секеј: Технологијатермическојобработкистаљи, Москва 1986, Металлургија, стр. 375-411.
[4] G. E. Totten: Steel heat treatment, Metallurgy and technologies, Handbook Second edition, Portland State University 2007, izd. Taylor&Francis Group,
[5] Г. Ф. Ивановскиј, В.И. Петров: Ионно-плазменнајаобработкаматериалов, Москва 1986, радио и свјаз, стр. 66-122.
[6] В. Д. Садовскиј, В.М. Счастливцев, Т.И. Табатчикова, И.Л. Јакољева: Лазернијнагрев и структурастаљи, Сверловск 1989, Уро АН СССР.
[7] N. Rykalin, A. Uglov, I. Zuev, A. Kokora: Laser and electron beam material processing, Handbook, Moscow 1988, MIR Publ, p.277-353.
[8] А. Г. Григорјанц, А.Н. Сафаров: Основилазерновоупрочњењијасплавов, Москва 1988, Висшајашкола, стр. 7-33.
[9] J. Kusinski, S. Kac, A. Kopia, et al.: Laser modification of the materials surface layer – a review paper, Bull. of the Polish akademy of sciences, Technical sciences, 60/2012/4, p. 711-728.
[10] P. Dinesh Babu, K.R. Balasubramanian: Laser surface hardening- a review, Int. J. Surface Science and Eng, 5/2011/2-3, p. 131-137.
[11] J. Sundqvist: Aspects of heat flow in laser materials processing, 2018, Doctoral Thesis, Lulea University of Technology, Sweden.
[12] M. Srećković, A. Bugarinović, Ž. Tomić, A. Kovačević, V. Rajković: Interakcijalaserasamaterijalom: Teorija, eksperimentirealnost, Beograd 2012, Regionalnicentar za talente Beograd II
[13] M. Srećković, S. Polić, A. Bugarinović, V. Svoboda: Laser iproblemikonzervacijekulrutnebaštine, Beograd 2016, Centralniinstitut za konzervaciju, Centar za talente Beograd 2.
[14] A-M. El-Batahgy, R.A. Ramadan, A-R. Moussa: Laser surface hardening of tool steels-Experimental and numerical analysis, J. Surface Engineered Materials and Advanced Technology, 2013, 3, p. 146-153.
[15] L. Xue, J. Chen, S.-H. Wang: Freeform Laser Consolidated H13 and CPM 9V Tool Steel, Metall. Microstruct. Anal, 2013/2, p. 67-78.
[16] M. Miralles: Laser Hardening of Cutting Steels, Master thesis, Lulea University – Sweden, 2013.

IMPACT OF EXTRAORDINARY SECURITY MEASURES TO EMPLOYEES DURING THE PANDEMIC COVID-19

Slavica Miletić[1], Dejan Bogdanović[2], Emina Požega[1]

[1]Mining and Metallurgy Institute Bor, Zeleni bulevar 35, 19210 Bor, Serbia

[2]Technical Faculty Bor, University of Belgrade, V.J. 12, 19210 Bor, Serbia

Abstract

Today's modern business organizations in times of pandemic caused COVIDE -19 are not in a situation to take place without the required extraordinary security measures. The implementation of extraordinary security measures is becoming increasingly important, especially in today's current wisdom changing market during the pandemic.The aim of this paper is to assess the progress of the impact of extraordinary security measures on employees during the COVID-19 pandemic.The evaluation of indicators / criteria was done by AHP method.Suppression progressthe COVID-19 pandemic demonstrates the effectiveness of the proposed approach.

***Keywords**: Security measures, Employees, COVID -19*

1. INTRODUCTION

During the pandemic caused COVIDE - 19 Government of the Republic of Serbia has declared the introduction of emergency measures for the safety of human health.All countries in the world during the pandemic declared an emergency situation in accordance with their national laws.Regulation on security measures for combating a pandemic, the Government of the Republic of Serbia published in the "Official Gazette of RS", No.151 / 2020The countries of the European Union have given a time frame for the implementation of sustainable security measures for the suppression of infectious diseases.Prescribed safety measures are implemented by employers / company managers.Employees need to know, understand and follow the prescribed measures in their workplace. They may also request additional information from their employer / manager.Employers / managers include their representatives of the Integrated Management System (ISM). ISM integrates: Quality Management System (ISO 9001, QMS), Environmental Protection System (ISO 14001, EMS) and Health and Safety Protection System (OHSAS 18001: 2007).It is the duty of the employer / manager to communicate with employees in terms of encouraging and caring for their health.It is assumed that jobs with a large number of contacts have a higher risk. Employees who have a close interaction with customers or other employees during a shift are at higher risk of infection. Close communication of employees with other clients enables the same greater danger of obtaining and transmitting viruses. It is assumed that excessive environment, crowded the workplace, confined space, frequency of contact with areas of high touch; frequently touching the employees have a higher risk of infection.

Analyses of the impact of security measures on employees during a pandemic COVIDE - 19 provide an opportunity for employers / managers a way to combat the infection. Employers / managers do not have the opportunity to know the health condition of individual employees; it is confidential or has the ability to implement appropriate safety measures.

Analysis of the impact of security measures on employees during a pandemic was made AHP (analytic hierarchy process) method. The following safety measures were analyzed: cleaning and disinfection, use of personal protective equipment (PPE), wearing non-medical masks or face masks, and physical distancing or separation.

The AHP method belongs to the methods of multi-criteria decision making (MCDM). MCDM methods belong to the field of operational research and management science, which include various techniques that facilitate the decision-making process [1, 2]. These methods are widely used in various areas of business: staff selection [3], supply chain [4], information technology [5], organizational culture selection [6] and many other areas.

2. EXPERIMENTAL

In order to assess the overall progress of the declared measures to combat the pandemic caused by COVID - 19, the following indicators are assessed: cleaning and disinfection, use of personal protective equipment (PPE), wearing non - medical masks or face masks, physical distancing or separation and communication with employees; prevention posters (Table 1).

Table 1. Indicators (criteria) and explanation

Indicators (criteria)	Explanation of indicators (criteria)
C_1 -cleaning and disinfection	Landscaping and cleaning, constant disinfection, hand washing reduces the risk of spreading COVID - 19.
C_2 - use of personal protective equipment (PPE)	Some employees cannot use protective equipment (dresses, boots, gloves, etc.).
C_3 - wearing non-medical masks or face masks	Wearing medical masks or face masks can prevent a person who is unknowingly infected from spreading the virus to other employees.
C_4 - physical distancing or separation	Separating people or separating from each other, reducing contact on common surfaces mitigates the risk. Somewhere this is not possible, so several measures are combined to increase security and reduce the risk of spreading the virus.
C_5 - communication with employees and prevention posters	Communication with employees on how to react as safely as possible to emergencies while the virus lasts. Prevention posters as notifications for employees as measures to be taken while COVID - 19 measures are in force.

Using the AHP method, we evaluate the indicators (criteria) with the help of the Sati scale, where we compare the two elements in relation to the goal. The goal is to make overall progress in curbing the spread of COVID - 19 to employees through security measures.When interpreting the results with the help of Satie's scale, one element is always more important than the other, depending on the set goal. These conclusions define the AHP method and make it suitable for evaluating the criteria.

Table2. Matrix comparing pairs

Indicators (criteria)	C_1	C_2	C_3	C_4	C_5
C_1	1	1/2	1	2	1
C_2		1	2	3	1/2
C_3			1	3	1
C_4				1	1/2
C_5					1

The AHP method has a strong mathematical basis and is one of the soft optimization methods. The degree of consistency is less than 0.10, which means that the decision maker gave an accurate assessment of the criteria. Table 2 shows a 5x5 matrix comparisons. Figure 1 shows the Hierarchy of the AHP method.

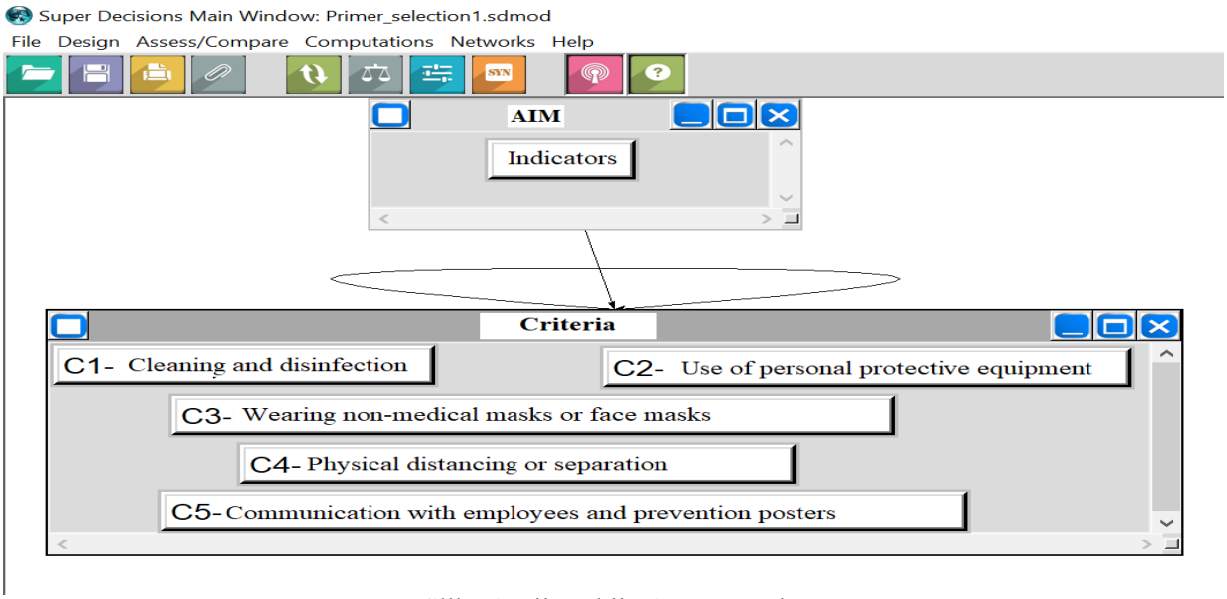

Slika 1.Hijerarhija AHP metode

3. RESULTS AND DISCUSSION

The obtained results are shown in Figure 1. The analysis was done by AHP calculation using Super Decision software.Criterion C_2, the use of personal protective equipment has the greatest progress for the suppression of the COVID-19 pandemic, because its weight coefficient is 0,27203.Communication with employees and posters for prevention, criterion C_5 is in second place in terms of progress in combating the pandemic, because its weighting factor is 0,25925.Criterion C_3, non-medical wearing masks or face masks with a weighting coefficient of 0, 19843 occupies third place.Cleaning and disinfection, the criterion C_1 is in fourth place.The weight coefficient of criterion C_1 is 0,18151. Physical distancing or separation, criterion C_4 with a weighting factor of 0.08878 is in fifth place in terms of progress to combat the pandemic.AHP analysis shows that: criterion C2 affects 27.2% on the reduction of COVIDA -19, criterion C5 with 25.9%, criterion C3 with 19.84%, criterion C1 with 18.1% and criterion C4 with 8.8%.We conclude that the prescribed safety measures impact on reducing the spread of a pandemic, which is a big improvement.

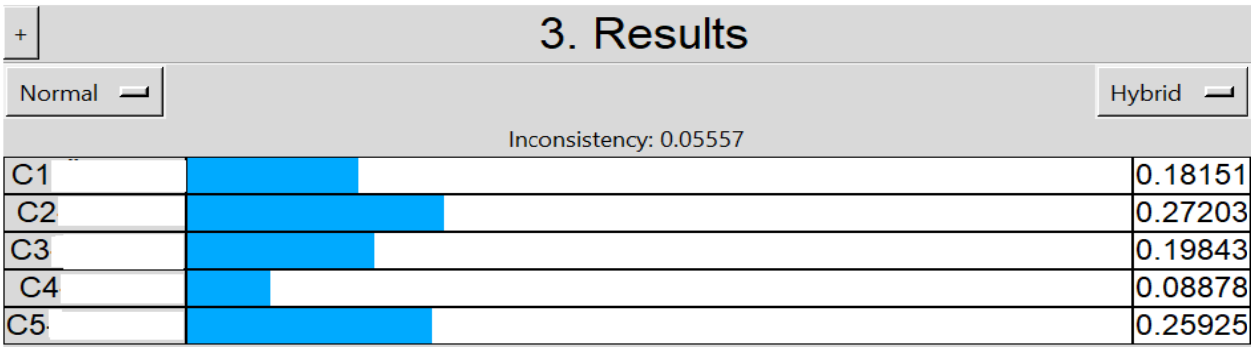

Figure 2. Weighting coefficients of the criteria

4. CONCLUSION

Emergency security measures prescribed by the Government of the Republic of Serbia have significant role in the progress of combating the spread of the pandemic COVIDE - 19.The implementation of prescribed security measures is important to combat the pandemic. Security measures are implemented by the employer / manager together with IMS representatives.In this paper, the AHP method for evaluation of indicators / criteria is proposed.During the evaluation of the indicators / criteria, there were three decision makers where they evaluated five criteria.Using personal protective equipment, criterion C2 has the greatest progress in combating the spread of the COVID-19 pandemic because its weighting factor is 0,27203.We can conclude that the implementation of the prescribed emergency security measures brings great progress in the fight against the pandemic to employees.The obtained results confirmed the applicability of this proposed method. For future research with a little modificationcan be used by other MCDM methods.

ACKNOWLEDGEMENTS

The research presented in this paper was done with the financial support of the Ministry of Education, Science and Technological Development of the Republic of Serbia, within the financing of scientific research work in the Institute of Mining and Metallurgy Bor, according to the Contract No. 451-03-9/2021-14/200052, and at the University of Belgrade, Technical Faculty in Bor, according to the Contract No. 451-03-9/2021-14/200131.

REFERENCES

[1] Stanujkic, D.; Karabaševi´c, D., An extension of the WASPAS method for decision-making problems with intuitionistic fuzzy numbers: A case of website evaluation,Oper. Res. Eng. Sci. Theory, 2018, 1, p. 29–39.

[2] JaukovicJocic, K., Jocic, G., Karabasevic, D., Popovic, G., Stanujkic, D., Zavadskas, E.K., Thanh Nguyen, P., A Novel Integrated PIPRECIA–Interval-Valued Triangular Fuzzy ARAS Model: E-Learning Course Selection, 2020, 12, p. 928.

[3] Bogdanović, D., Miletić, S., Personnel evaluation and selection by multicriteria decision making method, Econ. Comput. Econ. Cybern. Stud. Res.,2014, Vol. 48(3), p. 179-196.

[4] Yazdani, M.; Zarate, P.; Coulibaly, A.; Zavadskas, E.K., A group decision making support system in logistics and supply chain management, Expert Syst. 2017, 88, p. 376–392.

[5] Turskis, Z.; Goranin, N.; Nurusheva, A.; Boranbayev, S., Information security risk assessment in critical infrastructure: A hybrid MCDM approach,Informatica, 2019, 30, p. 187–211.

[6] Miletić, S.,Stanojević, Š.Z., Jovanović, I., Radivojević, M., Conić, V., AHP analysis of organizational culture in textile companies in Serbia, Ind. Textila,2020, 71, 2, p. 124–131.

KINETIC STUDY OF SOLID-PHASE REDUCTION OF POLYGRADIENT IRON-CONTAINING MATERIAL

Daniela Grigorova[1],Rossitza Paunova[1]

[1]University of Chemical Technology and Metallurgy, 1756 Sofia, 8 Kl. Ohridskyblvd., Bulgaria

Abstract

The kinetics of the direct reduction of iron-containing material with increased content of manganese, barium, and lead was studied. Coke breeze and brown coal/lignitewere used as reducing agents. The mechanism and kinetics of the reduction reaction were systematically studied by means of thermogravimetric analysis. The apparent activating energy of the dissociation and solid-phase processes that took place when heating pellets without a reducer was E = 98,62 kJ/mol. The reduction processes were significantly influenced by the Boudoir reaction. It was found that when using coke breeze, the speed of the processes was higher due to their higher reactivity. When using coke breezein the pellets, the activating energy was 240 kJ/mol, and when using brown coal - 158 kJ/mol. The reduction processes took place in the kinetic region. Brown coal can be successfully used as a reducing agent.

***Keywords**: kinetics, TGA analysis, activation energy, rate of reaction*

1. INTRODUCTION

The iron-containing material, the object of this study, is sludge that falls off after flotation enrichment of ore and is subsequently disposed of as waste. Modern devices for magnetic separation allow for the extraction of iron. The product after separation has a relatively high content of iron, but it also has a fine composition and a high content of barite, manganese, and lead. In our earlier research, the possibility for successful pelletization has been established.Reduction heating is one of the options for removing the accompanying impurities, including the reduction removal of lead and zinc from the pellets. The thermodynamics, mechanism, and kinetics of the direct reduction of pure iron oxides [1-3], manganese oxides [1, 4], ZnO [5], PbO [2] and $BaSO_4$ [6] have been the subject of numerous studies and have been well studied. To remove $BaSO_4$, it is necessary to process it to barium sulfide BaS. $BaSO_4$ is reduced using activated carbon, solid carbon graphite, coke, and carbon. Coke and coke breeze are the main reducing agents used in metallurgy. Brown coal has a lower cost and has significantly larger deposits in the earth.The present paper aims to study the kinetic characteristics (activating energy, rate constant, and reduction degree) in non-isothermal reduction heating of a multicomponent iron-containing material, by tracking the influence on the kinetic data when replacing the reducing agent – local production brown coal instead of coke breeze.

2. EXPERIMENTAL

The chemical composition of the polygradient iron-containing material used is presented in Table 1.

Table 1 - Chemical composition of initial iron-containing material,%.

Fe (total)	SiO_2	Al_2O_3	Cu	CaO	Zn	MgO	S	Mn	P	Pb	Ba
50,100	7,067	1,157	0,142	1,64	0,071	0,915	0,599	7,687	0,014	0,416	3,163

The phase analysis of the sample of iron-containing material was done with the help of X-ray diffraction analysis.The studied material consisted of complex oxide compounds, with a more crystalline or finely dispersed structure, acting as individual oxides. The main phases were synthetic magnetite Fe_3O_4, hematiteFe_2O_3, calcite $Ca(CO_3)$, quartz, cristobalite SiO_2, andbixbyiteMn_2O_3.This waste iron-containing material was used as the main raw material for making the pellets. Two types of reducing agents, coke breeze and brown coal/lignite were used:

- Pellets 1- consisted of iron ore material;
- Pellets 2- consisted of a homogenized mixture of iron ore material and crushed coke breeze;
- Pellets 3- consisted of a homogenized mixture of iron ore material and brown coal/lignite.

Green pellets of size 9-16 mm were prepared in a laboratory disc pelletiser of 1 m diameter with 0,6% bentonite as a binder.A strength level of 180 kg/pellet was achieved.The pellets were heated up to 1473 K. A STA PT1600 TG-DTA/DSC thermogravimetric apparatus was used in the experiments. The heating speed was 283 K/min. The kinetic parameters were determined using the Piloyan method.Figures 1 to 3 show the changes in mass and the differential change in temperature during the heating of the three samples. The XRDshown in Figure4 is the product of pellets 3 (containing iron ore material and reducing brown coal), obtained after heating to a temperature of 1473 K.

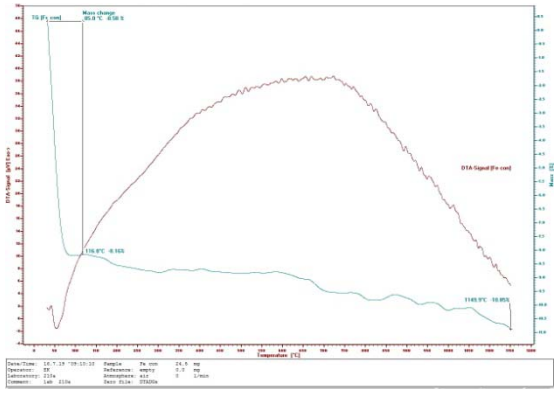

Figure 1. TG/ DTA analysis of pellets 1.

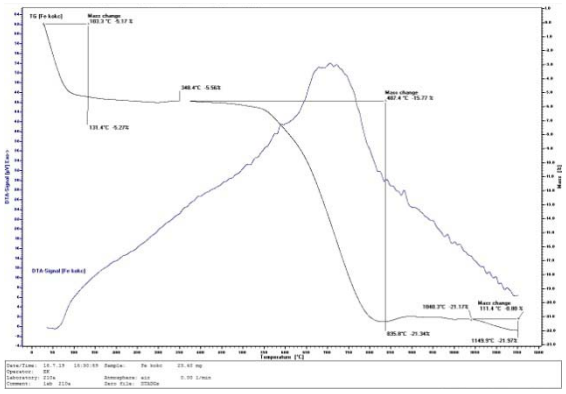

Figure 2. TG/ DTA analysis of pellets 2.

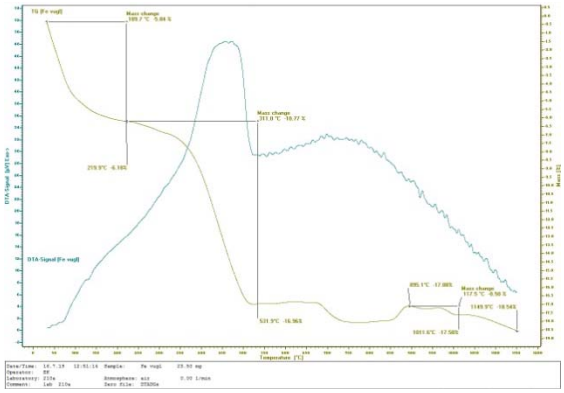

Figure 3. TG/ DTA analysis of pellets 3.

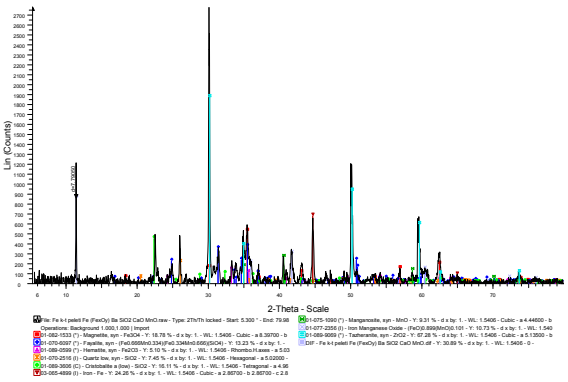

Figure 4. XRD analysis of pellets 3 after heat treatment.

The decrease in mass in the first sample-pellets 1 was due to the release of moisture and volatile substances; above the temperature of 845 K,it was due to the decomposition of iron oxides according to the scheme$Fe_2O_3 \rightarrow Fe_3O_4 \rightarrow FeO$.The exothermic effect, accompanied by mass loss, was observed in pellets using reducing agents. This effect was due to the combustion of carbon from coke and coal, as well as from thecompleted reduction processes, mainly of iron and

partly of manganese oxides. At temperatures above 850 K, solid-phase interactions between $Fe_2O_3$and SiO_2took place until the formation of Fe_2SiO_4 (fayalite).

The dependence of lgm – 2lgT = f(1/T) of the studied pellets is presented in Figures5- 7. Figure 8 shows the rate of the processes when heating the pellets using coke and brown coal. Two peaks were registered.The first one up to a temperature of 400 K shows the processes of dissociation and solid-phase interactions, whereas at a temperature of 980 K the rate of combustion of carbon contained in the material and in the reduction of iron and manganese oxides is clearly seen. When a coke reducer is used, the processes take place at a higher rate.

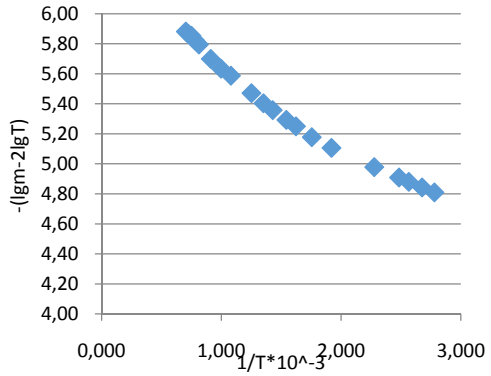

Figure 5. The dependence of lgm - 2lgT = f (1/T) of pellets 1.

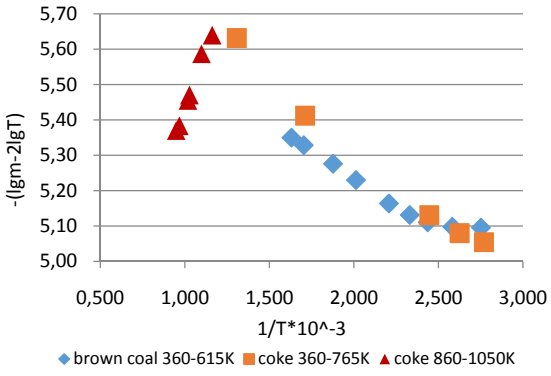

Figure 6. The dependence of lgm - 2lgT = f (1/T) of pellets 2 and 3 up to temperature 1050K

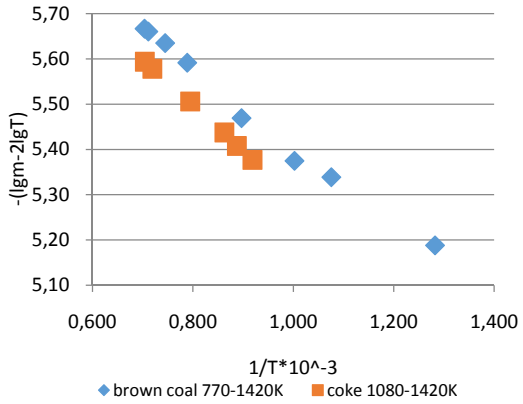

Figure 7. The dependence of lgm - 2lgT = f (1/T) of pellets 2 and 3 up to temperature 1420K

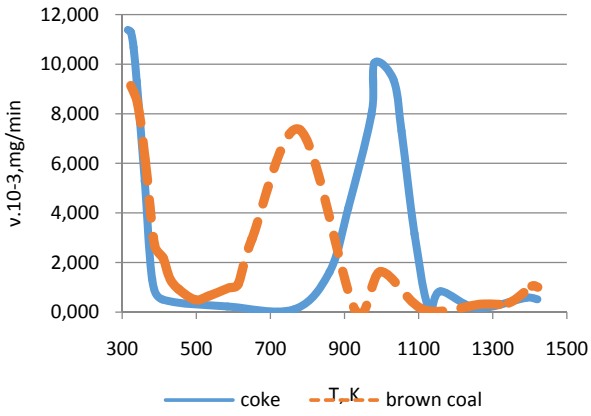

Figure8. Rate of the processes depending on the temperature of the pellets containing reducer agent

Using the graphical method, the activating energy was determined and the equations for the rate constant in the chosen temperature ranges were derived. The results are presented in Table 2.

Dissociation and solid-phase interactions are the main processes occurring in pellets 1; the processes take place in the external diffusion region. In the case of pellets 2 using coke breeze, the processes take place in three sub-stages. When using brown coal (pellets 3), the processes take place in two stages: the first is limited in the external diffusion region, and the second in the kinetic region.The activating energy in the reduction of $Fe_2O_3 \rightarrow Fe_3O_4$is 69- 100 kJ/mol; $Fe_3O_4 \rightarrow FeO$ = 64-78 kJ/mol; $Fe_xO \rightarrow Fe$ = 100-116 kJ/mol [7,8].The apparent activating energy in the reduction of zinc oxide pellets is between 165-242 kJ/mol [9-10]. The activating energy of the thermal dissociation of MnO_2 is 175 kJ/mol. Ea ofthe reduction of Mn_2O_3 - 226 kJ/mol, and

Mn_3O_4 is 289 kJ/mol, which is almost equal to that for the reaction of carbon gasification. The gasification reaction is catalyzed by Mn_3O_4 [11].

Table 2 - Activation energy and reaction rate equation of the studied pellets

Pellets	lnK	R^2	Activation energy (Ea)	temperature range, K
1	lnK= 521/T – 6,17	0.974	98,62 kJ/mol (23555 cal/mol)	355-1400
2	lnK_1 = 395/T – 6,12	0.988	75,51 kJ/mol (18040 cal/mol)	88-492
	lnK_2 = -1342/T –4,09	0.988	241,32 kJ/mol (57641 cal/mol)	587-780
	lnK_3 = 1009/T – 6,31	0.999	193,48 kJ/mol (46138 cal/mol)	816-1147
3	lnK_1 = 251/T – 5,74	0.948	43,36 kJ/mol (10356 cal/mol)	360-613
	lnK_2 = 853/T –6,26	0.989	158,03 kJ/mol (37744 cal/mol)	780-1150

3. CONCLUSION

Based on the experimental data, the apparent activating energy for the processes occurring during heating of pellets 1, 2, and 3 was determined. Equations for determining the rate constant lgK = f (1/T) were derived. It was found that at higher temperatures the processes took place in the kinetic region.The reduction of iron oxides took place with activating energy of 193,48 kJ/mol (coke breeze) and 158,03 kJ/mol (brown coal). The reduction of Mn_2O_3 at a temperature of about 700 K has Ea = 241,32 kJ/mol. At a temperature of 780K, a rate of 7,4. 10^{-3} mg/min was reported for the sample using brown coal, while in the sample containing coke breeze the maximum was drawn at a temperature of 980 K at a rate of 10,05 10^{-3} mg/min. During this period, the combustion and gasification of carbon took place, as well as the reduction of some oxides, such as zinc, iron, and manganese. The results show that brown coal can be successfully used as a reducing agent, achieving lower activating energy and high metallization.

REFERENCES

[1] I. Bornatskiy, Theory of metallurgical processes, Kiev-Donetsk, Press, “Vishchashkola”, 1978, pp 127, 129, 133. (in Russian).
[2] T.Nikolov, Theory of Metallurgical Processes, Tehnika Press, 1982, p. 249 (in Bulgarian).
[3] S.Filippov, Theory of metallurgical processes, Moscow, Metallurgy Press, 1967, p. 163.
[4] F.Sesen, Practical reduction of manganese oxide. J Chem Tech App., 1, 1, 2017.
[5] D.Ryzhonkov, Theory of metallurgical processes, Moscow, Metallurgy Press, 1989, p. 129. (in Russian).
[6] Y.Zhang, N. Dengpan, C.Jianxin. Thermodynamic and Kinetics Study of Carbothermal Reduction of Barite. J. Chem. Eng. Jpn., *52* (6) (2019)478-483.
[7] S. Trushenski, K. Li, W. Philbrook, Non-Topochemical reduction of iron oxides, Metall. Trans., 5 (1974) 1149-1158.
[8] W. Jozwiak, E. Kaczmarek, T. Maniecki, W. Ignaczak, W. Maniukiewicz, Reduction behavior of iron oxides in hydrogen and carbon monoxide atmospheres, Appl.Catal., 326 (2007) 17-27.
[9] C. Guger & F. Manning, Kinetics of zinc oxide reduction with carbon monoxide, Metall. Mater. Trans B,2(1971)3083–3090.
[10] B. Kim, J. Yoo, J. Park and J. Lee, A Kinetic Study of the Carbothermic Reduction of Zinc Oxide with Various Additives, Metall. Mater. Trans, 47, 9 (2006) 2421 - 2426.
[11] K. Terayama, M. Ikeda, Study on the Reduction of MnO_2 to MnO with Carbon by the Effluent Gas Analysis Method, J JPN I MET MATER45(9) (1981) 901-908

PART I: WHAT MAKES A GOOD THERMOELECTRIC

Emina Požega[1], Danijela Simonović[1], Saša Marjanović[2], Milenko Jovanović[1], Lidija Gomidželović[1], Milijana Mitrović[2], ZdenkaStanojević Šimšić[1]

[1]Mining and Metallurgy Institute Bor, Zelenibulevar 35, 19210 Bor, Serbia

[2]Technical Faculty Bor, University of Belgrade, V.J. 12, 19210 Bor, Serbia

Abstract

Starting from spectroscopy pure materials, a monocrystal sample of p type, $Bi_2Te_{2.8}Se_{0.2}$, was synthesized by the Bridgman method at the Serbian Academy of Sciences and Arts in Belgrade (SANU). The transport properties of single crystals were investigated. Transport properties have shown that with current increasing, mobility and Hall coefficient increase. Positive values of the Hall coefficient confirm that the material is of the p type with a high concentration of charge carriers,$n_b = 10^{18}$ cm^{-3}.

Keywords: *Bridgman technique, Hall and Van der Pauw method, doping*

1. INTRODUCTION

Based on the thermoelectric effect, waste thermal energy generated as a by-product of industrial processes can be converted into electricity. Known as "Peltier", "Seebeck" or "Thomson" effect, the thermoelectric effect is seen in semiconductor devices that generate voltage when a different temperature is present on each side, or create a temperature difference between the two sides when the voltage is on the device. The thermoelectric materials development is conditioned by finding materials with a high figure of merit. The parameter that evaluates the quality of thermoelectric materials, the Figure of merit (Z), is determined by the dimensionless quantity, ZT, [1,2] which is defined as:

$$ZT = \frac{\alpha^2 \cdot \sigma \cdot T}{k} = \frac{\alpha^2 \cdot T}{k \cdot \rho} = \frac{\alpha^2 \cdot T}{(k_e + k_l) \cdot \rho} \quad (1)$$

where: α - Sebek coefficient, σ - electrical conductivity, k - thermal conductivity, T - absolute temperature, ρ - electrical resistance.

Thermal conductivity has two components: electronic conductivity, k_e and lattice conductivity, k_l. The ratio α^2/ρ is defined as the power factor and determines the electrical properties. The combination of material properties required for thermoelectric materials to have quality and usable properties is also a challenge for scientists. The basic foundation in the research of thermoelectric materials is to satisfy properties that are in contradiction with each other, as can be seen from Equation 1. In order to maximize the quality factor (obtaining the highest possible thermal current, which is the absolute value of the Sebek coefficient), it must have high electrical conductivity and low thermal conductivity.In order to get as much thermal current as possible, we need only one type of charge carrier. Semiconductors are materials that are relatively easy to change the type of charge carrier (electrons and holes).
Best bulkthermoelectricmaterials at room temperature are Bi_2Te_3/Sb_2Te_3.

If doping isincreased, the electrical conductivity increases buttheSeebeck coefficient is reduced for almost all typical thermoelectric materials. Namely low gap semiconductors, almost all typical thermoelectric materials best compromise and still highly doped semiconductors are in charge concentrations range of 10^{18}-$10^{19}$$cm^3$ (Figure 1).

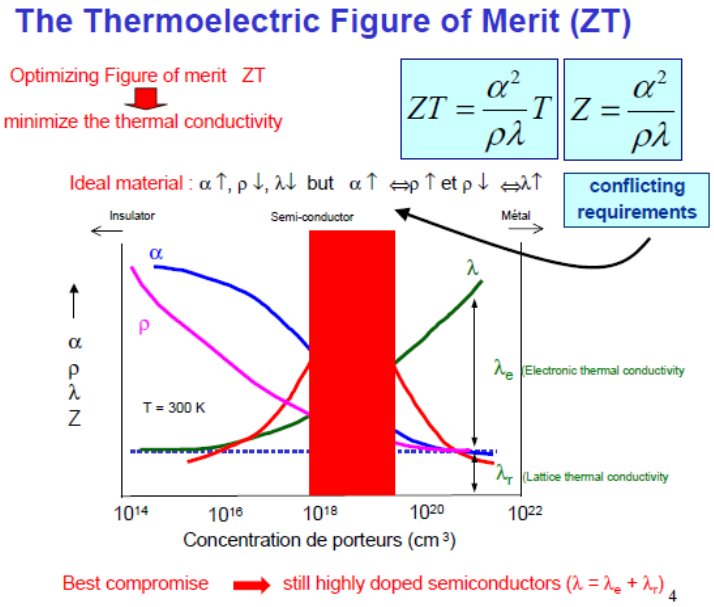

Figure 1. Best compromise of thermoelectric [3]

Best compromise of thermoelectric is marked with a red rectangle on the Figure 1.With special techniques and advances in modern material synthesis, especially in nano materials, a new time for complex thermoelectric materialsis approaching.

The significant contribution of our research is reflected primarily in the domain of materials science[4,5,6], especially in the field of thermoelectric materials. Successful synthesis of p type single crystal$Bi_2Te_{2.8}Se_{0.2}$by the Bridgman process obtained at the Serbian Academy of Sciences and Arts (SANU) in Belgrade was performed. A significant scientific contribution has been made in the application field of bismuth telluride as a thermoelectric material and selenium as its dopant. In this way, the conducted research enriched the set of data relevant for further research and for possible practical application.

2. EXPERIMENTAL

ThesampletestedbytheHalland Van derPauwmethodwascut from the ingot normally to thecrystallizationdirection(⊥). In thefollowing, thesesamplewill be referred to as 6/4(⊥).

Before the measurement starting, the sample waspreparedto be in the form of thin disc. The samples on which the measurements were performed had a uniform thicknessof 1.8 mm (Table). Sample did not have any irregularities on them. All measurements were carried out at room temperature (T =300 K). The source of magnetic field applied perpendicular to the Hall element was a permanent magnet of 0.37 T. Hall Effect measurements were done to obtain transport properties.

For resistance measure, voltage and current contacts were attached to 4 fixed contact terminals located at the sample ends and at different current intensities. Schottky contacts were used for tests performed at room temperature. The change of transport and electrical parameters with increasing current intensity was also monitored.

3.RESULTS AND DISCUSSION

The calculated data from the measurement results of the transport quantities for sample 6/4 (⊥) with a Schottky diode at room temperature (25 ° C) and magnetic induction of the permanent magnet B = 0.370 T are given in Table 1 and Table 2. Measurements were performed at currents of 0.1 and 0.5 mA.

Table 1. Results for sample 6/4 (⊥) at a current of 0.1 mA

Measured size	**Symbol**	**Result**	**Measuerment unit**
Bulk carrier concentration	n_b	$5.511x10^{18}$	$/cm^3$
Mobility	μ	$7.237x10^{1}$	cm^2/Vs
Specific resistivity	ρ	$1.565x10^{-2}$	Ωcm
Average Hall Coefficient	R_H	$1.133x10^{0}$	cm^3/C
A-C Cross Hall Coefficient	R_{H1}	$-1.784x10^{0}$	cm^3/C
B-D Cross Hall Coefficient	R_{H2}	$4.050x10^{0}$	cm^3/C
Sheet carrier concentration	n_S	$9.920x10^{17}$	$/cm^2$
Specific conductivity	σ	$6.389x10^{1}$	1/Ωcm
Magneto resistance	ΔR	$8.315x10^{-3}$	Ω
Vertical/Horizontal ratio of resistivity	α	$4.807x10^{-1}$	

Table 2. Results for sample 6/4 (⊥) at a current of 0.5 mA

Measured size	**Symbol**	**Result**	**Measuerment unit**
Bulk concentration	n_b	$4.150x10^{18}$	$/cm^3$
Mobility	μ	$1.594x10^{2}$	cm^2/Vs
Specific resistivity	ρ	$9.435x10^{-3}$	Ωcm
Average Hall Coefficient	R_H	$1.504x10^{0}$	cm^3/C
A-C Cross Hall Coefficient	R_{H1}	$1.173x10^{0}$	cm^3/C
B-D Cross Hall Coefficient	R_{H2}	$1.836x10^{0}$	cm^3/C
Sheet concentration	n_S	$7.469x10^{17}$	$/cm^2$
Specific conductivity	σ	$1.060x10^{2}$	1/Ωcm
Magneto resistance	ΔR	$2.968x10^{-3}$	Ω
Vertical/Horizontal ratio of resistivity	α	$1.079x10^{-1}$	

Mobility increases with currentincreasing. The Hall coefficient values are positive. This indicates that the samples are of p type and that the charge carriers majority are holes. That the samples are of p type was also confirmed by the hot point method. The mobility of most charge carriers decreases with increasing current, which indicates that the temperature of the samples increases, which affects on the mobility. For our sample the mobility value is increase from $\mu = 7.237x10^{1}cm^2/Vsat$ current intensity of 0.1 mA to $\mu = 1.594x10^{2}cm^2/Vsat$ current intensity of 0.5 mA.

4. CONCLUSION

This paper was the result of the selenium doped bismuth telluride monocrystalsemiconductor compoundproperties testing. Hall's and Van der Pauw's methods were used for material characterization.

The electrical properties of this crystal were measured and the mobility, concentration of the charge carriers majority and Hall coefficient were observed. On the basis of the Hall coefficient, it was determined that the majority carriers are holesin the monocrystal. The measured holes mobility was less than the holes mobility in pure bismuth telluride.
TheresultsofthesestudiesshowthattheseleniumdopedbismuthandtelluriummonocrystalwassuccessfullysynthesizedbytheBridgmanmethod, andsignificantlycomplementexistingbismuthtelluride single crystalsknowledge.

ACKNOWLEDGEMENTS

Authorswish to thankProfessorAcademician Pantelija Nikolić† on bigandselflesseffortsandassistance in allstagesofinvestigations. As wellauthorswish to thank Stevan Vujatović†, a specializedtechnician as well as Dr Ljiljana Živanovfullprofessor at the Department ofElectronics, Department ofEnergy, ElectronicsandTelecommunications from theFacultyofTechnicalSciences (FTN), Universityof Novi Sad andprofessorDr Milan Radovanović, researchassociate, to helpwiththeHallexperiment.

This work was financially supported by the Ministry of Education, Science and Technological Development of the Republic of Serbia, Grant No. 451-03-9/2021-14/ 200052.

REFERENCES

[1] H. J.,Goldsmid, R.W. Douglas, Br. J. Appl. Phys.5 (1954) 386 – 390.
[2] Tritt, T. M. Ed. Semiconductors and Semimetals, Recent Trends in Thermoelectric Materials Research: Part One to Three (Academic, San Diego, CA, 69 to 71, 2001, p. 352.
[3] https://www.fzu.cz/~knizek/pdf/ThermoelectricMaterials.pdf
[4] E. Požega, Sintezaikarakterizacijamonokristalabizmutaiteluradopiranihselenom, cirkonijumomiarsenom (Doktorskadisretacija), Univerzitet u Beogradu, Tehničkifakultet u Boru, Bor, 2018, p. 82.
[5] E. Požega, S. Ivanov, Z. Stević, Lj. Karanović, R. Tomanec, L. Gomidželović, A. Kostov, Trans. Nonferrous Met. Soc. China 25 (2015) 3279 - 3285
[6] E. Požega, P. Nikolić, S. Bernik, L. Gomidželović, N. Labus, M. Radovanović, S. Marjanović, Synthesis and investigation of BiSbTeSe single crystal doped with Zr produced using Bridgman method, Revista de Metalurgia 53 (3) (2017)

PART II: WHAT MAKES A GOOD THERMOELECTRIC

Emina Požega[1], Danijela Simonović[1], Saša Marjanović[2], Milenko Jovanović[1], Lidija Gomidželović[1], Milijana Mitrović[2], Slavica Miletić[1]

[1]Mining and Metallurgy Institute Bor, Zelenibulevar 35, 19210 Bor, Serbia

[2]Technical Faculty Bor, University of Belgrade, V.J. 12, 19210 Bor, Serbia

Abstract

Successful synthesis of p type single crystal $Bi_2Te_{2.8}Se_{0.2}$ by the Bridgman process obtained at the Serbian Academy of Sciences and Arts (SANU) in Belgrade was performed. A significant scientific contribution has been made in the application field of bismuth telluride as a thermoelectric material and selenium as its dopant. In this way, the conducted research enriched the set of data relevant for further research.

Keywords: *Bridgman technique, Hall and Van der Pauw method, doping*

1. INTRODUCTION

The best thermoelectric materials at temperatures from 300 K to 500 K [1,2,3] are Bi_2Te_3-based solid solutions, including $(Bi, Sb)_2Te_3$ and $Bi_2(Te, Se)_3$.

The commercial Bi_2Te_3-based thermoelectric of p and n type are generally prepared by unidirectional solidification methods, such as zone melting [4], Bridgman [5,6], and Czochralski [7].

Good thermoelectric is defined as:

$$ZT = \frac{\alpha^2 \cdot \sigma \cdot T}{k} = \frac{\alpha^2 \cdot T}{k \cdot \rho} = \frac{\alpha^2 \cdot T}{(k_e + k_l) \cdot \rho} \quad (1)$$

where: α - Sebek coefficient, σ - electrical conductivity, k - thermal conductivity, T - absolute temperature, ρ - electrical resistance.

For almost all typical thermoelectric materials with doping increasing Seebeck coefficient is reduced. It is necessary large Sebek coefficient and small resistivity and thermal conductivity as seen from the equation 1.

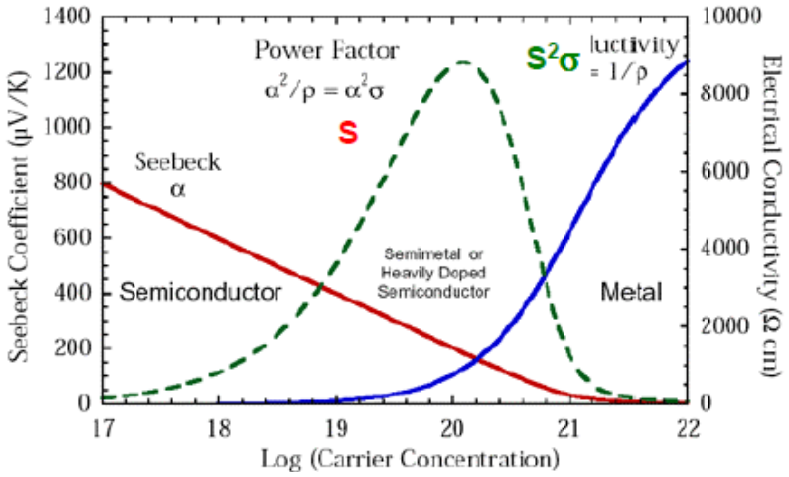

Figure 1. Materials with optimizing power factor[8]

Materials with good properties (Sebek coefficient, electrical conductivity, thermal conductivity, electrical resistance. carrier concentration, power factor) and which can be good thermoelectric are present on the Figure 1.

Best compositions for traditional bulk thermoelectric materials had largely been discovered by 1980[9].

2. EXPERIMENTAL

A monocrystal sample of p - type, $Bi_2Te_{2.8}Se_{0.2}$ was synthesized by the Bridgman method[10] at a temperature of 600°C starting from spectroscopic pure materials. Bismuth (Sigma - Aldrich, 99.999%), Selenium (Alfa Aesar, 99.999%) and Tellurium (Sigma - Aldrich, 99.999%) were taken in a certain proportion and sealed in a quartz ampoule under a pressure of 10^{-5} Pa. According to the stoichiometry of $Bi_2T_{3-x}Se_x (x = 0.2)$ alloy, high purity (5 N) elemental granules of Bi, Te and Se were weighed and then melted.

The lowering speed of the ampoule in the vertical furnace was about 2.2 mm/h. Structural, transport and thermoelectric properties were investigated. XRD analysis confirmed the monocrystal structure of $Bi_2Te_{2.8}Se_{0.2}$. Transport properties have shown that with increasing current, mobility increase. Positive values of Hall coefficient confirm that the material is p - type with high concentrations of charge carriers.

3.RESULTS AND DISCUSSION

The calculated data from the measurement results of the transport quantities for sample 6/4 (⊥) with a Schottky diode at room temperature (25 ° C) and magnetic induction of the permanent magnet B = 0.370 T are given in Table 1 and Table 2. Measurements were performed at currents of 1 and 5 mA.

Table 1. Results for sample 6/4(⊥) at a current of 1 mA

Measured size	Symbol	Result	Measuerment unit
Bulk carrier concentration	n_b	$4.876x10^{19}$	$/cm^3$
Mobility	μ	$1.700x10^{1}$	cm^2/Vs
Specific resistivity	ρ	$7.529x10^{-3}$	Ωcm
Average Hall Coefficient	R_H	$1.280x10^{-1}$	cm^3/C
A-C Cross Hall Coefficient	R_{H1}	$-4.388x10^{-1}$	cm^3/C
B-D Cross Hall Coefficient	R_{H2}	$6.948x10^{-1}$	cm^3/C
Sheet carrier concentration	n_S	$8.777x10^{18}$	$/cm^2$
Specific conductivity	σ	$1.328x10^{2}$	1/Ωcm
Magneto resistance	ΔR	$2.123x10^{-3}$	Ω
Vertical/Horizontal ratio of resistivity	α	$9.643x10^{-2}$	

Table 2. Results for sample 6/4(⊥) at a current of 5 mA

Measured size	Symbol	Result	Measuerment unit
Bulk concentration	n_b	$6.640x10^{18}$	$/cm^3$
Mobility	μ	$1.565x10^{2}$	cm^2/Vs
Specific resistivity	ρ	$6.008x10^{-3}$	Ωcm
Average Hall Coefficient	R_H	$9.401x10^{-1}$	cm^3/C
A-C Cross Hall Coefficient	R_{H1}	$9.863x10^{-1}$	cm^3/C
B-D Cross Hall Coefficient	R_{H2}	$8.940x10^{-1}$	cm^3/C
Sheet concentration	n_S	$1.195x10^{18}$	$/cm^2$
Specific conductivity	σ	$1.664x10^{2}$	1/Ωcm
Magneto resistance	ΔR	$2.442x10^{-3}$	Ω
Vertical/Horizontal ratio of resistivity	α	$8.606x10^{-2}$	

Mobility increases with increasing current. The Hall coefficient values are positive. This indicates that the samples are of p type and that the charge carriers majority are holes. That the samples are of p type was also confirmed by the hot point method. The mobility of most charge carriers decreases with increasing current, which indicates that the temperature of the samples increases, which affects on the mobility. For our sample the value of μ is increase from μ = $1.700x10^{1}cm^2/V$sat current intensity of 1 mA to μ = $1.565x10^{2}cm^2/Vs$ at current intensity of 5 mA.

4. CONCLUSION

Transport properties namely electrical conductivity (σ), Hall Effect (RH), bulk carrier concentration (n_b), sheet carrier concentration (n_S), mobility (μ) and specific resistivity (ρ)have been measured for the ternary system $Bi_2Te_{2.8}Se_{0.2}$as function of current intensity.

RH measurement indicates p-type conduction. The results were analyzed in order to establish the conduction mechanism in these compounds. The aim of our researches is to characterize transport properties and to detect the possibility of using these materials in thermoelectric devices.

ACKNOWLEDGEMENTS

Authorswish to thankProfessorAcademician Pantelija Nikolić† on bigandselflesseffortsandassistance in allstagesofinvestigations. As wellauthorswish to thank Stevan Vujatović†, a specializedtechnician as well as Dr Ljiljana Živanovfullprofessor at the Department ofElectronics, Department ofEnergy, ElectronicsandTelecommunications from theFacultyofTechnicalSciences (FTN), Universityof Novi Sad andprofessorDr Milan Radovanović, researchassociate, to helpwiththeHallexperiment.

This work was financially supported by the Ministry of Education, Science and Technological Development of the Republic of Serbia, Grant No. 451-03-9/2021-14/ 200052.

REFERENCES

[1] H. B. T. Goldsmid, Materials, 7 (2014) 2577 - 2592.
[2] G. J. Snyder, E. S.Toberer, Nat. Mater., 7 (2008), 9 - 114.
[3] Y. Yuan,W. Zhan,O.Cojocaru-Mirédin,Z. Bin,W. Xiao-Yu,G. Na,H.Zhong-Yue,Z.Fang-Qiu,Scientific Reports, 2463 (7) (2017) 1 - 10.
[4] D. Liu, J.Stoetzel,M.Seyring,M.Drüe,X. Li,R. Schmechel,M.Rettenmayr, Cryst. Growth Des. 16 (2016) 617 - 624.
[5] J. Laopaiboon, S. Pencharee, T. Seetawan, U. Patakham, B. Chayasombat, C. Thanachayanont, Mater. Lett. 141 (2015) 307 - 310.
[6] Požega, E. Sintezaikarakterizacijamonokristalabizmutaiteluradopiranihselenom, cirkonijumomiarsenom (Doktorskadisretacija), Univerzitet u Beogradu, Tehničkifakultet u Boru, Bor (2018) p. 82.
[7] L. Ivanova, Y. V. Granatkina, Inorg. Mater 36 (2000) 672 - 677.
[8] https://www.fzu.cz/~knizek/pdf/ThermoelectricMaterials.pdf
[9] E. Požega, S. Ivanov, Z. Stević, Lj. Karanović, R. Tomanec, L. Gomidželović, A. Kostov, Trans. Nonferrous Met. Soc. China 25 (2015) 3279 - 3285
[10] E. Požega, P. Nikolić, S. Bernik, L. Gomidželović, N. Labus, M. Radovanović, S. Marjanović, Synthesis and investigation of BiSbTeSe single crystal doped with Zr produced using Bridgman method, Revista de Metalurgia53 (3) (2017)

STUDY OF MICROSTRUCTURE AND THERMAL CONDUCTIVITY OF THE Ag–Bi–Sn ALLOYS

Dragan Manasijević[1], Ljubiša Balanović[1], Ivana Marković[1],Milan Gorgievski[1], Uroš Stamenković[1], Kristina Božinović[1], Duško Minić[2], Milena Premović[2]

[1]University of Belgrade,Technical Faculty inBor, V.J. 12, 19210 Bor, Serbia

[2]University of Priština, Faculty of Technical Science, KnezaMiloša, 7, 4000 Kosovska Mitrovica, Serbia

Abstract

Five Ag–Bi–Sn ternary alloys with changeable tin concentration ranging from 12.8 to 75.1 mass% and nearly equal mass contents of silver and bismuth were investigated in this study. Microstructures of as-solidified alloy samples were examined using scanning electron microscopy with energy dispersive X-ray spectrometry (SEM-EDS) The observed microconstituents were Ag_3Sn and (Bi) phases as well as ternary (Sn)+(Bi)+Ag_3Sn eutectic. The flash method was used for thermal diffusivity measurements in the temperature range from 25 to 100 °C. Based on the measured values of thermal diffusivity, thermal conductivity of the solid Ag–Bi–Sn alloys was obtained. Thermal conductivity of the studied Ag–Bi–Sn ternary alloys considerably increases with increasing tin concentration and slightly decreases with increasing temperature.

***Keywords**: Ag–Bi–Sn alloys, microstructure, ternary eutectic, thermal conductivity*

1. INTRODUCTION

In the past few decades, Pb-free solders have made great development and several main kinds of Sn-based lead-free solders such as Sn-Ag, Sn-Zn, Sn-Bi, Sn-Cu, and Sn-Ag-Cu have been extensively studied [1-4]. In the majority of cases, there is still no universal Pb-free alternative and the selection of the soldering alloy is based on specific requirements of an application [4]. The ternary Sn–Bi–Ag alloys have been recognized to be important lead-free solder materials [3]. The Sn–35Bi–1Ag alloy is especially attractive because it has a melting point (178 °C) close to the traditional Sn–Pb eutectic solder (183 °C), excellent mechanical property and wettability [3].

The aim of the present study is to investigate relations between chemical composition, microstructure and thermal properties of the Ag–Bi–Sn alloys. For this purpose, five Ag–Bi–Sn alloys from a wide composition range were prepared by induction melting of pure Ag, Bi and Sn and characterized using several experimental techniques.Microstructure, phase morphologyand thermal properties of the Ag–Bi–Sn alloys were examined. Microstructure of the samples was analyzed by SEM-EDS technique. Thermal diffusivity and thermal conductivity of the investigated alloys were determined by means of xenon-flash technique in the temperature range from 25 to 100 °C.

2. EXPERIMENTAL

All investigated alloy samples were prepared from Ag, Bi, and Sn (99.99 mass% purity) in an induction furnace under high-purity argon atmosphere. The average masses of the prepared ingots were about 5 g. The average loss of mass during melting of the samples was about 1 mass%. The microstructure was analyzed using scanning electron microscopy (SEM) in the backscattered electron (BSE) imaging mode using a TESCAN VEGA3 scanning electron microscope. The energy dispersive X-ray spectrometry (EDS) (Oxford Instruments X-act) was

employed for measurements of overall compositions and compositions of individual phases and the analysis was carried out with an accelerating voltage of 20 kV. The analyzed samples were prepared by classic metallographic procedure by polishing the specimens with diamond pastes without etching. The flash method was applied for determination of thermal diffusivity and thermal conductivity. This method was established by Parker et al. [5]. A xenon lamp (xenon-flash method) supplies an energy pulse to the front face of a thin disk specimen, and the temperature at the rear face is automatically recorded as a function of time. The thermal diffusivity is then determined according to the following equation suggested by Parker et al. [5]:

$$\alpha = \frac{1.37L^2}{\pi^2 t_{1/2}} = 0.1388\frac{L^2}{t_{1/2}} \quad \ldots(1)$$

Thermal diffusivity was measured using Discovery Xenon Flash (DXF-500) instrument over a range of temperatures from 25 to 100 °C. The Ag-Bi-Sn samples (12.6 mm in diameter and 2 mm thick with plane-parallel ground end faces) were placed in a vacuum furnace and heated at a constant rate of 10 °Cmin^{-1} to a measurement temperature. When the furnace temperature was sufficiently stable, the front surface of the specimen was heated by an energy pulse from the xenon lamp. Temperatures of the rear face of the samples were observed using the nitrogen-cooled IR detector (InSb sensor).

After the measurements of thermal diffusivity, thermal conductivity of the investigated samples was determined using the following fundamental relationship:

$$\lambda = \alpha \cdot \rho \cdot Cp \quad \ldots(2)$$

where λ is thermal conductivity (Wm^{-1}K^{-1}), α is thermal diffusivity (m^{2}s^{-1}), ρ is density (kgm^{-3}), and Cp is specific heat capacity (Jg^{-1}K^{-1}).

3. RESULTS AND DISCUSSION

3.1. Microstructure observation

The samples were characterized by SEM-EDS technique to examine microstructures, identify the microconstituents, and to measure their composition. The EDS data was acquired using area and point analysis. Firstly, the overall compositions of the alloy samples were determined by analyzing an as large as possible part of their surface. In order to determine the compositions of coexisting phases, each observed phase was analyzed at at least five different regions of the sample. Overall results of SEM-EDS analysis are given in Table 1. Examples of the microstructures are shown in Fig. 1.

Table 1 – Results of SEM-EDS analysis

Sample / mass%	Microstructure	Identified microconstituents	Composition/mass%		
			Ag	Bi	Sn
44.3Ag-42.9Bi-12.8Sn	Equiaxed Ag_3Sn grains in the (Bi) base	Ag_3Sn	75.4	2.2	22.4
		(Bi)	-	98.5	1.5
34.0Ag-33.4Bi-32.6Sn	Equiaxed Ag_3Sn grains, (Bi) dendrites and eutectic (Sn)+(Bi)+Ag_3Sn in the interdendritic regions	Ag_3Sn	75.1	-	24.9
		(Bi)	-	100.0	-
		(Sn)+(Bi)+Ag_3Sn eutectic	2.3	30.7	67.0
22.5Ag-23.9Bi-53.6Sn	Ag_3Sn and (Bi) dendrites and eutectic (Sn)+(Bi)+Ag_3Sn in the interdendritic regions	Ag_3Sn	75.2		24.8
		(Bi)	-	99.0	1.0
		(Sn)+(Bi)+Ag_3Sn eutectic	2.2	24.4	73.4
19.7Ag-18.5Bi-61.8Sn	Ag_3Sn and (Bi) dendrites with eutectic (Sn)+(Bi)+Ag_3Sn in the base	Ag_3Sn	75.6	-	24.4
		(Bi)	-	98.5	1.5
		(Sn)+(Bi)+Ag_3Sn eutectic	2.3	20.3	77.4
12.0Ag-12.9Bi-75.1Sn	Ag_3Sn and (Bi) dendrites with eutectic (Sn)+(Bi)+Ag_3Sn in the base	Ag_3Sn	75.5	-	24.5
		(Bi)	-	98.8	1.2
		(Sn)+(Bi)+Ag_3Sn eutectic	2.6	13.9	83.5

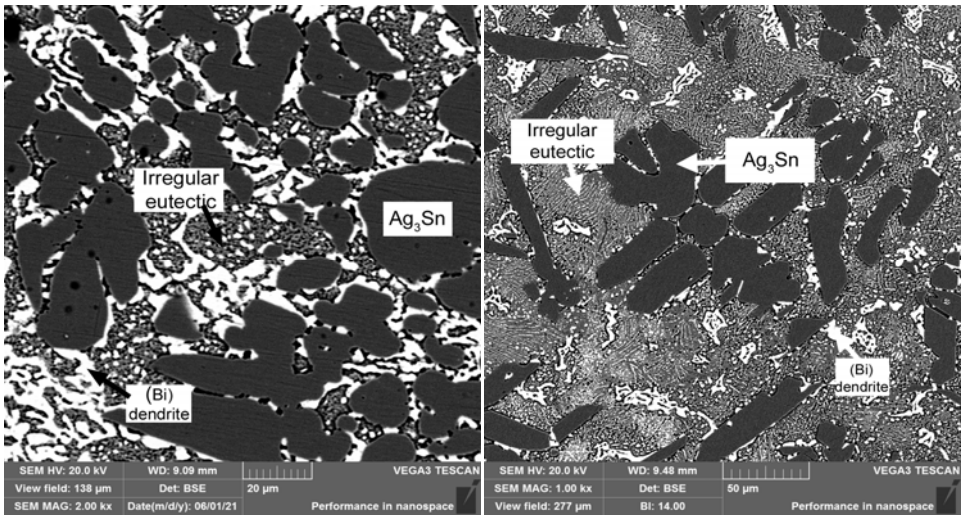

(a) (b)

Figure 1. SEM image: (a) 34.0Ag-33.4Bi-32.6Sn alloy; (b)22.5Ag-23.9Bi-53.6Sn alloy

3.2. Thermal conductivity measurements

The obtained values of density, thermal diffusivity, specific heat capacity and thermal conductivity for the solid Ag-Bi-Sn alloys in the temperature range from 25 to 100 °C are given in Table 2.Alloys densities were determined by using a buoyancy method based on the Archimedes' principle. Specific heat capacities of the studied alloys were calculated using thermodynamic parameters from [6]. The uncertainty for the thermal diffusivity measurements is ± 3% [4]. The total uncertainty for the thermal conductivity is estimated to be ± 6% [4].

4. CONCLUSION

The main conclusions of the present study may be summarized as follows:

The microstructure of studied alloys includes grains of Ag_3Sn and (Bi) phasesand ternary eutectic mixture of (Sn) Ag_3Sn and (Bi) phases.Density decreases and specific heat capacity

increases with increasing Sn content. Thermal diffusivity and conductivity monotonically increase with increasing Sn content and slightly decrease with increasing temperature.

Table 2 – Density, specific heat capacity, thermal diffusivity, and thermal conductivity of the investigated Ag–Bi–Sn alloys in the temperature range 25-100 °C

Alloy /mass%	Temperature /°C	Density/ gcm^{-3}	Calculated specific heat capacity /$Jg^{-1}K^{-1}$	Measured thermal diffusivity /mm^2s^{-1}	Thermal conductivity /$Wm^{-1}K^{-1}$
44.3Ag-42.9Bi-12.8Sn	25	9.73	0.183	8.00	14.24
	50	9.73	0.185	7.83	14.09
	100	9.73	0.187	7.65	13.92
34.0Ag-33.4Bi-32.6Sn	25	9.03	0.192	16.50	28.61
	50	9.03	0.194	16.23	28.43
	100	9.03	0.199	15.69	28.19
22.5Ag-23.9Bi-53.6Sn	25	8.19	0.201	25.86	42.57
	50	8.19	0.204	24.47	40.88
	100	8.19	0.21	23.43	40.3
19.7Ag-18.5Bi-61.8Sn	25	8.01	0.207	25.9	42.94
	50	8.01	0.211	24.80	41.91
	100	8.01	0.216	23.22	40.17
12.0Ag-12.9Bi-75.1Sn	25	7.73	0.213	27.80	45.77
	50	7.73	0.217	26.69	44.77
	100	7.73	0.223	24.89	42.91

ACKNOWLEDGEMENTS

The research presented in this paper was done with the financial support of the Ministry of Education, Science and Technological Development of the Republic of Serbia, within the funding of the scientific research work at the University of Belgrade, Technical Faculty in Bor, according to the contract with registration number 451-03-9/2021-14/200131.

REFERENCES

[1] F. Yang, L. Zhang, Z.Q. Liu, S.J. Zhong, J. Ma, L. Bao, Adv. Mater. Sci. Eng, (2016) Article ID 9265195.
[2] H.R. Kotadia, P.D. Howes, S.H. Mannan, Microelectron. Reliab. 54(6–7) (2014) 1253–1273.
[3] Y. Li, Z. Wang, X. Li, M. Lei, J. Mater. Sci. Mater. Electron,31 (2020) 4224–4236
[4] D. Manasijević, Lj. Balanović, I. Marković, M. Gorgievski, U. Stamenković, A. Đorđević, D. Minić, V. Ćosović, Solid State Sci., 119 (2021) 106685.
[5] W.J. Parker, R.J. Jenkins, C.P. Butler, G.L. Abbott, J. Appl. Phys. 32 (9)(1961) 1679-1684.
[6] L. A. Zabdyr, G. Garzeł, Calphad, 33 (2009) 187-191.

THE INFLUENCE OF THE PARTICLE SIZE ON CRYSTALLIZATION OF GLASS POWDERS FROM THE SYSTEM Li_2O-Al_2O_3-GeO_2-P_2O_5

Vladimir S. Topalović[1],Srđan D. Matijašević[1], Snežana R. Grujić[2], Jovica N. Stojanović[1], Jelena D. Nikolić[1],Veljko V.Savić[1], SnežanaN. Zildžović[1]

[1]Institute for the Technology of Nuclear and other Mineral Raw Materials, 86 Franchetd'Esperey St, 11000 Belgrade, Serbia

[2]Faculty of Technology and Metallurgy, University of Belgrade, Karnegijeva 4, 11000Belgrade, Serbia

Abstract

The glass was prepared by standard melt-quenching technique.The crystallization of powder glass from the system Li_2O-Al_2O_3-GeO_2-P_2O_5 was studied. The investigations were performed under non-isothermal and isothermal conditions using the DTA and XRD methods. The results showed that the glass crystallize by primary crystallization. As a primary phase the $LiGe_2(PO_4)_3$ is formed. The influence of particle size of the glass powder samples in the range 0-1 mm on the temperature of the DTA crystallization peak, T_p, the peak height $(\delta T)_p$ and the parameter $T_p^2/(\Delta T)_p$ was studied. It was indicated that for the particle size in the range 0.05-0.4 mm, surface and volume crystallization are significant, while for the particle size >0.4 mm the volume crystallization is dominant.

***Keywords**: particle size, glass crystallization, surface and volume crystallization*

1. INTRODUCTION

The studies of crystallization of Li_2O-Al_2O_3-GeO_2-P_2O_5 glasses showed that the $LiGe_2(PO_4)_3$ phase which belongs to the solid electrolyte is formed.This type of solid electrolyte generally crystallize in rombohedral R3-c(167) space group related to open structures and the monovalent Li^+cation can easily migrate in lattice with low activation energy [1,2]. The crystal structure of $LiGe_2(PO_4)_3$ consists of a three-dimensional framework of corner-shared GeO_6octahedra, LiO_6octahedra and PO_4tetrahedra. The basic unit of the framework consists of two GeO_6octahedra and three PO_4tetrahedrashare oxygen atoms corresponding to $[Ge_2(PO_4)]_3$. Both units are linked by their corners to form a three-dimensional network structure and this structure results in cavities where lithium ions reside and in bottlenecks in which they pass through [3].
This family of the crystalline phosphates are often referred to as "NASICONs" (acronym for "Na-Super Ionic Conductors") although they don't contain Na^+ ion [4]. NASICON-type materials are potential candidates as the solid electrolytes for utilization in high energy density batteries, sensors, displays, low expansion ceramics, thermal-shock-resistantmaterials,electrochemical devices and nuclear waste disposals[5, 6].

$LiGe_2(PO_4)_3$ can be synthesized by conventional ceramic method, glass-ceramics method, solution-sol-gel method or hydrothermal method. In comparison with the sintered materials, glass-ceramics have much advantage because they can be easily manufactured into desired size or shape and have dense microstructure. Therefore, it is significant to understand the process crystallization of these glasses.

In the present paper the mechanism and influence of the particle size on crystallization of germanophosphate glass under nonisothermal conditions was studied.

2. EXPERIMENTAL

The glass was prepared by melting a homogeneous mixture of reagent-grade Li_2CO_3, Al_2O_3, GeO_2 and $(NH_4)_2HPO_4$ in a covered platinum crucible. The components were thoroughly mixed together and heated stepwise up to 300°C to remove volatile substances.The melting was performed in an electric furnace BLF 17/3 at T=1400 °C during t=0.5 h. The melt was cast and cooled between two steel plates. The chemical analysis was performed using spectrophotometer AAS PERKIN ELMER Analyst 300.The experiments under non-isothermal conditions were performed using a Netzsch STA 409 EP device and Al_2O_3 powder as the reference material. Powder samples of the following granulations were prepared: <0.048; 0.048-0.063; 0.063-0.1; 0.1-0.2; 0.2-0.3; 0.3-0.4; 0.4-0.5; 0.5-0.65; 0.65-0.83 and 0.83-1.0 mm. The glass powders were prepared by crushing of bulk glass in an agate mortar and sieving it to appropriate grain size. In the experiments, a constant weight (m=100 mg) of the samples was heated at heating rate β=10 °C/min to T=800 °C. The experiments with bulk glass samples were performed in a one-stage regime. The samples were heated at heating rate β = 10 °C/min up to the chosen crystallization temperature at which they were maintained over 100 h in an electric furnace Carbolite CWF 13/13, with automatic regulation and temperature accuracy of ± 1°C. Finally, the samples were removed from the furnace and then crushed into an agate mortar. Powdered samples were used for XRD analysis.

The XRD method was used to determine the phase composition and the XRD patterns were obtained by using a Philips PW-1710 automated diffractometer. The XRD measurements were performed at room temperature in a stationary sample holder.

3. RESULTS AND DISCUSSION

The results of the chemical analysis show that a glass composition of $22.5Li_2O{\cdot}10Al_2O_3{\cdot}30GeO_2{\cdot}37.5P_2O_5$ (mol%) was obtained. In Fig. 1 the DTA curve of glass sample particle sizes of < 0.048 mm and 0.83-1 mm, recorded at heating rate of β=10 °C/min in the temperature range T=20-800 °C is shown.

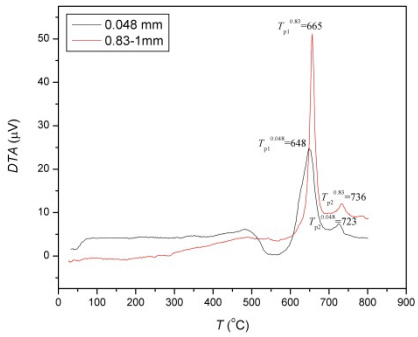

Figure 1. DTA curves recorded at a heating rate of β=10 °C/min for powder sample particle sizes: a) <0.048 mm and b) 0.83-1 mm

As can be seen in Fig. 1, two exothermal temperature peaks for both curves were registered. The higher peaks appeared at lower temperatures (T_{p1}). Also, only the peaks height is changed while their positions do not change markedly by increasing of the glass particle size. Similar peaks behavior was registered for all glass samples studied.

In order to identify the formed crystalline phases at the temperatures corresponding to peak T_{p1} and T_{p2}, the experiments under isothermal conditions were performed with bulk samples. In a one-step regime, the samples were heated at crystallization temperatures from DTA analysis.Powder X-ray diffraction (XRD) analysis confirmed the quenched melts to be vitreous.

The samples were transparent, without visible residual gas bubbles. XRD analyses revealed that at DTA peak 1 the $LiGe_2(PO_4)_3$ phase is formed with quantity of 97.6 %, and at DTA peak 2 the secondary phase GeO_2 with quantity of 2.4% appeared (figure not shown).

The glasses generally crystallize by either surface or volume mechanism. Although, both crystallization mechanisms can occur simultaneously and competitively, one mechanism usually dominates. The one of the procedure convenient for evaluating the dominant crystallization mechanism of glass powder is differential thermal analysis (DTA)[7]. Experimental and theoretical studies have shown that the particle size of glass powder influences the mechanism of its crystallization[8, 9]. In Fig. 2, the effects of particle size on the exothermal DTA peak temperatures, T_p, for all samples are presented.It can be seen (Fig.2) that the resistance to crystallization of the tested glass increases with the increase of the glass powder size, passing through the maximum for the sample of the largest granulation.

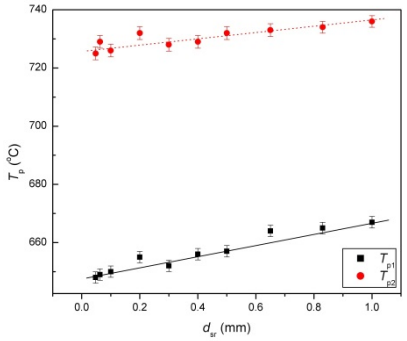

Figure2. The Effect of particle size on DTA exothermal peak temperatures T_p

The parameters of $T_p^2/(\Delta T)_p$ and $(\delta T)_p$ show the dependency on particle size and can be used as qualitative measure for the polymorphic as well as the primary surface and volume crystallization. The ratio $T_p^2/(\Delta T)_p$, where T_p is the DTA peak temperature and $(\Delta T)_p$ is the half-width of the DTA peak is related to the dimension of crystal growth. The height of the exothermal DTA peak $(\delta T)_p$ is proportional to total number of nuclei (volume and surface) contained in the glass particle. If surface and volume crystallization proceed simultaneously, three distinct regions can be distinguished as a function of particle size. They reflect the behavior arising from decreasing of surface-to-volume ratio with the increase of particle size.

The results of the influence of particle size on the ratio $T_p^2/(\Delta T)_p$ and DTA peak height $(\delta T)_p$ for peak 1 are shown in Fig. 3.

As can be observed from Fig. 3 (peak 1), the curves with two distinguishable regions were obtained. The ratio $T_p^2/(\Delta T)_p$ and $(\delta T)_p$ have a lowest values for average particle size <0.050 mm.Theoretically, for lowest particle size the surface crystallization can be favorable.

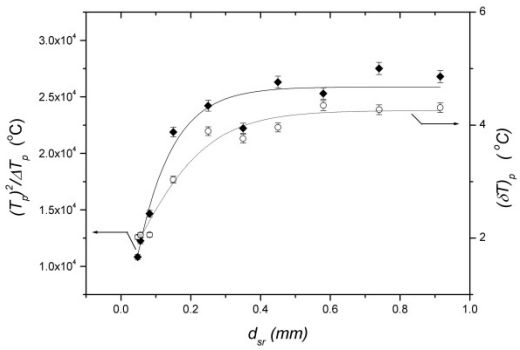

Figure3. The effect of particle size on $T_p^2/(\Delta T)_p$ and $(\delta T)_p$ for peak 1

Practically, only for this glass grain size the number of surface nuclei was comparable with volume oneand the total number of the present nuclei are smallest. In the particle size range of 0.05-0.4 mm, the both parameters increased to asymptotic values. In this case, with increasing particle size, the ratio of volume to surface nuclei increased as the number of volume nuclei increases with respect to the number of surface nuclei. Both mechanisms of crystallization are present also in this range. In the grain size range >0.4 mm, both parameters remain approximately constant. In this case, the number of volume nuclei dominates in the total number of nuclei and hence, the volume crystallization mechanism prevails. When the number of volume nuclei becomes dominant, a further increase in particle size does not significantly influence the change in the volume nuclei or the total number of nuclei.

4. CONCLUSION

The effect of particle sizeon crystallizationof the $22.5Li_2O{\cdot}10Al_2O_3{\cdot}30GeO_2{\cdot}37.5P_2O_5$ (mol%) glass powders was studied. The results showed the primary crystallization of this glass. A NASICON type material $LiGe_2(PO_4)_3$ was formed as the stable primary phase.

The effect of particle size of glass on the crystallization mechanism was analyzed. For particle size in the range 0.05-0.4 mm both surface and volume crystallization are significant, while for particle size >0.4 mm volume crystallization is dominant.

ACKNOWLEDGEMENTS

The authors are grateful to the Ministry of Education, Science and Technological Development of the Republic of Serbia for the financial support (grant contract No.: 451-03-9/2021-14/200023 and 451-03-68/2021-14/200135).

REFERENCES

[1] F.Zheng, M. Kotobuki, S.Song, M. O.Lai, L .Lu, *J. Power Sources*, **389** (2018) 198-213.
[2] P.P.Kumar, S.Yashonati, J.Chem.Sci. 118 (2006) 135-154.
[3] J. D. Nikolić, S. V. Smiljanjić, S. D. Matijašević, V. D. Živanović, M. B. Tošič, S. R. Grujić, J. N. Stojanović, Process. Appl. Ceram., 7 (4) (2013) 147-151.
[4] N.Anantharamulu, K.K.Rao, G.Rambabu, B.V.Kumar, V.Radha, M.Vithal, J.Mater.Sci. 46 (2011) 2821-2837.
[5] K.Arbi, M.Ayadi-Trabelsi, J.Sanz, J.Mater.Chem., 12 (2002) 2985-2990.
[6] J. A. Dias,S. H. Santagneli, Y. Messaddeq, J. Phys. Chem. C, 124 (2020) 26518-26539.
[7] C.S.Ray,Q.Yang, W.Haung and D.E.Day, J.Am.Ceram.Soc. 79 (1996) 3155-3160.
[8] S. D. Matijašević, S. R. Grujić, V. S. Topalović, J. D. Nikolić, S. V. Smiljanić, N. J. Labus, V. V. Savić, Sci. Sinter., 50 (2) (2018) 193-203.
[9] P. Svoboda, J. Malek, J. Non-Cryst. Solids, 358 (2012) 276-284.

The 52nd International October Conference on Mining and Metallurgy
November 29th – 30th, 2021
www.ioc.tfbor.bg.ac.rs

TECHNOLOGIES FOR PHYSICAL TREATMENT OF WATER CONTAINING SELENIUM: A REVIEW

Vesna Marjanović[1], Radmila Marković[1], Vesna Krstić[1, 2]

[1]Mining and Metallurgy Institute Bor,Zelenibulevar 35, 19210 Bor, Serbia

[2]University of Belgrade, Technical Faculty Bor, VJ 12, 19210 Bor, Serbia,

Abstract

This paper presents an overview of technologies for physical treatment of water containing selenium (Se) as a pollutant. Water with high content of selenium comes from the mining industry, production of pesticides and their use in agriculture, during coal combustion, etc. Physical treatment technologies include the reverse osmosis and nanofiltration. The reverse osmosis technology is applicable and the legal regulations can be met, as the concentration of Se in the final solution is less than 5 mg L^{-1}. The nanofiltration technology can be used to treat the mine wastewater that contains a low concentration of Se in the form of metals. As with the application of reverse osmosis, the legal regulations can be met.

Keywords: *selenium, wastewater, physical treatment technologies*

INTRODUCTION

Selenium in the environment is naturally present in rocks and soils in several oxidation states: as selenite, selenate, selenide, and elemental Se. It is a trace element in the natural ore deposits containing other minerals, such as heavy metal sulfides [1]. In addition to naturally occurring Se, its increase in concentration in the environment is caused by the human activities, especially mining, coal combustion, pesticide production, use in agriculture, etc. [2].

Nowadays, the industrial plants generate large amounts of various types of wastewaters that contain harmful chemicals and pollutants. Selenium is present in wastewater of the final stages of ore processing, mainly in the form of selenite (at low pH value) or selenate (at high pH value) [3].

The bio accumulative nature of Se in tissues, food and organisms has a dangerous impact and toxicity on human and animal life, so that the wastewater treatment with Se content makes it an urgent issue for the environment protection. However, the removal of Se from wastewater is a challenge because it is the result of its different solubilities, oxidation states, and the effect of other components. Thus, the identification of Se species in water systems, and adequate removal technology requires a deep understanding of its biogeochemistry and species[4].

TECHNOLOGIES FOR PHYSICAL TREATMENT

Technologies for physical treatment include the reverse osmosis (RO) and nanofiltration (NF). All these technologies are well understood and are applied to the wastewater treatment in other industries. However, with the exception of reverse osmosis, these selenium removal technologies have only been developed in the laboratory or pilot plant [4, 5].

The reverse osmosis is used to filter the contaminated water through a membrane that is impermeable to Se oxyions (Fig. 1). The process is applicable and easily adjustable, and it can be achieved that the concentration of Se in the final solution is less than <5 mg L^{-1}, which satisfies the legal regulations. The disadvantages of this process are high capital and operating costs, and the pre-treatment with coagulation/flocculation and/or ultrafiltration is required. The process

requires frequent maintenance, control and cleaning of membranes, high working pressure. Also, in some cases, the treatment of solution is required before discharge[6].

Reverse osmosis achieved the removal of selenium from mine wastewater by 98%, for an initial concentration of 0.4 mg L^{-1} in 24 hours, with the concentration in wastewater after treatment being 0.002 mg L^{-1}[7].

The nanofiltration is a potential technology for water treatment with Se content, which is performed by filtering the contaminated water through a membrane that is impermeable to Se oxyanions (selenate and selenite). This technology can be used to treat the mine water that contains a low concentration of Se in the form of metals. The low working pressure on a membrane separates on the basis of molecular size and ionic charge, which allows water to pass through the membrane, and at the same time the pollutants are separated (Fig. 1). The advantage of this technology is that the concentration of Se in the final solution can be less than <5 mg L^{-1}, which satisfies the legal regulations. The disadvantages of this process are high capital and operating costs, testing related to the effect of presence other anionic species, suspended particles and etc. Process maintenance and control costs are small [6].

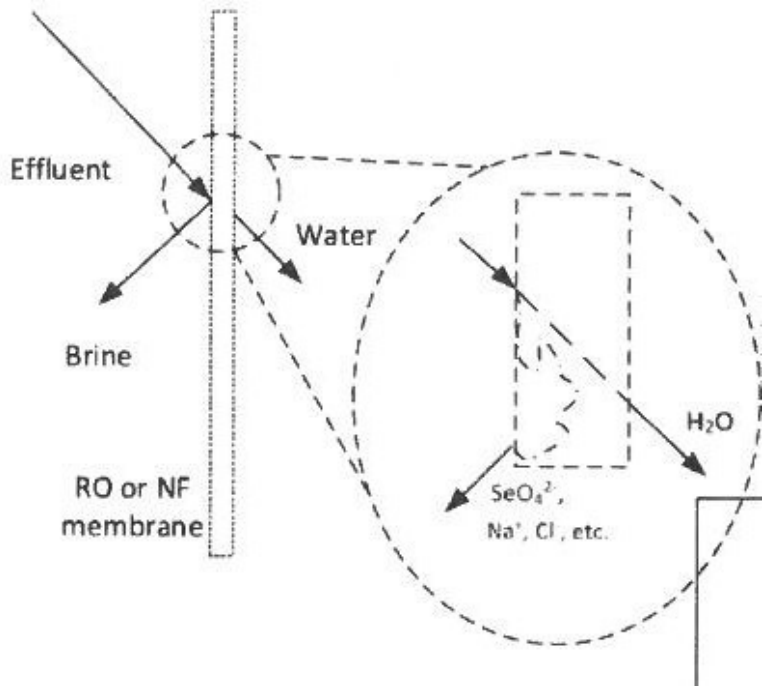

Fig. 1 *Process of membrane separation: reverse osmosis (RO) and nanofiltration (NF)*

Various types of composite membranes for nanofiltration have also been used to remove Se oxyanions. A new nanocomposite NF thin-plastic membrane containing a polyhedral oligometricsilsesquioxane in a selective layer (POSS) has been developed, which is in the form of such a thin-film [8]. For an initial selenite and selenate concentration of 1000 ppm, the removal percentage was 93.9% and 96.5% SeO_3^{2-} and SeO_4^{2-}, respectively. Also, a thin film composite membrane (TFC) consisting of zwitterionic water-soluble copolymer (P [MPC-co-AEMA]) was developed, which improved the removal efficiency to 98.2% and 99.1%, for SeO_3^{2-} and SeO_4^{2-}, respectively[9, 10, 11].

CONCLUSION

From the above results it can be concluded that NF is mainly applied only to synthetic waters, however, studies have shown that NF has the potential to remove both selenates and selenites above94%. RO and NF result in almost the same range of removal efficiencies, but RO achieved it in a significantly lower time interval (<24 h). Ceramic micropore filtration is a new technique that offers good low-cost removal efficiency, but a good assessment needs to be done for complex systems such as industrial water. This technique requires a longer removal time (> 48 h). Although RO and NF achieve high removal efficiencies, the number of studies to remove Se from wastewater has decreased significantly in recent decades. This could be due to the high operating costs and maintenance costs of the membranes, which forced the industry to focus on other treatments for effective removal. However, the potential replacement of membrane materials with natural organic fiber materials, as well as the reuse of NF membranes can help solve these problems, but operating and maintenance costs will not change significantly.

ACKNOWLEDGMENTS

Financial support for this study was partly provided by the Ministry of Education, Science and Technological Development of the Republic of Serbia (Contract No. 451-03-9/2021-14/200052).

REFERENCES

[1] Khamkhash, A., Srivastava, V., Ghosh, T., Akdogan, G., Ganguli, R., & Aggarwal, S. (2017). Mining-Related Selenium Contamination in Alaska, and the State of Current Knowledge. Minerals, 7(3), 1–13. https://doi.org/10.3390/min7030046

[2] He, Y., Xiang, Y., Zhou, Y., Yang, Y., Zhang, J., Huang, H., Shang, C., Luo, L., Gao, J., & Tang, L. (2018). Selenium Contamination, Consequences and Remediation Techniques in Water and Soils: A Review. Environmental Research, 164(February), 288–301. https://doi.org/10.1016/j.envres.2018.02.037

[3] Noreen, S., Mustafa, G., Ibrahim, S. M., Naz, S., Iqbal, M., Yaseen, M., Javed, T., & Nisar, J. (2020). Iron Oxide (Fe2O3) Prepared via Green Route and Adsorption Efficiency Evaluation for an Anionic Dye: Kinetics, Isotherms and Thermodynamics Studies. Journal of Materials Research and Technology, 9(3), 4206–4217. https://doi.org/10.1016/j.jmrt.2020.02.047

[4] Holmes, A. B., & Gu, F. X. (2016). Emerging Nanomaterials for the Application of Selenium Removal for Wastewater Treatment. Environmental Science: Nano, 3(5), 982–996. https://doi.org/10.1039/c6en00144k

[5] Etteieb, S., Magdouli, S., Zolfaghari, M., & Brar, S. K. (2020). Monitoring and Analysis of Selenium as an Emerging Contaminant in Mining Industry: A Critical Review. Science of the Total Environment, 698, 134339. https://doi.org/10.1016/j.scitotenv.2019.134339

[6] Richards, L. A., Richards, B. S., & Schäfer, A. I. (2011). Renewable energy powered membrane technology: Salt and Inorganic Contaminant Removal by Nanofiltration/Reverse Osmosis.Jour nal of Membrane Science, 369(1–2), 188–195. https://doi.org/10.1016/j.memsci.2010.11.069

[7] Man, M., Yin, X., Zhou, Z., Sparrow, B., Susie, L., & Frank, M. (2016). Extreme recovery membrane process and Zero Liquid Discharge low temperature crystallization for treating scaling mine waters. Annual Meeting of the International Mine-Water-Association (IMWA), 836–843.

[8] He, Yingran, Tang, Y. P., & Chung, T. S. (2016). Concurrent removal of selenium and arsenic from water using polyhedral oligomeric silsesquioxane (POSS)-polyamide thin-film nanocomposite nanofiltration membranes. Industrial and Engineering Chemistry

Research, 55(50), 12929–12938. https://doi.org/10.1021/acs.iecr.6b04272

[9] He, Yangzhuo, Xiang, Y., Zhou, Y., Yang, Y., Zhang, J., Huang, H., Shang, C., Luo, L., Gao, J., & Tang, L. (2018). Selenium contamination, consequences and remediation techniques in water and soils: A review. Environmental Research, 164(February), 288–301. https://doi.org/10.1016/j.envres.2018.02.037

[10] He, Yingran, Liu, J., Han, G., & Chung, T. S. (2018). Novel thin-film composite nanofiltration membranes consisting of a zwitterionic co-polymer for selenium and arsenic removal. Journal of Membrane Science, 555(February), 299–306. https://doi.org/10.1016/j.memsci.2018.03.055

[11] He, Yingran, Zhao, D. L., & Chung, T. S. (2018). Na+ functionalized carbon quantum dot incorporated thin-film nanocomposite membranes for selenium and arsenic removal. Journal of Membrane Science, 564(June), 483–491. https://doi.org/10.1016/j.memsci.2018.07.031

TECHNOLOGIES FOR BIOLOGICAL TREATMENT OF WATER CONTAINING SELENIUM: A REVIEW

Vesna Marjanović[1], Radmila Marković[1], Vesna Krstić[1, 2]

[1]Mining and Metallurgy Institute Bor,Zelenibulevar 35, 19210 Bor, Serbia

[2]University of Belgrade, Technical Faculty Bor, VJ 12, 19210 Bor, Serbia,

Abstract

Selenium (Se) is an important trace element for many organisms, including humans, but is bioaccumulative and toxic at higher levels than homeostatic. Selenium deficiency and toxicity are problems worldwide. The mines, coal-fired power plants, oil refineries and agriculture are important examples of anthropogenic sources, generation of polluted water and wastewater. Due to the harmfulness to the human health and ecotoxicity, the concentration of selenium in drinking water and wastewater must be controlled. This paper provides an overview of biological treatment technologies for the removal of selenium from water.

Keywords: *Selenium bioreduction, Bioreactors, Selenium pollution, Selenium wastewaters*

1. INTRODUCTION

The biological treatment technologies such as: biological reduction using microorganisms, usageof the UASB bioreactors (up-flow anaerobic sludge blanket bioreactor), GE's ABMet (Advanced Biological Metals Removal) technology and others have proven to be attractive and economical methods[1,19]. The choice of method depends on the specific situation and required quality of purified water (Se and other parameters). It is also important that during water treatment, not only selenium but also other parameters must be in accordance with increasingly strict legislation. This is generally achieved by combining the different treatment techniques and phases, which includes the pre-treatment as needed.

2. TECHNOLOGIES OF BIOLOGICAL TREATMENT

Biological reduction by microorganisms has emerged as a relevant and economical method, which can provide the purified water with a few mg of L^{-1} selenium. Bacteria used to reduce selenates and selenites are the terminal electron acceptors during cellular respiration. These methods are based on the natural ability of bacteria, fungi and algae for the methylation process of Se, and its conversion into gaseous forms. These methods are attractive, cheap and environmentally friendly, because few chemicals are used in the treatment. The advantages of these methods are the low price of maintenance costs, and possibility of in-situ application, and disadvantages are: adjustment of environmental parameters (pH, temperature and co-factors); it is necessary to provide the excess of nutrients; it is necessary to separate the plant species and water; long residence time of wastewater; insufficient efficiency of selenium removal[2,3].

The chemical and physical similarity between selenium (Se) and sulfur (S) shows that these two elements have common metabolic pathways in plants. The presence of compounds Se and S indicates that these elements take part in the biochemical processes that affect the uptake, transfer and assimilation during plant development. However, based on small but crucial differences in reactivity and other metabolic interactions, it is concluded that some biochemical processes involving Se may be excluded from those related to S. The such approaches may help in the future application of genetically engineered on the plants with ability forSeaccumulation regarding to the environmental protection [4].

Indian mustard (*Brassica juncea L.*) accumulates high concentrations of Se in the plant tissues and Se volatilizes in relatively non-toxic forms, such as dimethyl-selenide. Research has shown that the presence of bacteria in a rhizosphere of Indian mustard is necessary to achieve the best rates of accumulation and volatilization of selenate from the plants [5]. The advantages of these technologies are low costs, the possibility of in-situ application, minimum need for process monitoring, possibility for treatment the large amounts of solution. The disadvantages of these processes are the long average process time and large space requirement.

A significant number of studies have focused on the identification of new bacterial species with high tolerance and reduction capacity for Se removal. It has been observed that many bacterial groups have shown great potential for selenium removal, even under aerobic conditions, e.g., *Pseudomonas moraviensis* that rapidly reduces selenite to Se (0) in aerobic media[6]. The strain was ineffective against selenate, but selenite was removed by more than 95% at 2 days at high selenite concentration.

In the case of mine wastewater, the reduction of Se by bacteria can be inhibited by increased nitrate concentrations. To overcome this problem, a combination of several strains of bacteria (*Pseudomonas-*,*Lisinibacillus*- and *Thauera*-related species) was examined to simultaneously reduce selenates and nitrates from natural wetland sediment that were affected by mine water [7]. This combination can potentially treat wastewater that contains both pollutants at the same time.

Experimental studies of bioreactors use different communities of microorganisms to treat selenium-contaminated wastewater. Biological treatments can be divided into: passive biological treatment [8], sequencing batch reactor [9], electro biochemical reactor- EBR[10], fluidized bed reactor [11], hydrogen-based membrane biofilm reactor [12], ABMet® system[19], Up-flow anaerobic sludge blanket reactor[13], combined process of zero-valent iron and selenate reducing bacterium[14], combined process of activated alumina and bioreactor [15], fungal bioreactor [16].

The UASB (up-flow anaerobic sludge blanket reactor) bioreactors work in the anaerobic conditions and it is necessary to provide nutrients for the microbiological reduction of selenite and selenate to the elemental selenium. The end product of biological reduction is the elemental selenium, a fine precipitate, slightly toxic, which is easily removed from the aqueous phase by the precipitation or reverse rinsing [17,18]. This system requires a source of carbon (such as molasses) and macronutrients necessary to maintain a healthy biomass. Biological reduction in an anaerobic reactor with a charged bed showed the most consistent results. The realized laboratory experiments with bioreactors for selenium removal from the industrial wastewater from refinery have showed that after preconditioning of these water (adjustment the pH to 7, adjustment the salinity and addition of carbon sources), the initial Se concentration that was from 1.5 to 3.6 mg L^{-1} dropped to 0.1 mg L^{-1}, 15 days after the UASB treatment [18].

The GE's ABMet (Advanced Biological Metals Removal) technology is a patented treatment system, based on the bioreduction in active filters that reduces the concentrations of nitrates, selenium and toxic metals. This technology was chosen for the wastewater treatment from the metal recycling plants, coal mines and power plants (after flue gas desulphurization) [19]. The pre-treatment, such as solids, may be required selenium removal.

The biological treatment in a wetland is an integrated system of water, plants, animals, microorganisms and the environment (soil, sun and air), where pollutants are removed by the biological reduction [3]. Clearly, the first advantages of wetlands are low capital costs, maintenance and operation costs[20]. However, several aspects limit their application: a large area land is required; a long period of time to get good results after starting work; the performances affected by different environmental conditions; monitoring the need to maintain an ecologically healthy system; uncertainty about the consistency of the results; risk of groundwater pollution; periodic disposal of accumulated material; possible impact on the reproduction of avocets that feed and nest in the wetlands [3, 20].

3. CONCLUSION

Several conventional bioreactor systems can be used to remove selenates and selenites from wastewater in the form of elemental selenium. Biological treatment has emerged as a "best practice" for Se-containing wastewater due to its advantages such as low operation costs and easier operation system, the ability to adjust capacity as needed, no problems with chemical sludge disposal, the ability to recover Se regarding to reduce the total concentration of Se ions in wastewater. One of the main advantages of microbiological decreasing of selenium is the production of biogenic selenium which has a technical application. The bioreduction of selenium oxyions by various microorganisms that occur in natural and projected environments under different operating conditions has been relatively well researched. It is also necessary to take into account the actual parameters of wastewater such as pH, temperature and volume.

ACKNOWLEDGMENTS

Financial support for this study was partly provided by the Ministry of Education, Science and Technological Development of the Republic of Serbia (Contract No. 451-03-9/2021-14/200052).

REFERENCES

[1] PAUL, T., & SAHA, N. C. (2019). Environmental Arsenic and Selenium Contamination and Approaches Towards Its Bioremediation Through the Exploration of Microbial Adaptations: A Review. *Pedosphere*, *29*(5), 554–568. https://doi.org/10.1016/S1002-0160(19)60829-5

[2] Santos, S., Ungureanu, G., Boaventura, R., & Botelho, C. (2015). Selenium contaminated waters: An overview of analytical methods, treatment options and recent advances in sorption methods. *Science of the Total Environment*, *521–522*(1), 246–260. https://doi.org/10.1016/j.scitotenv.2015.03.107

[3] CH2MHILL, 2010. Review of Available Technologies for the Removal of Selenium from water-Final Report. Prepared for North American Metals Council

[4] Sors, T. G., Ellis, D. R., & Salt, D. E. (2005). Selenium uptake, translocation, assimilation and metabolic fate in plants. *Photosynthesis Research*, *86*(3), 373–389. https://doi.org/10.1007/s11120-005-5222-9

[5] De Souza, M. P., Chu, D., Zhao, M., Zayed, A. M., Ruzin, S. E., Schichnes, D., & Terry, N. (1999). Rhizosphere bacteria enhance selenium accumulation and volatilization by indian mustard. *Plant Physiology*, *119*(2), 565–573. https://doi.org/10.1104/pp.119.2.565

[6] Staicu, L. C., Van Hullebusch, E. D., Oturan, M. A., Ackerson, C. J., & Lens, P. N. L. (2015). Removal of colloidal biogenic selenium from wastewater. *Chemosphere*, *125*, 130–138. https://doi.org/10.1016/j.chemosphere.2014.12.018

[7] Subedi, G., Taylor, J., Hatam, I., & Baldwin, S. A. (2017). Simultaneous selenate reduction and denitrification by a consortium of enriched mine site bacteria. *Chemosphere*, *183*, 536–545. https://doi.org/10.1016/j.chemosphere.2017.05.144

[8] Luek, A., Rowan, D. J., & Rasmussen, J. B. (2017). N-P Fertilization Stimulates Anaerobic

Selenium Reduction in an End-Pit Lake. *Scientific Reports*, *7*(1), 1–8. https://doi.org/10.1038/s41598-017-11095-2

[9] Kim, H. W., Hong, S. H., & Choi, H. (2020). Effect of nitrate and perchlorate on selenate reduction in a sequencing batch reactor. *Processes*, *8*(3), 1–8. https://doi.org/10.3390/pr8030344

[10] Opara, A., Peoples, M. J., Adams, D. J., & Martin, A. J. (2014). Electro-biochemical reactor (EBR) technology for selenium removal from British Columbia's coal-mining waste waters. *Minerals and Metallurgical Processing*, *31*(4), 209–214. https://doi.org/10.1007/bf03402472

[11] Performance, B. C., Envirogen, A., & Whitepaper, T. (2011). Treatment of Selenium-Containing Coal Mining Wastewater with Fluidized Bed Reactor Technology Proven Systems Provide Major Cost Advantages. *An Envirogen Technologies Whitepaper*, *August*, 1–15.

[12] Yuan, Y., Lin, H., Lin, Z., & Wang, Y. (2018). A Review of Hydrogen-Based Membrane Biofilm Reactor to Remove Oxidized Pollutants from Water. *IOP Conference Series: Materials Science and Engineering*, *392*(4). https://doi.org/10.1088/1757-899X/392/4/042031

[13] Zeng, T., Rene, E. R., Zhang, S., & Lens, P. N. L. (2019). Removal of selenate and cadmium by anaerobic granular sludge: EPS characterization and microbial community analysis. *Process Safety and Environmental Protection*, *126*, 150–159. https://doi.org/10.1016/j.psep.2019.03.039

[14] Liu, J., Taylor, J. C., & Baldwin, S. A. (2018). Removal of selenate from brine using anaerobic bacteria and zero valent iron. *Journal of Environmental Management*, *222*(January), 348–358. https://doi.org/10.1016/j.jenvman.2018.05.095

[15] Ji, Y., Li, L., Wang, Y.T., 2020. 'Selenium removal by activated alumina in batch and continuous-flow reactors'. Water Environ. Res. 92 (1), p51–59. https://doi.org/ 10.1002/wer.1159. Jin, Z., Du, X., Xu, Y., Deng

[16] Sabuda, M. C., Rosenfeld, C. E., DeJournett, T. D., Schroeder, K., Wuolo-Journey, K., & Santelli, C. M. (2020). Fungal Bioremediation of Selenium-Contaminated Industrial and Municipal Wastewaters. *Frontiers in Microbiology*, *11*(September). https://doi.org/10.3389/fmicb.2020.02105

[17] Kashiwa, M., Nishimoto, S., Takahashi, K., Ike, M., & Fujita, M. (2000). Factors affecting soluble selenium removal by a selenate-reducing bacterium Bacillus sp. SF-1. *Journal of Bioscience and Bioengineering*, *89*(6), 528–533. https://doi.org/10.1016/S1389-1723(00)80051-1

[18] Soda, S., Kashiwa, M., Kagami, T., Kuroda, M., Yamashita, M., & Ike, M. (2011). Laboratory-scale bioreactors for soluble selenium removal from selenium refinery wastewater using anaerobic sludge. *Desalination*, *279*(1–3), 433–438. https://doi.org/10.1016/j.desal.2011.06.031

[19] Sonstegard, J., Harwood, J., Pickett, T., (2007). Full scale implementation of GE ABMetbiological technology for the removal of selenium from FGD wastewaters. Proceedings of the 68th International Water Conference vol. 2, p. 580 (Orlando, Florida, USA)

[20] Water, M. (2014). to Treatment Technologies for. March, 1–94.

USAGE SPECIFICS OF GEOGRIDS

Milenko Jovanović[1], Miomir Mikić[1], Miroslava Maksimović[1], Daniel Kržanović[1], Radmilo Rajković[1], Emina Požega[1]

[1]Mining and Metallurgy Institute Bor, Zeleni bulevar 35, 19210 Bor, Serbia

ABSTRACT

Geosynthetics and their variants play a major role in soil protection whether it is a landfill, a landslide, a road route or some other surface pollution.
Geosynthetics has experienced its development in recent decades, and all products in this field can still be considered relatively new, which does not mean that they have not proven themselves in many demanding projects (fields of activity) on different occasions and requirements, especially in mining and construction and ecology.
A special part of this area refers to geogrids and geotextiles made of organic material (from nature) in combination with more commonly used synthetic materials and the main topic of this paper. By crossing (combining) these types (materials) of geogrids (geotextiles, etc.) in the form of a certain hybrid technology of making these products, we get usage parameters suitable in the field of environmental protection and the necessary mechanical and temporal usability.
This would, seemingly contradictory requirements (appropriate - usage conditions), lead to a compromise, but at the same time effective fulfillment of the same in appropriate situations.
Keywords: Geogrids, geosynthetics, geomaterials, landfills, stability

1. INTRODUCTION

Geogrids are mainly made of polymeric materials such as polyethylene, polyester and polypropylene and are characterized by high tensile strength. The original geogrids were made by drilling holes in the sheet of material. Today, such geogrids are made by the so-called extrusion process. We now have geogrids made of polyester fibers coated with polyethylene. A multitude of continuous fibers are joined into a thread, which is then woven in the longitudinal and transverse direction with a certain distance between the ribs, and the folds are additionally strengthened, and then the fibers are coated.
Geogrids (Fig. 1.) are most often used to strengthen and stabilize poorly bearing soil. In some cases, the material, the size of the fraction of which is larger than the mesh opening of the mesh, is poured on the geogrid and the material is trapped in the geogrid openings and a system resistant to external forces is formed. In addition to stabilizing and strengthening poorly bearing soil, geogrids are also used to strengthen asphalt by installing a geogrid between the layers of asphalt. In this case, it is important to mention the use of geogrid in road rehabilitation, in order to prevent the reaction of existing cracks on a new layer of asphalt. The geogrid takes over the action of forces and prevents the formation of cracks on the newly installed layer of asphalt. The third important purpose of geogrids is to protect against soil erosion. For this purpose, there are two-dimensional geogrids that have small eye openings and three-dimensional geogrids. Depending on the manufacturer, geogrids may differ, but their primary function and mode of operation are the same.
• absorb the kinetic energy of erosive elements (rain, wind) and stabilize the soil surface, creating numerous micro-dams over it,
• keeps seeds and hydrosowing materials in place, even on a steep slope of the soil, which leads to successful seed germination
• helps water penetrate through the soil and retain moisture, leading to better seed germination and good grass growth.

Figure 1. Setting up a geogrid

The use of anti-erosion geotextiles can increase and support the effect of erosion control in areas with particularly steep slopes or in substrates susceptible to erosion [1,2,7,8].

1.1. Organic geogrids

The greatest role of vegetation in the protection of slopes from erosion and its stabilization is provided when its surface enables the establishment of a given vegetation and allows water to flow at a certain speed and intensity on the surface and thus prevents the degradation of vegetative cover.

Organic geogrids have unique characteristics, consisting of biologically and chemically photo degradable natural fibers. They are designed to keep the land in place until vegetation is established.

The organic geogrid has the following roles:

• To absorb the kinetic energy of erosive elements (rain, wind)
• To facilitate the penetration of rain into the ground
• To retain moisture from rain: In addition to being eco-friendly, they can absorb water about five times the dry weight
• Allows to avoid loss or dispersion of seeds necessary for revegetation
• Provides radical establishment of plant species
• Allows control of soil temperature by mitigating its natural oscillations: so that they can mitigate extreme temperatures and create a pleasant micro-climate for vegetation growth.
• Allows to reduce the loss of soil moisture

Organic geogrids are more flexible than most types of synthetic geogrids. This allows them to easily follow the contour of the soil surface. The ability to make direct contact between the fibers and the soil, enables the reduction of soil loss by 90% or more. In addition to the above, organic geogrids act as "mulch" and thus improve the establishment of vegetation. After degradation, they do not leave any toxic material in the soil [4,6,7,8].

1.2. Synthetic geogrids

Synthetic geogrids are synthetic products (geosynthetics) used to stabilize the terrain. The polymeric nature of the products makes them suitable for use in a country where high levels of durability are required. This type of geogrid is available in a wide range of shapes and (synthetic) materials.

In difficult conditions (such as slopes with a critical angle, channels with high flow, etc.), the vegetative cover, even when it is well placed, will not be able to survive under the erosive power of water.

Therefore, for the purpose of stabilization and strengthening of the terrain, the law should define the obligation to use (install - install) geogrids or geosynthetic networks and thus increase the resistance to erosion and thus the protection of the natural environment [7].

2. EXPERIMENTAL

2.1 Choosing the right material

Geogrid manufacturers strive to make their products as cheap as possible and make them as easy to use as possible. However, it is advisable not to focus on the manufacturer, but on your immediate tasks.

• For strengthening embankments and slopes - a geopronet made of polypropylene fibers is perfect.

• Railway - It is convenient to reinforce with two axle gratings or geogrids of increased strength. Slavros or his analogues will do their job well.

• Strengthen drainage systems and prevent shoreline turbidity - use geogrids 15-30 mm high or higher.

• In road construction - biased fiberglass and polymer mesh is perfect. For example, the Slavros SD 40 geogrid is perfect for that purpose.

• Parking and parking - designed to work with constant loads. That is why high-strength polyester and fiberglass nets are used here. As an option - instead of a grate, a lawn grate can be used here.

2.2. Application of geogrids in measures of reclamation of degraded land

In Serbia, there are a large number of coal mines, quarries, clays and similar areas that, after exploitation, are left to natural reclamation - a process that is very slow, measured for decades, while in some locations it is not possible. Proper approach to reclamation implies a planned procedure, based on a database.

New materials and technologies enable significant improvements in many areas of mining and construction in the field of faster, safer, more efficient construction, insurance, maintenance and rehabilitation of mining and construction facilities, especially civil engineering, although some materials are widely used in the field of environmental protection. and building construction.

Generally speaking, within the reclamation of degraded areas, it is necessary to apply technical, bio-technical and biological measures.

Technical measures contribute to the improvement of resistant and deformable characteristics of landfills, which directly affect the increase of erosion stability of slopes.

Bio-technical measures, together with technical measures, contribute to faster achievement and maintenance of permanent stability of landfills.

Biological measures include the application of agricultural and forest reclamation, which contribute to the stability and maintenance of reclaimed areas, but are much more important from the aspect of spatial revitalization and the establishment of natural biocenoses. Horticultural species play a significant role in biological measures.

Before the formation of the landfill, the first phase of technical measures is the stabilization of the base for the future landfill and its planning, drainage or installation of drainage systems. After this phase, tailings are dumped and a landfill is formed in phases (Fig. 3) [1,2,7,8].

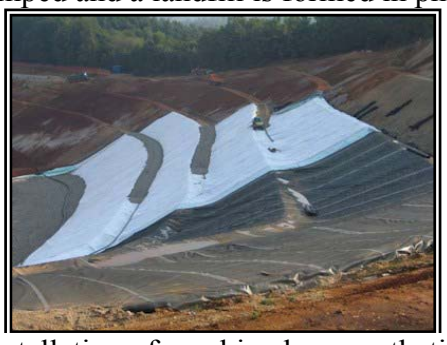

Figure 3. Installation of combined geosynthetic materials

3. CONCLUSION

Geogrids and geotextiles made of organic material (coconut, jute) are a natural and 100% biodegradable solution for erosion control using geogrids or geotextile mats made of coconut

fibers. Organic geogrids have unique characteristics, consisting of biologically and chemically photodegradable natural fibers. They are designed to keep the land in place until vegetation is established. Geogrid or permeable geotextile provides a natural system of assistance (improvement of characteristics) to the soil (soil, landfill…) and vegetation.

Due to a large number of factors that cause directly the negative effects of mining or construction works, special attention should be paid not only to the application of geogrids and other types of geosynthetics, but also to the application and selection of new materials and technologies.

The installation of these efficient systems (geogrids, geotextiles…) in various branches of economy and industry and their expediency directly depends on the materials from which they are made. The application and selection of types and materials in road construction is important because the application of these materials has an impact on savings and improvements in the field of faster, safer and more efficient construction of road construction and elements, their maintenance, as the impact on traffic safety and flow. It also refers to the protection and stabilization (strength) of the surfaces (slopes) of landfills and other mining facilities, where the choice of type and material of the cover layer depends on the deposited material, size and shape of the landfill itself [3].

As a possible saving solution in many cases, where an efficient result is required, both on the ecological and on the construction, safety, field security plan, there is a hybrid approach to the use of construction materials. Using the different types of materials in the production of geogrids or geotextiles, we can solve the seemingly contradictory requirements in their application.

Such hybrid materials, which would contain cross-beams of organic and synthetic origin, can, depending on the need (purpose) and their mutual relationship, be an "ideal compromise", that is, a saving solution. Material of organic origin would have a positive impact on the development and preservation of vegetation and the entire ecosystem, while geosynthetic materials would have the primary application of mechanical stabilization nature, as much stronger and more stable materials. In addition to the above, organic geogrids act as "mulch" and thus improve the establishment of vegetation. After degradation, they do not leave any toxic material.

It should be noted that many of the presented materials have a very wide application in the field of environmental protection, especially the prevention of groundwater and surface water pollution through infiltration control, as well as in the treatment and immobilization of various types of waste, especially hazardous waste.

Special attention in further development should be paid to the use of new natural materials and hybrid technology of geomaterials, as products of the future.

ACKNOWLEDGEMENTS

Note: This work was financially supported by the Ministry of Education, Science and Technological Development of the Republic of Serbia, Grant No. 451-03-9/2021-14/ 200052.

REFERENCES

[1] Veinović, Ž.,Kvasnička, P. (2007'): Surface landfills, Internal script, Faculty of Mining, Geology and Petroleum Engineering, University of Zagreb, Zagreb
[2] Zidar, M. (2009'): Landslide remediation methods, Faculty of Geotechnics, University of Zagreb, Varazdin
[3] MladenBogicevic - Gradjevinarstvo.rs (December 3, 2008)
[4] Dragan M. Đorđić (2016'); Investigation of deformation characteristics of nonwoven geotextile materials made of polyester and polypropylene fibers - Doctoral Dissertation.
[5] SRPS EN ISO 10318: 2015 - Geosynthetics - Terms and definitions: ISO 10318 (2015 ')
[6] Sandra Lenček; (2010'): Final paper: Application of geosynthetics in environmental management; Faculty of Geotechnics, University of Zagreb, Varaždin - k 3 6.
[7] MilenkoJovanović (June, 2019'), Study Research II (Doctoral Dissertation): "Geosynthetics - Purpose and Application (in Mining)", University of Belgrade, Technical Faculty in Bor.
[8] MilenkoJovanović (July, 2019'), Study Research III (Doctoral Dissertation):"OrganicGeogrids", University of Belgrade, Technical Faculty in Bor.

INTERMETALLIC BONDING BETWEEN A RING CARRIER AND AN ALUMINUM PISTON ALLOY

Srećko Manasijević[1], Zdenka Zovko Brodarac[2], Natalija Dolić[2], Mile Djurdjević[3], Radomir Radiša

[1]Lola Institute Ltd, KnezaVišeslava 70a, Belgrade, Serbia
[2]University of Zagreb Faculty of Metallurgy, Alejanarodnihheroja 3,Sisak, Croatia
[3]Nemak Europe, Zeppelins Trasse 24, 4020 Linz, Österreich

Abstract
This paper presents an analysis of the intermetallic bond between a ring carrier and an aluminum piston alloy. An optical microscope combined with the SEM / EDS analysis has been used to metallographically analyze the quality of the intermetallic bonding layer. The obtained results show that can be established intermetallic bond between two materials of different qualities.

***Keywords**: piston alloys, ring carrier, intermetallic bond, Ni-Resist, Al-Fin process.*

1. INTRODUCTION

Pistons are made mostly of aluminum multicomponent alloys (Al−Si−Cu−Ni−Mg), which are used in the automotive industry due to a combination of good casting and mechanical properties [1−5] high strength at elevated temperatures (up to 350 °C) [1,2] and also resistance to sudden temperature changes [1,3−5]. Depending upon the engine type and operating conditions, there are different design solutions for pistons.

This paper deals with pistons for highly-loaded diesel engines with a ring carrier. The ring carrier is specially designed to form the first piston ring groove. The ring carriers of standard features are made of austenitic cast iron (Ni-Resist) in order to increase the wear-resistance of the first ring groove, especially in engines with high loads [5−9]. Austenitic gray iron castings are used primarily for their resistance to heat, corrosion, and wear, as well as controlled expansion, temperature stability, castability, and machinability. The Ni-Resist ring groove inserts are manufactured into pistons to increase engine and piston life. In the meantime, they can also improve the air-tightness of the piston in the cylinder, increase the efficiency of combustion, reduce emissions and air pollution, and contribute to the environment.

The alfin process is a method for preparing a ferrous surface for intermetallic bonding [5−9]. The alfin bonding process is commonly used to bond a non-ferrous Al alloy and a ferrous alloy. It is well known that cast iron contains carbon as a result of the casting process[5−9]. During the piston casting, the ring carrier is soaked by the alfin bond process, which results in a strong connection with the piston material. During this process, an intermetallic layer composed of Fe_xAl_y is formed on the border between the two different materials by the diffusion of atoms[5−9].

The aim of this paper is to conduct a detailed analysis of the intermetallic bonding layer that is formed between the ring carrier and the piston.

2. EXPERIMENTAL

The tests were performed on an Ø89 mm piston for a diesel engine. A cross-section of the investigated piston casting with its macrostructure and indicated sampling point is shown in

Figure 1a. The chemical compositions of the piston alloys and ring carrier given are in Table 1. In this case, the hardness of the ring carrier is 140−150 HBS (the standard is 120−160 HBS)[5].

Table 1. Chemical composition of the experimental alloy (wt. %).

Alloy	Element/chemical composition										
AlSi13Cu4Ni2Mg	Si	Cu	Ni	Mg	Fe	Mn	Cr	Ti	Zr	V	Al
	13.05	3.80	2.01	0.90	0.52	0.19	0.09	0.07	≈0.03	≈0.01	residual
Sample of the ring carrier	Ni	Cu	C	Cr	Si	Mn					Fe
	15.10	6.32	2.81	2.21	1.89	1.23					residual

The instruction for forming connections between the ring carrier and the piston casting is a trade secret of all producers.

The melting of the alloy for piston casting was performed in a tub-like electro-resistant furnace-type RIO 750 (80 kW and a melting capacity of 120 kg/h). The preparation of the Al-alloy was performed in an electro-resistant muffler-like furnace type RIO 250 (85 kW). During preparation, the piston casting was exposed to melt-treatment processes (refining, modification, and degasification at 725±5 °C) to improve its mechanical properties. The temperature of the melt was measured using a Ni−Cr−Ni digital pyrometer.

The casting of the investigated pistons was performed on semi-automatic machines in the PDM-Serbia concern according to a predefined internal procedure by the manufacturer. After being removed from the tool, the piston castings were air-hardened (the air pressure was 4 bar). A "CER Čačak EPC 200/300" furnace with a capacity of 3,000 kg/h and a maximum temperature of 350 °C was used for the stabilization.

An optical microscope (Olympus GX51) with a magnification of up to 1,000x was used to visualize the microstructure. The samples were observed under a scanning electron microscope (SEM) using magnifications between 200x and 5,000x. Qualitative and quantitative assessments of the chemical compositions of the phases were done using an energy dispersive spectrometer (EDS).

3. RESULTS AND DISCUSSION

Figure 1 showsthemicrostructure ofthe piston cross-section, where the successfull intermetallic bond between the ring carrierand the pistonalloy is shown. The microstructure of the ring carrier is shown in the following figures: Figure 1b with a magnification of 200x; Figure 1e with a magnification of 500x; and Figure 2h shows a SEM analysis with a magnification of 2,000x. In this case, the microstructure of the ring carrier consists of lamellar graphite distribution in austenite: ASTM type A or B, size 4−6.

The thickness of the diffusion layer was measured (Figure1f). The results show that the thickness of the diffusion layer formed in the piston alloy is within the range 14.60 to 45.17 μm (the average is 31.19 μm). According to international pistons manufacturer, the thickness of the diffusion layer should be in the range between 10−70 μm [5].

In addition to characterization by optical and SEM microscopy, a qualitative analysis of the phases in the intermetallic bonding layer was conducted by EDX scanning electron microscopy.In the first step, an EDS mapping of the intermetallic bonding layer was made. In addition to the conventional SEM image, the EDX mapping provides a meaningful picture of the element distribution of a surface.

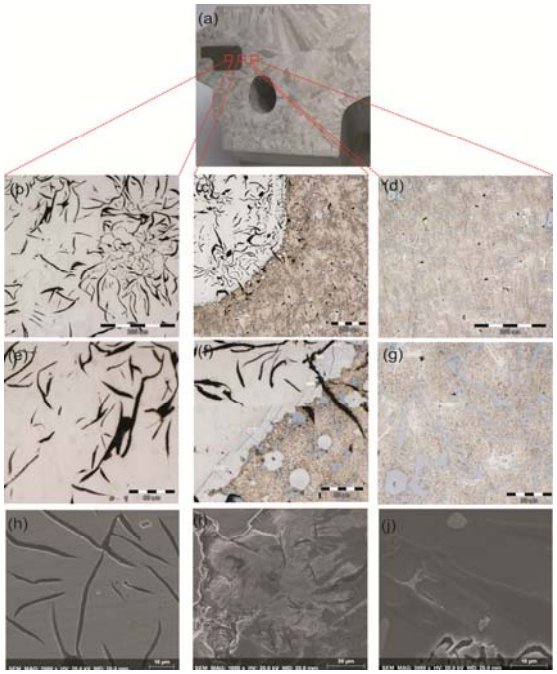

Figure1. Microstructure of the ring carrier-alfin bond-piston

The EDS mapping was done to better identify the precipitated phases. Additionally, the EDS mapping also provides useful information to predict the possible phases where the key elements show higher contrast. Figure 2a shows a SEM analysis while Figure 2b shows an EDS mapping of all the elements in the intermetallic bonding layer. Figures 2c to 2h show the EDS mapping of other important elements (Fe, C, Ni, Cu, Si and Al).

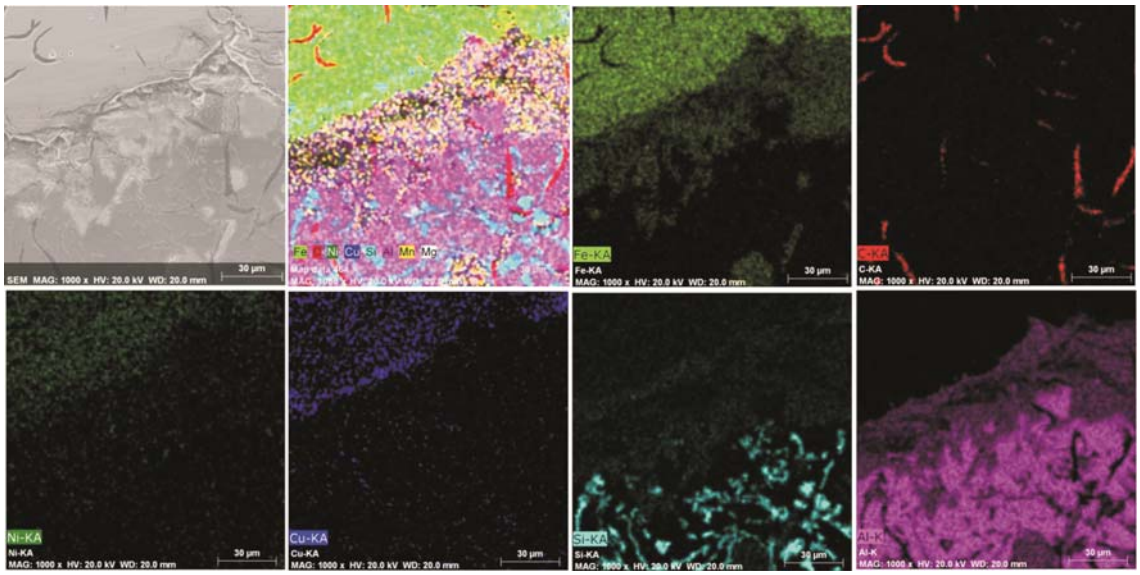

Figure2. The intermetallic bonding layer:a: SEM, 1000x; b: EDS mapping of all elements and EDS mapping; c: Fe; d: C; e: Ni; f: Cu; g: Si; and h: Al [15]

In the second step, a line EDS analysis of element distribution in the intermetallic bonding layer was made. The results of this analysis are shown in Figure 3. The point of line analysis is indicated in Figure 3a while in Figure 3b only for Al and Fe. Based on the obtained results, it can be seen that the Fe concentration decreases and that the Al concentration increases uniformly along the analyzed ring carrier-alfin bond-piston line, depending on the presence of other alloying elements (i.e., there is no discontinuity). Figure 3b shows the corresponding EDS

spectra for the phase identified in the intermetallic bonding layer. The EDX results were used to identify the stoichiometry for the particular phases based on the data reported in the literature. The alfin bond is a real bond, which has a chemical composition close to Fe_xAl_y and is formed by the Fe and Al alloy (Fig. 3d).

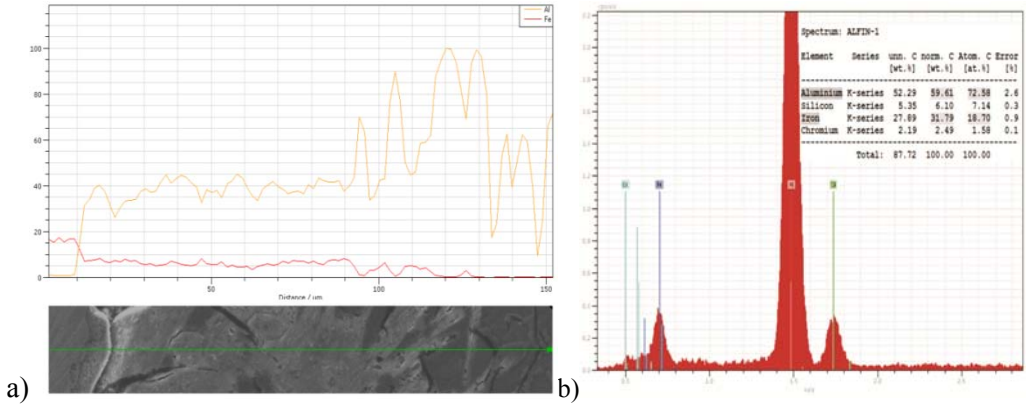

a) b)

Figure3. Analysis of the intermetallic bonding layer: a: SEM, 1000x; b: EDS analysis changes in all elements; c: EDS analysis, changes in Al and Fe; and d: EDS identification of Fe_xAl_y[15].

4. CONCLUSION

Based on the analysis of the experimental test results presented in this paper and the available data from the literature, it can be concluded that if the manufacturer's instructions defined for casting pistons with the ring carrier are applied completely, a good metal connection can be formed between the two quality materials.

The results presented in this paper are only an introduction to further, ongoing research.

REFERENCES

[1] S. Manasijevic, R. Radisa, S. Markovic, Z. Acimovic,Pavlovic, K. Raic: Intermetallics, 19 (2011) 486–492.
[2] S. Manasijevic, R. Radisa, S. Markovic, K. Raic, Z. AcimovicPavlovic: Practical Metallography, 46 (2009) 565–579.
[3] R. Gholizadeh, S.G. Shabestar: Metall. Mater. Trans. A, 42 (2011) 3447–3458.
[4] N. Belov, D. Eskin, N. Avxenieva: ActaMater.,58 (2005) 4709–4722.
[5] S. Manasijevic: Aluminum Piston Alloys,Published by the LOLA Institute Belgrade, 2012.
[6] Patent Number: 6,127,046. United States Patent. Date of Patent, Oct. 3. 2000.
[7] Patent Number: 6,112,802. United States Patent. Date of Patent, Sep. 5. 2000.
[8] A.F. Acar, F.Ozturk, M. Bayrak: Mater. Technol., 2010, vol. 44, pp. 391–395.
[9] Engine Australia Pty Ltd: Alfin (Ni-Resist) Ring groove inserts, Service Engineering Bulletin, 2012.
[10] J.C. Viala, M. Peronnet, F. Barbeau, F. Bosselet, J. Bouix: Composites Part A, 33 (2002) 1417–1420.
[11] M.C.J. Marker, B. Skolyszewska-Kühberger: Intermetallics, 19 (2011) 1919−1929.
[12] M. Willcox: Ultrasonic inspection equipment for Al-Fin insert diesel pistons, Insight NDT equipment Ltd, The Old Cider Mill Kings Thorn Herefordshire HR2 8AW, 2000.
[13] R.C. Hernández, J.H. Sokolowski: J. Alloys Compd., 419 (2006) 180−190.
[14] C.L. Chen, R.C Thomson: J. Alloys Compd., 490 (2010) 293−300.
[15] S. Manasijevic, N. Dolic, Z. Zovko Brodarac, M. Djurdjevic, R. Radisa, Metallurgical and Materials Transactions A, 45(10) (2014) 4580−4587.

PATENTED INVENTIONS OF LJUBOMIR KLERIĆ

Snežana Šarboh[1]

[1]Intellectual Property Office, KneginjeLjubice 5, 11000 Beograd, Serbia, ssarboh@zis.gov.rs

Abstract

LjubomirKlerić, the one of the most important Serbian scientists, was also a prolific inventor. In this paper are presented results of an investigation relating to his patented inventions. Briefly, Klerić had patented some of his known inventions, such as a drill for boring wells, a cartridge for mining purposes and a polypantograph, but not a logarithmograph, a curvimetre and a tractoriograph. Instead, he had patented some other inventions, such as a rotary engine, a differential pulley and a clutch. It is shown that Klerić had at least 36 patents from 7 different countries.

Keywords:*LjubomirKlerić, invention, patent, polypantograph.*

1. INTRODUCTION

Ljubomir Klerić (1844-1910) was a man of many talents and one of the most important scientists in the Kingdom of Serbia at the end of XIX century and the beginning of XX century. During his career, he was a mining engineer, a geologist and a full member of the Serbian Royal Academy (from 1887). He also served as a minister of education and ecclesiastical affairs, a minister of the national economy and a member of the State Council, as mentioned in [1]. Nevertheless, he is best known as a professor of the Belgrade University, who educated and inspired numerous generations of students. It is also known that Klerić inclined more to the applied than to theoretical science and that he was prolific inventor. He also admired other inventors, especially Nikola Tesla, whom he proposed as a member of the Serbian Royal Academy.

Although Ljubomir Klerić died 110 years ago, an exceptionally small number of papers refers to his activities related to protection of his inventions, such as [1]. The most often mentioned Klerić's inventions are a new drill for deep wells, a cartridge for mining purposes, polypantograph (a kind of writing apparatus), a logarithmograph, a curvimetre and a tractoriograph. Also his first published paper [2] deals with his new cartridge for blasting and mining purposes. In [1] is also cited his statement that he had patented a drill for boring wells "in all the European countries", wherein he specified France and Germany as examples. Additionaly, he mentioned that he had got royalty payment for the right to use the drill in Germany. Nevertheless, respective patents had not been identified at least by patent number and country of grant. Instead, it seems that it have been taken for granted that all of the mentioned Klerić's inventions had been patented, but real situation turned out to be quite different.

Namely, during author's own investigation on Nikola Tesla's and Michael Pupin's patents in the state archives and the archives of industrial property authorities of different countries, the author came across some of Klerić's patents and decided to include them in the investigation. The obtained results will be presented in the continuation of this paper. However, first will be briefly explained basic terms from patent law, because it is not possible to understand the presented material properly without knowing these terms.

2. INVENTIONS AND PATENTS

In public, the terms "invention" and "patent" are often used as synonyms. However, their true meanings are very different. In patent law, an invention is the technical solution of a particular

technical problem, as explained in more detail in [3]. On the other hand, the term "patent" refers to the rights acquired by the patent owner, who prepares a patent specification, which is a document describing the invention and generally containing a description of the invention with figures (if any) and claims. A patent is not automatically protected, just by creating an invention or by announcing it to the public, but only upon carrying out the stipulated administrative procedure, which is initiated by filing a patent application containing the patent specification to the competent authority in charge.

Duration of a patent rights is temporally limited (20 years in most countries) from the filing date of the patent application. More important is, that the patent validity is territorially limited, i.e. it is in force only in the country, the competent authority of which granted that patent.

3. RESULTS AND DISCUSSIONOF THE INVESTIGATION

3.1 Registered patents of Ljubomir Klerić

In Table 1 is given the current list of registered Klerić's patents, which has been compiled on the basis of the author's own investigation conducted in resources of [4-8]. The majority of provided data is not available both in free-of-charge (such as ESPACENET or WIPO Patentscope) and expert patent databases (such as EPODOC by the EPO).

Table 1. The current list of LjubomirKlerić's patents

Nr.	Patent Nr.	Title of Invention	Filing Date	Grant Date
1.	**US131548**	**Drill for boring wells**	**-**	**24.09.1872**
2.	RU1569	Веревчатыйбуровойснарядъ	05.05.1872.	28.11.1873.
3.	**AT21/000343**	**PatronezumSprengen des GesteinsbeiBergwerksarbeiten**	**18.05.1871**	**01.08.1871**
4.	GB1871/02335	A new cartridge for blasting and mining purposes	04.09.1871	-
5.	**AT21/000560**	**KontinuierlichwirkenderZiegelofen**	**18.05.1871**	**15.11.1871**
6.	**AT21/000392**	**RädersystemmitspeziellerAnwendung auf Räderfahrzeuge und Flaschenzüge**	**22.05.1871**	**23.08.1871**
7.	**DE64785**	**Apparat zurgleichzeitigen Anfertigungmehrerer übereinstimmender Gebildeode rSchriftstücke**	**19.11.1891**	**03.10.1892**
8.	AT42/001174	Polypantograph	21.11.1891	10.05.1892
9.	BE97407	Polypantograph	01.12.1891	15.12.1891
10.	FR217772	Polypantographe	01.12.1891	02.07.1892
11.	US512718	Polypantograph	10.05.1892	16.01.1894
12.	**AT42/002356**	**Kräftepaarmotor**	**23.09.1891**	**07.12.1892**
13.	DE69284	KraftmaschinemitkreisendemKolben und beweglichenFlügeln	28.09.1891	19.06.1893
14.	BE96592	Moteur á couple de force	29.09.1891	15.10.1891
15.	FR216430	Moteur á couple de force	29.09.1891	02.07.1892
16.	GB1891/16643	A new or improved rotary engine	30.09.1891	-
17.	**AT42/003843**	**Seildifferentialflaschenzug**	**25.02.1892**	**27.12.1892**
18.	DE65467	Seil-Differentialflaschenzug	11.03.1892	10.11.1892
19.	FR220107	Moufle á cordedifférentielle	12.03.1892	24.09.1892
20.	BE98784	Moufle á cordesdifférentielles	14.03.1892	31.03.1892
21.	US516098	Differential pulley	03.06.1892	06.03.1894
22.	**AT42/004110**	**Polypantograph**	**09.07.1892**	**28.12.1892**
23.	FR223080	Poly-pantographe	09.07.1892	27.02.1893
24.	DE74515	VorrichtungzurgleichzeitigenAnfertigungmehrererübereinstimmenderZeichnungen und Schriftstücke	23.07.1892	12.04.1894
25.	DE76776	VorrichtungzurgleichzeitigenAnfertigungmehrererübereinstimmenderZeichnungen und Schriftstücke (a patent of addition for DE74515)	07.09.1893	15.08.1894
26.	US512719	Polypantograph	13.09.1892	16.01.1894
27.	**AT43/000186**	**Wasserstandanzeiger**	**17.10.1892**	**27.01.1893**
28.	**DE74328**	**Schraubenband-Reibungskupplungmitlosem, anpressbaren Mantel**	**27.07.1892**	**06.04.1894**
29.	FR223632	Accouplement pour embrayer et desembrayer les arbres de transmission	12.08.1892	27.02.1893
30.	AT43/000240	Kupplung	16.10.1892	26.01.1893
31.	**AT43/000525**	**Wasserstandanzeiger**	**13.09.1892**	**07.03.1893**
32.	BE101409	Niveaul'eaumagnetique	23.09.1892	15.10.1892
33.	FR224506	Niveaul'eaumagnetique	23.09.1892	27.02.1893
34.	US 530,592	Magnetic water-gage	27.03.1893	11.12.1894
35.	**DE76492**	**Geschwindigkeitsmessermit von FlüssigkeitgefülltenGefassfürRegulatoren**	**25.10.1893**	**02.08.1894**
36.	AT44/002317	Apparat zumRegulieren und messen von Geschwindigkeiten	26.10.1893	26.03.1894
37.	**CH9225**	**NeuerTourenanzeiger**	**11.10.1894**	**15.05.1895**

In Table 1 the two-letter codes have the following meanings: AT – Austria, BE - Belgium, CH – Switzerland, DE – Germany, FR – France, GB – Great Britain, RU - Russia and US – the United States. Data dealing with the basic patents (i.e. the ones that were filed first) are printed in bold, unlike data on their equivalents (which relate to the same inventions, but in the other countries). .

3.2 Brief analysis of Klerić's patents

As can be seen from Table 1, Klerić(who wrote his family name as "Kleritj" in these documents) had registered 36 patents in 7 different countries (Austria – 11 patents, Belgium – 4 patents, France – 6 patents, Germany – 7 patents, Great Britain – 2 patents, Switzerland – 1 patent and the U.S.A. – 5 patents). Based on consideration that there are still other available resources, it can be assumed that this is not the final number of Klerić's patents.

Above mentioned Klerić's patents can be divided in two groups: the first group containing his earliest patents filed in 1871 and the second group containing the rest, which had been filed in the period between 1891-1894. It seems that Klerić filed his first 4 patent applications immediately after his departure from Serbia. The first two ones relate to his drill for boring wells (American patent US 131,548) and a cartridge for blasting and mining purposes (Austrian patent AT21/000343, shown in Figure 1, and British patent GB1871/02335), which have already been mentioned in [1], but without appropriate patent data. The subject matter of the next one, Austrian patent AT21/000560, is a kiln for continuous baking of bricks, while the fourth one, also Austrian patentAT21/000392,relates to a wheel system with special application on wheeled vehicles and pulley blocks.

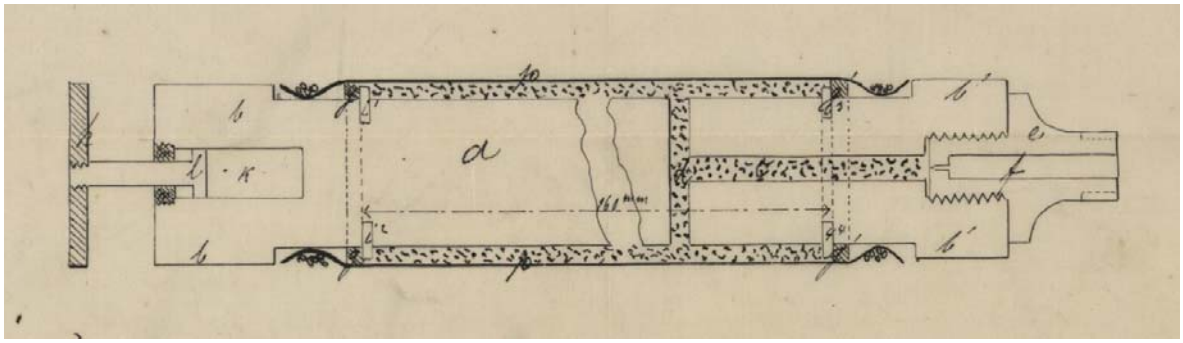

Figure 1. A figure from Austrian patent AT21/000343 for a cartridge for blasting and mining purposes

During next 20 years, when Klerić returned to Serbia and become a professor of the Belgrade University, he had not filed a single patent application. Then, between 1891 and 1894 he filed a large number of patent applications and had got another 32 patents for his inventions. Although some of them are well known, such as his polypantograph, others have not been mentioned in the available references. The most of them relates to measuring devices and the most cited one is his American patent US530,592 for magnetic water-gage. He also patented a rotary engine (Austrian patent AT42/002356), differential pulley (Austrian patent AT42/003843) and a clutch (German patent DE74328). On the other hand, it seems that he had not patented a logarithmograph, a curvimetre and a tractoriograph. Also, it appears that he stopped patenting his inventions when he was appointed for a minister of education and ecclesiastical affairs in 1894.

It is certain that Klerić had never patented any of his numerous inventions in the Kingdom of Serbia. The reason for it is following: through the Kingdom of Serbia, as one of 11 founding countries of the Paris Union (it took place in 1883) was obliged to establish an institution for the protection of industrial property, it had set up the Administration for the Protection of Industrial

Property considerably later, more precisely on 15 November 1920 (see [9]), i.e. over 10 years after Klerić's death.

4. CONCLUSION

In this paper are presented results of an investigation relating to patented inventions of LjubomirKlerić,a significant Serbian scientist and a professor, who was also a prolific inventor. It has been found that Klerić had patented some of his known inventions, such as a drill for boring wells, a cartridge for mining purposes and a polypantograph, but not a logarithmograph, a curvimetre and a tractoriograph. Instead, he had patented some other inventions, such as a rotary engine, a differential pulley and a clutch. His patenting activity took part in 1871 and between 1891 and 1894. It has been shown that Klerić had at least 36 patents from 7 different countries, but none in the Kingdom of Serbia.

ACKNOWLEDGEMENT

I would like to express my deep gratitude to my late colleague Slobodan Stojković, both for his enthusiastic encouragement and great help in collecting needed archive materials.

REFERENCES

[1] KaticaStevanovićHedrih, LjubomirKlerić, in Lives and work of the Serbian Scientists, volume 1, Serbian Academy of Science and Arts, Belgrade, 1996, p.129-179.
[2] Ljubomir Klerić,Die theoretische und praktische Verwendung einer neuen Sprengpatrone und Ladungsmethode, Erfunden von Ljubomir Kleritj. - Mit Holtzschnitten, Separat - Abdruck aus der Berg- und Hattenmannischen Zeitungen, Jahrgang 1872, p. 1-15.
[3] SnežanaŠarboh, The patents of Nikola Tesla: towards the definite catalog, Nikola Tesla Museum, Belgrade 2007. p.15-18.
[4] French patent specifications - Archives of Institut National de la PropriétéIndustrielle (INPI), Paris, France
[5] Austrian privileges - Archives of ÖsterreichischesPatentamt, Wienna, Austria
[6] German patent specifications - Archives of Deutsches Patent- und Markenamt (DPMA), Munich, Germany
[7] Belgium patent specifications - Archives de l'Ėtaten Belgique, Brussels, Belgium
[8] EPOQUE (EPO QUEry service) the inhouse host computer of the EPO
[9] Intellectual Property Office - About the Office (http://www.zis.gov.rs/about-us/about-us.103.html)

DEGRADED AREA OF VELIKI KRIVELJ QUARRY RECULTIVATION

Miomir Mikic[1], Milenko Jovanović[1], Radmilo Rajković[1], Daniel Kržanović[1], Emina Požega[1]

[1]Mining and metallurgy Institute Bor, Zeleni Bulevar, 19210 Bor, Serbia

Abstract

Veliki Krivelj Quarry is located north of Bor, near the village of Brezanik. Itoperates within Serbia Zijin Copper doo Bor. During the exploitation of limestone, waste material was obtained, which is deposed of in the southeast in relation to the quarry. In order to protect the environment and improve the landscape, an analysis will be performed to determine the optimal method of recultivation. Using technics of technical and biological recultivation, a new ecosystem will be established and the degraded areas will be translated into their new function.

***Keywords**: quarry, waste dump, waste, recultivation.*

1. INTRODUCTION

The Veliki Krivelj Quarry operates within Serbia Zijin Copper doo Bor. It is located north of Bor, at a distance of about 4.5 km, near the village of Brezanik (Figure 1). Of the larger facilities nearby, there is the Veliki Krivelj flotation plant and the open pit Veliki Krivelj. The main goal of obtaining limestone is for smelter Bor needs. During the exploitation of limestone waste was obtained, which is deposited southeast in relation to the open pit (Figure 1).

The morphology of the terrain Kriveljski kamen is such that it is located within the hill that dominates the surroundings (Figure 1). The terrain with the lowest elevation of 350 m is at the foot of the hill at the confluence of the Ujova and Kriveljska rivers, while the highest elevation at the top of Kriveljski kamen is 655 m.

The Kriveljski kamen limestone deposit is isolated in the central part of the deposit and there is no natural boundary on all sides (Figure 1). The deposit is built of Cretaceous sediments: limestone, marble and andesite (phase II) and of Paleogene marbles and quartz dioritporphyrite breakthroughs, of which limestones and marbles are the most widespread. Limestones are characterized by low compactness, they belong to the crack-cavernous type with tectonic fracture along faults. Along the caverns and fault lines, which are usually filled with the decomposition products of the original basic mass, it is possible for water to penetrate into deeper parts of the reservoir.

Figure 1. Spatial view of Quarry Veliki Krivelj location

2. DEGRADED AREA

Exploitation of limestone at the Veliki Krivelj Quarry implies degradation of the surrounding area during the formation of the projected contours of the open pit. The total area that will be degraded is 48,735 m^2. The projected waste dump occupied an area of 8,760 m^2, and the projected open pit area of 39,975 m^2.

Open pit and waste dump degraded areas are intended for landscaping by applying recultivation for raising forest plantations.

During the exploitation of the Veliki Krivelj quarry, no layers of soil material were found, even in the surface layers, due to the characteristic terrain, while the obtained waste will be disposed of at the designed waste dump.

Since the recultivation requires soil material that is used to fill the seedling pits, it is necessary to obtain it, in this case, from the area near quarry.

The total area where soil material will be obtained is 3,010 m^2. Bearing in mind that 20-30 cm of surface layer will be used, a sufficient amount of soil material was obtained to perform recultivation. The location plots that will represent the borrowing of soil material are located southeast of the open pit and south of the waste dump.

3. CHOOSING RECULTIVATION METHOD

The main goal of recultivation of physically, chemically and biologically damaged soils is to establish the function of land management, as a resource that is disturbed by anthropogenic activities.

The goal of reclamation is to "return" in some form, through the activities envisaged by the recultivation project, what was previously borrowed from nature through exploitation.

For the reclamation of the quarry Veliki Krivelj, reclamation with the method of afforestation is proposed. Reclamation works take place in the following phases of reclamation:Technical phase of reclamation and Biological phase of reclamation.

4. TECHNICAL PHASE OF RECULTIVATION

Technical reclamation includes the areas of the plateau of the waste dump and all benches of the open pit.

The technical phase of reclamation at the tailings dump at the Veliki Krivelj Quarry represents the stage of preparatory works (subsequent leveling of the final plane), which enable the performance of biological reclamation. Subsequent planning or leveling of the final bench (plateau) is done with a bulldozer before the start of recultivation. During the final process of disposal of the last excavated piles of tailings on the final plane, due to the stability of the landfill, they are not leveled (the piles do not allow the formation of ponds and lakes during atmospheric precipitation and infiltration of water in the landfill body). The bottom of the open pit will also be leveled.

After this phase of technical recultivation, the degraded areas for planting will be prepared, ie the formation of pits for seedlings on the open pit benches and the plateau of the tailings dump.

This implies the process of drilling and blasting in order to form (excavate) pits (funnel) for seedlings on the benches of open pit. This is necessary because it is such a type of substrate that the pits cannot be dug by hand or by mechanization.On the plateau of the tailings dump, pits for seedlings will be excavated by machine because it is a matter of filled material, so the base is adequate for this type of excavation.

After that, the soil material is transported to the benches of open pit and the plateau of the waste dump, which will be used to fill the pits for seedlings.

5. BIOLOGICAL PHASE OF RECULTIVATION

The biological phase of reclamation implies a complex of biotechnical and phytomeliorative measures for growing forest crops on the prepared surfaces of open pit and waste dump in order to greening and restore ecosystems.

The most effective measures to prevent erosion and improve landfill stability is afforestation. [1]. The development of seedlings leads to better binding of the substrate in the landfill, which prevents erosion, as well as raising dust by the wind [1].

The biological phase of reclamation includes afforestation of all areas of waste dump and open pit.

Pits made as part of technical reclamation will be used for afforestation. Planting seedlings is done manually. During planting, the seedlings are also fertilized with mineral fertilizer.

Pits for seedlings are dug in two rows at a distance of 3 m from each other on the flat surfaces – open pit benches.

The bottom of open pit is at K + 540 m and represents a flat surface in the limestone and when the exploitation at the open pit ceases, this area will be intended for raising forest plantations (Figure 2).

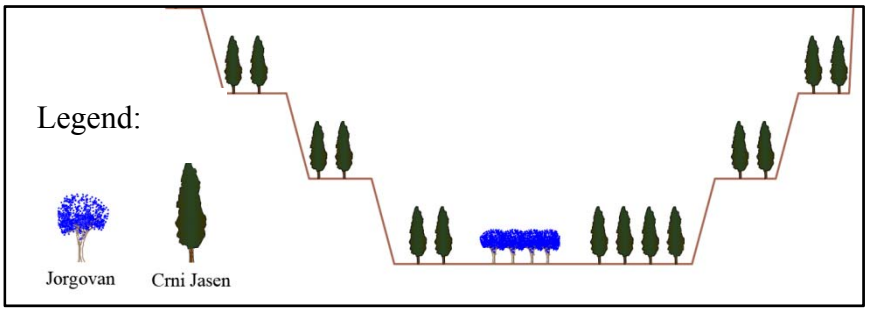

Figure 2. Profile of a surface mine with the arrangement of plant cultures

For greening of degraded areas at the subject location, the biological method of recultivation will be applied, as follows:

- Shrubby plants: Lilac - Syringa vulgaris. As this crop is drought resistant and is satisfied with modest soil, gives abundant root shoots, it was chosen for afforestation of degraded areas.
- Woody plants: Black ash - Fraxinus ornus L. It was chosen because of its characteristics to bind the soil well on steep terrain.

Lilac - Syringa vulgaris, which is a deciduous shrub, was chosen as a shrubby plant. It is a natural habitat in Eastern Serbia and the Ibar Valley. It has excellent characteristics that are necessary for the subject area, the most important of which is that it is resistant to drought, is satisfied with modest soil and gives abundant root shoots. It is also valued as an ornamental plant and is often grown in backyards and parks.

The woody plant that will also be used in biological reclamation is black ash. A tall tree that can grow up to 20 meters in height. It thrives on rocky and shallow skeletal soils, suitable for areas with steep terrain up to 1200 m above sea level.

Planting deciduous shrub crops means a square pattern, on flat surfaces, with a mutual distribution of 2.24 m, and about 2000 seedlings can be planted on one hectare.

The planting of deciduous trees at the bottom of the open pit and the plateau of the waste dump will be done according to a square scheme at a distance of 3 m from each other. This means that 1,100 seedlings can be planted on one hectare.

Planting deciduous trees on the benches of a open pit, since the width of the floor is 7.5 m, it is possible to plant trees in two rows according to a square scheme at a distance of 3 m from each other. This means that 1,100 seedlings can be planted on one hectare.

In order to determine the total cost of procurement of seedlings, it is necessary to determine the total number of seedlings. This number is determined based on the areas covered by these crops. The total required number of seedlings for planting has been determined, and amounts to:

- for lilac- 91 seedlings
- for black ash - 2385 seedlings

5.1 PLANTING METHOD

The general rule when planting seedlings is to plant the plant 1-2 cm deeper than the position in which it was in the nursery. When the soil around the seedling settles, the root collar will be at ground level.

Up to 1/3 of the height of the earth is first inserted into the excavated pits. The seedling is placed vertically in the pit so that the root veins take as natural a position as possible along the entire depth. The remaining amount of soil is poured on the root of the plant to fill the seedling pit so that the root neck is 1-2 cm below the level of the trampled soil. After planting, tread the immediate surroundings of the seedling well in order to compact the soil, thus eliminating the danger of forming "air pockets" along the root of the seedlings, which lead to drying of the seedling. According to previous experiences, the most common cause of poor seedling reception is, in addition to the lack of moisture in the soil, improper planting.

Healthy seedlings with a free root system, age 2 + 1, are used for planting. 150 g of NPK (15:15:15) of mineral fertilizer is added per planted seedling.

Fertilizer is added around the planted seedling only when the root is completely covered with soil, ie the pit is filled. In the spring, when hoeing, fertilize the seedlings with KAN in the amount of 100 g per seedling.

6. CONCLUSION

Occupying large areas of land, ecosystem degradation and population relocation, ie. changes in the network of settlements are, of course, the most significant structural changes caused by the exploitation of mineral resources in large mining basins [2]. To this should be added the relatively high degree of pollution of the environment: air, water, soil and wildlife from harmful emissions from the industrial complex [2].

Recultivation and revitalization of the space is the last, very important phase (after the end of exploitation) and requires appropriate planning activities for its implementation.

Today, significant results are being achieved in the world on the restoration of degraded land. Restored areas sometimes reach a higher ambient value compared to the state before the start of exploitation.

In this case, the effects of reclamation of degraded areas are reflected in the fact that:

- Forest plantations enable better binding of the soil, stimulate the development of ground flora, activate pedological processes in the substrate by the root system, prevent insolation and drying of the soil, blowing strong winds and raising dust.
- Afforestation of degraded areas contributes to environmental protection, improvement of the microclimate and aesthetic appearance of the environment.

ACKNOWLEDGEMENTS

This work was financially supported by the Ministry of Education, Science and Technological Development of the Republic of Serbia, contract no. 451-03-9 / 2021-14 / 200052.

REFERENCES

[1] Miomir Mikić, Sanja Petrović, Ivana Jovanović, Radmilo Rajković: Reclamation the inner landfill of the coal open pit Cementara in Pljevlja, Montenegro. 48th International october conference on mining and metallurgy. Universitet of Belgrade Technical Faculty Bor. Bor, 2016. ISSN / ISBN 978-86-6305-047-1. DOI 226011916. pp. 285-288

[2] Nenad Spasić, Božidar Stojanović, Marija Nikolić: „Uticaj rudarstva na okruženje i revitalizacija degradiranog prostora”.UDK 622.271:502.171. Prostorno planiranje 75-85 str.

EFFECTS OF TAILINGS ON GROUNDWATER ALONG BOR AND BELA RIVERS IN THE BOR MINING AREA, EASTERN SERBIA

Dragana Adamović[1,2], Daizo Ishiyama[1], Hiroshi Kawaraya[1], Ogawa Yasumasa[1]

[1]Gaduate School of International Resource Sciences, Akita University, Tegatagakuen-machi 1-1, Akita Pref. 010-8502, Japan

[2]Mining and Metallurgy Institute Bor, ZeleniBulevar 35, 19210 Bor, Serbia

Abstract

Contamination of water bodies is a large problem in many mining areas in the world. Groundwater in mining areas can be polluted by different mechanisms and the pollution can often be severe. Mixing calculations are useful to clarify the mechanism of pollution as well as to define the source of pollution. Based on the mixing calculation between interstitial water in tailings along strongly polluted rivers and unpolluted groundwater, it is thought that interstitial water in tailings along Bor River and Bela River located in the Bor mining area is causing pollution of groundwater in the vicinity of those rivers.

***Keywords**: groundwater pollution, calcium, sulfate, interstitial water, mixing calculation.*

1. INTRODUCTION

Mining development in the Bor mining area started in 1903. Mining activity has been the main economic activity in Eastern Serbia in the last 120 years. The long history of mining in the Bor mining area leads to serious environmental problems, which are most pronounced on air, soil and surface water pollution around the mining sites [1,2,3,4,5]. Adamović, 2021[6] defined the earlystage of groundwater pollution based on Ca^{2+} and SO_4^{2-} concentrations at Slatina Village, Rgotina Village and Vražogrnac Village along strongly polluted Bor River and Bela River. The early-stage groundwater pollution was detected by using a combination of geochemical maps and threshold values. However, the mechanism of groundwater pollution is not clear. Given this reason, the aim of this study was to clarify the mechanism of groundwater pollution and to define the source that affects groundwater quality in the study area by using mixing analysis considering geochemical reactions.

2. MATERIALS AND METHODS

A field survey was carried out for field observation and sample collection in August 2019. Thirty-seven groundwater samples were collected at Slatina Village, Rgotina Village and Vražogrnac Village, while 3 groundwater samples were collected outside the mining area as background samples. In addition, 3 polluted river water samples were collected. In this study, interstitial water in tailings that have been collected in 2017 was also considered.

In the field, pH, Eh, water temperature and bicarbonate concentrations were measured at each sampling site. All samples were filtrated using cellulose acetate hydrophilic filters with a pore size of 0.20 μm. Finally, two kinds of samples were collected, one non-acidified sample for determination of major cations and anions by ion chromatography (IC), and one acidified sample for determination of trace elements by inductively coupled plasma mass spectrometry(ICP-MS). After the field survey, all of the samples were transported to Japan where chemical analyses were done (Akita Industrial Technology Center in Akita City, Japan).

3. RESULTS AND DISCUSSION

3.1 General features of water samples

Polluted river water had an acidic pH ranged from 2.9 to 3.7. All of the river water samples were classified as Ca-Mg-SO_4-dominant type water (Figure 1) having high SO_4^{2-} concentrations as well as high concentrations of Cu, As, Fe and Mn.

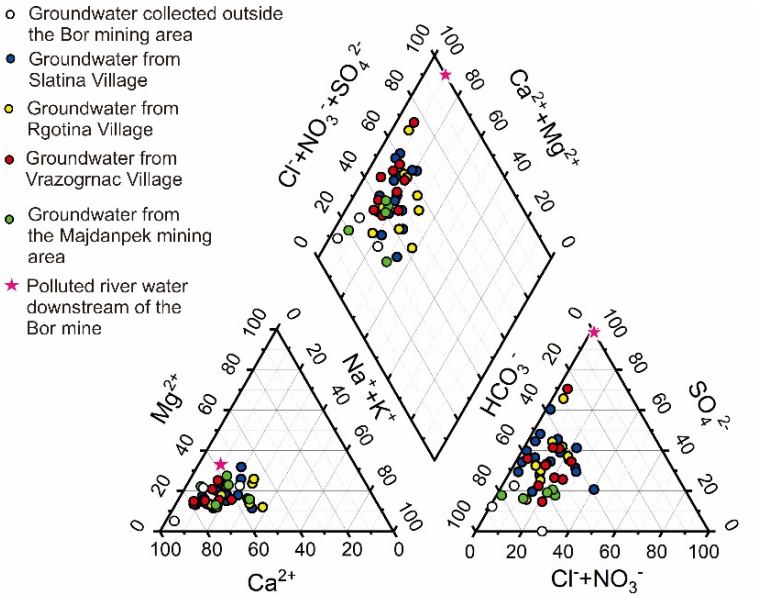

Figure 1 Piper diagram showing the chemical composition of groundwater and polluted river water in the study area.

All of the groundwater samples considered in this study had a near-neutral character. Groundwater samples that were collected outside the mining area at Luka, Donja Bela Reka and Zlot Villages are classified as Ca-Mg-HCO_3-dominant type water (Figure 1). Ca-Mg-HCO_3-dominant type water is typical in areas where carbonate bedrocks are present, which is the case with Eastern Serbia[7]. On the other hand, groundwater samples that were collected at Slatina Village, Rgotina Village and Vražogrnac Village are classified either as Ca-Mg-HCO_3-dominant type water or Ca-Mg-SO_4-dominant type water. These groundwater samples are plotted in the Piper diagram between polluted river water samples and groundwater samples collected outside the mining area, indicating the presence of groundwater pollution in the Bor mining area (Figure 1). Content of heavy metals and arsenic in all groundwater samples resulted to be low, which is to be expected for water having a near-neutral character.

3.2 Mechanism of groundwater pollution

Early-stage groundwater pollution was defined based on Ca^{2+} and SO_4^{2-} concentrations along polluted rivers downstream of the Bor mine. However, not all of the collected groundwater samples at Slatina, Rgotina and Vražogrnac Villages showed pollution. Higher concentrations of Ca^{2+} and SO_4^{2-} were found along Bela River at Rgotina and Vražogrnac Villages which are located farther from the Bor mine compared with Slatina Village. To know the mechanism of groundwater pollution along polluted rivers, mixing analyses were performed. Mixing diagrams are shown in Figures 2, 3 and 4.

For the creation of mixing diagrams, two polluted end-members and one unpolluted end-member were considered. The polluted end-membersconsistedofconcentrations of Ca^{2+} and SO_4^{2-} obtained for polluted river water and interstitial water in tailings along the banks of polluted rivers, while an unpolluted end-member consisted of concentrations of Ca^{2+} and SO_4^{2-} obtained

for groundwater samples that were collected outside the mining areas.In the mixing diagrams, groundwater samples collected near polluted rivers, intermediate part and far from the riversare marked by circles in red, orange and yellow, respectively. End-members in the mixing diagrams are shown in different colors (Figures 2, 3 and 4).

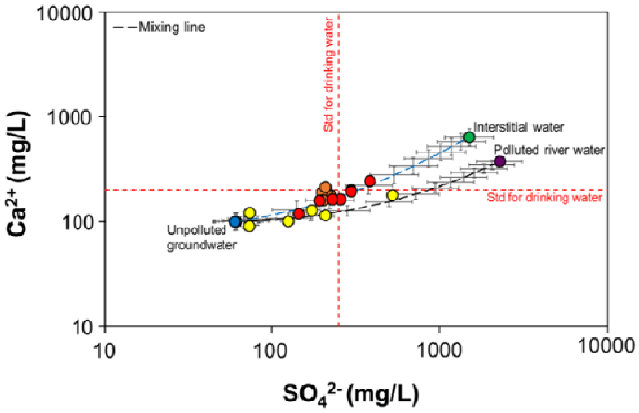

Figure 2 Diagram showing two end-members/two components mixing lines for groundwater samples collected in Slatina Village.

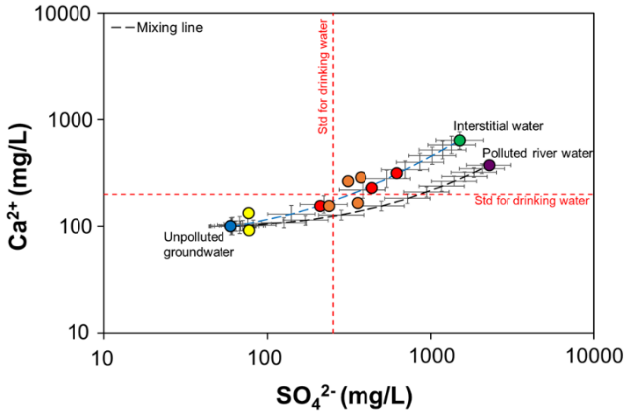

Figure 3 Diagram showing two end-members/two components mixing lines for groundwater samples collected in RgotinaVillage.

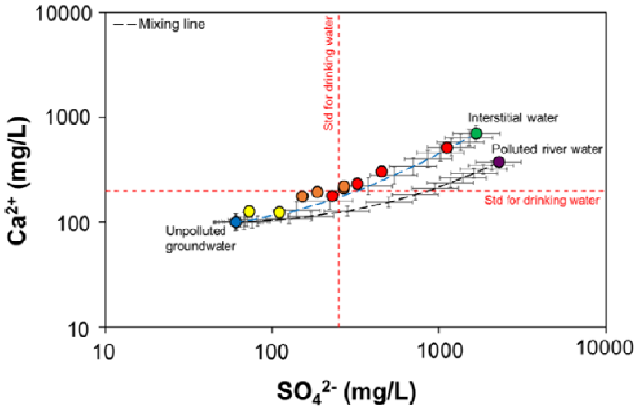

Figure 4 Diagram showing two end-members/two components mixing lines for groundwater samples collected in VražogrnacVillage.

Based on the distribution of actual Ca^{2+} and SO_4^{2-} concentrations of groundwaterin mixing diagrams (Figures 2, 3 and 4), groundwater samples collected near polluted rivers and from the intermediate parts are plotted on the mixing line created for interstitial water in tailings and unpolluted groundwater. These results indicate that mechanism of groundwater pollution in the

study area is the infiltration of interstitial water in tailings into groundwater. In the mixing diagram created for groundwater samples collected at Slatina Village, some samples are plotting on the mixing line created for polluted river water and unpolluted groundwater (Figure 2). However, these samples were collected far from the Bor River. Therefore, the possibility of mixing between groundwater and polluted river water in this region of Slatina Village is denied.

4. CONCLUSIONS

Mixing analyses showed that the mechanism of groundwater in the area downstream of the Bor mine is infiltration of interstitial water in tailings along the banks of polluted Bor and Bela Rivers into groundwater, not mixing between polluted river water and groundwater. Moreover, higher concentrations of Ca^{2+} and SO_4^{2-} were found in the downstream area of Bela River. Therefore, attention should be alsopaid to the areas located far from the mining facilities not only in its vicinity.

ACKNOWLEDGEMENTS

This study was undertaken as a part of the project "Research on the Integration System of Spacial Environment Analyses and Advanced Metal Recovery to Ensure Sustainable Resource Development that belongs to the SATREPS program (Science and Technology Research Partnership for Sustainable Development) supported by Japan International Cooperation Agency (JICA) and Japan Science and Technology (JST).

REFERENCES

[1] S.M.Serbula, J.S. Milosavljevic, J.V. Kalinovic,T.S.Kalinovic, A.A. Radojevic, T.Lj. ApostolovskiTrujic, V.M. Tasic, Arsenic and SO_2 hotspot in South-Eastern Europe: An overview of the air quality after the implementation of the flash smelting technology for copper production. Sci. Tot. Env., 777 (2021) 145981.

[2] M.Pejović, B. Bajat, Z. Gospavić, E. Saljnikov, M. Kilibarda, D. Čakmak, Layer-specific spacial prediction of As concentration in copper smelter vicinity considering the terrain exposure. J. Geo.Explo. 179 (2017) 25-35.

[3] J.V. Petrović,S.C.Alagić,S.M. Milić, S.B. Tošić, M.M. Bugarin,Chemometric characterization of heavy metals in soils and shoots of the two pioneer species sampled near the polluted water bodies in the close vicinity of the copper mining and metallurgical complex in Bor (Serbia): Phytoextraction and biomonitoring contexts. Chemosphere. 262, (2021) 127808.

[4] S. Đorđievski, D. Ishiyama, Y. Ogawa, Z. Stevanović, Mobility and natural attenuation of metals and arsenic in acidic waters of the drainage system of Timok River from Bor copper mines (Serbia) to Danube River. Env. Sci. Poll. Res. 25 (2018) 25005-25019.

[5] D. Adamovic, D. Ishiyama, S. Dordievski, Y. Ogawa, Z. Stevanovic, H. Kawaraya, H. Sato, Lj. Obradović, V. Marinković, J. Petrović, V. Gardić, Estimation and comparison of environmental impacts of acid mine drainage-bearing river water in the Bor and Majdanpek porphyry copper mining areas in Eastern Serbia. RGE., 71 (2021) 123-143.

[6] D. Adamović, Geochemical and stable isotope studies of groundwater and river water in the Bor and Majdanpek porphyry copper mining areas in Eastern Serbia: Implications for the environmental impact on groundwater. Doctoral Dissertation, Akita Univerity, Akita, Japan. 2021.

[7] C. Appelo and D. Postma, Geochemistry, groundwater and pollution. Boca Raton: CRC Press, p.668.2005.

CHARACTERIZATION OF ALLOYS CuAlAu0.5

Ana Kostov[1], Zdenka Stanojević Šimšić[1], Aleksandra Milosavljević[1],

[1]Mining and Metallurgy Institute Bor, Zeleni bulevar 35, 19210 Bor, Serbia

Abstract

Phase equilibria of alloys CuAlAu0.5 was examined using optical microscopy (LOM), scanning electron microscopy with energy dispersive spectroscopy (SEM-EDS) and differential thermal analysis (DTA) methods. Based on the structural analysis of the examined alloys the existence of all expected phases was confirmed: solid solutions based on copper, aluminum and gold (Cu, Al, Au) and β phase. The characteristic temperatures of phase transformations of alloys were determined too. By measuring the hardness of the alloys, it was determined that the highest values of hardness were measured in alloys whose composition includes the β phase.

Keywords: *CuAlAu0.5 alloys, characterization, martensite structure.*

1. INTRODUCTION

Shape memory alloys include special materials that are characterized by two unique properties, the phenomenon of shape memory and pseudoelasticity. [1] It is these characteristics that have made these materials interesting for research for several decades. The motive for testing these materials is not purely academic in nature, but it is also the possibility of their application in technology, electronics, energy, medicine, bioengineering, space technology, etc. Alloys with a shape memory effect belong to a group of modern materials known as smart materials. It is characteristic for these materials to react to the influence of the environment, i.e., depending on the change of external conditions, there is a change in the properties of the material (mechanical, electrical, structural) [2]. In the last few years, due to high technical - technological development and market needs, primarily in the automotive and oil industries and robotics [3], there is a need for alloys that remember shape with high temperatures of phase transformations. It is characteristic of these alloys that the temperature of the beginning of the transformation of martensite into the initial phase is above 120^{o}C under stress - free conditions. [4] The most important and well-known alloys that show the shape memory effect are alloys based on nickel and titanium, as well as based on copper. Copper-based alloys are cheaper and can be produced in a simpler and more economical way, which, with appropriate thermal, mechanical, etc. properties, makes it suitable for application in engineering, energy, space technology, medicine, bioengineering, etc. [5] Today, the alloys of the Cu-Zn-Al and Cu-Al-Ni systems are the most widely used, but numerous studies indicate that intensive work is being done on the production and use of other copper-based alloys and a number of other elements.

2. EXPERIMENTAL

For experimental investigations in the concentration range of the Cu-Al-Au, the cross section with a constant gold content Au = 50at% was selected. As-cast alloys were used in all tests. All samples were prepared by inductive melting of pure metals in a protective argon atmosphere. The total weight loss of the prepared ingots was less than 1% by weight. The compositions and masses of the tested alloys are given in Table 1.The following methods were used for characterizationof the alloys CuAlAu0.5: optical microscopy (LOM), scanning electron microscopy with energy dispersive spectroscopy analysis (SEM-EDS), differential thermal

analysis (DTA), measurement of microhardness and Vickers hardness and electrical conductivity measurement.

Table 1 -Composition and mass of tested alloys

Alloy	X_{Cu}	X_{Al}	X_{Au}	m_{Cu}(g)	m_{Al} (g)	m_{Au} (g)
Alloy 1	0.3	0.2	0.5	0.4697	0.1329	2.4273
Alloy 2	0.35	0.15	0.5	0.5400	0.0982	2.3917

The optical microscopy was used a Reichert MeF2 microscope with a maximum magnification of up to 500 times. SEM-EDS analysiswas performed on a scanning electron microscope Sem Tescan Vega TS 5136MM (resolution 3nm at 20kV and maximum magnification up to 100000 times), with an energy dispersive spectroscope brand Bruker. DTA tests were performed on a device for simultaneous thermal analysis of materials Netzsch STA 449F1 Jupiter operating in the temperature range from -150^{o}C to 2400 ^{o}C and heating rate from 0.001 K/min to 50 K/min. DTA measurements were performed in an argon atmosphere with samples weighing up to 50 mg, at a constant heating and cooling rate of 10 ^{o}C/min. Al_2O_3 was used as a reference material. The hardness of the samples was determined using the standard Vickers method.

3. RESULTS AND DISCUSSION

SEM photographs of the tested samples of the alloys CuAlAu0.5 are shown in Figures 1 and 2.For the investigated alloys the presence of β phase was confirmed. The surface of the investigated alloys given in Figures 3 and4, is corroded by imperial water. The microstructure of the alloy 1, composed of $Cu_{30}Al_{20}Au_{50}$, is characterized by the existence of polygonal, coarse β-phase grains in which a martensite structure is just emerging. In the alloy 2, composition $Cu_{35}Al_{15}Au_{50}$, the martensite structure is well developed, which is expected considering that the composition of this alloy is in the region of the β phase.Determinations of temperatures of phase transformations in the alloys CuAlAu0.5 were performed by DTA. After homogenization, the tested samples were heated and cooled with a heating and cooling rate of 10^{o}C/min. Onset was determined when determining the characteristic phase transformation temperatures, while peaks were taken for liquidus and temperatures of other phase transformations.The DTA heating and cooling curves of selected samples of the investigated alloys are shown in Figures 5 and 6, respectively.

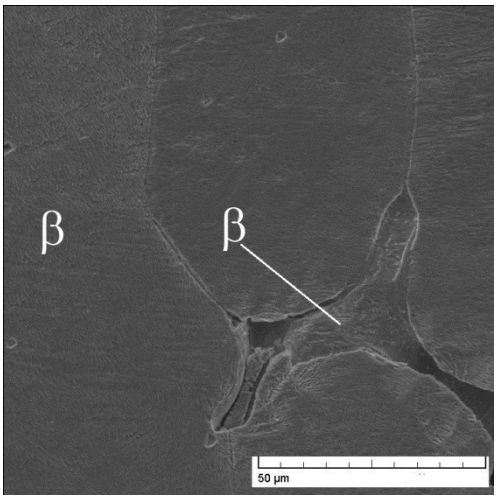

Figure 1. SEM of alloy 1 - $Cu_{30}Al_{20}Au_{50}$

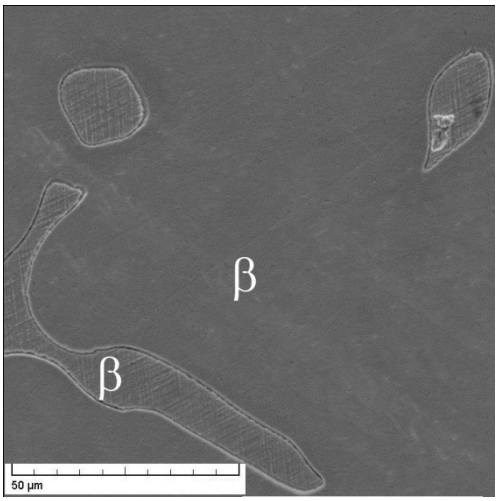

Figure 2. SEM of alloy 2 - $Cu_{35}Al_{15}Au_{50}$

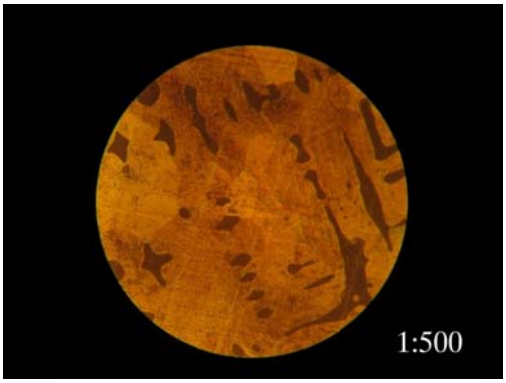

Figure 3. LOM for alloy 1 - $Cu_{30}Al_{20}Au_{50}$

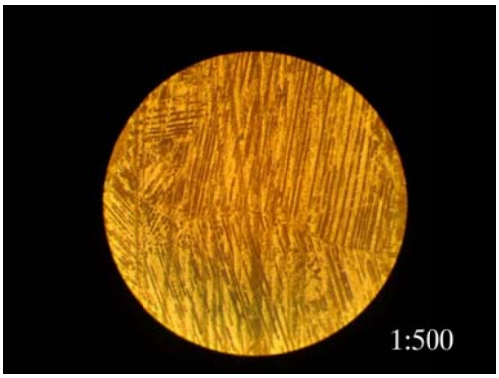

Figure 4. LOM for alloy 2 - $Cu_{35}Al_{15}Au_{50}$

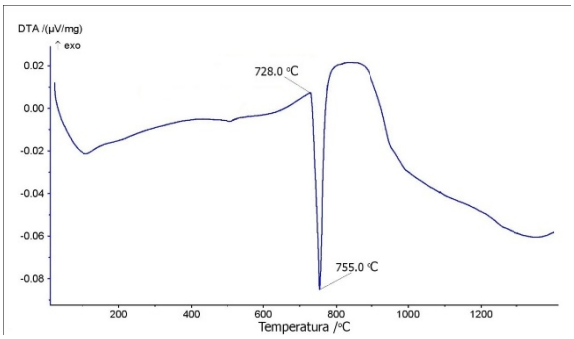

a)

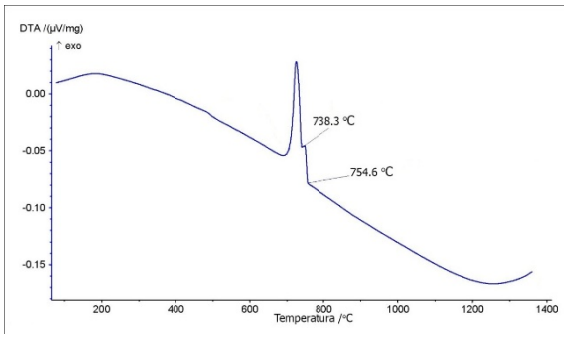

b)

Figure 5. DTA curves for alloy 1: a) heating; b) cooling

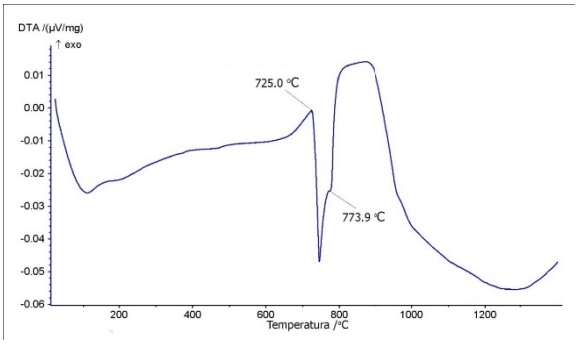

a)

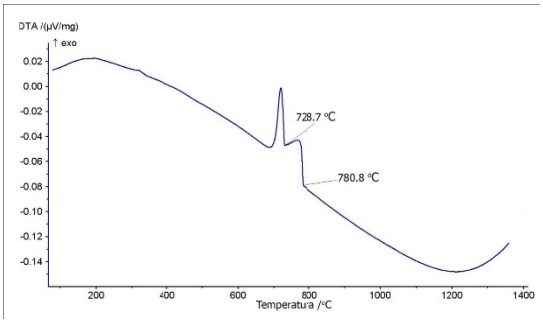

b)

Figure 6. DTA curves for alloy 2: a) heating; b) cooling

The results of measuring the hardness of the investigated alloys are given in Table 2. It can be noticed that between the measured hardness of alloys 1 and 2, the difference is almost insignificant, which is expected because the compositions of these alloys are very similar.The load used in measuring the microhardness of the samples of the alloys was 100 g. The obtained measurement results are presented in Table 3.

Table 2 - Results of hardness measurements

Alloy	Chemical composition	HV10
Alloy 1	$Cu_{30}Al_{20}Au_{50}$	174
Alloy 2	$Cu_{35}Al_{15}Au_{50}$	164

The measured values of electrical conductivity of alloys 1 and 2 in Table 4, do not differ, which is in accordance with the compositions of these alloys.

Table 3 - Results of microhardness measurements

Alloy	Chemical composition	HV0.1
Alloy 1	$Cu_{30}Al_{20}Au_{50}$	267
Alloy 2	$Cu_{35}Al_{15}Au_{50}$	149

Table 4 - Results of electrical conductivity measurements

Alloy	Electrical conductivity (MS/m)			
	Measured values			Mean value
Alloy 1	5.643	5.604	5.591	5.613
Alloy 2	5.626	5.317	5.310	5.418

4. CONCLUSION

Based on the structural analysis of the investigated alloys CuAlAu0.5, which was performed using optical microscopy and SEM-EDS method, the existence of all expected phases was confirmed: solid solutions based on copper, aluminum and gold (Cu, Al, Au) and β phase. Using differential thermal analysis (DTA), the characteristic temperatures of phase transformations of the tested alloys were determined. By measuring the hardness of the alloys, it was determined that the highest values of hardness were measured in alloys whose composition includes the β phase. The results of measuring the microhardness of the alloys show that a high value of microhardness. By measuring the electrical conductivity of alloys, it was determined that the alloys possess high values of electrical conductivity. Based on the obtained results, the further thermodynamic analysis can be validated based on obtained structural, mechanical and electrical characteristics of the alloys.

ACKNOWLEDGEMENTS

The research presented in this paper was done with the financial support of the Ministry of Education, Science and Technological Development of the Republic of Serbia, within the financing of scientific research work at the Mining and Metallurgy Institute Bor, according to contract no. 451-03-9/2021-14/200052.

REFERENCES

[1] A. Milosavljević, A. Kostov, R. Todorović, Bakar, 36 (1) (2011) 39-44.
[2] K. Otsuka, K. Shimizu, Y. Suzuki, Y. Sekiguchi, C. Taki, T. Homma, S. Miyazaki, Splavi s Effektom Pamjati Form, Metallurgija, Moskva, 1990, p. 123.
[3] Y. Zheng, Y. Liu, N. Wilson, S. Liu, X. Zhao, H. Chen, J. Li, Z. Zheng, L.Bourgeois, J-F. Nie, Acta Materialia, 184 (2020) 17-29.
[4] H. Hosoda, T. Hori, T. Morita, A. Umise, Journal of the Japan Institute of Metals, 80(1) (2015) 27-36.
[5] Y. Zheng, Y. Liu, N. Wilson, S. Liu, X. Zhao, H. Chen, J. Li, Z. Zheng, L. Bourgeois, J-F. Nie, Microsc. Microanal.,25 (2019) 1700-1701.

The 52nd International October Conference on Mining and Metallurgy
November 29th – 30th , 2021
www.ioc.tfbor.bg.ac.rs

MULTICRITERIA ANALYSIS OF THE LEVEL OF SUSTAINABLE DEVELOPMENT OF THE TOPLICA DISTRICT USING THE ELECTRE METHOD

Marija Milenković[1],VioletaJovanović[2], Jane Paunković[2],Vesna Krstić[3,4]

[1]University of Niš, Univerzitetskitrg 2, Niš, Serbia
[2]Faculty for Management Zajecar, Megatrend University, Park šumaKraljevica bb, 19000 Zaječar, Serbia
[3]Mining and Metallurgy Institute Bor, ZeleniBulevar 35, 19210 Bor, Serbia
[4]University of Belgrade, Technical Faculty Bor, VJ 12, 19210 Bor, Serbia

Abstract
Multicriteria analysis and optimization is applied as a procedure in situations when there are a large number of criteria and variants for defining the solution of the problem. Multi-criteria evaluation can be applied in various activities. In this paper, it was applied in order to rank the municipalities of the Toplica district (Kursumlija, Prokuplje, Blace and Zitoradje) in order to determine which of them is the most developed. The ranking of municipalities according to a number of criteria at the same time, contributes to determining the real situation regarding the factors of sustainable development. Common to all methods of multicriteria analysis is that they solve a given problem on the basis of quantitative analyzes between several alternatives with a larger number of criteria. The procedure for selecting criteria and their weights is very important for their application, which is why these methods mostly differ. All used mathematical models proved to be useful, and the paper presents the results obtained by the method of multicriteria analysis ELECTRE (Elimination and (Et) Choice Translating Reality).

***Keywords**: Multicriteria analysis, sustainable development, ELECTRE, Toplica district.*

1. INTRODUCTION

An integrated approach to the strategy and policy of regional development enables, in addition to defining the degree of regional development and considering its development possibilities, the connection of factors and development goals, so that in the end the result of development is in the function of population interest and general well-being [1-3].

According to the available theoretical and practical knowledge, the integral approach in the analysis of the situation and decision-making on regional development is mainly reduced to the application of some of the methods based on factor, branch-regional or analysis that monitors the basic determinants of economic and sustainable development.

The factor approach is the closest to a complete systemic approach, which analyzes the impact of all relevant factors on the development of the region. By introducing the methods of multicriteria analysis and optimization, the factor approach also gained the status of a suitable integrated model for research and planning of regional sustainable development [4-8].

Having in mind the complexity of the problem of regional development, it is necessary to, in addition to modern theoretical and practical knowledge, establish a more active relationship between local, regional and state institutions in mutual coordination in the process of implementing strategic development plans. Only in this way can the concept of regional sustainable development meet the set goals and objectives [9-17].
The paper takes the Toplica district as an example, which was chosen as a demo region due to poor development, long-term trend of population depopulation, modest qualification structure of

the active population, agriculture as the leading industry, and the area whose natural boundaries are defined by the Toplica river basin. they coincide with the administrative borders, within which there are significant, but untapped natural potentials, which are the key factors for the future sustainable development of this region. Based on this example, it can be concluded that multicriteria analysis can be successfully applied to identify inequalities in the degree of sustainable regional development.

2. METHODOLOGY

2.1Multicriteria analysis of sustainable development of Toplica district

Planning the development of the Toplica district, based on the principles of sustainability, implies the simultaneous monitoring of the development of its municipalities under the influence of selected economic, social and environmental factors of development. The number and value of these factors and its influences on the development of municipalities in the Toplica district have conditioned the need to use mathematical models, which are based on their multi-criteria analysis, offering a sequence of alternative solutions (position of municipalities in sustainable development). For the selected influencing development factors, the initial quantification matrix was formed, as a starting point for the application of multicriteria analysis using the ELECTRE method [11,12]. Consideration of this method for multi-criteria analysis aims to verify the obtained solutions, their compatibility and reliability in determining the final solution on the position of the municipalities of Toplica district in the field of sustainable development.

3. RESULTS

3.1 Multicriteria analysis - ELECTRE method

The ELECTRE method is one of the methods of multicriteria analysis that are often used when solving problems with several alternatives and influencing factors of different origins and units of measure. From the initial matrix for ranking the municipalities of the Toplica district, all the complexity and diversity of development factors can be seen, which justifies the choice of this method for further analysis. By forming a normalized matrix from the initial decision matrix by applying the norm of decision criteria ($\sqrt{\Sigma Xi^2}$jwhere Xij is one of the development criteria), the problem of dimensional discrepancy between development factors was eliminated and conditions were created for conducting multicriteria analysis for obtaining solutions in quantitative form and its evaluation.

The ELECTRE method bases its analysis on the comparison of alternative solutions in pairs (each with each alternative), with the aim of obtaining first the degree of agreement between their weights, and then the degree of disagreement according to which the analyzed alternatives differ in weight.

The procedure of applying the method itself is iterative and consists of the following steps:

1. Calculation of the normalized decision matrix (N)
2. Calculation of weight normalized matrix (TN) (two variants of weight criteria)
3. Determining sets of agreement and disagreement (Sij, Nij)
4. Determining the compliance matrix (MS)
5. Determining the non-compliance matrix (MNS)
6. Determination of matrix aggregate dominance (MAD)
7. Ranking of alternative solutions and conclusion

An overview of the practical application of this method with its procedures on the problem of defining the state of sustainable development of the municipalities of the Toplica district is given in Table 1.

Table 1. Initial matrix for decision-making on sustainable development of Toplica district - ELECTRE method

Alternative-municipality / **Development factor criterion**		**Kuršumlia** **a1**	**Blace** **a2**	**Prokuplje** **a3**	**Žitorođa** **a4**	**Normof decision criteria** $\sqrt{\Sigma Xij^2}$
I Population						
f_1- Age index	min	1.284	1.890	1.230	1.383	8.646 = 2.9400
f_2- Coefficient of working capacity of the population	min	0.284	0.416	0.283	0.350	0.4563= 0.6375
f_3- Degree of education	max	2.510	2.480	2.630	2.260	√24.475= 4.9472
II Economy - activity of the population						
f_4-Economic Sustainability Index I	min	1.135	1.004	1.452	0.729	√4.936= 2.2217
f_5-Economic Sustainability Index II	max	1.720	2.040	1.766	1.347	√12.0532= 3.4718
f_6- Sustainability ratio	max	0.85	0.74	0.88	0.89	√2.803= 1.6742
III Social standard						
f_7-Education-density of primary and secondary schools	max	0.1777	0.5000	0.3364	0.700	√0.8847= 0.9406
f_8- Health care standard	max	0.0018	0.0016	0.0037	0.0010	√0.00002= 0.0045
f_9- Degree of road construction (km/h)	max	0.0290	0.0170	0.0080	0.0060	√0.00123= 0.0351
IV Ecology and environment						
f_{10}- Available land per household	max.	3.37	3.12	3.17	2.44	√39.651= 6.2970
f_{11}- Degree of forest exploitation	min	1.26%	1.66%	1.40%	0.70%	√6.7932= 2.6063
f_{12}- Degree of water utilization for water supply	min	35%	44%	55%	121%	√23852= 144.32

Based on the data of the aggregate dominance matrix (MAD) for variant (1), the following follows: Alternative a3 (municipality of Prokuplje) dominates in the field of sustainable development over other alternatives (municipalities): a1, a2, a4 (Kuršumlija, Blace, Žitorođa), respectively; Alternative a1 (Kuršumlija) and a2 (Blace), dominate in sustainable development over alternative (municipality) a4 (Žitorođa); Alternative a4 (Žitorođa) does not dominate any alternative (municipality); Alternative a1 (Kuršumlija) and a2 (Blace) have equal dominance in sustainable development.

Based on the data obtained from the analysis conducted by the ELECTRE method with the application of two, variant proposals of weight criteria, it can be concluded that for both variants: Alternative a3 (Prokuplje municipality) dominates in the field of sustainable development over other alternatives a1, a2, a4 and Žitorođa), respectively; Alternative a4 (Žitorođa) does not dominate any alternative (municipality of Toplica district); Alternatives a1, a2 (municipalities of

Kuršumlija, Blace), respectively, dominate over alternative a4 (municipality of Žitorođa) and Alternative a1 (Kuršumlija) because they have a slight advantage of sustainable development compared to alternative a2 (municipality of Blace).

4. CONCLUSIONS

Economic development is one of the changing factors of development, relying primarily on the available natural and human resources of the region and its municipalities. As these potentials also differ between municipalities within the region, this is consequently transferred to their economic and overall development. The methodological approach for the analysis of their condition and status within the region is completely equivalent to the new concept, which is defined in this paper, and refers to sustainable regional development, starting from the process of preparing and defining research programs to the final solution on the state and directions, further economic and overall sustainable development of the municipalities of the Toplica region.

ACKNOWLEDGEMENTS

This paper is partly supported by the Registration N°451-03-9/2021-14/200052 administered by Ministry of Education and Science of the Republic of Serbia.

REFERENCES

[1] Milenković, M., Vaseashta, A., Vasović, D., Strategic Planning of Regional Sustainable Development Using Factor Analysis Method. Pol. J. Environ. Stud. 30 (1) (2021) 1-7.
[2] Cvijanović, D., Rodica, B. Factors of Regional and Local Economic Development, Institute for Agricultural Economics, Beograd, 2013.
[3] Frankowski, P., Zbierska, J., Stansisyewski, R., Kayzer, D. Effect of Newly Created Water Reservoirs on Agricultural Landscape Stability, Polish Journal of Environmental Studies 28 (5) (2019) 3173.
[4] Statistical Office of the Republic of Serbia, Official Gazette of the Republic of Serbia, Beograd (2016) 222-287.
[5] Panchal, R., Singh, A., Diwan, H., Does circular economy performance lead to sustainable development? – A systematic literature review. Journal of Environmental Management 293 (2021) 112811.
[6] Ciplet, D., From energy privilege to energy justice: A framework for embedded sustainable development. Energy Research & Social Science 75 (2021) 101996.
[7] Opricović, S. Multi-criteria Optimization in Construction, Faculty of Civil Engineering, Beograd, pp. 119-171, 1998.
[8] The World Commission on Environment and Development, Our common Future, Oxford, New York, Oxford University Press, 1997.
[9] Volkan Oral, H., EhsanKakar, A., Saygin, H., Feasible industrial sustainable development strategies for the Herat Province of Afghanistan. Technology in Society 65 (2021) 101603.
[10] National Sustainable Development Strategy of the Republic of Serbia, Official Gazette of the Republic of Serbia, No. 57/2008, 14, 2008.
[11] Chen, Z.-S., Martínez, L., Chang, J.-P., Wang, X.-J., Xionge, S.-H., Chin, K.-S., Sustainable building material selection: A QFD- and ELECTRE III-embedded hybrid MCGDM approach with consensus building. Engineering Applications of Artificial Intelligence 85 (2019) 783-807.
[12] Opricović, S., Tyeng, G.-H. Extended VICOR method in comparison with outranking methods, European Journal of Operational Research 178, 514-529, 2007.
[13] National Strategy for Sustainable Use of Natural Goods and Resources. Official Gazette of the Republic of Serbia, No. 32/2012 Beograd, 2012.
[14] Government of the Republic of Serbia, Public Policy Secretariat, Serbia and Agenda 2030, Beograd, 2019.
[15] Ronan Cooney, Alex H L Wan, FearghalO'Donncha, Eoghan Clifford, Designing environmentally efficient aquafeeds through the use of multi-criteria decision support tools. Current Opinion in Environmental Science & Health (2021) 100276.
[16] Frankowski, P., Zbierska, J., Stansisyewski, R., Kayzer, D. Effect of Newly Created Water Reservoirs on Agricultural Landscape Stability, Pol. J. Environ. Stud. 28 (5), 3173, 2019.
[17] Yarnall, K., Olson, M., Santiago, I., Zelizer, C., Peace engineering as a pathway to the sustainable development goals. Technological Forecasting and Social Change 168 (2021) 120753.

The 52nd International October Conference on Mining and Metallurgy
November 29th – 30th , 2021
www.ioc.tfbor.bg.ac.rs

LONG-TERM PLANNING OF MINING THE LEAD AND ZINC ORE DEPOSIT IN THE BRSKOVO ORE FIELD, THE REPUBLIC OF MONTENEGRO

Daniel Kržanović[1], Radmilo Rajković[1], Dejan Stevanović[2],Miomir Mikić[1], Milenko Jovanović[1], Sanja Petrović[1]

[1]Mining and Metallurgy Institute Bor, Zelenibulevar 35, 19210 Bor, Serbia

[2]Faculty of Mining and Geology, University of Belgrade, Djusina 7, 11120 Belgrade, Serbia

Abstract

Profitable mining of mineral deposits requires some assessment and planning. The objective of these efforts is to determine the most profitable excavation plan and the highest rate of return on investment. These tasks are performed in the field of long-term planning.Using the Whittle software for strategic planning and optimization of excavation boundary and software Gems for construction the open pits, the long-term directions of exploitation the lead and zinc ore deposits in the Brskovo ore field are defined depending on the flotation processing capacity, quality of mineral raw material in terms of useful and harmful components. and making the maximum profits in that production process.

***Keywords**: long-term planning, Brskovo ore field, optimization, Whittle and Gems software packages.*

1. INTRODUCTION

The basic, primary input in the planning and design process of the open pit is a geological block model of the ore body. It is very important to accurately calculate the block value in optimization, because the wrong calculation leads to the wrong optimal contour of the open pit [1].

The most commonly accepted objective, in complex production systems, in optimizing the open pit boundary is to maximize the net present value of future cash flows. To achieve this objective, the spatial relationship of variables in the deposit (such as the geographical location of deposit and its geological properties) as well as the temporal relationship of variables (including the order in which the ore will be mined and processed) must be taken into account, and consequently a derived cash flow.

The Brskovo ore field includes four lead and zinc deposits: Brskovo, Igrišta, ŽutaPrla and Višnjica. All deposits are located about 6 km east of Mojkovac and belong to the Municipality of Mojkovac.

Deposits of the Brskovo ore field were exploited in the period 1976-1987 using the open pit and underground mining methods. About 960,000 t of ore from the Brskovo deposit and about 2,020,000 t of ore from the ŽutaPrla deposit were excavated. The exploitation of mentioned deposits was suspended due to poor economic effects, caused by the high exploitation costs and low recovery of useful elements from the lead and zinc ore deposits.

2. SOFTWARE MODELING OF THE DEPOSIT

Block models for the lead-zinc ore deposits "ŽutaPrla-Višnjica" (hereinafter ZPV) and "Brskovo" were made in the Geovia Gems software package and represent the block models with regular blocks sizes 10x10x5. The economic value of the deposit is determined on the basis of

the value of metals present in the ore, i.e. lead, zinc, copper and silver. The economic effects of ore exploitation are calculated on the basis of the selling price of payable metals in the ore, i.e. lead, zinc, copper and silver. Based on this, the cut-off grade of equivalent lead and zinc (Pb + Zn) metals in the ore was determined, which is GS = 0.6% Pb + Zn. Blocks with content for Pb + Zn below GS are treated as waste.

One of the key factors in creating an economic model for the ZPV and Brskovo deposits is the assessment of mercury content in concentrate, i.e. the value limitation to 900 ppm.

To estimate the mercury content in concentrate, the following formula was developed, on the basis of conducted experimental research:

$$Hg_{\_CON} = \left(\frac{Hg[ppm]}{Zn[\%] \times 0.01}\right) \cdot 0.406 \quad [ppm] \tag{1}$$

The formula is based on the mean contents of mercury (Hg, ppm) and zinc (Zn,%) in the run-of-mine ore. The next step is to create a new attribute of mercury content called ZnHg, which contains ≤900ppm Hg. A script is written using a scripting language that defines the ore with mercury content of ≤900ppm.

The panel in Figure 1 shows a script used by the Gems software to separate the ore with mercury content ≤900ppm and ore with mercury content > 900ppm.

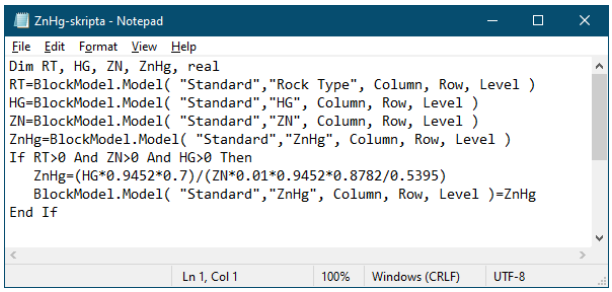

Figure 1. Script used by the Gemssoftware for separation the defined ore types

3. OPTIMIZATION THE BOUNDARY OF THE OPEN PTIS - SELECTION OF OPTIMAL FINAL CONTOURS AND PUSHBACKS

Optimization of the open pits at the Brskovo site was made on the basis of two block models of deposits and defined the input techno-economic parameters.

Optimization of the open pits was made on the balance reserves using the Whittle software that is the industry standard for this area. The Whittle software package uses a modified Lerch Grosmman algorithm in the optimization process, according to which the optimal contour of the open pit is obtained on the basis of economic value of individual mini blocks in the deposit. The software has the ability to change the size of revenue applying the revenue factor to the metal prices and thus generate more possible contours of the open pits [2].

Taking into account the amount of exploitation reserves affected by the open with a coefficient of revenue factor of 1, which corresponds to the optimal open pit based on undiscounted profit, the ore excavation capacity, minimum width between excavations of 50m, a decision was adopted to determine the final limit of optimal open pit for discounted profit based on the excavation of the final open pit in two pushbacks [3]. Based on this solution, the analysis of potential contours of the first pushback and optimal final contour of the open pit ZPV was carried out. The results of carried out analysis are shown graphically in Figure 2.

Analyzing the optimal development of the open pit ZPV, for the case of phase development with one Pushback (open pit 12 in the analysis), it was obtained that the optimal final contour of the

open pit ZPV, the open pit under ordinal number 30 (revenue factor = 0.94). The open pit 30 provides the maximum Net Present Value ("Specified case") for the analyzed phase development.

Analyzing the optimal development of the open pit Brskovo, for the case of phase development with one Pushback (open pit 16 in the analysis), it was obtained that the optimal final contour of the open pit Brskovo, the open pit under number 33 (revenue factor = 0.96). The open pit 33 provides the maximum Net Present Value ("Specified case") for the analyzed phase development. Also, the result of analysis the Brskovo open pit showed a low sensitivity to the Net Present Values in the selection of potential Pushbacks, which is evident in the small difference in Net Present Value between the "Best case" and the "Worst case" analysis. The reason for small difference in the Net Present Values between the analyzed variants is a short service life for the Brskovo open pit [4].

a) 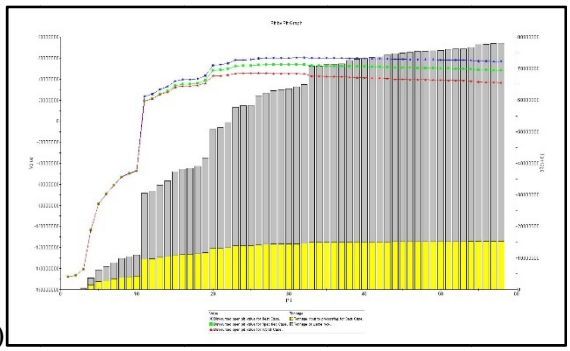 b) 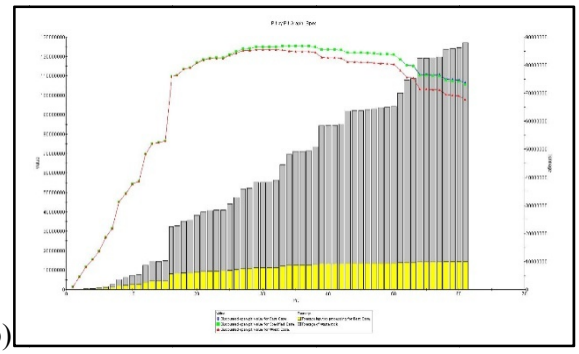

Figure 2. Pit by Pit graphs for the open pits: a) ZPVand b) Brskovo

4. OPTIMIZATION OF EXCAVATION DYNAMICS

After selection of pusbacks and final contours of the open pits, defining the order in which the blocks will be excavated is approached, i.e. the optimization of excavation dynamics is performed. This process was carried out in the Whittle software, using the Milawa algorithm-balancing mode, Figure 3. Excavation dynamics includes the period of excavation at the open pit ZPV (Period 0) and additional 7 years of excavation at the open pits ZPV and Brskovo.

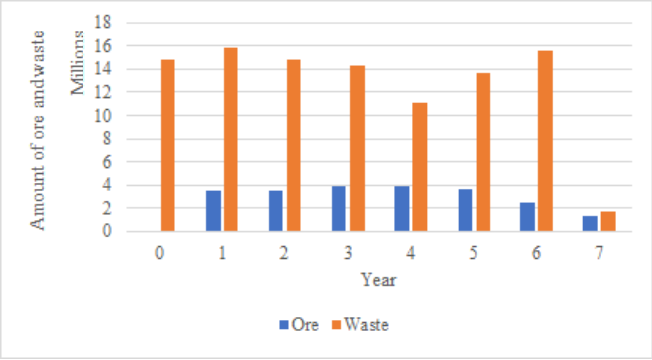

Figure 3. Dynamics of ore excavation at the open pits ZPV andBrskovo

5. NET PRESENT VALUE

Discounted cash flow analysis (DCF analysis) is a universally used method for evaluating the economic performances in a project. As such, it is often incorporated into algorithms, for optimization and production planning, commercial software packages (Whittle). The most common type of economic analysis comes down to the projection of cash flow during the project life.

The results of the carried out DCF analysis is shown in the graph of discounted cash flow, Figure 4. The realized net present value by exploitation of lead and zinc ore in the Brskovo ore field is 84,746,781 $ (discounted with 10%).

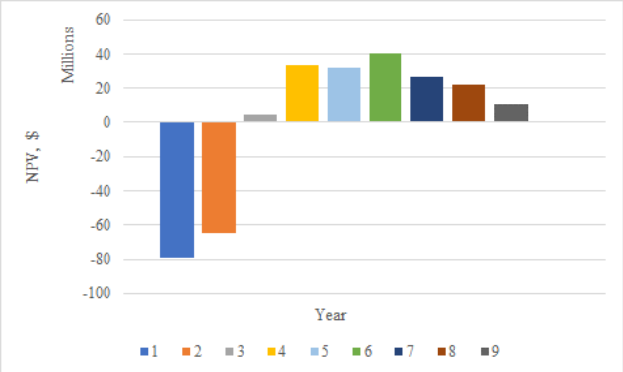

Figure 4. Graph of discounted cash flow

6. CONCLUSION

The applied approach of comprehensive understanding the process of planning the deposit exploitation in the Brskovo ore field using the modern software tools, which are based on the optimization algorithms such as the Lerchs - Grossmann algorithm, Milawa algorithm, and other procedures based on computer programs, provides a profitable exploitation. The result of such approach is the improvement of exploitation the lead and zinc ore deposits ŽutaPrla-Višnjica and Brskovo, which are characterized by the presence of high mercury content in certain batches of deposits in the complex working conditions, and which is reflected in better financial effects in the mine operations

The discounted cash flow analysis shows a net present value of $ 84,746,781 $. Based on that, the conclusion follows that the future exploitation of lead and zinc deposits in the Brskovo ore field is profitable.

ACKNOWLEDGEMENTS

This work was financially supported by the Ministry of Education, Science and Technological Development of the Republic of Serbia, Grant No. 451-03-9/2021-14/ 200052.

REFERENCES

[1] D. Kržanović, M. Ljubojev, I. Jovanović, N. Vušović, An Analysis the Effects of Changes in Price of Metal and Operating Costs to the Profit in Exploitation the Copper Ore Deposits, A Case Study: Copper Mine Majdanpek, Serbia, Mining & Metallurgy Engineering Bor, No. 3-4 2017, pp. 51-58.

[2] D. Kržanović, N. Vušović, M. Ljubojev, R. Rajković, Importance of Planning the Open Pits in the Conditions of Contemporary Mining - A Case Study: The Open Pit South Mining District Majdanpek, Mining & Metallurgy Engineering Bor, No. 1-2 2017, pp. 15-22.

[3] D. Kržanović, N. Vušović, M. Ljubojev, Selection of the Optimum Pushbacks in a Long-Term Planning Process of the Open Pit – A Condition for Maximization the Net Present Value: Case Study: The Open Pit VelikiKrivelj, Serbia, Mining Engineering, Mining and Metallurgy Institute Bor, No. 1-2/2018, pp.37-44.

[4] D. Kržanović, R. Rajković, N. Vušović, M. Jovanović,Selection of the Optimal Contour of the Open Pit in Mining the Lead and Zinc Ore Deposit with the Increased Mercury Content, Mining & Metallurgy Engineering Bor, No. 1-2 2021, pp. 35-42.

The 52nd International October Conference on Mining and Metallurgy
November 29th – 30th , 2021
www.ioc.tfbor.bg.ac.rs

CALCULATION OF SAFETY DISTANCE FOR THE OPERATION OF MINING EQUIPMENT IN THE WORKING ENVIRONMENT WITH WEAKENED CHARACTERISTICS AT THE OPEN PIT "NORTH MINING DISTRICT" OF THE COPPER MINE MAJDANPEK

Radmilo Rajković[1], Daniel Kržanović[1], Miomir Mikić[1], Milenko Jovanović[1]

[1]Mining and Metallurgy Institute Bor, Zelenibulevar 35, 19210 Bor, Serbia

Abstract

At the Open Pit "North Mining District" of the Copper Mine Majdanpek, exploitation is planned in the northeastern part of the deposit. The total height of excavation is 195 m with floors of 15 m high. The works are partly performed in the working environment with weakened geomechanical characteristics. This paper presents the calculation of a safety distance for the operation of mining equipment on each floor of the exploitation.

***Keywords**: OP "North Mining District", stability calculation, safety distance.*

1. INTRODUCTION

The Copper Mine Majdanpek is located in eastern Serbia, in the immediate vicinity of the town of Majdanpek, in the south and west of it, in the Mali Pek river basin. Within the copper deposits "North Mining District" and "South Mining District", there are the same named open pits at a distance of 0.5 km from each other. In the immediate vicinity of the deposit there are the infrastructure facilities, which are used for the ore processing, as well as the waste and flotation tailings dumps.

Until 1977, within the Copper MineMajdanpek, only the open pit "South Mining District" was in operation, when the open pit "North Mining District" started operation. Until 1993, only copper ore was mined and copper concentrate was produced, when the excavation of zinc and lead ore began as well as the production of this concentrate. The works at the open pit "North Mining District" were developed within three work sites: "Central part", "Tenka" and "Dolovi".

The open pit "North Mining District" has an elliptical shape of approximate length along the larger axis of 1,900 m and along the smaller axis of 1,100 m. The highest point of the open pit is approximately at the level of k675 m. The lowest point that the open pit currently reached is k360 m. The operation was carried out on a floor with a floor height of 15 m. Up to the level of k452 m, the open pit is of a height type, and below the level of k452 m the open pit passes into a depth type. The current view of the open pit "North Mining District" is shown in Figure 1.

So far, about 33.5 Mt of copper ore and 600,000 tons of polymetallic ore have been produced from the open pit "North Mining District". About 130 Mt of waste was excavated [1].

During 2021 and 2022, it is planned to continue the works in the northeastern part of the open pit. A part of the working environment in which the excavation will be performed has the weakened geomechanical characteristics. The excavation technology is discontinuous: drilling, blasting, loading and transport, with the auxiliary mining works and drainage of the open pit. Therefore, it is necessary to determine a safety distance from the edge of floors for heavy equipment operation (hydraulic excavators and trucks) at all floors of excavation.

Figure 1 The Open Pit "North Mining District"

2. STARTING BASES FOR CALCULATION THE SAFETY DISTANCE

Calculation the safety distance for equipment operation in the working environment zone with weakened geotechnical characteristics was made on a geotechnical profile 3 - 3'[2], Figures 2 and 3. The calculated parameters of the working environment [3] are shown in Tables 1 and 2.

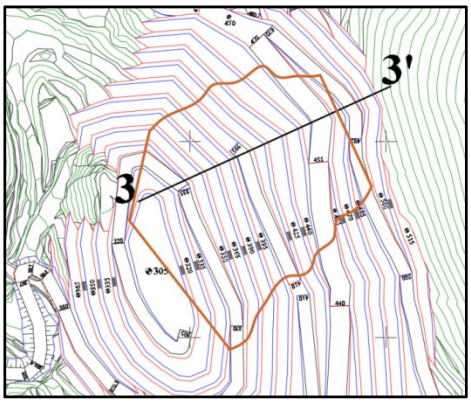

Figure 2 Position of geotechnical profile 3 – 3'

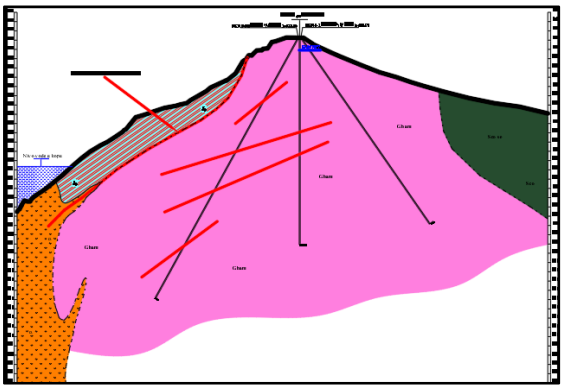

Figure 3 Geotechnical profile 3 – 3'

Table 1 Calculating parameters of the working environment 1

Working environment	Cohesion kPa	Angle of internal friction °	Bulk density kN/m^3
Massive and banked limestones	32	31	26.65

Table 2 Calculating parameters of the working environment 2 and 3

Working environment	UCS kPa	m	s	Bulk density kN/m^3
Gneisses - biotitic, amphibolitic, muscovitic	38.880	1.210300	0.000121896	27.00
Andesites and tectonic breccias	24.500	0.786973	0.000074391	26.03

A hydrogeological model of the deposit has not been developed yet. To determine the safety distance, the pore water coefficient ru = 0.2 was adopted for all working environments [3].

Technology of landslide removal is such that a complete floor is excavated, and then it is moved to a lower floor. The maximum surface load from equipment at the open pit was adopted on the basis of data on the types of excavators and trucks that are planned to be used. These loads are:
Hydraulic excavator: 2 x 61 kN/m; Rear axle of full truck: 2 x 324 kN/m

According to the Rulebook on technical requirements for the open pit exploitation of mineral deposits (Official Gazette of RS, No. 96/2010), for calculation the stability of the working slopes of the floor system for solid rocks at the open pits, the minimum allowable safety factor is Fs = 1.05.

3. SAFETY DISTANCE CALCULATION

The stability calculation was performed with the Rocscience software package [4, 5], i.e. its Slide tool on the basis of boundary equilibrium conditions [4 - 12]. Calculations were performed by the Morgenstern - Price and Bishop methods for the arbitrary sliding surfaces. The program allows automatic search of the critical sliding surface with a minimum safety factor.

Stability analysis on the 3 - 3'profile was performed for each floor of excavation, with the existing water lake up to elevation k383.5 m and for the situation that the water was removed.

The area of sliding surfaces with a safety coefficient of less than 1.05 is defined on each floor, i.e. the safety distance of excavators and trucks from the edge of floor. This distance is increased by 20% for safety, Figure 4.

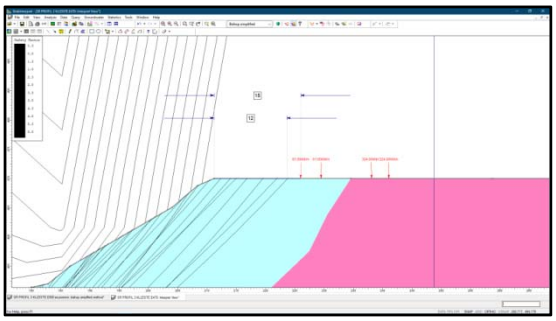

Figure 4 Safety distance from the edge of floor for equipment operation

The output interface of the Slide program for calculation the stability on 3 - 3'profile for one floor is shown in Figures 5 and 6. The safety distances from the edge for equipment operation on each floor are shown in Table 3.

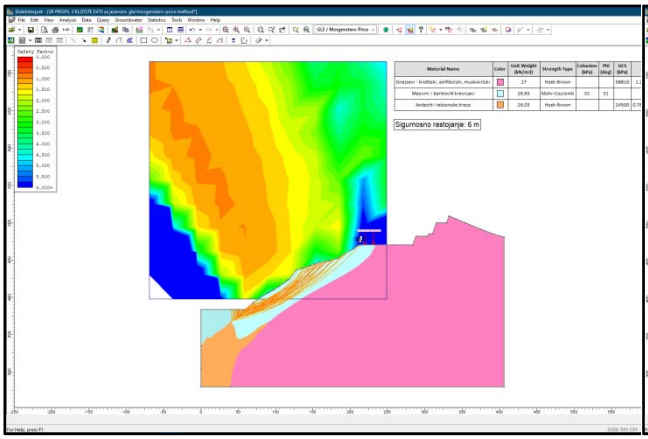

Figure 5 Calculation of stability with a water lake for thefloor E470 by the Morgenstern – Price method

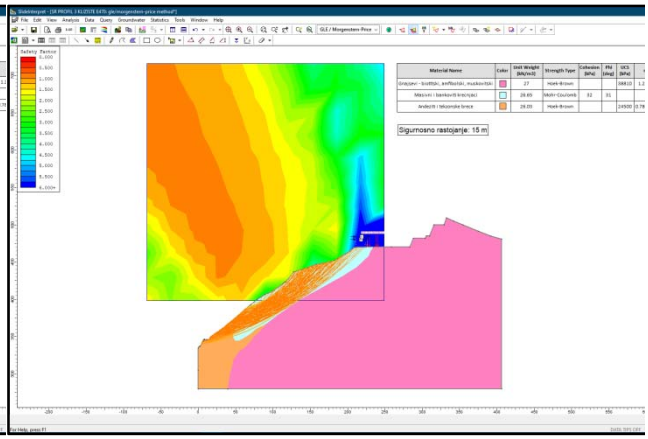

Figure 6 Calculation of stability without a water lake for thefloor E470 by the Morgenstern – Price method

Table3 Safety distances in the zone of weakened material

Floor	Without a lake on the open pit bottom		With a lake up to K383.5 m	
	Zone with Fs<1.05	Adopted safety distance from the floor edge m	Zone with Fs<1.05	Adopted safety distance from the floor edge m
E500	15	18	<10	10
E485	12	15	10	12
E470	12	15	<10	10
E455	20	24	<10	10
E440	49	59	29	35
E425	32	40	10	12
E410	23	28	<10	10
E395	<10	10	-	-

4. CONCLUSION

The safety distance of loading and transport machinery from the outer edge of floor was calculated on the basis of geomechanical characteristics of the working environment and load of machinery, with the required safety coefficient.

The existing accumulation of water on the bottom of the open pit has a great effect on the safety distance of floor from the outer edge of floor. The existence of a water accumulation reduces the safety distance because it acts as a ballast. Due to this reason, the dynamics of water pumping must follow the dynamics of excavation works. Only the amount of water that interferes with the descent to the lower floors should be pumped out.

Loading and transport equipment as well as transport routes on the floor level must be located within the safety zone.

From the moment of possible occurrence, the slope deformations, they must be visually and instrumentally observed. For each specific situation, a program of organized monitoring the occurrence of slope deformations must be made.

ACKNOWLEDGEMENTS

This work was financially supported by the Ministry of Education, Science and Technological Development of the Republic of Serbia, Grant No. 451-03-9/2021-14/200052.

REFERENCES

[1] Radmilo Rajković, Igor Svrkota, Dragan Milanović, Mile Bugarin: Uzdizanjeproizvodnje bakra u Srbiji, stanjei perspektive – Deo 1. Rudarskikompleks; IX kolokvijum o pripremimineralnihsirovina; Univerzitet u Beogradu, Rudarsko – geološkifakultet, Katedra za pripremumineralnihsirovina; Beograd 26. oktobar 2018; str. 174 – 202; ISBN 978-86-7352-326-2

[2] Izveštaj o inženjerskogeološkimistraživanjimanapovršinskomkopu Severnirevir u Majdanpeku;Institut za rudarstvoimetalurgijuBor, 2021.

[3] Elaborat o stabilnostiprojektovanogzavršnogstanjapovršinskogkopa Severnirevir; Institut za rudarstvoimetalurgijuBor, 2021.

[4] Radmilo Rajković, LjubišaObradović, DanielKržanović, MiomirMikić: Stabilityofthe Dam ”PrevojŠaška“ oftheFlotationTailingDump ‘ValjaFundata“ in Majdanpek; MiningandMetallurgyEngineering Bor, 1-2/2019, pp. 9-18; ISSN 2334-8836, UDK (045)=111, DOI 10.5937/mmeb1902009R

[5] Radmilo Rajković, DanielKržanović, MiomirMikić, Milenko Jovanović: StabilityoftheAshandSlagLandfill "Maljevac" – PljevljaforOvertop to thePeakElevation K+832 m; MiningandMetallurgyEngineering Bor, 1-2/2018, pp. 17-26; ISSN 2406-1395, UDK 626.877:622.613.11/.13:681.51(045)=111, DOI 10.5937/mmeb1802017R

[6] Radmilo Rajković, DanielKržanović, MiomirMikić: StabilityDump Pit Mine “CerovoCementacija 1“, 46th InternationalOctoberConference on MiningandMetallurgy, 01-04 October 2014 BorLake, Serbia; pp. 309-313; ISBN: 978-86-6305-026-6

[7] Radmilo Rajković, DanielKržanović, MiomirMikić: StabilityofFlotationTailings in LeposavićUsing Software Package GeoStudio2007, Mining 2014 Vrnjačka Banja; pp. 390-397; ISBN: 978-86-80809-84-7

[8] Radmilo Rajković, LjubišaObradović, MiomirMikić, DanielKržanović: ApplicationofStandardsforDesigningEmbankmentsandEarthDams in theStabilityCheckDamsFlotationTailing RTH in RTB Bor; Rudarstvo 2016, pp. 298-307, SremskiKarlovci 24-26.05.2016. ISBN: 978-86-80420-03-5

[9] Radmilo Rajković, Mile Bugarin, VladanMarinković: StabilityAnalysis on Dumping „Oštreljskiplanir“ ofthe Open Pit Mine “Bor“ in a FunctionofWaterQuantity, MiningandMetallurgyEngineering Bor 3/2013, pp. 49-64, UDC: 622.271:621.65:681.51(045)=20, DOI: 10.5937/MME1303049R, ISSN: 2334-8836

[10] Radmilo Rajković, DanielKržanović, MiomirMikić, VladanMarinković: StabilityofAshandSlugDump on ThermalPowerPlant Gacko withthe Software Geostudio 2007; pp. 227-231; Mining 2013 PlansforDevelopmentandImprovementofMining; VelikoGradište, Srebrnojezero 28-31 May 2013; ISBN: 978-86-80809-78-6

[11] Radmilo Rajković, DanielKržanović, RužicaLekovski: StabilityAnalysisofInnerWasteDump “Kutlovaca” oftheCoal Open Pit Mine “Potrlica“– PljevljaUsingtheGeoStudio 2007 Software; MiningEngineering 1/2010; pp. 69 – 80; ISSN: 1451-0162

[12] Radmilo Rajković, DanielKržanović, Branislav Rajković; AnalysisofStabilityduringtheCleaningofCassettes 1 and 2 ofSettingPond Filter oftheWastewaterPurificationFacilitiesof Kolubara – PreradaVreoci bythe Software Geostudio 2007; 42. InternationalOctoberConference on MiningandMetallurgy; pp. 33-40; ISBN 987-86-80987-79-8

HARDENSS, MICROHARDNESS AND ELECTROCONDUCTIVITY OF ALLOYSWITH VARIABLE Cu CONTENT INCu-Al-Ag SYSTEM

Zdenka Stanojević Šimšić[1], Ana Kostov[1], Aleksandra Milosavljević[1], Emina Požega[1]

[1]Mining and Metallurgy Institute Bor, Zeleni bulevar 35, 19210 Bor, Serbia

Abstract

The results obtained from the experimental determination of hardness, microhardness and electrical conductivity of the selected as-cast alloys along Ag0.5Al0.5-Cu vertical section in the ternary Cu-Al-Ag system, are represented in this paper. All microhardness and hardness measurements were carried out using standard procedure by Vickers method.Electrical conductivity was determined using"Institute dr. Förster SIGMATEST 2.06" device.

***Keywords**: Hardness, Microhardness, Electroconductivity, CuAlAg Alloys.*

1. INTRODUCTION

For many years various groups of materials known as smart materials, have been studied regarding their special characteristics, by different disciplines of materials science.The main characteristic of these materials is that the change of external conditions leads to a change in the properties of the materials (mechanical, electrical, structural) [1]. A part of this large group are shape memory materials which include different kinds of materials from metal alloys to textile[2-3]. It is already well known that these materials are characterized with some special properties which are unique among all kinds of smart materials such as the shape memory effect,pseudoelasticity and in some cases biocompatibility. Among many different systems, Cu-Al based alloys belong to the shape memory materials, too. These materials have been studied for a long time in details and some of them have practical application, like the alloys of the Cu-Zn-Al and Cu-Al-Ni systems, but the interest does not cease and a huge number of investigations are carried on[1-10]. Such interest is caused by the fact that beside the appropriate properties, the production of alloys is less complicated and the costs are lower comparing to the alloys of other systems [10].So, Cu-Al based materials are very good for application in engineering, space technology, medicine, bioengineering and others.

In the frame of research conducted in order to investigate as-cast alloys of the ternary Cu-Al-Ag system regarding thermal behavior, microstructure and phase equilibria, hardness,microhardness and electrical conductivity were determined, too. Obtained results of hardness,microhardness and electrical conductivity measurements for the alloys located in the area with constant Al:Ag molar ratio equal to 1:1 and variable molar ratio of Cu of the ternary Cu-Al-Ag system, are presented in this paper.

2. EXPERIMENTAL

As it was already mentioned above, all investigations were done with as-cast alloys. Samples were prepared by induction melting under argon atmosphere with total metal losses of the masses less than 1%.The purities of theconstituent metals Cu, Al and Ag were 99.99%. Obtained samples were of cylindrical shape weighing about 3g, diameter 7mm and length 20mm. The hardness and microhardness measurements were done by Vickers standard method.

Hardness was determined at load of 10, 20 and 30N while microhardness at load of 100g. Microhardness measurements were done on the PMT-3 microscope hardness meter. All measurements were done in three points for each sample. Electrical conductivity measurements were carried out on "Institute dr. Förster SIGMATEST 2.06"device.

Composition and mass of selected as-cast alloys are presented in Table 1.

Table 1 - Composition and mass of investigated alloy samples

Sample	X_{Cu}	X_{Al}	X_{Ag}	m_{Cu}	m_{Al}	m_{Ag}
$Cu_{20}Al_{40}Ag_{40}$	0,2	0,4	0,4	0,5720	0,4858	1,9422
$Cu_{40}Al_{30}Ag_{30}$	0,4	0,3	0,3	1,1575	0,3686	1,4738
$Cu_{60}Al_{20}Ag_{20}$	0,6	0,2	0,2	1,7570	0,2487	0,9943
$Cu_{80}Al_{10}Ag_{10}$	0,8	0,1	0,1	2,3710	0,1258	0,5031

3. RESULTS AND DISCUSION

Selected alloys were located in section with variable molar ratio of Cu and equal molar ratios of Ag and Al, in ternary Cu-Al-Ag system, i.e. in the area along Ag0.5Al0.5-Cu vertical section,according to their chemical compositions. Micrographs of investigated sample alloys, obtained by optical light microscopy are presented in Figure 1.

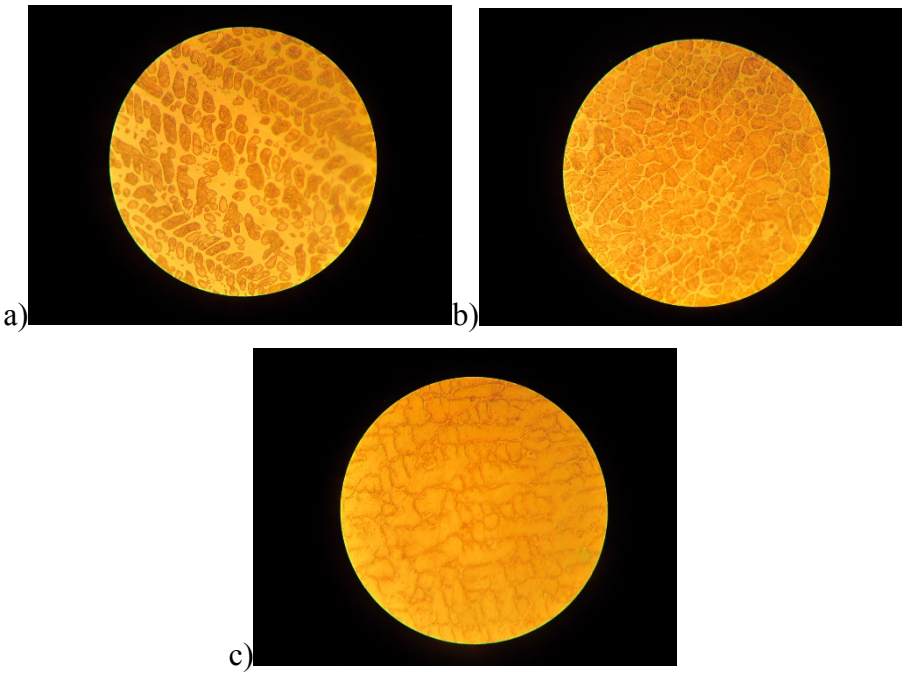

Figure 1. Microstructure of selected alloy samples (magnification 500x): a) $Cu_{40}Al_{30}Ag_{30}$, b) $Cu_{60}Al_{20}Ag_{20}$,c) $Cu_{80}Al_{10}Ag_{10}$

3.1 Hardness measurements

Obtained results of the hardness measurement of the investigated sample alloys are shown in Table 2.The fact that various loads have been used for different samples leads to the conclusionthat the maximal hardness value is measured at the sample alloy$Cu_{40}Al_{30}Ag_{30}$ at a load of 30 kg.

Table 2 - Results of the hardness measurements for selected alloy samples

Sample	HV
$Cu_{20}Al_{40}Ag_{40}$	284(HV20)
$Cu_{40}Al_{30}Ag_{30}$	299(HV30)
$Cu_{60}Al_{20}Ag_{20}$	149(HV10)
$Cu_{80}Al_{10}Ag_{10}$	87,3 (HV10)

3.2 Microhardness measurements

Microhardness measurements of the selected sample alloys was carried out at a load of 100 g. Obtained results of the microhardness measurement of the investigated samples are presented in Table 3.

Table 3 - Results of the microhardness measurements for selected alloy samples

Sample	HV0.1			
	Measuring point 1	Measuring point 2	Measuring point 3	Mean values
$Cu_{40}Al_{30}Ag_{30}$	102	81	116	100
$Cu_{60}Al_{20}Ag_{20}$	211	198	216	208
$Cu_{80}Al_{10}Ag_{10}$	144	136	169	150

The maximum value ofmicrohardnesswas determined for the $Cu_{60}Al_{20}Ag_{20}$ alloy sample and minimal for the alloy $Cu_{40}Al_{30}Ag_{30}$.

3.3Determination of electrical conductivity

Values of electrical conductivity were determined only for sample alloy $Cu_{60}Al_{20}Ag_{20}$.

Table 4 - Results of electrical conductivity measurements

Alloy	Electrical conductivity (MS/m)			
	Measured values			Mean value
$Cu_{60}Al_{20}Ag_{20}$	6.5	6.1	7.1	6.566

4. CONCLUSION

As additional methods of characterization,hardness,microhardness and electrical conductivity measurements for selected as-cast alloys of the ternary Cu-Al-Ag system with variable molar ratio of Cu and equal molar ratios of Ag and Al,were carried out, too. Hardness and microhardness measurements were done by Vickers standard method. Loads of 10, 20 and 30 kg were used for hardness measurements. The maximal measured hardness value is obtained for sample $Cu_{40}Al_{30}Ag_{30}$at load of 30 kg. Maximal microhardness was determined for the sample $Cu_{60}Al_{20}Ag_{20}$ and minimal for $Cu_{40}Al_{30}Ag_{30}$ alloy sample.Electrical conductivity was determined only for sample alloy $Cu_{60}Al_{20}Ag_{20}$and its value was 6.566 MS/m.

ACKNOWLEDGEMENTS

This work was done with the financial support of the Ministry of Education, Science and Technological Development of the Republic of Serbia, within the financing of scientific research work at the Mining and Metallurgy Institute Bor, according to contract no. 451-03-9/2021-14/200052.

REFERENCES

[1] K. Otsuka, K. Shimizu, Y. Suzuki, Y. Sekiguchi, C. Taki, T. Homma, S. Miyazaki, Splavi s EffektomPamjati Form, Metallurgija, Moskva, 1990, p. 123.
[2] R. Dasgupta, J. Mater. Res. 29 (16) (2014) 1681-1698.
[3] Mustafa O. Göka, Mehmet Z. Bilira, Banu H. Gürcüm, World Conference on Technology, Innovation and Entrepreneurship, Procedia - Social and Behavioral Sciences 195 (2015) 2160 – 2169.
[4] W. Witusiewicz, U. Hecht, S. Rex, F. Sommer., J. Alloy. Comp., 337 (2002) 189-201.
[5] W. Witusiewicz, U. Hecht, S. G. Fries, S. Rex., J. Alloy. Comp., 385 (2004) 133-143.
[6] A. T. Adorno, R. A. G. Silva., J. Alloy. Comp., 473 (2009) 139-144.
[7] U. Böyük, N. Marasli, E. Çadırlı, H. Kaya, K. Keslioglu., Curr. Appl. Phys., 12 (2012) 7-1
[8] Z. StanojevićŠimšić, D. Manasijević, D. Živković, T. HoljevacGrgurić, A. Kostov, D. Minić, Ž. Živković., J. Therm. Anal. Calorim., 120 (2015) 149-155.
[9] Z. StanojevićŠimšić, A. Kostov, A. Milosavljević, Proceedings of 50th International October Conference on Mining and Metallurgy, 30th September-3rd October 2018, Bor Lake, Bor, Serbia, 2018, p. 211.
[10] Y. Zheng, Y. Liu, N. Wilson, S. Liu, X. Zhao, H. Chen, J. Li, Z. Zheng, L. Bourgeois, J-F. Nie, Microsc. Microanal., 25 (2019) 1700-1701.

The 52nd International October Conference on Mining and Metallurgy
November 29th – 30th , 2021
www.ioc.tfbor.bg.ac.rs

STRATIGRAPHY AND AGE OF ROCK UNITS AND MINERALIZATION IN THE TIMOK MAGMATIC COMPLEX ANDTHE BOR METALLOGENIC ZONE – A REVIEW

Miodrag Banješević[1],

[1]Technical Faculty Bor, University of Belgrade, V.J. 12, 19210 Bor, Serbia

Abstract

This study reports of stratigraphy and geochronology of rock units and mineralization of the Timok Magmatic Complex (TMC) and the Bor Metallogenetic Zone (BMZ)which belongs to theLate Cretaceous Apuseni-Banat-Timok-Srednogorje Belt (ABTS, part of the Tethyan-Eurasian Metallogenic Belt).Existing data are supplemented and systematized by the latest geological, stratigraphic and mineral exploration.The TMC developed on a continental crust composed of different types of the Proterozoic to the Lower Cretaceous rocks. The TMC consists of the volcanic/magmatic, volcanogeno-sedimentary and sedimentary units. The sedimentary processes and magmatism lasted nearly continuously throughout nearly the whole Late Cretaceous. The sedimentation lasted from the Albian-Cenomanian to the Maastrichtian. Magmatism occurred in two phases from the Upper Turonian to the Upper Campanian: V1 (90-83 Ma), V2 (83-78 Ma), with a steady decrease in age from east to west. Cu-Au porphyry mineralization take place between 87-80 Ma. Major mineralizationis related to the V1 magmatic phasepredominantly developed in the easternmost part of the BMZ.

***Keywords**: Timok Magmatic Complex, stratigraphy, aga data, volcanism, mineralization.*

1. INTRODUCTION

The Timok Magmatic Complex (TMC) almost totally overlap of the Bor Metallogenetic Zone (BMZ) which belongs to the Late Cretaceous Apuseni-Banat-Timok-Srednogorje Belt (ABTS, [1,2]) and together belong to the transcontinental Tethyan-Eurasian Metallogenic Belt [3].

Because the TMC and the BMZ as the entire ABTS are known to host some of the largest Cu and Au deposits in Europe, their geology has been frequently studied in the last several decades (e.g.,[4,5,6,7,8,9,10,11], among others). The studies covered various geological aspects of the origin and evolution of many parts of this belt and established solid genetic links between volcanic/magmatic processes and mineralization events. In this respect, the information based on stratigraphic relationships and high precision geochronology that includes Ar/Ar[5,6], U/Pb zircon dating (e.g., [4,9,11,12]) and Re/Os molybdenite dating [7] was of supreme importance.

In this study will be revised, supplemented and systematizedstratigraphy, geochronology and mineralization relationshipof the BMZ. The BMZ is famous for its large porphyry copper systems accompanied by high- and subordinate low-sulphidation epithermal Au ore deposits [13,14,15,16,17]. It has long been thought that the massive sulphide deposits had been mined out long ago, the recent discovery of a world class copper and gold deposit of ČukaruPeki seriously arouse new interests for further investigating the BMZ, both in the exploration and the scientific context[18,19,20].

2. GEOLOGY, STRATIGRAPHY, ROCK AND MINERALIZATION AGE DATA OF THE TMC AND THE BMZ

The areas of the BMZ and the TMC almost totally overlap (Figure 1). The geology of the TMC along with the main ore deposits within the BMZ, the available geochronology age determinations are given in Figure 1 and Table1. The stratigraphy and time space development

of the TMC and relationship of published sediment formations and magmatic suites[21,8] are given in Figure 2. The TMC developed on a continental crust composed of different types of the Proterozoic to the Lower Cretaceous rocks, partially overlaid by Miocene and Holocene sediments. After continuous carbonate sedimentation from the Early Jurassic to the Lower Cretaceous, a new sedimentation period commenced with the Albian transgression. These Albian–Cenomanian sedimentation processeshad clastic character and were related to oscillations of the depositional environment (Lenovac Formation, [21], Figure 2). After a hiatus, the Turonian–Senonian evolution commenced with a newsedimentary cycle. The sediments overlie the Cenomanian clastites, started with basal conglomerate and continues continuously, over wide area in the TMC with clastic to carbonate sediments (OštreljFormation,[21], Figure 2). The lowest part of the sediments contains microfauna (*Helvetoglobotruncanahelvetica*), indicating the Lower to the Middle Turonian age [21].During the Upper Turonian tothe Senonian, the whole TMC area shows a considerable difference in the evolution between the eastward and the westward tectonic block (Figure 2, [22]).

The volcanism/magmatismoccurred in two phases from the Upper Turonian to the Upper Campanian: V1 (90-83 Ma), V2 (83-78 Ma), Figure 2, Table 1. It predominantly consists of extrusive volcanics, shallow intrusions and volcaniclastics that are at places associated with volcano-sedimentary and sedimentary rock series, with a steady decrease in age from east to west.

In the eastward block, predominate volcanic rocks of biotite-hornblende andesite (±dacite) compositions (TimokAndesite, V1, [8,12], I volcanic phase in Figure 1). These rocks stratigraphically overlie the Cenomanian siliclastic sediments or the Turonian clastic to carbonate sediments (Figure 2). The available U/Pb zircon ages of the Timok Andesite (V1) range 90-83 Ma ([4,9,12], Table 1). In the same time, the available U/Pb zircon ages and volcanological analyses reveal that the first volcanic phase (V1) can be split into two sub-phases: V1A and V1B [12].

The V1A sub-phase andesite can betermed plagioclase-hornblende phyric, has mostly holocrystalline groundmass and is substantially altered and mineralized. It is represented by coherent, brecciated and volcaniclastic facies. The age of V1A ranges widely from 90 to 85 Ma ([4,12], Table 1).

The V1B can be termed hornblende-plagioclase phyric andesite. It is a fresh, non-mineralized rock displaying holo- to hypocrystalline texture and occasionally fluidal fabric. The V1B is represented by coherent lava flows or shallow intrusions, monomictic breccia and volcaniclastic rock.The V1B sub-phase shows an age range of ~85 to 83 Ma ([4,12], Table 1).

During the volcanismand especially after its interruption, in a shallow water environment, andesite volcanics begin to be resedimented, transported and formedvolcano-sedimentary package - epiclastics. The epiclastics are represented by polymictic andesite breccia, volcaniclastic conglomerate and sandstone, which matrix is often composed of clay, fine grained sandstones or reddish marls.These rocks are known as the MetovnicaEpiclastite([8], Epiclastic in Figure 1), are usually interlayered with marls and siltstoneand sometimes, contain well-preserved microfauna the Coniacian–Campanian age [22,23,12].

The sedimentary series of the Oštrelj Formation are continuously developed and can be found over the Early Cretaceous rocks of the volcanic basement rock but also as underlying or overlying the V1 and V2volcanites and their epiclastic products (MetovnicaEpiclastite, Figure 2). The sediments are represented by layered to laminated grayish siltstones, marls, sandy limestones and calcareous sandstones and contain Turonian–Campanian micropaleontological content [21,12].

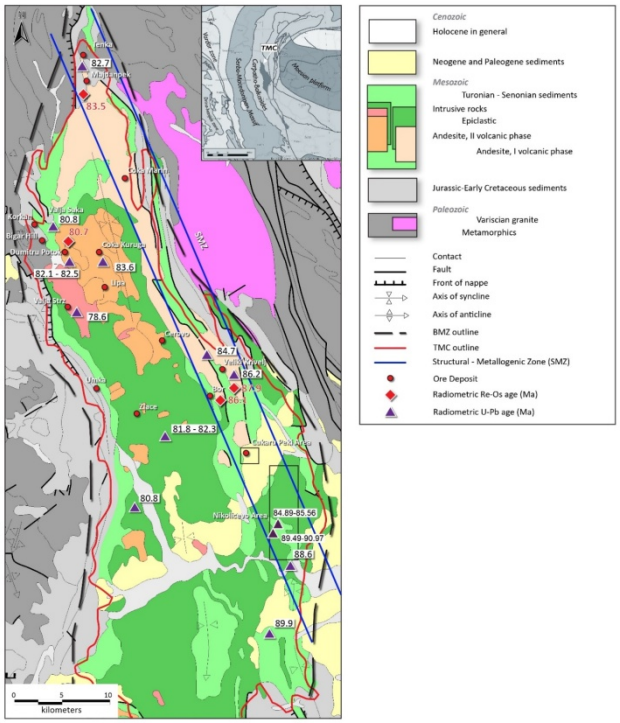

Figure 1. A geological-metallogenetic map of the Timok Magmatic Complex (TMK) and the BorMetallogenetic Zone (BMZ); the numbers are literature U/Pb and Re/Os age data [4,7,9,11,129]; theinset shows the regional geotectonic position; note that the legend is organized in the form of asimplified geological column.

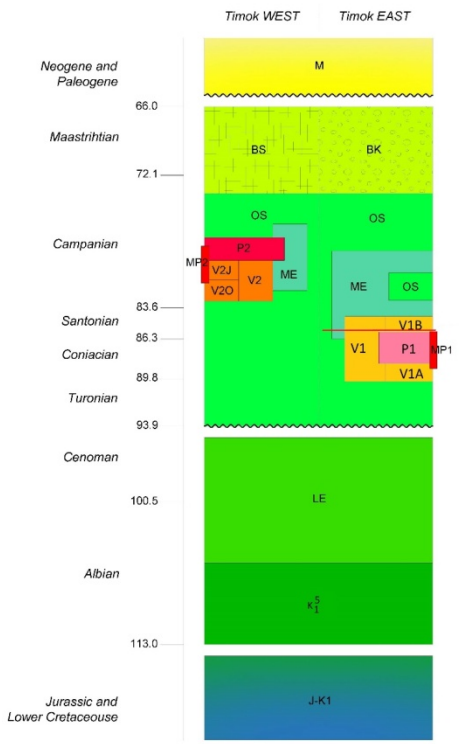

Figure 2.The stratigraphy and time space development of the TMC and relationship of sediment formations and magmatic suites [22,21,8]. On the left side is schematic stratigraphic chart with epoch and age in Ma. LE – Lenovac Formation, OS – Oštrelj Formation, V1 – Timok Andesite, volcanic/magmatic first phase, V1A–Timok andesite sub-phase, V1B – Timok andesite sub-phase, P1 – Shallow intrusions in V1, MP1 – Porphyry mineralization, ME – Metovnica Epiclastic, V2 – volcanic/magmatic second phase, V2O – Osnić basaltic andesite, V2J – Ježevica andesite, P2 – ValjaStržplutonite, MP2 – Porphyry and skarn mineralization, BS – Bukovo Formation, BK – Bor Clastic, M – Miocene sediments, TimokEAST – The eastward tectonic block, Timok WEST – the westward tectonic block Red line highlighted schematic unconformity of porphyry mineralization in the eastward tectonic block.

Towards the west of the TMC, the V1 andesite grade into the hornblende-pyroxene- to pyroxene andesite and basaltic andesite -V2 phase (Ježevica andesite and Osnić basaltic andesite,[8]). They are predominantly emplaced as submarine extrusive volcanics, shallow intrusions and associated epiclastic rocks (II volcanic phase in Figure 1). These volcanic rocksreveal U/Pb zircon ages range of 83-81 Ma, but related to andesite or trachyte dykes ([4], Table 2). They are also stratigraphically interlayered with the above mentioned the Senonian sediments (Oštrelj Formation, Figure 2) and are at places covered by their epiclastic products (Epiclastic in Figure 1). In the westernmost part of the TMC occur plutonic of monzodiorite-granodiorite-gabbrodiorite compositions (ValjaStržplutonite, [8],Intrusive rocks in Figure 1). This rock intruded in to the basaltic andesite and andesite and surrounding sediments (Figure 2). The plutonic rock is dated at 83-78 Ma (Table 1, [4,11]).

From the Upper Campanian to Maastrichtian, in the westward block of the TMC, reef sedimentation commenced (Bukovo Formation, [21]). At the same time, in the eastwardblock,coarse-grained and regressive clastites were deposited (Bor Clastic, ([21], Figure 2). This was the period when the TMCuplifted and its existence as an area of active volcanism/magmatismand marine sedimentation terminated[22].

Table 1 –Summary of rock and mineralization age data in the TMC [4,5,6,7,9,11,12], zr-zircon, ho-hornblende, bi-biotite, mo-molybdenite, wm-white mica.

Location	Lithology	Method	Age Ma	Volcanic phase
Majdanpek	Andesite-Dacite	U/Pb zr	85.2±4.2-86.0±7.2 [9]	V1A
VelikiKrivelj	Andesite dyke	U/Pb zr	86.17±0.15-86.29±0.32 [4]	
VelikiKrivelj	Andesite dyke	Ar/Ar ho	85.5±1.3 [5]	
Bor	Andesite	Ar/Ar ho	83.4±1.7-84.6±1.1 [6]	
Bor	Andesite	Ar/Arbi	89.0±0.6 [5]	
Nikoličevo	Andesite	U/Pb zr	89.49±0.42-90.97±0.39 [12]	
Gamzigrad	Andesite	U/Pb zr	88.6±8.0 [9]	
Lenovac	Volcaniclastic	U/Pb zr	89.9±6.0 [9]	
VelikiKrivelj	Cu-Mo Porphyry	Re/Osmo	87.88±0.5 [7]	
Bor	Andesite	Re/Osmo	85.94±0.4-86.24±0.5 [7]	
Bor	Borskareka Porphyry	Ar/Arwm	86.3±1-86.9±1.1 [6]	
Nikoličevo	Andesite	U/Pb zr	84.89±0.75-85.56±0.53 [12]	V1B
VelikiKrivelj	Andesite	U/Pb zr	84.66±0.5 [4]	
Majdanpek-Dolovi	Andesite dyke	U/Pb zr	82.73±0.03 [4]	V2
Brestovac cross road	Trachyte dyke	U/Pb zr	81.79±0.5-82.27±0.35 [4]	
Podgorac	Basaltic andesite	U/Pb zr	80.8±4.8 [9]	
Majdanpek	Cu-Au-Mo Skarn	Re/Osmo	83.37±0.4-83.77±0.5 [7]	
Majdanpek		Ar/Arwm	83.15[5]	
ValjaStrž	Monzonite	U/Pb zr	78.62±0.44 [4]	
ValjaStrž	Granodiorite	U/Pb zr	78.9±5.2-82.2±5.4 [9]	
ValjaStrž	Diorite	U/Pb zr	78.5±1.3-82.5±0.4 [11]	
ČokaKuruga	Diorite	U/Pb zr	83.6±0.5 [11]	
Dumitru Potok	Diorite	U/Pb zr	82.1±0.7-82.2±1.2 [11]	
KrakuRiđi	Diorite	U/Pb zr	80.8±0.6 [11]	
Dumitru Potok	Cu Porphyry	Re/Osmo	80.69±0.4-80.82±0.45 [7]	

The Bukovo Formation overlies theOštrelj Formation. There are moderate beddedsiltstonesand marls overlain by sandy limestones with intercalated layers of claystonesand contain Upper Campanian to Maastrichtian micropaleontological content [21].

The Bor Clastic are polymictic coarse to fine-grained conglomerate and sandstone.It is built by pebbles of the Upper Cretaceous volcanites and sediments originated from the TMC, pebbles of the Paleozoic metamorphic and igneous rocks, the Paleozoic sediments, the Jurassic and the Lower Cretaceous carbonate rocks, that originated from the basement of the TMC[24]. Micropaleontological content inthe Bor Clastic suggest the Upper Campanian to the Maastrichtian age [25,21,24].

The BMZ hosts more than hundred significant metallic occurrences out of which 22 have been recorded as ore deposits (see review of [16]. The location of 14 economically most significant ore deposits is indicated in Figure 1.

The world-class high-sulfidation Cu-Au deposit of Bor and ČukaruPeki-Upper zone and large porphyry Cu-Au deposits of VelikiKrivelj, Majdanpek,Bor-BorskaReka and ČukaruPeki-Lower zone are all situated along the eastern margin of the BMZ (Figure 1), more precisely inside a narrow structural-metallogenetic zone oriented SSZ-JJI (blue lines in Figure 1, [12]). In the same structural-metallogenetic

zone occur smaller polymetalicepithermal deposits ofhigh-sulphidation, such as Čoka Marin [26], which do not exhibit obvious links to larger porphyry systems.

The western part of the BMZ is less promising and hosts generally different morphogenetic types of mineralization [11]. There are smaller porphyry Cu-Au, high sulphidation-style, polymetallic replacement, and skarn-type deposits connected with plutonic rocks (e.g.Tenka, Valja Saka, Umka, Dumitru Potok, ČokaKuruga, ValjaStrž, Lipa, among others, Figure 1). This zone also hosts a low-sulphidation deposit of Zlaće and a sediment-hosted Au mineralization Korkan-Bigar Hill ([27,11], Figure 1). In the last several years, in this part of the TMC occurrences of manganese ore were also reported and are interpreted as having been related to VMS/SEDEX-type of mineralization [16,11,28].

The age of porphyry mineralization andmineralized and hydrothermally altered andesitic host rocks clearly corresponds (Table 1). The porphyry mineralization ofVelikiKrivelj and Borska Reka deposits is associated with the V1A volcanics and may take place between 87-85.5 Ma roughly[6,7]. The porphyry-skarn mineralization of Majdanpek-Dolovi deposit related with andesitic dykes and dated around 83 Ma. The youngest dated mineralization is in the western part of the TMC, at Dumitru Potok deposit, range of 81-80 Ma and correspond with ValjaStrž plutonic.

3. CONCLUSION

The review of stratigraphy, time space development, relationship ofsediment formations and magmatic suites and available geochronology age determinationsof the TMC and the BMZ imposed the following conclusions:

- After a generally uniform development from the Early Jurassic to the Lower Cretaceous, during the Upper Turonian to the Senonian, the whole TMC area shows a considerable difference in the evolution between the eastward and the westward tectonic block.

- The sedimentary processes and magmatism lasted nearly continuously throughout nearly the whole Late Cretaceous.

- The volcanism/magmatism occurred in two phases from the Upper Turonian to the Upper Campanian: V1 (90-83 Ma), V2 (83-78 Ma).

- The available U/Pb zircon ages and volcanological analyses reveal that the first volcanic phase (V1) can be split into two sub-phases: V1A and V1B.The Timokandesite V1A is older (90-85 Ma) and is both in time and space associated to ore mineralization, whereas the V1B is younger (85-83 Ma) and clearly postdates the main mineralization event.

- The porphyry Cu-Au mineralization in the BMZ ranges widely from 87-80 Ma.

- The structural-metallogenetic zone along the eastern margin of the BMZ is probably one of the most prospective areas in Europe for exploration. The discovery testifies that even old and presumably well-investigated mining areas may host significant ore deposits that await to be found, in particular in deeper parts of the existing systems.

ACKNOWLEDGEMENTS

The research presented in this paper was done with the financial support of the Ministry of Education, Science and Technological Development of the Republic of Serbia, within the funding of the scientific research work at the University of Belgrade, Technical Faculty in Bor, according to the contract with registration number 451-03-9/2021-14/ 200131.

REFERENCES

[1] Berza, T.; Constantinescu, E.; Serban-Nicolae, V. Upper Cretaceous Magmatic Series and Associated Mineralisation in the Carpathian-Balkan Orogen. Resource Geology 1998, 48, 291-306. (DOI 10.1111/j.1751-3928.1998.tb00026.x)

[2] von Quadt, A.; Moritz, R.; Peytcheva, I.; Heinrich, C. Geochronology and geodynamics of Late Cretaceous magmatism and Cu-Au mineralization in the Panagyurishte region of the Apuseni-Banat-Timok-Srednogorie belt, Bulgaria. Ore Geology Reviews 2005, 27, 95-126. (DOI 10.1016/j.oregeorev.2005.07.024)

[3] Janković, S. The Copper Deposits and Geotectonic Setting of the Tethyan Eurasian Metallogenetic Belt. Mineralium Deposita 1977, 12, 37-47.

[4] von Quadt, A.; Peytcheva, I.; Cvetković, V.; Banješević, M.; Koželj, D. Geochronology, geochemistry and isotope tracing of the Cretaceous magmatism of East-Serbia as part of the Apuseni-Timok-Srednogorie metallogenic belt. GeologicaCarpathica, 2002 53, 175-177.

[5] Clark, A.H.; Ullrich, T.D. 40Ar/39Ar age data for andesitic magmatism and hydrothermal activity in the Timok Massif, eastern Serbia: implications for metallogenetic relationships in the Bor copper-gold subprovince. Mineralium Deposita 2004, 39, 256-262. (DOI 10.1007/s00126-003-0370-3)

[6] Lips, A.; Herrington, R.; Stein, G.; Koželj, D.; Popov, K.; Wijbrans, J. Refined timing of porphyry copper formation in the Serbian and Bulgarian portions of the Cretaceous Carpatho–Balkan Belt. Economic Geology 2004, 99, 601-609. (DOI 10.2113/gsecongeo.99.3.601)

[7] Zimmerman, A.; Stein, H.; Hannah, J.; Koželj, D.; Bogdanov, K.; Berza, T. Tectonic configuration of the Apuseni–Banat–Timok–Srednogorie Belt, Balkans–South Carpathians, constrained by high precision Re-Os molybdenite ages. Mineralium Deposita 2008, 43, 1-21. (DOI 10.1007/s00126-007-0149-z)

[8] Banješević, M. Upper Cretaceous magmatic suites of the Timok Magmatic Complex. Annales Geologiques De La PeninsuleBalkanique, 2010, 71, 13-22. (DOI 10.2298/GABP1071013B

[9] Kolb, M.; von Quadt, A.; Peytcheva, I.; Heinrich, C.A., Fowler, S.J.; Cvetković, V. Adakite-Like and Normal Arc Magmas: Distinct fractionation paths in the East Serbian segment of the Balkan Carpathian Arc. Journal of Petrology 2013, 54, 421-451. (DOI 10.1093/petrology/egs072)

[10] Gallhofer, D.; von Quadt, A.; Peytcheva, I.; Schmid, S.M.; Heinrich, C.A. Tectonic, magmatic, and metallogenic evolution of the Late Cretaceous arc in the Carpathian-Balkan orogen: Tectonics 2015, 34, 1813-1836. (DOI 10.1002/2015TC003834)

[11] Knaak, M.; Marton, I.; Tosdal, R.M.; Van der Toorn, J.; Davidović, D.; Strmbanović, I.; Zdravković, M.; Živanović, J.; Hasson, S. Geologic Setting and Tectonic Evolution of Porphyry Cu-Au, Polymetallic Replacement, and Sedimentary Rock-Hosted Au Deposits in the Northwestern Area of the Timok Magmatic Complex, Serbia. Society of Economic Geologists, Inc., Special Publication 2016, 19, 1-28.

[12] Banješević, M.; Cvetković, V.; von Quadt, A.; LjubovićObradović, D.; Vasić, N.; Pačevski, A.; Peytcheva, I. 2019. New Constraints on the Main Mineralization Event Inferred from the Latest Discoveries in the Bor Metallogenetic Zone (BMZ, East Serbia). Minerals, Special Issue Mineral Deposits of Central Europe V.9, Iss. 11, 672.

[13] Janković, S. Metallogenic features of copper deposits in the volcanointrusive complexes of the Bor district, Yugoslavia. In Monograph European copper deposits, Janković, S., Sillitoe, R.H., Eds.; Society of Economic Geologists, Department for Economic Geology, Faculty of Mining and Geology: Belgrade, Serbia, 1980; 42–49.

[14] Janković, S. Types of copper deposits related to volcanic environment in the Bor district, Yugoslavia. GeologischeRundschau 1990, 79, 467-478.

[15] Koželj, D. Epithermal gold mineralization in the Bor metallogenic zone: Morphogenetic types, structural-texture varieties and potentiality, Special ed.; Copper Institute: Bor, Serbia, 2002. (In Serbian)

[16] Jelenković, R.; Milovanović, D.; Koželj, D.; Banješević, M. The Mineral Resources of the Bor Metallogenic Zone: A Review. GeologiaCroatica 2016, 69/1, 143-155. (DOI 10.4154/GC.2016.11)

[17] Klimentyeva, D.; Thomas, D.; von Quadt, A.; Tončić, T.; Heinrich, C. Silicate-replacive high sulfidation massive sulfide orebodies in a porphyry Cu-Au system: Bor, Serbia. Mineralium Deposita, 2020, published online (DOI.org/10.1007/s00126-020-01023-2)

[18] Banješević, M.; Large, D. Geology and mineralization of the new cooper and gold discovery south of Bor – Timok Magmatic Complex. XVI Serbian Geological Congress, DonjiMilanovac, Serbia, 2014; Cvetković, V., Ed.; Serbian Geological Society: Beograd, Serbia, 739-740.

[19] Canby, V.M.; Koželj, D.; Naftali, L. ChukaruPeki Cu-Au deposit, Serbia, Discovery History, Geology and Ore Types. NewGenGold 2015 Conference in Perth, Australia, 2015.

[20] Velojić, M.; Jelenković, R.; Cvetković, V. Fluid Evolution of the ČukaruPeki Cu-Au Porphyry System (East Serbia) inferred from a fluid inclusion study. GeologiaCroatica 2020, 73/3, 197-209. (DOI: 10.4154/gc.2020.14)

[21] Ljubović-Obradović, D.; Carevac, I.; Mirković, M.; Protić, N. Upper Cretaceous volcanoclastic-sedimentary formations in the Timok Eruptive Area (eastern Serbia): new biostratigraphic data from planktonic foraminifera. GeologicaCarphatica 2011, 62/5, 435-446. (DOI 10.2478/ v10096-011-0031-x

[22] Đorđević, M.; Banješević, M. Geology of northern part of the Timok Magmatic Complex, Booklet and Geological Map 1:50 000. SaveznoMinistarstvo za privredu 1997, 171 str., Beograd (in Serbian).

[23] Đorđević, M. Volcanogenic Turonian and epiclastics of the Senonian in the Timok Magmatic Complex between Bor and the Tupižnica Mountain, eastern Serbia. Annales Geologiques De La PeninsuleBalkanique 2004-2005, 66, 63–71.

[24] Banješević, M.; Đorđević, M.; Ljubović-Obradović, D.; Đokić, B. The composition and age of Borclastites from the B2 drill hole at ČukaruPeki. 46th International October Conference on Mining and Metallurgy, Bor lake. Bor 2014, Serbia. Eds: N. Štrbac, D. Živković, S. Nestorović, Proceedings, 61-65.

[25] Đorđević, M.; Mihajlović, Š.; Ljubović-Obradović, D.; Đajić, S.; Banješević, M.; Zupančič, N. New details of the age and location of Bor conglomerates and sandstones southwardly from Bor (east Serbia). Vesnik, A i B – Geologija 1994, 46, 169-176.

[26] Živković, P. Petrology and alterations of Čoka Marin 1 ore deposit. MSc Thesis, Faculty of Mining and Geology, Belgrade University, Belgrade, Serbia, 1987. (In Serbian)

[27] Van der Toorn, J.; Davidović, D.; Hadijeva, N.; Strmbanović, I.; Márton, I.; Knaak, M.; Tosdal, R.M.; Davis, B.; Hasson S. A new sedimentary rock-hosted gold belt in eastern Serbia. 12th Biennial SGA Meeting – Mineral deposit research for a high-tech world, Uppsala, Sweden, 2013; Jonsson, E., et al., Eds.; Society for Geology Applied to Mineral Deposits: Genève, Suisse; 2, 691–694.

[28] Pačevski, A.; Cvetković, V.; Šarić, K.; Banješević, M.; Hoefer, H.E.; Kremenović, A.Manganese mineralization in andesites of Brestovačka Banja, Serbia: evidence of sea-floor exhalations in the Timok Magmatic Complex. Mineralogy and Petrology 2016, 110/4, 491-502. (DOI 10.1007/s00710-016-0425-7)

The 52nd International October Conference on Mining and Metallurgy
November 29th – 30th , 2021
www.ioc.tfbor.bg.ac.rs

DUALPHASED FOURWAYINTERSECTION REGULATED BY TRAFFIC LIGHTS WITH FIXED AND ADAPTIVE MOD OF OPERATION

Milan Radivojević[1*], Zoran Stević[2], Marko Tanasković[3]

[1]Mining and Metallurgy Institute Bor, Zelenibulevar 35, 19210 Bor, Serbia

[2]Technical Faculty Bor, University of Belgrade, V.J. 12, 19210 Bor, Serbia

[3]UniversitySingidunum Belgrade, ul. Danijelova 32, 11000 Belgrade, Serbia

Abstract

Road traffic in many populated areas is mainly regulated using a traffic light, which in many cases is not sufficiently effectively configured. This can lead to unnecessary long waiting times and increase total time losses when passing through the intersection. This paper presents the results of the application program of the adaptive semaphore system of the four-way two phase intersection, made using the LabVIEW software package, as well as the data and results of the analysis of the functioning of the intersection with adaptive and fixed traffic mode.

Keywords: *adaptive traffic mode, fixed traffic mode, traffic regulation, traffic lights, virtual instrument.*

1. INTRODUCTION

From the functional point of view, surface intersection is the most complex element of the traffic network.Namely, the paths of traffic flows of different directions are crossed, the flows may change directions, the vehicle and pedestrian flows are crossed, different maneuvers take place. This indicates that surface intersections are areas with increased concentration of conflicts and increased risk of traffic accidents. That is precisely why it is necessary to have in mind that, while designing and constructing intersections,their main role is to ensure safe traffic and quickly and economically distribute traffic flows, in order to ensure that the conflicts among the participants in traffic are less frequent and that the congestion delay is as little as possible. These conditions have to be met by using minimal financial investments.

The main role of the traffic lights, i.e. light signals for traffic regulation at surface intersections, is the separation of conflicts between vehicles and pedestrians at characteristic points. Light signals regulate traffic flows in such a way as to allow vehicles of one group of flows (non-conflict or conflict-compatible) to pass in a given time period (phase), whereby the vehicles of the second group of flows will be collected at the same time. Then, the second group of vehicles is accommodated, during the same, or different time interval, then the third, possibly the fourth and so on, after which the cycle is repeated periodically. Vehicle accommodation is carried out on the basis of a signalling plan, which, in a unified way, accommodates all the flows grouped within the phases. The main problem that needs to be solved, when it comes to signalized intersection, is calculating and optimization of the signal plan, which implies determining the cycle duration, the number of phases, as well as calculating the distribution of green time intervals to each phase. The maximum recommended duration of the cycle is 120sec. Light signals can operate in a fixed mode when signal plans are determined based on previously collected traffic data, and also as adaptive systems, when light signals operate depending on changes in traffic parameters such as flow, speed, density, and more.

2. THE CYCLE, CAPACITYAND DEGREE OF SATURATIONOF THESURFACE INTERSECTION

The Webster method is used in order to determine the duration of the cycle (C) and the green times of the corresponding phases (gi) of the traffic lights:

$$C = \frac{1.5 \cdot L + 5}{1 - Y},\ g_i = \frac{Y_i}{Y} \cdot (C - L),\ L = n \cdot d + \sum_{i=1}^{n} \Delta t_i \ \text{i} Y = \sum_{i=1}^{n} Y_i \qquad (1)$$

where: L - represents the total lost or unused time at the intersection during the cycle, Yi = maxj {yj (i)} = maxj (Qi / Si) and yi = Qi / Si - the coefficient of utilization capacity of the i-traffic lane, number of phase of the signal plan, d - average time losses-congestion delays, per vehicle during the "green phase" and Δti – clearance interval between the phase "i" and the next phase. The Qi, Si and Y represent the traffic flow intensity of the i-th access lane,the saturated traffic flow of the i-th lane and the coefficient of utilization of the intersection capacity. Saturated traffic flows are determined on the basis of special tables and, as a rule, for this intersection, are constant.On the other hand, the intensity of traffic flows Qi can change over time (daily, weekly, monthly, etc) and are most often determined by counting or by using special detectors installed at the intersections. Intersections with constant cycle values are constant, calculated on the basis of pre-collected data on traffic flow intensity values, constitute a group of intersections with a fixed mode of traffic light system operation.

The intersections where the optimum cycle value is calculated and the distribution of green time to each phase is carried out in such a way that the values are adapted to the changes in traffic flows, belong to the group of intersections with the adaptive system of traffic lights mode of operation.

Adaptive traffic management systems are very complex systems. The functioning of such systems, as a rule, is based on the use of computer systems and corresponding software solutions. The basic components of the adaptive system are the data parameters, the traffic parameters, the corresponding computer system, the light source controller and the traffic lights (Figure 1a.).

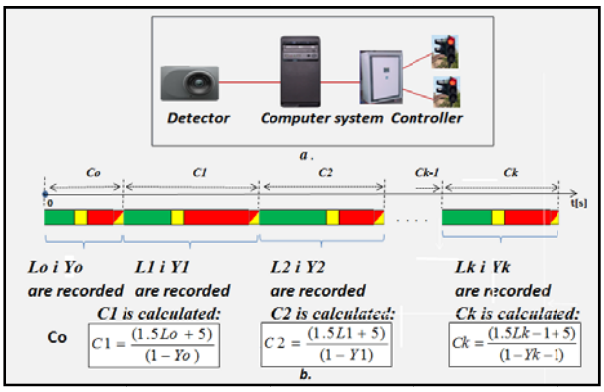

Figure 1. System elements and cycle calculation

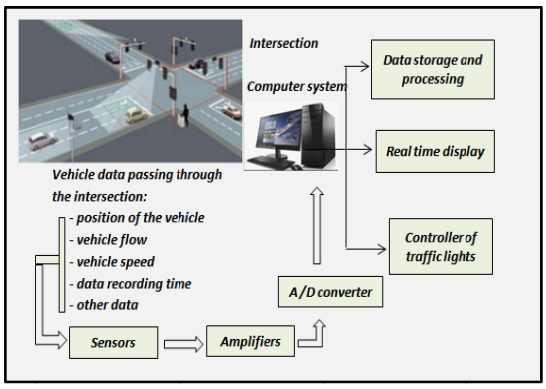

Figure 2. Functional structure of the adaptive system

Figure 2 shows the functional structure of the adaptive traffic management system at intersections regulated by traffic lights.

The aim of this paper is to offer one of the possible solutions for an adaptive traffic management system, based on the use of LabView software package. The basis of the solution lies in the fact that is necessary is to the measure of the intensity of traffic flows in the intersection lanes, during

the current cycle (with the help of appropriate detectors), and use the values to calculate the duration of the next cycle (Figure 1b.):

$$C_{k+1} = (1.5L_k + 5)/(1 - Y_k) \quad (2)$$

where k represents the current cycle and, in accordance with the relation (1) and the length of the green light for each phase, the capacity (ci), the saturation level (Xi) for each traffic lane:

$$g_{i,k+1} = (Y_{i,k}/Y_k)(C_{k+1} - L_k), \; c_{i,k+1} = S_i(g_{i,k+1}/C_{k+1}) \text{i} X_{i,k+1} = Q_{i,k}/c_{i,k+1} \quad (3)$$

When the saturation values for all traffic lanes are equal or less than one, then, the traffic takes place under conditions of unsaturated traffic flows, which means that vehicles stop only once in front of the stop line, and that all vehicles that "requested" pass through the crossroads are accommodated during the cycle. If the saturation level is larger than one, on one or more lanes, then the traffic takes place under conditions of oversaturated flows, which means that not all vehicles are accommodated during the cycle and that a certain number of vehicles stop several times before they pass through the intersection.This further leads to a significant increase in congestion delays, as well as an increase in the concentration of exhaust gases, increased anxiety and other undesirable occurrences.

3. RESULTS OF TESTING THE ADAPTIVE SYSTEM PROGRAM SOLUTION

The program solution for the adaptive traffic management system is calculated for a four-way, two phased isolated intersection regulated by traffic lights. The solution is based on the software platform called LabVIEW software package - a standard in the field of virtual instrumentation.

The graphic user interface package has two panels: a control panel for process control and tracking and a panel for making an application solution, or a block diagram. The testing of the software solution and comparing the obtained results was performed on two identical two-phase intersections, one of which works with the adaptive, and the other with a fixed traffic light mode of operation (with a cycle duration of 52 seconds). The testing was carried out by computer simulation, where the simulation program was also done in LabVIEW. This program is, in its essence, identical to that used by an adaptive mode of operation of traffic lights in real-life conditions. The only difference is that a special simulator (instead of the appropriate detectors) is used as the basis for the traffic flow in the simulation program, and that the elements of the signal timing plan are sent directly to the traffic lights. Figures 3 and 4 show the results of the test, ie the average value of traffic flows at the end of the current cycle (used to calculate the duration of the next one) and saturation levels within the respective cycles.

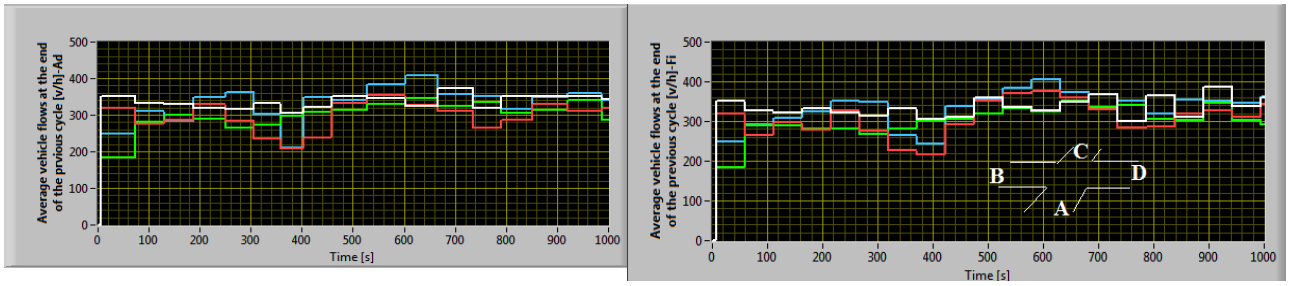

Figure 3. Average values of traffic flows during testing times at intersections crossings with adaptive and fixed mode

The test results show (Figure 4) the advantages of adaptive mode of operation in relation to the intersections with the fixed mode of traffic lights operation. In the first one the traffic takes place in unsaturated traffic flows and with significantly smaller changes in the degree of saturation. However, the intersection with a fixed mode of operation, after the fourth cycle, undergoes the

state of oversaturated flows, and under such circumstances, with minor changes, the traffic takes place until the end of the test period.

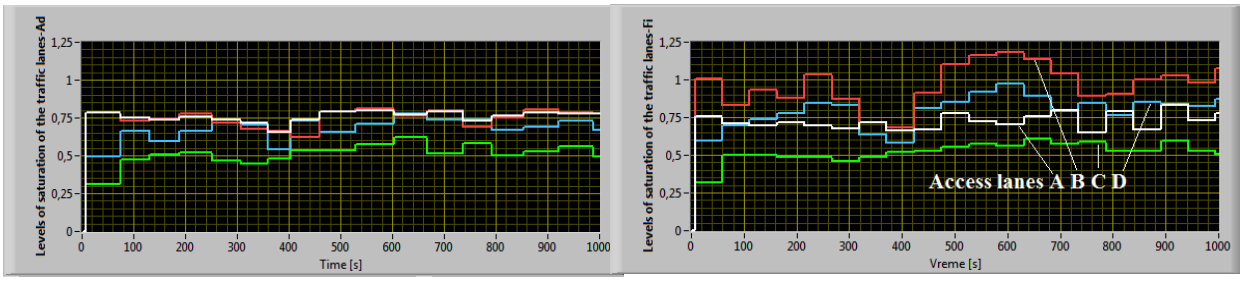

Figure 4. Levels of saturation of intersection with adaptive and fixed mode of traffic light

4. CONCLUSION

The testing process was carried out for different cycle lengths of the system with a fixed mode of operation and different values of average traffic flows, and results are similar to those shown in the following tables. The software solution shows the benefits of the adaptive system when vehicles are in the dilemma zone, and when emergency vehicles are passing through the intersection.

The development of computers, the rapid development of new technologies and different types of sensors for detecting conditions and traffic parameters data, have enabled the creation of adaptive systems designed to control the light signals operation, not only on isolated and intersections regulated by traffic lights, but also on at-grade intersection. Nowadays, there is a large number of adaptive systems around the world installed in different locations, use different equipment, work under different conditions and achieve different results. What is common to most systems is the lack of information on essential modes of operation, used algorithms and other elements of management control.

ACKNOWLEDGEMENTS

This work was financially supported by the Ministry of Education, Science and Technological Development of the Republic of Serbia, Grant No. 451-03-9/2021-14/ 200052.

REFERENCES

[1] Krsto P. Lipovac, BEZBEDNOST SAOBRAĆAJA, udžbenik, Beograd, 2008, 105-188
[2] Docent drŽeljkoRanković, dipl.ing., Regulisanjesaobraćaja (Materijalsapredavanja), TEHNIKUM TAURUNUM, Visokainženjerskaškolastrukovnihstudija Beograd – Zemun, smerDrumskiigradskisaobraćaj, Beograd, 2011, p. 85
[3] *CALCULATION OF TRAFFIC SIGNAL TIMINGS - WEBSTER'S METHOD,* http://www.rhd.gov.bd/Documents/ExternalPublications/Trl/Calculation%20of%20traffic%20signal%20timings-Webster's%20method%20Note13.pdf, p. 7.
[4] Mingmin Wu, Wanjing Ma, Li Li, Characterize Dilemma Zone and Minimize its Effect *at Coordinated Signalized Intersections,*https://core.ac.uk/download/pdf/82213153.pdf, p.13
[5] *Priručnik za projektovanjeputeva u RepubliciSrbiji*, Funkcionalnielementiipovršineputeva, Raskrsniceipriključci, JavnopreduzećePuteviSrbije, Beograd, 2012, p. 25.

The 52nd International October Conference on Mining and Metallurgy
November 29th – 30th , 2021
www.ioc.tfbor.bg.ac.rs

USE OF COPPER TAILING AND COPPER SLAG IN 3D PRINTED CONCRETE PROCESSES

Filip Gramić[1], Nemanja Rančić[1], Sandra Filipović[1], Jelena Đorđević[1],

[1]Mining and Metallurgy Institute Bor, Zeleni bulevar 35, 19210 Bor, Srbija

Abstract

Climate change and global warming due to greenhouse gas emissions have become an increasing problem in recent years. As one of the largest industries with carbon dioxide emissions, the cement and concrete industry is caused by fuel for blasting and transport of raw materials. It is estimated that the cement industry emits about 7% of the total CO2 [11] In the modern practice of production of non-ferrous, rare and precious metals, increasing attention is paid to the possibility of treating raw materials with low metal content, since they are missing or very limited reserves of rich ores. At the same time, the intensive development of technology in the world leads to higher consumption of metals, which results in a multiple increase in the price of metals in recent years. [12]. In the copper mines of Bor, which at the beginning of the 20th century was classified as the mine with the highest copper content (between 5% and 6%), today the average copper content in the ore is below 0.4% and is among the poorest in the world. . According to estimates from 2013, annual copper production increased from 0.5 Mt to 21 Mt between 1900 and 2012 [13].

***Keywords**: 3D printing, copper tailing, concrete.*

1. INTRODUCTION

The harmful impact of mining activities is reflected in the degradation and destruction of large areas of land (surface mines), the disposal of large amounts of solid waste (mine overburden, tailings and flotation tailings) and the occurrence of acidic mine waters. During the metallurgical processing of polymetallic ores and concentrates, in addition to obtaining basic metals, intermediate products (slag, dust and sludge) are created. 11133 tons of overburden and tailings were deposited for each inhabitant of the Bor municipality [12].

The use of waste or recyclable materials as primary raw materials for the production of 3D printing materials can greatly promote 3D printing to reach its maximum economic potential [3].

With the rapid progress of urbanization and industrialization, current problems such as a shortage of skilled labor, resource depletion, and safety issues have seriously accelerated the development of construction [7].

Figure 1. Copper prices on the world market (US $ / t) from 1957 to 2020.

2. EXPERIMENTAL

The goal of concrete printing is to ensure that each printed layer has the capacity to retain its original shape due to its own load and due to the load of subsequent layers immediately after extrusion, and yet remain fluid enough to fill the gaps between adjacent layers. There is a delicate balance between the properties of the material (liquid, extrudability, possibility of installation, curing time, etc.) and process parameters (print speed, nozzle size, extrusion speed, etc.) [6].

One of the mechanisms used in previous research on 3D printers is shown in Figure 2.

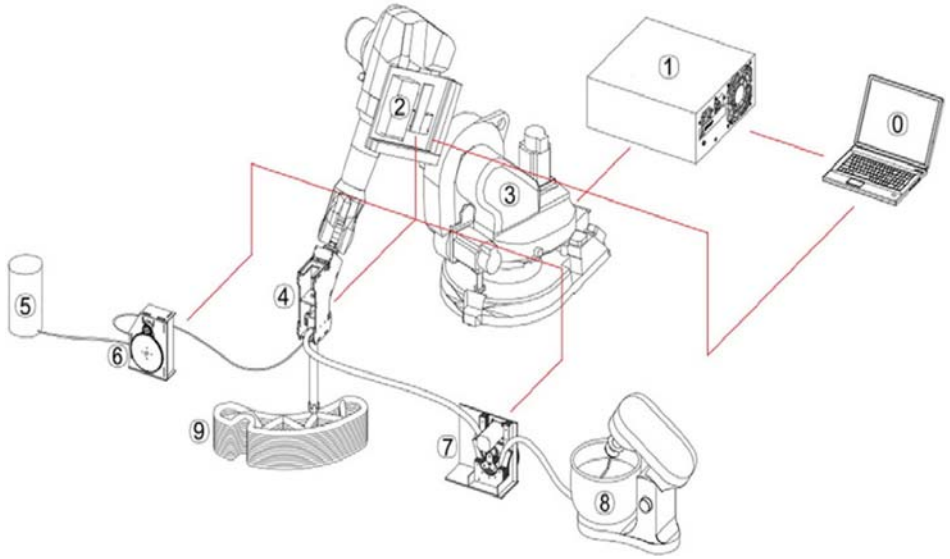

Figure 2. 3D printing procedure scheme: 0. System command; 1. Robot control; 2. Press control; 3. Robot arm; 4. Printer head; 5. Binding agent; 6. Binding agent pump; 7. Premix pump; 8. Premix mixer; 9. 3D printed object.

Including ordinary Portland cement and silicate dust used as binders, a highly effective polycarboxylate-based superplasticizer has been adopted to achieve the required fluidity and stability of the mixture. An appropriate amount of basalt fiber is used to reduce shrinkage due to early drying and increase toughness. Composite materials with a mass fraction of copper slag of up to 35% with a step of 5% are proposed in order to achieve a mixture more resistant to

electromagnetic radiation and as compact a mixture as possible due to the angular grains of copper slag [4].

Ma et al. [3] uses copper tailings in cementitious materials for 3D printing, mainly in the study of printing properties such as extrudability, mountability, setting time, flowability and hardening properties. In his research, he replaced copper tailings up to 50% by weight in relation to river sand with a step of 10%.

3. CONCLUSION

Etringite, CHS gels and other cement crystals found in the used mining waste help to form a complex three-dimensional crystal structure and thus improve the mechanical properties of the concrete thus printed. Therefore, the entire cement matrix will lead to a compact structure with low porosity. In addition, the toxicity of leaching and the radioactivity of the 3D building material for printing were tested, and the results show that the 3D building material for printing composed of copper tailings and steel slag is environmentally friendly [1].

The influence of copper tailings content on the hardening time of 3D printed concrete is reflected in the reduction of hardening time, reduction of fluidity and viscosity reduction due to the size of copper tailings particles that are like clay and have the possibility of higher water absorption [1].

Tests show that a mixture with a mass fraction of 30% copper tailings in relation to sand is the best choice for printing free-form components, which have a water-binder ratio of 0.26 and a sand ratio of 3: 2, containing 70% cement, 20% volatile ash and 10% silica gel, plus 1.2 kg / m3 micro polypropylene fibers. This mixture also required 1.083% superplasticizer to achieve optimal workability [3].

It can be noticed that mixtures R0 - R30 have good workability, while mixtures R40 and R50, with a share of copper tailings of 40% and 50%, respectively, are not suitable for 3D printed concrete processes due to relatively high liquidity and low stiffness.

The average compressive strength of samples with the addition of copper tailings in the amount of 10, 20, 30, 40 and 50% is 36 MPa after 3 days of concrete printing, which proves that the addition of mining tailings does not have a large impact on strength after 3 days. On the samples examined after 14 and 28 days with the addition of 40%, it is 47 MPa and 53.2 MPa, i.e. 21% and 23.2% higher compressive strength than the reference samples without the addition of mining tailings [3].

REFERENCES

[1] Xinjian Li, Na Zhang, Jianbo Yuan, Xinke Wanga, Yonghong Zhang, Feixu Chen, Yihe Zhang, Preparation and microstructural characterization of a novel 3D printable building material composed of copper tailings and iron tailings, Construction and Building Materials 249 (2020) 118779

[2] B. Zareiyan, B. Khoshnevis, Interlayer adhesion and strength of structures in contour crafting - effects of aggregate size, extrusion rate, and layer thickness, Autom. Constr. 81 (2017) 112–121.

[3] G. Ma, Z. Li, L. Wang, Printable properties of cementitious material containing copper tailings for extrusion-based 3D printing, Constr. Build. Mater. 162 (2018) 613–627.

[4] Guowei Maa,b, Junbo Sunb, Li Wanga, Farhad Aslanib,c, Miao Liub Electromagnetic and microwave absorbing properties of cementitious composite for 3D printing containing waste copper solids, Cement and Concrete Composites 94 (2018) 215–225

[5] Z. Li, L. Wang, G. Ma, Method for the enhancement of buildability and bending resistance of 3D printable tailing mortar, Int. J. Concrete Struct. Mater. 12 (1) (2018) 37–48.

[6] G. Ma, L. Wang, A critical review of preparation design and workability measurement of concrete material for largescale 3D printing, Front. Struct. Civ. Eng. 6 (2017) 1–19.
[7] Mehta PK, Monteiro PJM. Concrete: microstructure, properties and materials. McGraw-Hill; 2006.
[8] https://www.3printr.com/3d-concrete-printing-market-reach-56-4-million-2021-123966/.
[9] Jingchuan Zhanga, Jialiang Wanga, Sufen Donga, Xun Yub, Baoguo Han, A review of the current progress and application of 3D printed concrete, Composites Part A 125 (2019) 105533
[10] Chao Zhanga, Zeyu Houa, Chun Chena, Yamei Zhanga, Viktor Mechtcherineb, Zhengming Suna Design of 3D printable concrete based on the relationship between flowability of cement paste and optimum aggregate content, Cement and Concrete Composites 104 (2019) 103406
[11] Baisui Hana, mBatnasan Altansukhb, Kazutoshi Hagac, Zoran Stevanović, Radojka Jonovićd, Ljiljana Avramovićd, Daniela Urosević, Yasushi Takasakib, Nobuyuki Masudab, Daizo Ishiyamab, Atsushi Shibayamab Development of copper recovery process from flotation tailings by a combined method of high–pressure leaching–solvent extraction, Journal of Hazardous Materials Volume 352, 15 June 2018, Pages 192-203
[12] Grozdanka Bogdanović, Milan Trumić, Maja Trumić, Dejan V. Antić (2011.), Upravljanje otpadom iz rudarstva-nastanak i mogućnost prerade, Reciklaža i održivi razvoj 4, 37-43.
[13] Khaloo AR. Crushed tile coarse aggregate concrete. Cem Concr Aggr 1995; 17:119–25.

POSSIBILITY OF USING MINING WASTE IN THE PRODUCTION OF BRICK PRODUCTS

Filip Gramić[1], Nemanja Rančić[1], Sandra Filipović[1], Jelena Đorđević[1],

[1]Mining and Metallurgy Institute Bor, Zelenibulevar 35, 19210 Bor, Srbija

Abstract

Long-term exploitation leads to the degradation of large areas of land (surface mines), the disposal of large volumes of solid waste (overburden and tailings), the occurrence of wastewater and air pollution. Most of the industrial waste can be used today, and it is a secondary raw material. Recycling of waste raw materials generated during the exploitation and processing of mineral raw materials and melting of concentrates, enables the reuse of materials that have no use value. In this way, the waste generated in mining is given a new use value and at the same time reduces the negative impact on the environment [1].

***Keywords**: bricks, copper tailing, mine tailing.*

1. INTRODUCTION

Mining production in Bor began in 1903 with underground exploitation. The Bor open pit was opened in 1912 and was exploited until 1986. There are two more surface mines of copper ore in the municipality - in VelikiKrivelj (opened in 1979) and Cerovo (opened in 1990) [1]. Within the National Strategy for Sustainable Development based on the analysis of the existing mineral resource complex in the Republic of Serbia, sectoral goals in the field of sustainable development of mineral resources are defined, which include finding new deposits and rational use of existing natural resources using cleaner technologies. and testing the value of residual mineral raw materials in tailings and landfills[2].

At all stages of metal production, waste is generated which can be composed of natural materials that are only crushed (ordinary mining waste, unusable mineralized materials) or of natural materials that have been processed to varying degrees during the concentrate and processing phases, which contain chemical, inorganic and organic additives [6].

Mining waste represents 99.95% of the total landfilled waste on the territory of the municipality of Bor[4]. It is deposited in the immediate vicinity of processing capacities, and also, from 700 to 1000 t of slag is generated daily, depending on the processing capacity [5]. More than 450 x 106 t of overburden, 207 x 106 t of flotation tailings and 23 x 106 t of smelter slag have been deposited so far.

Table 1. Amount of mine waste and metallurgical slag and copper content[4]

		Deponije otpada	Količine (Mt)	Sadržaj Cu (%)	Cu (t)	Vrednost (miliona US$)
Jalovina površinskih kopova	Bor	''Visoki planir''	150	0,15	225000	1691,0
		''Severni planir''	20	0,3	60000	450,9
		''Planir RTH''	60	0,1	60000	450,9
		''Unutrašnje odlagalište''	28	0,2	56000	420,9
	V. Krivelj	''Planir V. Krivelj''	170	0,1	170000	1277,7
	Cerovo	''Planir Cerovo''	22	0,18	40000	300,6
Flotacijska jalovina	Bor	Staro flotacijsko jalovište	27	0,3	81000	608,8
		Flotacijsko jalovište RTH	50	0,2	100000	751,6
	V. Krivelj	Flotacijsko jalovište V. Krivelj	130	0,15	195000	1465,5
Metalurška šljaka	Bor	Metalurška šljaka	16,5	0,65	107000	804,2
		Ukupno:	**673,5**		**1094000**	**8222,1**

* Cena bakra na dan 21.12.2011. godine 7515,6 US$/t

2. EXPERIMENTAL

Brick is a building and construction material that is widely used. Conventional brick production usually uses clay and shale as a source material and requires firing at high temperatures (900-1000 ° C) not only consumes a significant amount of energy but also affects global warming. environment and can release large amounts of waste material [7].

The main raw materials for the production of limestone bricks are limestone sand with a high content of SiO and lime. However, in some areas there is a lack of sand with a high content of SiO_2, which has limited the production and application of limestone bricks. On the other hand, metal ore mining produces thousands of tons of tailings that carry SiO_2 daily. The use of tailings carrying SiO_2 as a substitute for natural and/or artificial sand for the production of autoclaved sand-lime bricks is a possible way to solve the problem of sand scarcity resources and environmental and safety problems caused by tailings [13].

The brick production process simply involves mixing the tailings with an alkaline solution, forming a brick by compressing the mixture in a mold under a certain pressure, and hardening the brick at a slightly elevated temperature. Unlike the conventional method of brick production, the new procedure does not use clay and slate nor does it require baking in a high-temperature furnace, which has significant environmental and environmental benefits [7].

Due to the fact that a large amount of tailings from copper mines is created every year and that the tailings of copper mines are rich in silicon and alumina and can be used as a potential source of materials for the production of geopolymers [11].

In order to protect clay and shale resources and protect the environment, some countries, such as China, have begun to restrict the use of clay and shale bricks [8,9].

Morchhale et al. [6] studied brick production by mixing copper mine tailings with different amounts of ordinary Portland cement and then compressing the mixture into a mold. The results show that bricks have higher compressive strength and lower water absorption when the content of ordinary portland cement increases.

Recently, researchers have started using geopolymerization technology to produce bricks from waste. Geopolymerization is a reaction that aluminosilicates undergo in a highly concentrated solution of alkaline hydroxide or silicate, forming a very stable material called a geopolymer having amorphous polymer structures [7].

3. CONCLUSION

Based on the previous experimental results of other authors, the following conclusions can be drawn in the production of bricks by autoclaving:

1) Higher initial water content means higher amount of NaOH and thus increases the strength of geopolymer brick samples.

2) Higher molding pressure leads to a higher degree of compaction, and thus to a higher UCS if no water is expelled during the molding process. When the forming pressure is too high, some water, and thus NaOH, will be lost, and the strength will decrease.

3) The hardening temperature is an important factor that affects the geopolymerization, and thus the strength of geopolymer brick samples. The hardness increases with the curing temperature to a certain level, and then decreases with the curing temperature. For the copper mine tailings used in previous research, the optimal hardening temperature is around 90 °C [7].

REFERENCES

[1] GrozdankaBogdanović, Milan Trumić, Maja Trumić, Dejan V. Antić (2011.), Upravljanjeotpadomizrudarstva – nastanak I mogućnostprerade, Reciklaža I održivirazvoj 4, 37-43.
[2] Nacionalnastrategijaodrživograzvoja, naosnovučl. 17, st. 1. I čl. 45, st. 1 Zakona o Vladi, „Službeniglasnik RS", br. 55/05, 71/05-ispravka i 101/07.
[3] Gorai, B.; Jana, R.; Premchand, K. Characteristics and utilisation of copper slag. Resources, Conservation and Recycling 2003, 39: 299-313.
[4] Program dugoročnograzvoja RTB Bor, Hidrometalurgija bakra, Univerzitet u Beogradu, Tehničkifakultet u Boru, 1993.
[5] Stanojlović, R.; Štirbanović, Z.; Sokolović, J. Primenanovetehnologije u funkcijiodrživepreradetopioničkešljake. Reciklaža I održivirazvoj 2008, 1, 34-42.
[6] BRGM: Management of mining, quarrying and ore- processing waste in the European union, Decembar 2001.
[7] Saeed Ahmari; Lianyang Zhang Production of eco-friendly bricks from copper mine tailings through geopolymerization. Construction and Building Materials 29 (2012) 323–331
[8] Chen Y, Zhang Y, Chen T, Zhao Y, Bao S. Preparation of eco-friendly Construction bricks from hematite tailings. Constr Build Mater 2011;25: 2107–11.
[9] Chou MI, Chou SF, Patel V, Pickering MD, Stucki JW. Manufacturing fired bricks with class F fly ash from Illinois basin coals. Combustion Byproduct Recycling Consortium, Project Number 02-CBRC-M12, Final Report; 2006.
[10] Morchhale RK, Ramakrishnan N, Dindorkar N. Utilization of copper mine tailings in production of bricks. J Inst Eng, Indian Civ EngDiv 2006;87:13–6.
[11] Drechsler M, Graham A. Innovative material technologies: bringing resources sustainability to construction and mining industries. In: 48th institute of quarrying conference, Adelide SA, Australia; 2005.
[12] Sungwon Sim; Dongho Jeon; Do Hoon Kim; Woo sung Yum; Seyoon Yoon; Jae Eun Oh. Incorporation of copper slag in cement brick production as a radiation shielding material. Applied Radiation and Isotopes 176 (2021) 109851
[13] Yonghao Fang; YaminGu; Qiubo Kang; Quan Wen; Pin Dai. Utilization of copper tailing for autoclaved sand–lime brick. Construction and Building Materials 25 (2011) 867–872

GOLD-SILVER ALLOYS ANODIC DISSOLUTION RESEARCH IN HYDROCHLORIC ACID ELECTROLYTES

Stepan O. Vydysh[1]

[1]The National University of Science and Technology MISiS, 2-Y Donskoy Proyezd, 119071Moscow, Russia

Abstract

The article is concerned with the electrochemical processing of gold-silver alloys with an increased concentration of silver (30%) in hydrochloride acid electrolytes. The absence of silver chloride formation on the gold-silver anode surface during the electrolysis in pure hydrochloride acid solutions was established. Au-Ag alloy dissolution rate specificity with silver concentration 30 % from electric current density at voltage 0.8-1.4 V was identified.

***Keywords**: precious metals, gold, silver, alloy, electrolysis.*

1. INTRODUCTION

Wohlwill method is classic solution for producing refining gold. Anode passivation is proceeded by silver chloride when alloy contains more than 5-6% of silver [1]. Reverse current allows dropping producing silver chloride layer [2]. This permit processing of alloys that contain not above 20-25% of silver. The increase of gold-silver alloys amount with high silver percentage requires alternative processing options.

Silver chloride generation is impossible without an oxidizing agent in the Ag-HCl system [3]. The silver oxidizing agent in AuAg|HAuCl4, HCl|Au system would be chloroauric acid HAuCl4 or nitric acid. Nitric acid might be in solution from the clean electrolyte by nitric-chloric dissolution or added for passivation layer dissolution [4]. Therefore, it is of interest to study the gold-silver alloy electrochemical processing with an increased silver content (30%) in pure hydrochloric acid.

2. EXPERIMENTAL

Au-Agalloywasmadebypowdermetallurgyforresearches, alsohydrochloric acid GOST 3118, potassium chloride GOST 4568, distilled water GOST 670 were used.

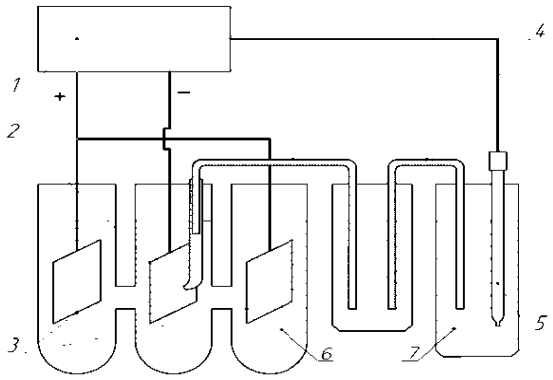

1 − rectifier; 2 –Au-Aganode; 3 − cathodes; 4 – saltbridges; 5 – Ag/AgCl electrode; 6 – hydrochloric acid electrolyte; 7 –KCl solution.
Figure 1 – Schematic electrolysis installation scheme

Technologicalinstallation (Figure 1) consistofarectifier (1) withavoltageregulator, Au-Ag anode (2) that immersed in hydrochloric acid electrolyte (100 g/l) (6). Titanium cathodes are placed in the cells on both sides of the anode (3). Theanodeisinstalledin the cell closeto one of the salt bridgescapillaryend (4). Ag/AgClelectrode (5)wasusedin the capacity of reference electrode, which representing the Ag|AgCl, KCl_{sat}. system. The electrode was immersed in KCL solution (7).

3. RESULTS AND DISCUSSION

TheresearchresultsoftheanodicpolarizationvariationaccordingtodurationoftheAu-Agalloyanodicdissolution, which contains 30% of silver, are shown in Figures 2-4. Itwasrevealedthatthegold-silveralloyelectrochemicaldissolutiondidnotproceedat 0.8 V and current densities of 100 and 4000 A/m^2 -gold cathode deposit was not found (Figure 2). Silveroxidesedimentationwasidentifiedin black dots form on the anode at 4000 A/m^2currentdensity

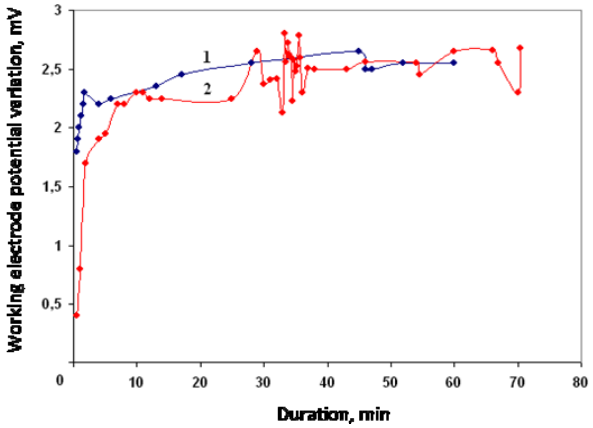

Figure 2 – Anodic polarization variation depending on the duration for test gold-silver alloy at U=0.8 V, j_a=100 (1) и 4000 (2) A/m^2

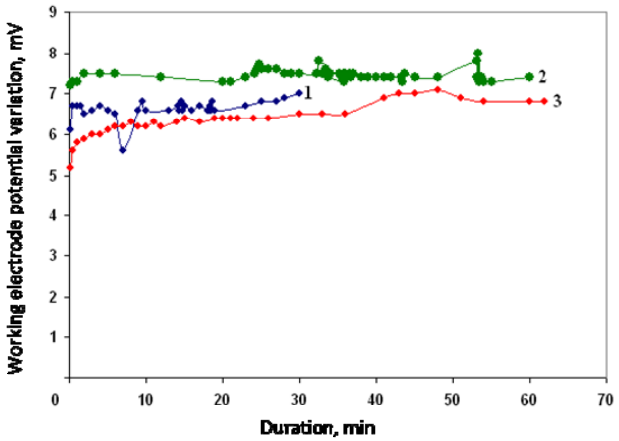

Figure 3 – Anodic polarization variation depending on the duration for test gold-silver alloy at U=1.2 V, j_a=1000 (1), 2000 (2), 4000 (3) A/m^2

Electrochemicaldissolutionproceededwithcathodegold precipitationat 1.2 Vand 1000, 2000, 4000 A/m^2 current densities (Figure 3).Anodedissolutionproceedsmoreintensivewithcurrent density increasingfrom 1000 to 4000 A/m^2. In each case, the silverchloridelayerwasnotfound.

Electrochemical dissolution is also a possibility at 1.4 V and 1000, 2000, 4745 A/m^2 current densities (Figure 4). Anodedissolutionofgoldwasobservedunderallconditions and reached the peak at 1.4 V and 2000 A/m^2.

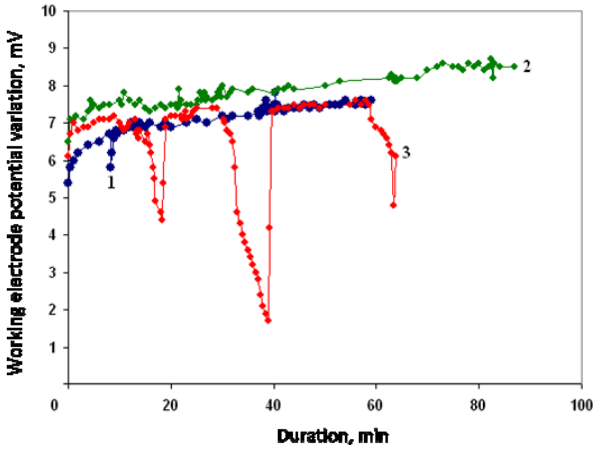

Figure 4 - Anodic polarization variation depending on the duration for test gold-silver alloy at U=1.4 V, j_a=1000 (1), 2000 (2) и 4745 (3) A/m^2

Innoneofthemodes silver chloride layer was not formed. Curvetypeofanodicpolarizationattract interest atthelargestcurrentdensity: sharp working electrode potential drops might be associated with chlorine evolution on the anode.

Anode dissolution specific rate depending on anodic current density for test alloy in hydrochloric solution at the voltage 1.2 and 1.4 Vare shownin Figure 5.

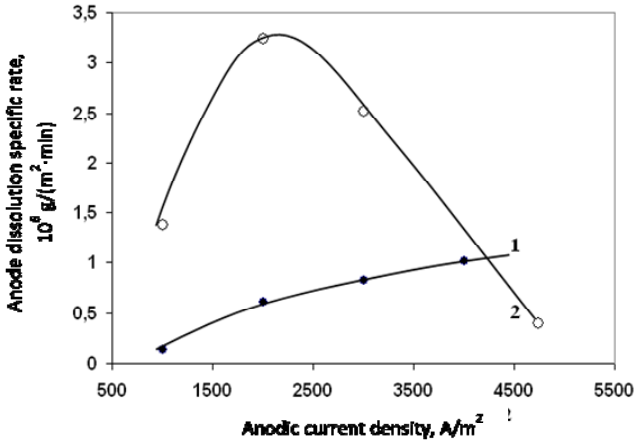

Figure 5 - Anode dissolution specific rate depending on anodic current density for test alloy in hydrochloric solution at the voltage, V: 1) 1,2; 2) 1,4

Electrochemicaldissolutionofgoldisobservedinallmodesatvoltage 1.2 and 1.4 V,howeverthe dissolution specific rate curvetypes are clearly different from each other.

ThetopdissolutionratewasobtainedatthemodeU=1.4 V, j_a=2000 A/m^2 and was $3{,}24 \cdot 10^{-6}$g/(m^2·min).

4. CONCLUSION

Theconductedresearchapprovedtheabsenceofsilverchloridelayeron gold-silver anode surface during electrolysis from pure hydrochloric acid electrolytes. Cathodegoldprecipitationwasobservedatavoltageofatleast 1.2 V. The radical dependence of dissolution rate from current density was established at 1.4 V. The maximum dissolution rate of gold-silver alloy, which contained 30 % of silver with was reached at$U$=1.4 V, j_a=2000 A/m^2. Theprocessmechanismrequiresadditional researches in order to establish the reason for the difference between dissolutions rate dependencies.

REFERENCES

[1] E. Wohlwill., Z. Elektrochemie., №4 (1898), p. 379-423.
[2] N.P. Fedotyev., Prikladnayaelektrokhimiya, Goshimzdat, Leningrad, 1962, p. 625.
[3] R.A. Lidin, Konstantyneorganicheskikhveshchestv: spravochnik, Drofa, Moscow, 2008, p. 685.

ADSORPTION ISOTHERMS FOR COPPER IONS ADSORPTION ONTO WALNUT SHELLS

Milan Gorgievski[1], Miljan Marković[1], Dragana Božić[2], Velizar Stanković[1], Nada Štrbac[1], Vesna Grekulović[1], Milica Zdravković[1]

[1]Technical Faculty Bor, University of Belgrade, V.J. 12, 19210 Bor, Serbia

[2]Mining and Metallurgy Institute Bor, Zelenibulevar 35, 19210 Bor, Srbia

Abstract

In this paper Langmuir, Freundlich, and Temkin adsorption isotherm models were used for describing the adsorption of copper ions onto walnut shells. The adsorption was performed in a batch system. The obtained isotherm data were fitted using the mentioned models, and the isotherm parameters were calculated from the linearized plots corresponding to each model. The Langmuir adsorption isotherm model showed the best agreement with the analyzed experimental data, with the correlation coefficient R^2 = 0.993. According to this model, the adsorption process occurs until a complete monolayer of copper ions is formed on the surface of the walnut shells. The maximum adsorption capacity, according to this model, was 7.71 mg g^{-1}.

***Keywords**: Adsorption isotherms, walnut shells, adsorption capacity, copper ions, batch system.*

1. INTRODUCTION

Environmental pollution, which includes water, air, and soil pollution, is a serious environmental problem. Waters contaminated with heavy metals are one of the biggest environmental problems of today. These waters affect the flora and fauna, and through the food chain also human health. Many industries, for example, metallurgy processing plants,discharge heavy metals into their wastewaters, thus polluting the environment[1, 2].Conventional technologies which are used for the removal of heavy metals from wastewaters including chemical precipitation, cementation, ion exchange, solvent extraction, adsorption, different membrane processes, etc, are already in use on an industrial level. These methods have their downsides, including an insufficient degree of metal ions removal, high costs, the need for excessive amounts of chemicals used in the process, and the formation of significant amounts of sludge. As a potential alternative method to conventional technologies for the removal of heavy metals from wastewaters emerges biosorption [3]. To describe the mechanism of the adsorption process as well as to obtain the information about the maximum adsorption capacity of selected adsorbent, the adsorption isotherms are used [4].

In this paper, the adsorption isotherm data of copper ions adsorption onto walnut shells was fitted using the Langmuir, Freundlich, and Temkin adsorption isotherm models.

2. EXPERIMENTAL

Walnut shells were used as an adsorbent for the adsorption experiments. Adsorption isotherm data was obtained by bringing into contact 0.5 g of walnut shells with 50 mL of synthetic solutions of copper ions with different initial concentrations ranging from 5 to 500 mg dm^{-3}. The suspension was stirred using a magnetic stirrer for 60 minutes, assuming that this process time is long enough to reach the equilibrium between phases [3]. After that, the suspension was filtered, and the filtrate was analyzed for the residual amount of copper ions.

3. RESULTS AND DISCUSSION

3.1 Langmuir adsorption isotherm model

This model was implemented theoretically assuming that the adsorption occurs in a monolayer, at a finite number of localized sites [5].

The Langmuir model can be expressed in the following form:

$$q_e = \frac{q_m K_L C_e}{1 + K_L C_e} \tag{1}$$

Linearization of the equation (1) results in the following expression:

$$C_e / q_e = \frac{1}{K_L q_m} + \frac{1}{q_m} C_e \tag{2}$$

where C_e is the equilibrium concentration of metal ions (mg dm^{-3}), $q_e$is the equilibrium adsorption capacity (mg g^{-1}), $q_m$is the maximum adsorption capacity (mg g^{-1}) and K_L (dm^3 g^{-1}) is the Langmuir equilibrium constant.

Graphical dependence of C_e/q_e in function of C_e, shown on Figure 1b, gives the straight-linewith the slope $1/q_m$and the intercept $1/K_Lq_m$.

3.2 Freundlich adsorption isotherm model

This model is often used to describe the non-ideal and reversible adsorption processes. The Freundlich model can also be applied to multilayer adsorption [5].

This model is represented by the following expression:

$$q_e = K_f C_e^{1/n} \tag{3}$$

Linearization of the Eq. (3) gives:

$$\log q_e = \log K_F + \frac{1}{n} \log C_e \tag{4}$$

where $C_e$is the equilibrium concentration of copper ions in the solution (mg dm^{-3}); q_e is the adsorbent capacity defined as mass of the adsorbed metal per unit mass of the adsorbent (mg g^{-1}) at equilibrium; K_F is the Freundlich equilibrium constant ((mg g^{-1}) (dm^3 mg^{-1})$^{1/n}$), and $1/n$ is the coefficient of heterogeneity in the Freundlich adsorption isotherm equation.

Graphical dependence of *log* $q_e$in function of *log* C_e, shown on Figure 1c, gives the straight line, with the slope $1/n$ and the intercept K_F.

3.3 Temkin adsorption isotherm model

Temkin adsorption isothermmodel is based on the assumption that the heat of adsorption in all layers of molecules decreases linearly with coverage, and that there is a uniform distribution of ion binding energy in the adsorbent-adsorbate system [6].

Temkin isotherm model is represented by the following expression:

$$q_e = B \ln\left(K_T C_e\right) \tag{5}$$

Linear form of the equation (5) is:

$$q_e = B \ln K_T + B \ln C_e \tag{6}$$

where $B = RT/b$ is the Temkin constant, which refers to the adsorption heat (J mol^{-1}); b is the variation of adsorption energy (J mol^{-1}); R is the universal gas constant (J mol^{-1} K^{-1}); T is the temperature (K); K_T is the Temkin equilibrium constant (dm^3 g^{-1}); q_e is the adsorption capacity defined as mass of the adsorbed metal per unit mass of the adsorbent (mg g^{-1}) at equilibrium; $C_e$is the equilibrium concentration of copper ions in the solution (mg dm^{-3}). Constants B and K_T can be determined from the graph $q_e = f(ln\ C_e)$, which is shown in Figure 1d, where B is the slope, and $K_T$the intercept.

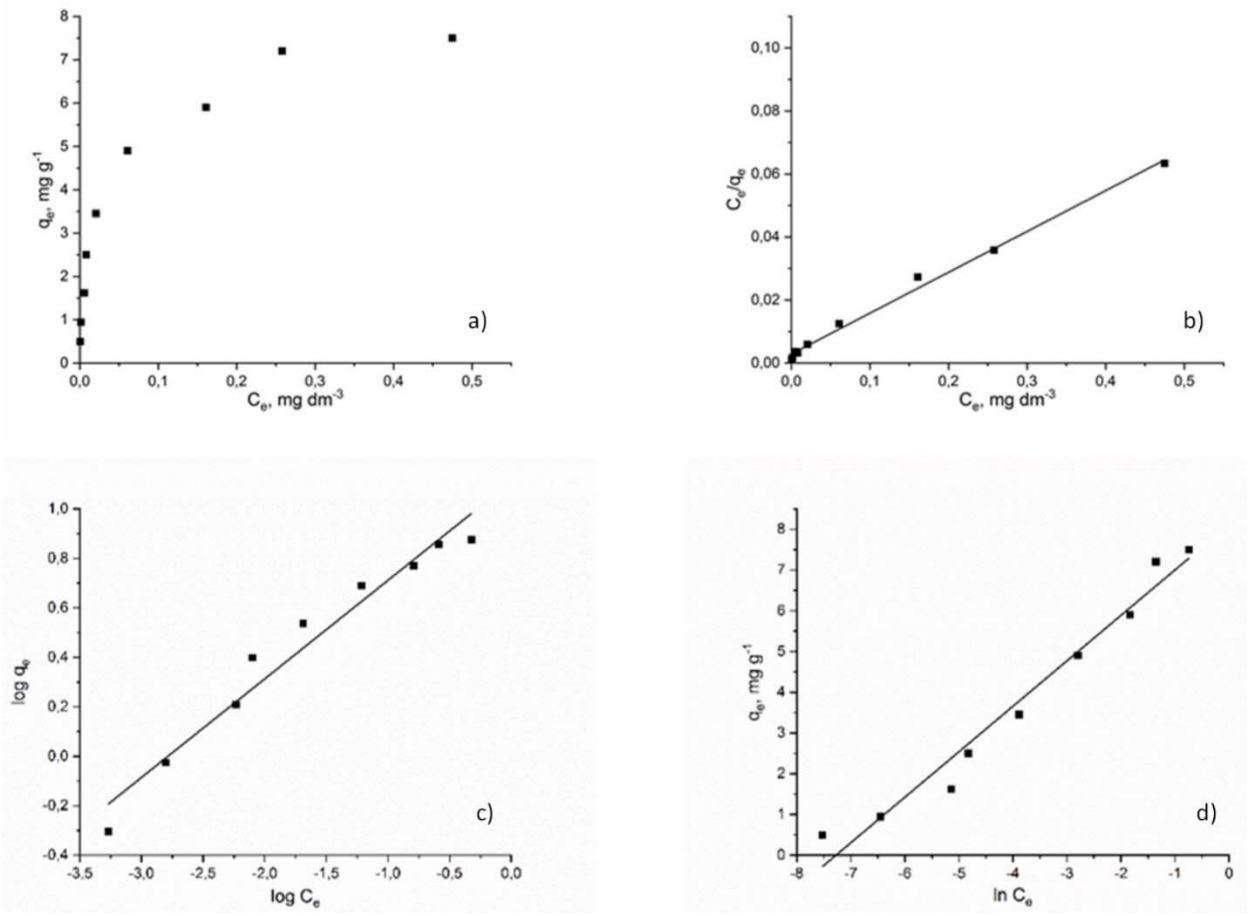

Figure 1. a) Adsorption isotherm data, b) Langmuir adsorption isotherm model, c) Freundlich adsorption isotherm model and d) Temkin adsorption isotherm model for copper ions adsorption onto walnut shells

The obtained adsorption isotherm data, shown in Figure 1a, was fitted using the Langmuir, Freundlich, and Temkin adsorption isotherm models, and the corresponding diagrams are shown on Figures 1 b-d. The equilibrium parameters for the analyzed models were determined using Equations (2), (4), and (6). The obtained parameters and correlation coefficients R^2 are given in Table 1.

Table 1. Obtained parameters for Langmuir, Freundlich and Temkin adsorption isotherm models for copper ions adsorption onto walnut shells

Langmuir				Freundlich			Temkin		
K_L dm^3 mg^{-1}	q_{exp} mg g^{-1}	q_m mg g^{-1}	R^2	K_F	1/n	R^2	B J mol^{-1}	K_T dm^3 g^{-1}	R^2
45.19	7.50	7.71	0.993	12.87	0.4	0.960	1.11	8.11	0.968

According to the data given in Table 1, the Langmuir model shows the best agreement to the analyzed data, with the correlation coefficient R^2 = 0.993. The experimentally determined adsorption capacity, and the maximum capacity determined by the Langmuir model are approximately equal, which further proves very good agreement of the Langmuir model with the analyzed data, and indicates that the adsorbent is almost completely saturated, where all of the active sites areoccupied by copper ions.The maximum adsorption capacity, obtained by the Langmuir adsorption isotherm model was 7.71 mg g^{-1}.

4. CONCLUSIONS

Walnut shells were used as an adsorbent for copper ions adsorption from aqueous solutions. The adsorption isotherm data were fitted using three theoretical adsorption isotherm models, i.e. Langmuir, Freundlich, and Temkin adsorption isotherm model. The obtained results, shown in Table 1, indicate that Langmuir model shows the best agreement with the analyzed experimental data, with the correlation coefficient R^2 = 0.993. This leads to the conclusion that the biosorption process occurs in a monolayer. The maximum adsorption capacity, obtained by the Langmuir adsorption isotherm model,according to Table 1, was 7.71 mg g^{-1}.

ACKNOWLEDGEMENTS

The research presented in this paper was done with the financial support of the Ministry of Education, Science and Technological Development of the Republic of Serbia, within the funding of the scientific research work at the University of Belgrade, Technical Faculty in Bor, according to the contract with registration number 451-03-9/2021-14/200131, and the Mining and Metallurgy Institute Bor, Grant No. 451-03-9/2021-14/ 200052.

REFERENCES

[1] R. B. Garcia-Reyes, J. R. Rangel-Mendez, Bioresour. Technol. 101 (2010) 8099-8108.
[2] R. Perez-Lopez, J. M. Nieto, G. R. Almodovar, Appl. Geochemistry. 22 (2007) 1919-1935.
[3] M. Gorgievski, D. Božić, V. Stanković, N. Štrbac, S. Šerbula, Ecol. Eng. 58 (2013) 113-122.
[4] M. J. Mohammed-Ridha, A. S. Ahmed, N. N. Raoof, NJES 20 (2017) 298-310.
[5] X. Chen, Information 6 (2015) 14-22.
[6] S. Puttamat, V. Pavarajarn, Int. J. Chem. Eng. 7 (4) (2016).

pH AND CONDUCTIVITYCHANGE DURING THE RINSING AND ADSORPTION OF COPPER IONS ONTO WALNUT SHELLS

Miljan Marković[1], Milan Gorgievski[1], Nada Štrbac[1], Vesna Grekulović[1], Aleksandra Mitovski[1], Kristina Božinović[1], Milica Zdravković[1]

[1]Technical Faculty Bor, University of Belgrade, V.J. 12, 19210 Bor, Serbia

Abstract

The change in pH and conductivity values during the rinsing of the walnut shells as well as during the adsorption of copper ions wasinvestigated in this study. The pH value increases during the rinsing of the adsorbent, reaching a constant value after the passing of 100 ml of distilled water. The increase in the pH value during the rinsing of the adsorbent occurs as a result of the transfer of H^+ ions from the aqueous phase into the molecular structure of the adsorbent, where they are exchanged with alkali and alkaline-earth metal ions. As for conductivity change, a sudden increase in conductivity occurs after passing the first 50 ml of distilled water, followed by a decrease in conductivity with further rinsing. The increase in conductivity is most likely caused by the increase in the concentration of alkali and alkaline earth metal ions in the solution, which are being transferred from the adsorbent structure into the aqueous phase. During the adsorption process, the pH value rapidly increases for the first few minutes, after which starts to decline. The release of H^+ ions from the adsorbent structure into the aqueous phase causes a rapid decrease in pH value as a result of the deprotonation of functional groups in the adsorbent molecular structure. The conductivity increases during the adsorption process. This increase is due to an increase in the concentration of alkali and alkaline earth metal ions in the solution, which are exchanged with copper ions during the adsorption process.

***Keywords**: Adsorption, copper ions, walnut shells, pH, conductivity.*

1. INTRODUCTION

The growing development of the mining and metal processing industry in the 21st century, which aims to process ores, metals, minerals, and other raw materials as efficiently as possible, has led to the creation of a huge amount of wastewater [1]. For an industry to be able to operate smoothly, it is necessary to comply with legal laws that require efficient wastewater treatment systems [2].During the last two decades, there has been an increase in environmental awareness in the world, which has contributed to the development of new, efficient, ecological, and economically acceptable technologies for wastewater treatment.Removal of heavy metals from wastewaters can be achieved by already existing conventional technologies such as: chemical precipitation, coagulation and flocculation, adsorption, ion exchange, solvent extraction, electrochemical methods, cementation, and various membrane processes [3].A new potential method of wastewater treatment, especially wastewaters with low content of pollutants, is adsorption using natural adsorbents–biosorption [4]. The main advantages of the biosorption process, compared to the conventional technologies, are: high efficiency in treating very dilute effluents, low operating costs, natural adsorbents are often with low or without economic value, and minimizationof obtained sludge [5].

In this paper, walnut shells were used as an adsorbent for copper ions adsorption from aqueous solutions. The pH and conductivity values were monitored during the rinsing of the adsorbent as well as during the adsorption process.

2. EXPERIMENTAL

The adsorption experiments were performed by bringing into contact 0.5 g of walnut shells with 50 ml of a synthetic copper ions solution of initial concentration 0.2 g dm^{-3}. Prior the experiments, walnut shells were firstly ground, then sieved through a set of laboratory sieves, and the sieve fraction (-1+0.4) mmwas used for the experiments.All the sampleswere rinsed with 200 ml of distilled water before the adsorption experiments.

3. RESULTS AND DISCUSSION

3.1 Change of pH value during the rinsing of walnut shells with distilled water

The change in pH value during the rinsing of walnut shells is shown in Figure 1. It can be seen that the pH value rises quickly at the beginning of the adsorption process, reaching a near-constant value after passing 100 ml of distilled water. The increase in pH value most likely occurs due to the transfer of H^+ ions from the aqueous phase into the structure of the walnut shells, where they are exchanged with the alkali and alkaline earth metal ions from the walnut shells structure.

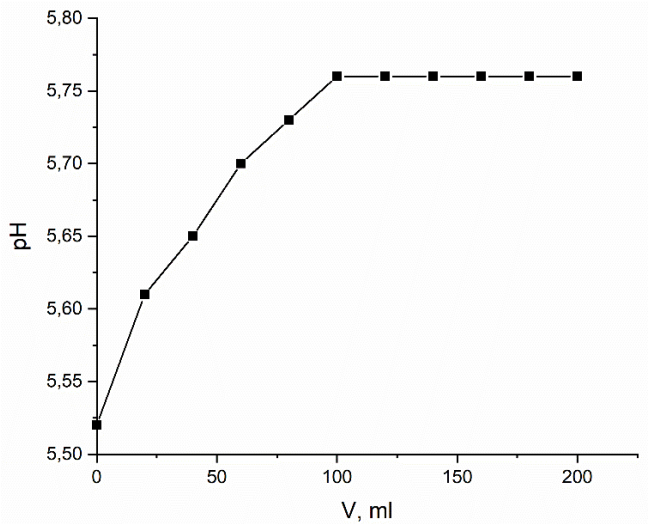

Figure 1. Change in pH value of the solution during the rinsing of the walnut shells

3.2 Change in conductivity of the solution during the rinsing of walnut shells with distilled water

The change in conductivity of the solution during the rinsing of walnut shells with distilled water is shown in Figure 2. It can be seen, that the conductivity first rises up to around 50 ml of distilled water passed, where it reaches its maximum value. After that, with further rinsing, a decrease in the conductivity of the solution is noted. The increase in the conductivity occurs due to the increase in the concentration of alkali and alkaline earth metal ions in the solution, which are transferred from the walnut shells structure into the aqueous phase. With further rinsing, the conductivity decreases as a result of a decrease in the concentration of these ions due to the dilution of the solution.

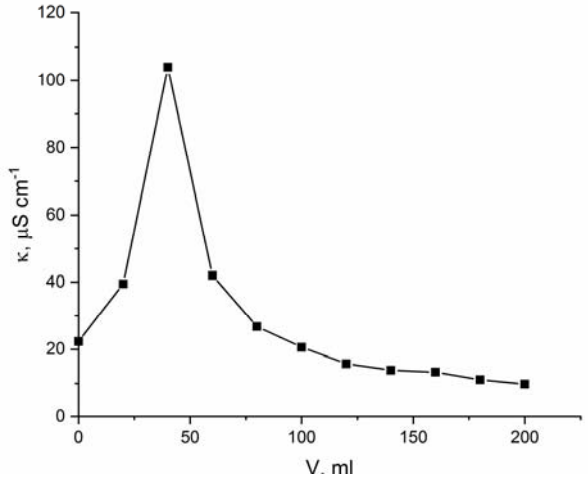

Figure 2. Change in conductivity of the solution during the rinsing of walnut shells with distilled water

3.3 Change of pH value during the adsorption of copper ions onto walnut shells

Quite a different change in pH value was noted during the adsorption process, opposed to the rinsing of the adsorbent. The change in pH value of the solution during the adsorption of copper ions onto walnut shells is shown in Figure 3. As can be seen from Figure 3, the pH value sharply increasesin the first few minutes of the process, after whichdecreases,reaching almost a constant value after 30 minutes of the adsorption process. The decrease in pH value occurs due to the deprotonation of functional groups existing in the structure of the walnut shells, and the transfer of H^+ ions into the solution, where they are exchanged with copper ions.

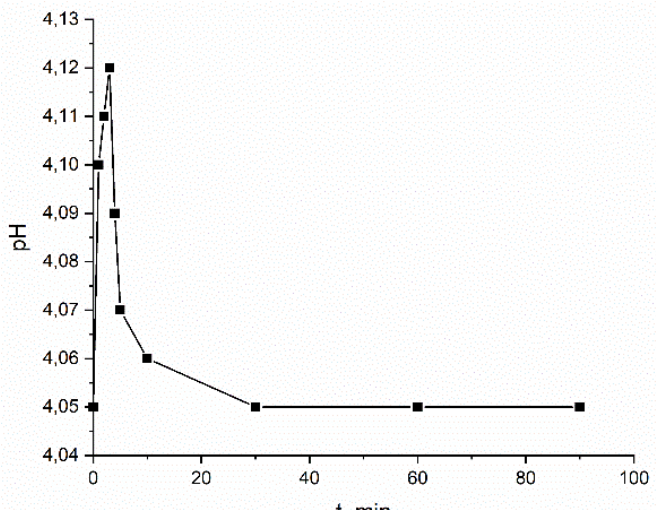

Figure 3. Change in pH value of the solution during the adsorption of copper ions onto walnut shells

3.4 Change in conductivity of the solution during the adsorption of copper ions onto walnut shells

The change in conductivity of the solution during the adsorption of copper ions onto walnut shells is shown in Figure 4. As can be seen from Figure 4 the conductivity of the solution increases during the adsorption process. Thisincrease in conductivity occurs due to the increase in the concentration of alkali and alkaline earth metal ions in the solution, which are being exchanged with copper ions during the adsorption process.

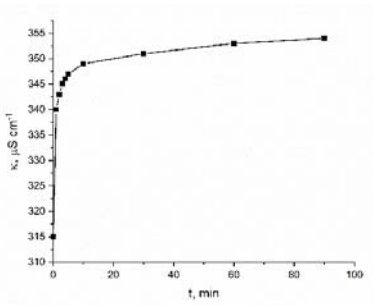

Figure 4. Change in conductivity of the solution during the adsorption of copper ions onto walnut shells

4. CONCLUSIONS

During the rinsing of the adsorbent, the pH value of the solution increases due to the transfer of H^+ ions from the aqueous phase into the structure of the walnut shells. The conductivityof the solution first rises up to around50 ml of distilled water passed, where it reaches its maximum value. After that, with further rinsing, a decrease in the conductivity of the solution is noted. The increase in the conductivity occurs due to the increase in the concentration of alkali and alkaline earth metal ions in the solution, which are transferred from the walnut shells structure to the aqueous phase. With further rinsing, the conductivity decreases as a result of a decrease in the concentration of these ions due to the dilution of the solution. For the adsorption experiments,the pH value sharply increases in the first few minutes of the process, after which decreases, reaching almost a constant value after 30 minutes of the adsorption process. The decrease in pH value occurs due to the deprotonation of functional groups existing in the structure of the walnut shells, and the transfer of H^+ ions into the solution, where they are exchanged with copper ions. The conductivity of the solution increases during the adsorption process. This increase occurs due to the increase in the concentration of alkali and alkaline earth metal ions in the solution, which are being exchanged with copper ions during the adsorption process.

ACKNOWLEDGEMENTS

The research presented in this paper was done with the financial support of the Ministry of Education, Science and Technological Development of the Republic of Serbia, within the funding of the scientific research work at the University of Belgrade, Technical Faculty in Bor, according to the contract with registration number 451-03-9/2021-14/200131.

REFERENCES

[1] T. V. Ramchadra, N. Ahalya, R. D. Kanamadi, CES Technical Report 110 (7) (2005) 1-34.
[2] H. A. Qdais, H. Moussa, Desalination 164 (2) (2004) 105-110.
[3] S. E. Ghazy, A. H. M. Gad, Arab. J. Chem. 7 (2014) 277-286.
[4] N. Ahalya, T. V. Ramchadra, JACEN 7 (2003) 71-79.
[5] D. Kratochvil, B. Volesky, Trends Biotechnol. 16 (1998) 291-300.

ELECTROCHEMICAL BEHAVIOR OF COPPER IN CHLORIDE MEDIUMIN THE PRESENCE OF WALNUT SHELL MACERATE

Vesna Grekulović[1], Aleksandra Mitovski[1], MirjanaRajčićVujasinović[1], Nada Štrbac[1], MilicaZdravković[1], Milan Gorgievski[1], MiljanMarković[1]

[1]Technical Faculty Bor, University of Belgrade, V.J. 12, 19210 Bor, Serbia

Abstract

The use of plant extracts to inhibit the corrosion of copper and its alloys has been the subject of numerous scientific studies. This paper presents the results of researchthe electrochemical behavior of copper during oxidation in a solution of 0.5 mol/dm^{3}NaCl in the absence and presence of walnut shell macerate in different concentrations. The electrochemical behavior of copper was investigated by method of open circuit potential measurement and cyclic voltammetry method. The results of measuring the open circuit potential show that the values obtained in the presence of walnut shell macerate are more positive in relation to the value recorded without the addition of walnut shell macerate. Three current peaks that correspondto copper chloride and copper oxide formation appear on the anode polarization curve obtained without the presence of walnut shell macerate. The value of current peaks decreases with increasing concentration of walnut shell macerate in the electrolyte. Lower current valuesin the presence of walnut shell macerate indicate that walnut shell macerate has got an inhibitory effect on processes resulting with these current peaks.

***Keywords**: copper, electrochemical behavior, chloride medium, walnut shell macerate.*

1. INTRODUCTION

Due to its properties,copper is one of the most important metals used in industry. First of allit has good electrical and thermal conductivity, good mechanical workability and partly noble properties. It has found wide application in the electronic industry, in the production of wires, sheets, pipes for households, in the computer and microelectronic industry, as well as in the production of a large number of alloys [1]. Copper corrosion and its inhibition in different environments, especially those containing chloride ions, have been subject of numerous scientific studies [2-4]. The possibility of protecting copper from corrosion is attracting the attention of numerous researchers, so that a large number of possible inhibitors have been tested to date. Inhibitors are substances that are added in various concentrations to a given solution that contains aggressive ions. They can have organic or inorganic origin. However, many inhibitors have shown negative effects like damaging the environment, so the discovery and development of new environmentallyfriendly inhibitors and the study of the mechanism of their action is the subject of many actualscientific studies[5, 6].

Plant extracts as potential corrosion inhibitors have become the subject of numerous scientific studies in recent years. Extracts of various parts of plants, such as seeds, bark and flowers can be used as metal corrosion inhibitors.

2.EXPERIMENTAL

The experiments were performed on a system consisting of:
- electrochemical cellwith three electrodes (working, reference and auxiliary),
- hardware (PC, AD/DA converter PCI-20428W manufactured by Burr-Brown and analog interface developed at the Technical Faculty in Bor) [7],

- measurement and control software (LabVIEW platform and specially developed application for electrochemical measurements) [7].

Experimentstestingelectrochemical behavior of copper in 0.5 mol/dm^{3}NaCl without and with the addition of walnut shell macerate (in further text: w.s.m) were performed by measuring the open circuit potential in relation to the saturated calomel electrode (SCE) during 60 seconds, and recording anode polarization curves in the potential range of -0.4 V vs. SCE up to 1 V vs. SCE with a scan rate of 20 mV/s.

The substances used for the preparation of working solutions are NaClp.a purity, manufactured byd.d. "ZorkaPharma" Šabac, chopped walnut shells and distilled water. The macerate was prepared as follows: 100 g of chopped walnut shells were added to 1000 mL of distilled water and heated to 60 ˚C. The mixturewas stirred four hours on a magnetic stirrer at a mixing speed of 400 min^{-1}. After four hours, the obtained macerate was filtered on a Bihner apparatus and stored in the refrigerator.

3. RESULTS AND DISCUSSION

The results of measuring the open circuit potential for pure copper in 0.5 mol/dm^{3}NaCl with and without the presence of w.s.m.during 60 seconds are shown in Figure 1.

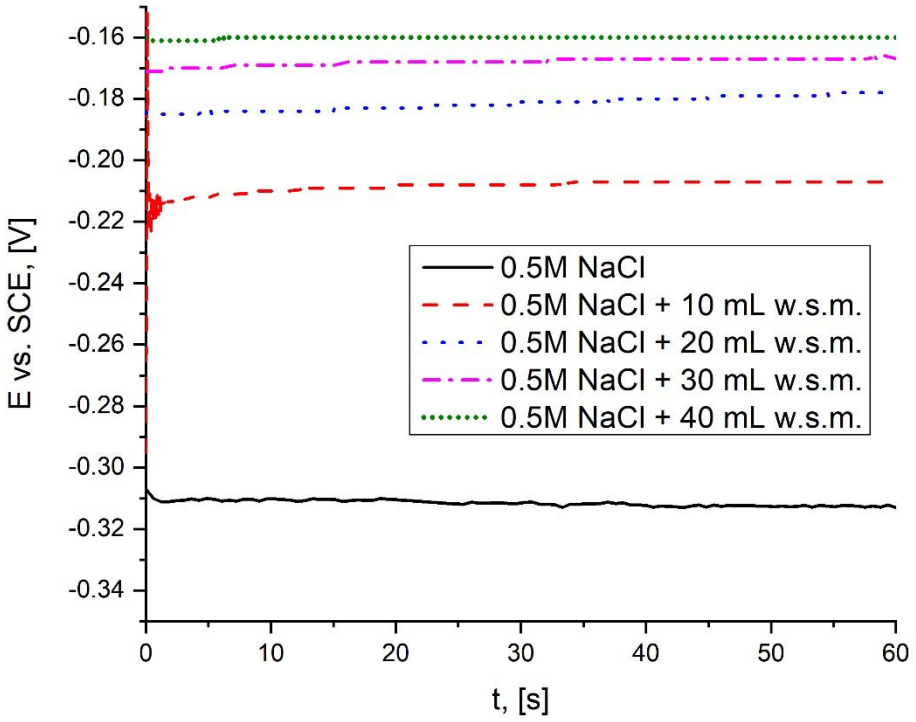

Figure 1.Open circuit potential of copper in 0.5mol/dm^{3}NaCl, with and without the addition of walnut shell macerate;(w.s.m. - walnut shell macerate)

Based on the measurement of the open circuit potential, it can be noticed that the open circuit potential for copper in pure 0.5 mol/dm^{3}NaCl is the most negative with the value of -0.313 V vs. SCE. With the addition of 10 mL of w.s.m.the open circuit potential is -0.207 V vs. SCE,after stabilization. With the addition of 20 mL of w.s.m., the open circuit potential is -0.178 V vs. SCE. With the addition of 30 mL and 40 mL of w.s.m.the open circuit potential stabilizes very quickly and with the addition of 30 mL of w.s.m.the open circuit potential is -0.166 V vs. SCE, while with the addition of 40 mL the open circuit potentialis -0.160 V vs. SCE.

Figure 2 shows the anodic polarization curves for pure copper without and in the presence of w.s.m.in different concentrations.

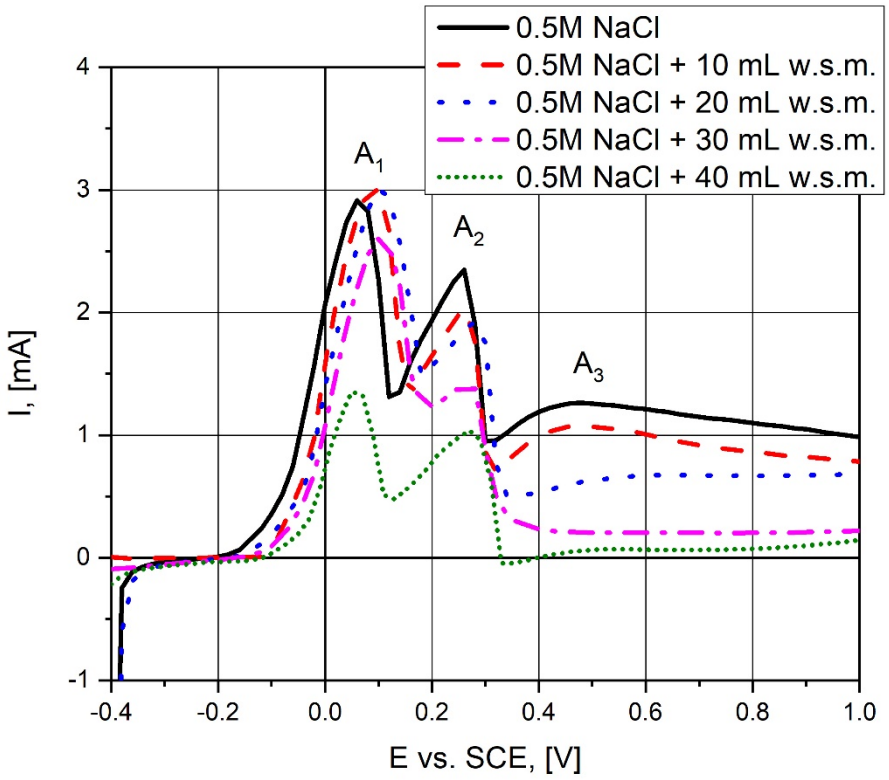

Figure 2.Anodic polarization curves for copper in 0.5 mol/dm^{3}NaCl, with and without the addition of walnut shell macerate;(w.s.m. - walnut shell macerate); scan rate 20 mV/s

Three current peaks were observed on the anode polarization curve recorded for copper in 0.5 mol/dm^{3}NaCl. Current peak A_1 appears at 0.06 V vs. SCE, current peak A_2 at 0.26 V vs. SCE, and the current peak A_3 at 0.46 V vs. SCE.

The current peaks A_1 and A_2 correspond to the formation of copper chloride by the following mechanism[8,9]:

$$Cu + Cl^- = CuCl_{ads} + e^- \quad (1)$$

$$CuCl_{ads} + Cl^- = CuCl_2 \quad (2)$$

$$Cu + CuCl_2^- = 2CuCl + e^- \quad (3)$$

The current peak A_3 corresponds to the formation of Cu_2O oxide according to the equation[10]:

$$2CuCl + 2OH^- = Cu_2O + H_2O + 2Cl^- \quad (4)$$

With the addition of 10 mL and 20 mL of w.s.m., the current valuesfor peak A_1 are higher than the current without the addition of w.s.m, while with the addition of 30 mL and 40 mL of w.s.m., the current valuesare lower than the current obtainedin pure NaCl solution. In the potential range where current peaks A_2 and A_3 occur, the current valuesare lower at all w.s.m. concentrations than the current valuesin pure NaCl solution. Also, current peaks obtained in the presence of w.s.m.appear at more positive potentials. The results obtained by the cyclic voltammetry method show that w.s.m.acts as an anodic inhibitor of copper corrosion.

4. CONCLUSION

Increasing concern for the environment has led to stricter regulations regarding the use of chemicals that can have a detrimental effect on the environment, which has resulted with the reduction or complete suspension of the use of a number of highly effective copper corrosion

inhibitors. Recently, the focus of research has been put on the inhibitory effect of so-called green inhibitors.

Green inhibitors can be of animal or plant origin. They are biodegradable, cheap and do not harm the environment. The inhibitory effect of some plant extracts is achieved thanks to the presence of tannins, vitamins and natural polymers in their composition.The possibility of using walnut shell macerate to protect copper from corrosion was investigatedin this paper.

Based on the performed experiments, the following conclusions can be made:

- According to the obtained results of measuring the open circuit potential for copper in 0.5 mol/dm^{3}NaCl without and with the addition of walnut shell macerate, it can be concluded that the open circuit potential valuesare more positive in the presence of the macerate than the open circuit potential without macerate addition.
- Examination of the electrochemical behavior of copper by the method of cyclic voltammetry in 0.5 mol/dm^{3}NaCl showed that three current peaks appear on the anode polarization curve. The current peaks A_1 and A_2 correspond to the formation of copper chloride, while the current peak A_3 corresponds to the formation of copper oxide on the surface. In the presence of walnut macerate, the inhibitory effect of macerate is achieved in the area of potential A_1 with the addition of more than 20 mL, while in the area ofpotentials A_2 and A_3, walnut macerate has an inhibitory effect at all tested concentrations of walnut macerate.

ACKNOWLEDGEMENTS

The research presented in this paper was done with the financial support of the Ministry of Education, Science and Technological Development of the Republic of Serbia, within the funding of the scientific research work at the University of Belgrade, Technical Faculty in Bor, according to the contract with registration number 451-03-9/2021-14/200131

REFERENCES

[1] P. Gertik, Noble Metals, GIP “Slobodan Jovic”, Belgrade, 1997 (in Serbian)
[2] E.M. Sherif, P. Su-Moon,Electrochem. Acta, 51 (2006) 6556-6572.
[3] V. Grekulović, M. Rajčić-Vujasinović, Corrosion 68 (2012) 025003-1.
[4] M.Antonijević, S.Milić, S.Šerbula,G.Bogdanović, Electrochim.Acta, 50 (2005) 3693–3701.
[5] M.Emad, M.AL-Rasheedi, J. Mater. Environ. Sci., 6 (1) (2015) 201-206.
[6] A. Y.El Etre, Corros. Sci., 40,11 (1998) 1845-1850.
[7] Z. Stević, M. RajčićVujasinović, Hem. Ind., 61 (2007) 1-6.
[8] T. Kosec, I. Milosev, B. Pihlar, Appl. Surf. Sci., 253 (2007) 8863–8873.
[9] S. Mamas, T. Kıyak, M. Kabasakaloglu, A. Koc.Mater. Chem. Phys., 93 (2005) 41–47.
[10] M. M.Antonijević, S. M.Milić, M. B. Petrović.,Corros. Sci., 51 (6) (2009) 1228-1237.

The 52nd International October Conference on Mining and Metallurgy
November 29th – 30th , 2021
www.ioc.tfbor.bg.ac.rs

EXPERIMENTAL DESIGN APPROACH IN RADIONUCLIDE SORPTION

Marija Šljivić-Ivanović[1], Slavko Dimović[1], Ivana Jelić[1],

[1]Vinča Institute of Nuclear Sciences, University of Belgrade, M.P.A. 12-14, 11351 Belgrade, Serbia

Abstract

This paper presents the utilization of experimental design for investigation of sorption from multi-component systems. i.e. suspensions similar to real liquid radioactive waste (LRW).Experimental design methodology is a powerful tool in the examination of selected ions/radionuclides competition during the sorption. For better understanding, an example of competitive sorption of a multi-component solution of strontium, cobalt, and nickel divalent ions onto waste concrete is shown.

Keywords*: liquid radioactive waste, immobilization, solidification.*

1. INTRODUCTION

Experimental design methodologyis a powerful tool inthe examination of selected ions (radionuclides) competition during the sorption from multi-component suspensions (systems)which are similar to real liquid radioactive waste (LRW) [1-4]. The experimental design represents a practical method, applicable in all research disciplines, able to investigate relations between the cause and the effect. The main characteristic of this approach is the simultaneous variation of independent variables input. This is anexcellentmechanism to minimize the total number of experimental trials, in regard to classic approach (one factor at a time). Depending on problem type and purpose of the investigation, different full or fractional factorial designs, surface methodology, block designs, and others could be utilized. These methodologies are especially useful for the investigation of the experimental conditionsmodification effects. Otherwise, the influence of mixture composition variation on system response can be investigated using a mixture design as a type of surface response methodology.

2. EXPERIMENTAL DESIGN

The first investigation with elements of experimental planning was performed in 1747 when surgeon James Lind performed a systematic study of the effect of drugs on patients suffering from scurvy [5-7]. Yet, the development of statistical methods in the design of experiments began with the statistician Ronald Fisher in 1825 [7].

Experimental design is a statistical method that allows simultaneous variation of all factors of an examined process, whereby a large amount of information about a given process is obtained with a relatively small number of experiments. This design allows the definition of empirical mathematical models that describe a given process. Proper selection of independent variables, their variation, and monitoring of system responses can define the influence of factors and the influence of their mutual interactions on the system response, i.e. dependent variable [1-4].Depending on problem type and testpurpose, different types of experimental designs are developed. If the goal is to define significant process variables (screening), factorial design (complete or fractional) and Plackett-Burman design are most often used. In order to optimize a process, different types of response surface designs are used (e.g. Box-Behnken design, central composite design, Taguchi design, etc.) [5-6].

Mixture design is a special design type in which the quantities or shares of different components in the mixture (whose influence is examined on some specific property of the mixture: dependent variable, system response, etc.), which are assumed to be only a function of the mixture composition, are varied as independent factors. Three mixture designs are available: Simplex Lattice, Simplex Centroid, and Extreme Vertices design [5].The experimental domains of Simplex designs cover all components in the mixture, i.e. covers the entire surface of Simplex, while the design of extreme peaks covers only part of Simplex and is used when there are restrictions on the amount/share of some or all components in the mixture [5-8].

3. SIMPLEX CENTROID DESIGN

The Simplex Centroid experimental design is customarilyused to examine ion sorption competitiveness in multi-component solutions during the sorption process.If a three-component mixture is considered (q = 3, where*q*is a number of components in the mixture), the number of experimental points corresponding to the number of one-, two- or three-component equimolar mixtures in Simplex Centroid design is 7 (2q – 1 = 7).Graphical interpretation of the obtained results could be presented in the form of ternary contours. The given points represent three points of the one-component mixture, three points of the two-component equimolar mixture, and one point of the three-component equimolar mixture which are located at the vertices of the triangle, in the middle of the sides, and one in the triangle center, respectively.It is possible to add three more points which refer to three-component mixtures of composition 2/3 of one component and 1/3 of total other components, i.e. 1/6 of the remaining two components. These three points correspond to the composition of the mixture with all permutations, which are 2/3:1/6:1/6, 1/6:2/3:1/6,and 1/6:1/6:2/3. In this way, a total of 10 points are obtained(Figure 1) [5-6].

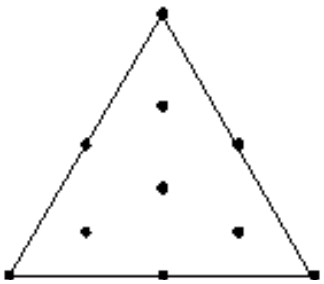

Figure 1. The point's positions in the Simplex Centroid design [6]

This methodology is used, firstly, to determine empirical mathematical models that could be used to predict system responses for any component ratio in a mixture and, secondly, to define the effect of each component individually or in combination with other components on system response.

The most complex model that can be used to describe the results of the Simplex Centroid design for a three-component mixture is a special cubic model, whose solution resulted in:

$$Y = \beta_1\ x_1 + \beta_2\ x_2 + \beta_3\ x_3 + \beta_{12}\ x_1x_2 + \beta_{13}\ x_1x_3 + \beta_{23}\ x_2x_3 + \beta_{123}\ x_1x_2x_3 + \epsilon \qquad (1)$$

where Y is the system response, x_1, x_2, and x_3 are the initial metal concentrations (independent variable), x_1x_2, x_1x_3, x_2x_3, and $x_1x_2x_3$ are interactions terms, β_1, β_2, and β_3 are regression coefficients, β_{12}, β_{13}, β_{23}, and β_{123} are coefficients that correspond to quadratic and ternary terms, ϵ is residual.

4. SIMPLEX CENTROID DESIGN EXAMPLE

An example of competitive sorption tests of a multi-component solution of strontium, cobalt, and nickel divalent ions onto waste concreteis given below [2].

Table 1 - Caption of table [2]

Experimental run	Molar proportions of cations in the mixtures		
	Sr	Co	Ni
1	2/3	1/6	1/6
2	0	1/2	1/2
3	1/3	1/3	1/3
4	0	1	0
5	1/2	0	1/2
6	1/2	1/2	0
7	1/6	1/6	2/3
8	0	0	1
9	1	0	0
10	1/6	2/3	1/6

Sorbed amounts of the investigated cations are presented in Figure2, as a function of solution composition defined in Table 1.[2].

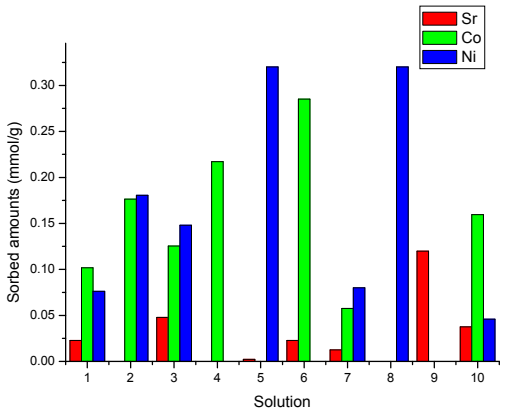

Figure 2. Sorbed amounts of Sr^{2+}, Co^{2+}, and Ni^{2+} from multi-component solutions by waste concrete [2]

A special cubic model is used for the description of data obtained by the Simplex Centroid design. For a three-component solution, this general model can be presented by equitation (1) and the following equations are derived (including only statistically significant terms) [2]:

$$\text{Concrete}-\text{Sr} = 0.082151\text{Sr} + 0.006431\text{Co} - 0.008789\text{Ni} \quad (2)$$

$$\text{Concrete}-\text{Co} = -0.001552\text{Sr} + 0.221311\text{Co} + 0.011582\text{Ni} + 0.576376\text{Sr}-\text{Co} \quad (3)$$

$$\text{Concrete}-\text{Ni} = 0.04441\text{Sr} - 0.01226\text{Co} + 0.31937\text{Ni} \quad (4)$$

These equations imply that the sorption of investigated cationsis directly proportional and principally affected by their own concentration in the multi-component solution. A significant interaction was found only in the case of Co^{2+} sorption from the mixture, i.e., the interaction between Sr^{2+} and Co^{2+} ions enhanced the efficiency of Co^{2+} removal. According to coefficients in equations 2 – 4, both positive and negative effects of coexisting cations were at least one order

of magnitude lower in respect to the most dominant effect [2].These equations can be graphically presented by the construction of ternary contour plots (Figure 3) [2].

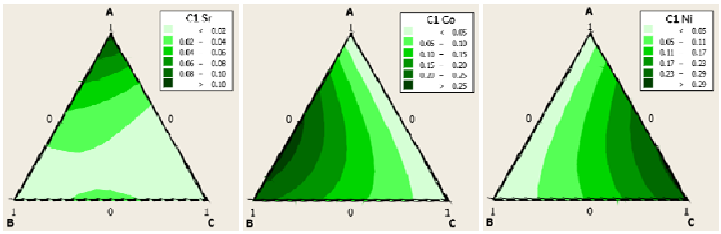

Figure 3. Ternary contour plots of (a) Sr^{2+}, (b) Co^{2+}, and (c) Ni^{2+}sorbed amounts onto waste concrete [2]

5. CONCLUSION

The experimental design represents a practical method, applicable in all research disciplines, able to investigate relations between the cause and the effect. This design allows the definition of empirical mathematical models that describe a given process. It is a powerful tool in the examination of selected ions (radionuclides) competition during the sorption from multi-component suspensions (systems) which are similar to real liquid radioactive waste (LRW). The Simplex Centroid experimental design is customarily used to examine ion/radionuclide sorption competitiveness in multi-component solutions during the sorption process. For the clarity, the example was shown, with given equations and their graphical presentation.

ACKNOWLEDGEMENTS

The research presented in this paper was done with financial support of the Ministry of Education, Science and Technological Development of the Republic of Serbia, within the funding of scientific research work at the University of Belgrade, Vinca Institute of Nuclear Sciences (Contract No. 451-03-9/2021-14/200017).

REFERENCES

[1] I. Jelic, M. Sljivic-Ivanovic, S. Dimovic, D. Antonijevic, M. Jovic, Z. Vujovic, I. Smiciklas, Water Air Soil Pollut, 230 (10) (2019).
[2] M. Sljivic-Ivanovic, I. Jelic, S. Dimovic, D. Antonijevic, M. Jovic, A. Mrakovic, I. Smiciklas, Clean Technol Environ Policy 20(6) (2018) 1343-1354.
[3] M. Sljivic-Ivanovic, I.Jelic, A.Loncar, D.Nikezic, S.Dimovic, B.Loncar, Nucl Technol RadiatProt 32 (3), (2017) 281-287.
[4] I. Jelic, M. Sljivic-Ivanovic, S. Dimovic, D. Antonijevic, M. Jovic, R. Serovic, I. Smiciklas, Process Saf Environ Prot 105 (2016) 348-360.
[5] G. Limousin, J. Gaudet, L.Charlet, S.Szenknect, V. Barthes, M. Krimissa,Appl Geochem 22, (2007) 249-275.
[6] Ž. Lazić, Design of experiments in chemical engineering, Wiley-VCH, Weinheim, Germany, 2004.
[7] P.Dunn,Arch Dis Child 76 (1)(1997) 64-65.
[8] R. Fisher, The design of experiments. Oliver and Boyd, Edinburg, 1947.

The 52nd International October Conference on Mining and Metallurgy
November 29th – 30th , 2021
www.ioc.tfbor.bg.ac.rs

INFLUENCE OF SILICA FUME ON SCC CONCRETE PROPERTIES

Ivana Jelić[1], Aleksandar Savić[2], Marija Šljivić-Ivanović[1], Slavko Dimović[1]

[1]Vinca Institute of Nuclear Sciences, University of Belgrade, M.P.A. 12-14, 11351Belgrade, Serbia

[2]Faculty of Civil Engineering, University of Belgrade, B.K.A. 73, 11000 Belgrade, Serbia

Abstract

The use of recycled materials or waste increases sustainability in the construction sector. Likewise, the self-compacting concrete (SCC) has shown improvement in mechanical properties, when made with some waste pozzolanic materials. The differences in the compressive strength of the SCC concrete sample in the case of 5% by mass share of silica fume compared to samples with 7% were explored. The results shown that optimal replacement of Ordinary Portland Cement by silica fume is 5%, under applied experimental conditions.

***Keywords**: sustainability, recycling, compressive strength.*

1. INTRODUCTION

The durability of concrete can be improved by limiting size and type of aggregate, the w/c ratio, and also by the usage of pozzolanic materials like: silica fume, nano-silica, fly-ash, blast furnace slag, etc. [1]. On the other hand, the use of recycled materials or waste increases sustainability in the construction sector [2]. Substitution of Ordinary Portland Cement (OPC) by waste pozzolanic materials in concrete also increases the energy efficiency of the processes involved.

Silica fume represents a by-product from the exhaust gases of ferrosilicon, silicon, and metal alloys smelting furnaces [1]. Silica fume addition in concrete might refine pore structure which leads to improvement in permeability and durability of concrete. By the utilization of optimum dosage of silica fume, a significant increase in strengths could be achieved. A concrete of high durability can be developed using fine ground pozzolanic admixture silica fume [3]. The better performance of concrete could be attributed to the fact that it exhibits lesser micro cracking and dense microstructure due to silica fume and calcined clays as pozzolans for concrete [4].

Also, the self-compacting concrete (SCC) has revealed improvement inmechanical properties made by using silica fume [5]. Due to the higher fineness of silica fume, it reacts very fastwith some hydration products of cement and thereby reducesthe porosity of concrete, hence resulting in improvement ofmechanical and durability properties of the concrete. In the earlystages, silica fume remains an inert material in concrete. Thehydration of cement produces C-S-H (Calcium Silicate Hydrate)and calcium hydroxide (free lime). C-S-H isresponsible for strength. The pozzolanic action takes placebetween calcium hydroxide and silica fume, which further producesadditional C-S-H in the voids left after hydration of cement.The extra C-S-H improves mechanical and durability properties by providing a much denser matrix [6].

According to the literature data, the author's opinions are divided regarding the participation of silica fume. By some authors, the optimized dosage of silica fume lies in 7 – 10 or 8–10% share of cement (by weight) [7]. However, some investigation showed that the optimal rate of silica fume in concrete is 5%. It is observed that the optimum dose of silica fume is 5% when used as a partial replacement of OPC. The silica fume inclusion increases the workability and strength of concrete considerably[8].

The aim of this study was to investigate the effect of reducing the recommended silica fume dose in SCC with recycled aggregate. The differences in the compressive strength of SCC concrete in the case of a 5% share of silica fume compared to samples with 7% were explored.

2. EXPERIMENTAL

Materials of sampleswere:

- Silica fume (0.1μm average particle size);
- OPC, PC35 M (V-L) 42.5 R,Beočin, Serbia;
- Limestone filler, Granit peščar, Ljig, Serbia;
- Superplasticizer, TKK, Slovenia;
- Aggregate, Gradient, Serbia;
- Recycled aggregate, smashed experimental samples;
- Water.

Namely, all samples had to achieve values of slump flowmore than 800 mm according to recommendations [9], therefore a required amount of superplasticizer was used.

The defined compositions of the SCC samples are listed in Table 1.

Table 1 –Compositions of the samples

Materials	Amounts	
	SCC7	SCC5
OPC	353.4 kg/m^3	368.6* kg/m^3
Limestone filler	223 kg/m^3	223 kg/m^3
Superplasticizer	1.1%	1.1%
Water	178 kg/m^3	178 kg/m^3
Aggregate (I, II, and III faction)	860; 265; 155 kg/m^3	860; 265; 155 kg/m^3
Recycled aggregate (I, II, and III faction)	0; 265; 155 kg/m^3	0; 265; 155 kg/m^3
Silica fume	7%	5%

*OPC mass was increased due to the reduced mass of silica fume

The extremely fine, amorphous, and latently reactive silica fume was used. Before water addition, silica fume was mixed with OPC. The optimal mixing time was 90 s.

Dry materials, i.e. recycled aggregate, limestone filler, and cement/silica fume mixture were mixed for one minute. Water was added for the next 30 s, after which the superplasticizer was dosed with the addition of water. Stirring was continued until 5 min. had elapsed. The samples were demolded after 1 day andcured in 20˚C water for 28 and 90 days (in total).

3. RESULTS AND DISCUSSION

The compressive strength tests were performed according to the standard SRPS EN 12390-3:2010 for cubic samples [10].

The results are presented in Figure 1. for SCC7 and SCC5 samples after 28 and 90 days marked as SCC7-28, SCC5-28, SCC7-90, and SCC5-90, respectively.

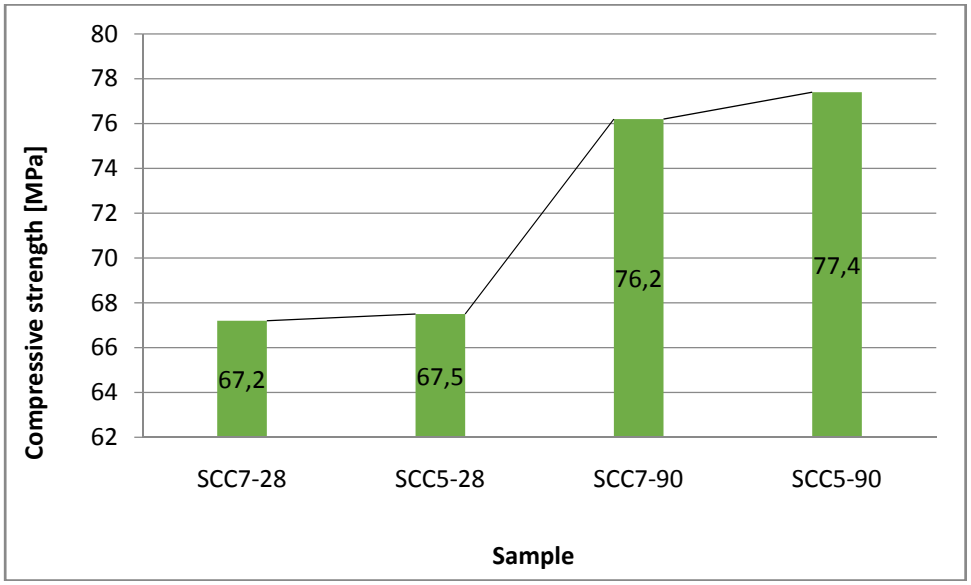

Figure 1. Compressive strengths of samples

The results showed that the compressive strength after 28 days was not significantly affected by the reduction in the amount of silicate fume. However, measurements after 90 days indicated that the sample with 5% silica fume (SCC5-90) showed slightly higher compressive strength.

Based on the results, it could be noted that the improvement in compressive strength due to silica fume incorporation in concrete occurs because of the chemical pozzolanic activity and filler action. However, an increase in thecompressive strength in SCC5 samplescould be explained by silica fume higher amount in SCC7than it was requiredfor pozzolanic actions, and hence reduction in strength [8].Likewise, the amount of OPC in SCC5 samples was higher relative to SCC7, and compressive strength was expected to be elevated. This investigation indicated that the optimal replacement of OPC by silica fume is 5%, under applied experimental conditions.

4. CONCLUSION

The effect of the recommended silica fume amount reduction in SCC with recycled aggregate was explored. The compressive strength of samples after 28 and 90 days were performed. The results for samples SCC7-28, SCC5-28, SCC7-90, and SCC5-90, were 67.2, 67.5, 76.2, and 77.4 MPa, respectively. An increase in compressive strength in samples with 5% silica fume could be explained by silica fume higher amount in SCC7 than it was required for pozzolanic actions and a higher amount of OPC.

ACKNOWLEDGEMENTS

The research presented in this paper was done with the financial support of the Ministry of Education, Science and Technological Development of the Republic of Serbia, within the funding of scientific research work at the University of Belgrade, Vinca Institute of Nuclear Sciences (Contract No. 451-03-9/2021-14/200017) and the University of Belgrade, Faculty of Civil Engineering (No. 200092).

REFERENCES

[1] S.K. Verma, C.S. Singla, G. Nadda, R. Kumar, Mater. Today, 32 (4) (2020) 882-887.
[2] M. Yilmaz, A. Bakiş, Procedia Soc.Behav. Sci., 195 (2015) 2253-2262.

[3] O. Zaid, J. Ahmad, M.S. Siddique, F. Aslam, H. Alabduljabbar, K.M. Khedher, Sci. Rep. 11, 12822 (2021).
[4] M. Antoni, Fac. Sci. Tech. L'Ingeniur, 1 (2013).
[5] H.A.F. Dehwah, Constr. Build. Mater. 26 (1) (2012) 547-551.
[6] V. Srivastava, V.C. Agarwal, R. Kumar, J. Acad. Ind. Res. 26 (4) (2012) 347-357.
[7] A. Imam, V. Kumar, V. Srivastava, Adv. Concr. Constr., 6 (2) (2018) 145-157.
[8] V. Srivastava, R. Kumar, V.C. Agarwal, P.K. Mehta, J. Environ. Nanotechnol., 3 (3) (2014) 32-35.
[9] G. Ke, J. Zhang, J. Adv. Concr. Technol., 18, (2020) 17-26.
[10] SRPS EN 12390-3:2010, Testing hardened concrete – Part 3: Compressive strength of test specimen.

L-LYSINE AS CORROSION INHIBITOR OF STAINLESS STEEL IN RINGER'S SOLUTION

Milan Radovanović[1], Ana Simonović[1], MarijaPetrović Mihajlović[1], Žaklina Tasić[1], Vladan Nedelkovski[1], Milan Antonijević[1]

[1]Technical Faculty Bor, University of Belgrade, V.J. 12, 19210 Bor, Serbia

Abstract

The effects of L-Lysine on stainless steel 316L corrosion in Ringer's solution were investigated. The investigation comprised different electrochemical techniques: measurement of open circuit potential and linear potentiodynamic polarization. The results obtained by polarization measurements show that the L-Lysine successfully inhibits the corrosion processes on stainless steel, in Ringer's solution, acting like mixed type inhibitor with a more pronounced influence on cathodic processes. Also, potentiodynamic curves indicate that L-Lysine acts through adsorption onto the steel surface without changing the mechanism ofcorrosion of steel. Quantum chemical parameters indicate that L-Lysine may be used as a corrosion inhibitor which was confirmed by electrochemical measurements.

***Keywords**: stainless steel; amino acids; corrosion; Ringer's solution; inhibition.*

1. INTRODUCTION

Steel is an alloy composed of iron and carbon, which in fact represents primary alloy widely used as a material in structural/civil engineering, because of its properties and cost efficiency. Stainless steel 316L is one of the most used material, especially in medicine, due to high corrosion resistance which is higher than at other steel due to the presence of certain alloying constituents [1].The most often use of 316L in medicine was for surgical and orthopedic implants. Steel corrodes during utilization as medical implants in human body due to exposure to aggressive ions such as chlorides present in blood plasma. High concentration of chloride ions will cause localized corrosion, while the low concentrations will cause uniform corrosion. Because of their high diffusivity, chloride ions are capable to penetrate through passive layer and cause pitting corrosion on stainless steels. If the concentration of chloride ions in the solution is high enough, accelerated corrosion with the occurrence of deeper and wider pits is to be expected [2]. The most used organic inhibitors are toxic which leads to aspiration to develop so called green inhibitors which are harmless to the environment [3].

Extracts and plant oils are recent years intensively studied as green inhibitors of metal corrosion in different solutions. Obtained results available in the literature show that plant extracts achieved inhibition efficiency which provides promise application of plant extract as potential good corrosion inhibitors [4]. Besides that, amino acids are another very promising group of compounds which already proved as green corrosion inhibitors for different metals and alloys in aggressive environment. Also, amino acids have numerous benefits: low cost of production, high purity, high degree of inhibition efficiency [5].

2. EXPERIMENTAL

The experiments were performed in the Ringer's solution without and with addition of different amount of L-Lysine (Lys). Concentration of L-Lysine used during experiments was from $1 \cdot 10^{-4}$ M up to $1 \cdot 10^{-2}$ M. The composition of Ringer's solution was shown in Table 1.

Table 1 – Composition of Ringer's solution

Component	Concentration, g/dm^3
NaCl	8.60
KCl	0.3
$CaCl_2$	0.33

Forelectrochemicaltesting of the corrosion behaviorof stainless steel 316Lpotentiostat(IVIUM XRE, IVIUMTechnologies) was used, with the appropriatesoftware. The systemis made up ofthreeelectrodes,stainless steel electrodes working, platinum as theauxiliaryelectrode andstandardcalomel electrode (SCE) as the referenceelectrode. Applied methods were measuring of the open circuit potential for 30 min andpotentiodynamic polarization. The linear potentiodynamic measurements were performed from OCP to -0.5 V vs. SCE in cathodic and to +0.4 V vs. SCE in anodic direction. Applied scan rate was 1 mV/s. All measurements were conducted at room temperature in naturally aerated solutions.

3. RESULTS AND DISCUSSION

Variations of OCP over time for stainless steel electrode in Ringer's solution, without and with the addition of different concentrations of L-Lysine are present in Figure 1a.

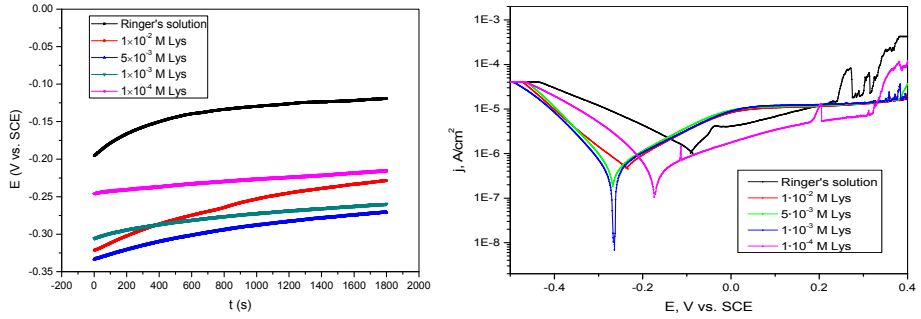

Figure 1 - Open circuit potential (a) and potentiodynamic polarization curves (b) recorded for stainless steel in Ringer's solution without and with the addition of different amount of L-Lysine

In bare Ringer's solution increase of OCP values is related with formation of protective oxide layer on steel surface.In solutions with addition of L-Lysine in whole investigated concentration range OCP values are increased from beginning indicating formation of protective layer in which structureinhibitor molecules are incorporated [6].Acquired curves presented in Figure 1a reveal that in the presence of L-Lysine OCP values become more negative in comparison with OCP obtained in bare Ringer's solution suggesting that inhibitor molecules are more favourable adsorbed on cathodic active sites [7]. Nevertheless, shift of OCP values is not significant in the presence of inhibitor which indicates that L-Lysine is more likely to act as a mixed-type inhibitor[8].

According to the obtained polarization curves presented in Figure 1b current density decrease in the presence of L-Lysine. A decrease in current density is the most pronounced in the vicinity of corrosion potential and reveal inhibitive action of L-Lysine. Also, L-Lysine shows a stronger influence on decrease of the cathodic current density. The highest tested concentration of L-Lysine decreases anodic current density not only in the vicinity of corrosion potential.Anodic peak obtained in bare Ringer's solution is omitted on polarization curves obtained in Ringer's solution with the addition of L-Lysine due to the formation of protective film on the stainless steel surface [9]. According to the polarization curves (Figure 1b) at higher potentials pitting corrosion occurs.Moreover, electrochemical kinetic parameters were obtained from polarization

curves (Figure 1b) and calculated values were presented inTable 2.Furthermore, inhibition efficiency (IE) of L-Lysine is presented also in Table 2 beside to the kinetic parameters.Inhibition efficiency was calculated according to the equation:

$$IE(\%)=[(j_{corr}-j_{corr(inh)})/j_{corr}]\times 100$$

where j_{corr} and $j_{corr(inh)}$ stand for corrosion current density recorded without and with inhibitor, respectively.

Table 2 – Electrochemical parameters of stainless steel 316L obtained using data presented in Figures 1b

Solution	E_{corr} (V vs. SCE)	j_{corr} (A/cm^2)	b_c (mV/dec)	b_a (mV/dec)	IE (%)
Ringer's solution	-0.092	$1.238\cdot10^{-6}$	-0.0189	0.0271	/
$1\cdot10^{-4}$ M Lys	-0.172	$3.284\cdot10^{-7}$	-0.123	0.085	73.5
$1\cdot10^{-3}$ M Lys	-0.265	$2.125\cdot10^{-7}$	-0.129	0.12	82.8
$5\cdot10^{-3}$ M Lys	-0.267	$1.882\cdot10^{-7}$	-0.144	0.095	76.7
$1\cdot10^{-2}$ M Lys	-0.236	$5.075\cdot10^{-7}$	-0.091	0.092	59.0

Considering the results shown in Table 2, it can be concluded that with an increase of L-Lysine concentrations, negative shift of corrosion potential (E_{corr}) values occurs. Decrease of current densities (j_{corr}) in solutions with addition of L-Lysine indicates inhibitory effect of this compound. It is also noticed that with the increase of L-Lysine concentration, inhibition efficiency drops, due to saturation of active sites on the stainless steel surface. A higher concentration of inhibitor means that in solution exist too many molecules of L-Lysine which are in confrontation for available active sites which leads to the decrease in adsorption of inhibitor molecules and to the decrease in inhibition efficiency.According to the values of Tafel slopes, molecules of inhibitor block active sites on the electrode surface due to adsorption without changing the reaction mechanism.

Quantum chemical calculations and molecule geometry optimization were performed using ArgusLab 4.0 [10]PM3-SCF method. The calculated parameters are summarized in Table 3 and they are the values of highest occupied molecular orbital energy (E_{HOMO}), lowest unoccupied molecular orbital energy (E_{LUMO}), energy gap ($\Delta E = E_{LUMO} - E_{HOMO}$), dipole moment of inhibitor (μ),ionization potential (I), electron affinity (A), electronegativity (χ), global hardness (η), maximum number of electrons transferred (ΔN_{max}) and number of transferred electrons (ΔN). The proposed spatial distribution of HOMO and LUMO is presented in Figure 2.

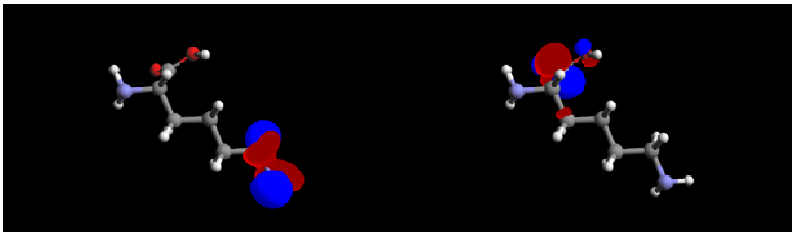

Figure 2 - Distribution of HOMO (left) and LUMO (right) of L-Lysine

Table 2 - Quantum chemical parameters

Parameter	E_{HOMO}, eV	E_{LUMO}, eV	ΔE, eV	μ, D	ΔN
value	-9.582	0.820	10.402	2.42109886	0.252
Parameter	I, eV	A, eV	χ, eV	η, eV	
value	9.582500204	-0.820332952	4.381083626	5.201416578	

Orbital energy values are indicators of the tendency of L-Lysine molecule to donate (high E_{HOMO}) or accept (low E_{LUMO}) electrons and hence to be adsorbed on the metal surface (small ΔE). Small value of η shows that it reacts with surface more readily and corrosion effect decreases, on the other hand great μ facilitates interaction with metal surface. Similar observations are already presented in literature [11]. Parameter ΔN also known as electron-donating ability, indicates the tendency of a molecule to donate electrons to the metal surface if $\Delta N>0$ [12].

4. CONCLUSION

L-Lysine acts like mixed type inhibitor of stainless steel 316L corrosion in Ringer's solution with more pronounced effect on cathodic processes. Potentiodynamic measurements indicate that L-Lysine forms protective film on steel surface which prevent contact between metal and aggressive ions. Corrosion mechanism of stainless steel is unchanged in the presence of L-Lysine.Quantum chemical parameters indicate that L-Lysine may be used as a corrosion inhibitor which was confirmed by electrochemical measurements.

ACKNOWLEDGEMENT

The research presented in this paper was done with the financial support of the Ministry of Education, Science and Technological Development of the Republic of Serbia, within the funding ofthe scientific research work at the University of Belgrade, TechnicalFaculty in Bor, according to the contract with registration number 451-03-9/2021-14/ 200131.

REFERENCES

[1] S. L. Assis, S. O. Rogero, R. A. Antunes, A. F. Padilha, I. A. Costa, J. Biomed. Mater. Res. B, 73 B (1) (2005) 109-116.
[2] M. Talha, Y. Ma, P. Kumar, Y. Lin, A. Singh, Colloid. Surface. B, 176 (2018) 494-506.
[3] B. El Ibrahimi, A. Jmaiai, L. Bazzi, S. El Isami, Arab. J. Chem., 13 (2020) 740-771.
[4] C. Verma, E. E. Ebenso, I. Bahadur, M. A. Quraishi, J. Mol. Liq., 266 (2018) 577-590.
[5] R. T. Loto, J. Mater. Res. Technol., 8 (2019) 484-493.
[6] O. Kaczerewska. R. Leiva-Garcia, R. Akid, B. Brycki, I. Kowalczyk, T. Pospieszny, J. Mol. Liq., 249 (2018) 1113-1124.
[7] M. B. Radovanović, Ž. T. Tasić, A. T. Simonović, M. B. PetrovićMihajlović, M. M. Antonijević, ACS Omega, 5 (2020) 12768-12776.
[8] M. B. Radovanović, Ž. T. Tasić,M. B. PetrovićMihajlović,A. T. Simonović, M. M. Antonijević, Sci. Rep., 9 (2019) 16081.
[9] S. Bashir, V. Sharma, H. Lgaz, I. Chung, A. Singh, A. Kumar, J. Mol. Liq., 263 (2018) 454-462.
[10] M.A. Thompson, Planaria Software LLC, Seattle, WA. http://www.arguslab.com.
[11] M. B. PetrovićMihajlović, M. B. Radovanović, Ž. Z. Tasić, M. M. Antonijević, J. Mol. Liq., 225 (2017) 127-136.
[12] B. El Ibrahimi, A. Soumoue, A. Jmiai, H. Bourzi, R. Oukhrib, K. El Mouaden, S. El Issami, L. Bazzi, J. Mol. Struct., 1125 (2016) 93-102.

The 52nd International October Conference on Mining and Metallurgy
November 29th – 30th , 2021
www.ioc.tfbor.bg.ac.rs

THE INFLUENCE OF CALCIUM IONS ON DEINKING FLOTATION RECOVERY UNDER DIFERENT CONDITIONS

Dragana Marilović[1], Maja Trumić[1], Milan Trumić[1],Ljubiša Andrić[2]

[1]Technical Faculty Bor, University of Belgrade, V.J. 12, 19210 Bor, Serbia

[2]Institute for Technology of Nuclear and other Mineral Raw Materials, Franšd'Epere 86, Serbia

Abstract

Deinking flotation is the most commonly used method in recycling paper process. Better understood of the interactions between added surfactant and the solid surfaces of ink can be accomplished by studying the fundamental mechanism. The effect of reagents on the flotation of offset paper was investigated for the purpose of efficiency removing the toner particles and fiber purification under different pH values in the presence of calcium ions. The results showed that calcium ions in combination with oleic acid remove toner particles with high efficiency in a short flotation time.

***Keywords**: deinking flotation, offset paper, calcium ions, toner recovery.*

1. INTRODUCTION

The use of secondary raw materials has several advantages, which are reflected in the conservation of natural resources and the reduction of environmental pollution and energy consumption [1]. Recycling of old paper is based on a combination of different technologies used to remove toner particles from the paper used for printing. When the particles are mechanically separated from the fibers, they are separated from the pulp by various operations. These operations include washing, screening, flotation, or a combination of these methods [2]. Many scientists have researched this area and made the conclusion that deinking flotation is most commonly used to remove ink from printed paper [3-5]. The mechanism of deinking flotation is similar to the flotation of mineral resources. Hydrophobic, non-wetting particles attach to the air bubbles and together with them float as aggregates to form a foam which is mechanically removed, while the hydrophilic fibers remain in the aqueous phase [6-8]. Practically, deinking flotation is a two-stage process which includes detaching of ink from the fibers and fillers and separation of ink particles from fibers and fillers. Deinking flotation of offset paper was researched throw experimental and simulations [9,10,11,12].

2. EXPERIMENTAL

2.1 Materials and methods

The pulp was formed from synthetic samples of white unprinted offset paper and toner cartridge from a laser printer. The pH value was regulated by 0.1 M HCl and 0.1 M NaOH. Flotation was performed with the oleic acid collector (125g/t) and $CaCl_2$ (35 kg/t). Distilled water was used for the flotation experiments. Before pulping, paper was mechanically fragmented in paper shredder into 4 mm x 40 mm. The paper type was MAESTRO standard A4, 80 g/m^2.

Figure 1 Shredded paper sample

After shredding, the sample needed to be soak in the liquid phase to allow the fibers swell for more efficient disintegration. The solid phase was soaked with about 200 ml of distilled water heated to 40 °C followed by the disintegration phase in the blender. To accelerate the swelling process of the cellulose fibers, another 200 ml of heated distilled water was added to the disintegrated sample and the cellulose fiber sample was allowed to stand for 17 hours. Synthetic toner sample was prepared by melting toner from an HP LaserJet CB435A cartridge, for 60 min at 100 °C, to provide a representative realistic sample.

Figure 2 Toner sample before melting

Flotation was performed using the oleic acid collector (125 g/t) and $CaCl_2$(35 kg/t) added to the pulp during the conditioning phase.The operating conditions for the toner flotation phase were adopted based on the values of optimal conditions from the literature [1, 11, 12, 14] and were the same for all experiments: rotation speed 1100 rpm, air flow 270 dm^3/h, pulp temperature 21-23 °C, solid phase content in pulp 1 %, conditioning time 15 min. The samples were extractedfrom the froth at 2, 4, and 20 min and then were filtered on ash less filter paper. The filter pads was transferred to an oven at 525 □ for at least two hours. The ash was analyzed by X-ray fluorescence to determine the total iron concentration.The efficiency of the process was monitored through the toner recovery in the foam product (It) and the fiber recovery in the sink product (Im).Optimization of the flotation process should provide recoveries greater than 90 % [11].

3. RESULTS AND DISCUSSION

Table 1 shows the flotation results of toner and fiber recovery for all tested conditions. The obtained results show that the greater impact of pH value is on the toner recovery than on fiber recovery.

Table 1 - Results of deinking flotation under different conditions

Flotation time t (min)	2		4		20	
pH	It (%)	Im (%)	It (%)	Im (%)	It (%)	Im (%)
3	66.03	94.51	68.40	91.46	68.71	88.21
5	69.81	93.71	71.38	90.39	71.45	86.67
7	83.38	92.22	84.50	88.67	84.81	85.97
9	68.12	93.42	69.39	91.72	69.79	88.29
12	***98.28***	***90.96***	98.95	86.80	99.38	81.01

From Table 1 can be seen that after 20 minutes of flotation in a very acidic condition (pH 3) to weakly basic (pH 9) environment, or after 4 minutes in a neutral conditions (pH 7), there is a reduced fiber recovery to about 88 %. With extended flotation time, there is a loss of fibers in the foam product. The loss of fibers from sink products to the foam layer is greatest in the highly alkaline environment, where after 20 minutes of flotation fiber recovery is 81 %. At shorter flotation times, up to 2 minutes, in a highly acidic to slightly alkaline environment, value of toner recovery increased by about 4 % on average, while in a strongly alkaline environment this increase is about 30 %. Generally, maximum values for toner recovery are reached at all pH values after 4 minutes of flotation. These results indicate a negligible effect of pH on the rate of separation of toner particles into the foam product under shorter flotation times. The highest recovery values under the given conditions were reached after 2 minutes of flotation in a strongly alkaline medium(pH = 12; Im = 98.28 % It = 90.96 %).The results are showed on Figure 3.

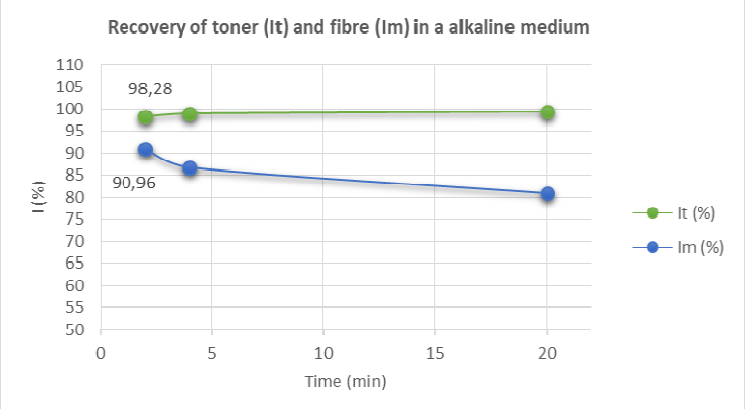

Figure 3 Toner (It) and fibre (Im) recovery at pH 12

Analyzing the maximum values obtained for fiber and toner recovery under the tested conditions in the presence of calcium chloride, it can be concluded that the optimal toner flotation time is 2 minutes. With increasing flotation time, toner recovery remains constant while fiber recovery decreases. The analysis of the results can confirm the statement of many researchers [11,13, 14]that with the increase of alkalinity under optimal conditions in the flotation process the efficiency of the toner particles flotation also increases.Comparing with the results obtained in the experiments without the addition of calcium ions [15], may say that the addition of $CaCl_2$ has an effect on the toner flotation. At the shortest flotation time at all pH values, without the addition of calcium ions, the toner recovery was less than 60 % except at pH 9, and with the addition of calcium chloride toner recovery was over 66 %. Fatty acid and calcium soap are good combination of reagents because of their mechanism. Primary mechanisms imply calcium soap precipitation which creates a layer around the toner particles through a hetero-coagulation mechanism, followed by a bubble-ink capture step [14].

4. CONCLUSION

The paper describes influence of calcium ions under different conditions on deinking flotation process. Previous flotation experiments were performed at different pH values using only oleic acid as a collector. In this research experiments were done with addition of $CaCl_2$ and by analysis the toner and fiber recovery, it has been confirmed that the calcium has a positive effect on deinking flotation of offset paper. It showed that the addition of calcium ions reduces the flotation time at alkaline conditions. In experiments performed without the addition of calcium ions, toner and fiber recovery over 90 % was not achieved. Addition of calcium ions achieved a toner and fiber recovery greater than 90 % at shorter flotation time.

REFERENCES

[1] C.A.Costa, J.Rubio, Deinking flotation: influence of calcium soap and surface-activesubstance, Laboratorio de Tecnologia Mineral e Ambiental-LTM, Minerals Engineering 18 (2005) 59–64.
[2] T.Moon, R.Nagarajan, Deinking xerographic and laser-printed paper using block copolymers, Colloids and Surfaces, A: Physicochemicaland Engineering Aspects 132 (1998) 275-288.
[3] M.Kemper, State-of-the-art and new technologies in flotation deinking, International Journal of Mineral Processing 56, 1-4, 1999, 317-333.
[4] S.Vashisth, C.P.J. Bennington, J.R.Grace, R. J. Kerekes, Column Flotation Deinking: State of-the-art and opportunities, Resources, Conservation and Recycling, 55(12), 2011, 1154-1177.
[5] R.Prakash, S.Kumar Majumder, A.Singh, Flotation technique: Its mechanisms and design parameters, Chemical Engineering & Processing: Process Intensification 127 (2018) 249–270.
[6] A.Larsson, P.Stenius, L.Odberg, Surface chemistry in Flotation Deinking – Part 1. The Flotability of Model Ink Particles, SvenskPapperstidn 87, 1984, 158-164.
[7] L.D.Ferguson, Deinking chemistry: part 2, Tappi Journal, (1992), 49-58.
[8] M.S.Trumić, M.Antonijević, M. Ž.Trumić, G.Bogdanović, Reciklažaštampanogpapiraprimenomprocesapriprememineralnihsirovina, Reciklaža I održivirazvoj 9, 2016, 48-57.
[9] A.Santos, B.Carre, A.Roring, Contribution to a better understanding of the basic mechanisms involved in the pulping and flotation of offset ink particles. Proceedings: Recycling Symposium,1996,339-347.
[10] M.A.D.Azevedo, J.Drelich, J.D.Miller, The effect of pH on pulping and flotation of mixed office wastepaper, Journal of Pulp and Paper Science, 25 (9) (1999), 317.
[11] M.S. Trumic, Kinetic model of toner separation from fiber suspension, (Dissertation),University of Belgrade, Technical Faculty in Bor, Bor, Serbia, 2015, 173.
[12] M.Vukoje, S.Jamnicki, M.Rožić, Deinkability of thermochromic offset inks, Nordic Pulp and Paper Research Journal 31 (4) 2016.
[13] R.Svensson, The influence of surfactant chemistry on flotation deinking, Dissertation, University of Technology, Sweden, (2011) 12-31,
[14] K.Theander, R. J.Pugh, Surface chemicals concepts of flotation deinking, Colloids and Surfaces A: Physicochem. Eng. Aspects, 240, 2004, 111–130,
[15] D.Marilović, M.Trumić, M.Trumić, LJ.Andrić, The influence of pH value on deinking flotation, XIII International Mineral Processing and Recycling Conference Belgrade, Serbia 8-10 may 2019, 106-110.

The 52nd International October Conference on Mining and Metallurgy
November 29th – 30th , 2021
www.ioc.tfbor.bg.ac.rs

OPTIMIZATION OF CATHODIC MATERIAL LEACHING PROCESS IN ACID-SULPHATE SOLUTION

Dragana Medić[1], Snežana Milić[1], Slađana Alagić[1], Maja Nujkić[1], Stefan Đorđievski[2], Aleksandra Papludis[1]

[1]Technical Faculty Bor, University of Belgrade, V.J. 12, 19210 Bor, Serbia

[2] Mining and Metallurgy Institute Bor, Bor, Serbia

Abstract

Lithium cobalt oxide is the first commercialized electrode material with the greatest potential for recycling. In this paper, the influence of different process parameters (leaching agent concentrations, solid phase concentrations and temperatures) on the degree of cobalt leaching was investigated. It was found that the maximum degree of cobalt leaching (about 100%) is achieved at the followingprocess parameters: sulfuric acid concentration was 3 mol/dm^3, solid phase concentration was 33 g/dm^3, volume flow of sulfur dioxide was 2 dm^3/min, temperature was 85°C and leaching process durationwas 60 minutes.

Keywords: *$LiCoO_2$, leaching, sulfur dioxide.*

1. INTRODUCTION

Sony commercialized the production of lithium-ion batteries in 1991, and their use in many electronic devices and electric vehicles has grown since then [1]. Improper disposal of waste batteries enables the release of cobalt into the environment, which presence in water systems can cause intestinal disorders, hearing loss, ischemia of the heart muscle, etc. [2]. Battery recycling technology protects the environment, preserves natural metal resources, and achieve significant economic benefits [1]. The methods that can be applied in the process of battery recycling are: hydrometallurgical, pyrometallurgical and biometallurgical [3,4]. Although the pyrometallurgical process is characterized by high efficiency, its application leads to high energy consumption, material loss and emissions of gaseous pollutants [5]. Compared to the traditional pyrometallurgical process, the hydrometallurgical process requires less energy consumption, emits less harmful gases and provides a high degree of metal valorization [6]. In order to reduce costs and increase process efficiency, biometallurgical processes have been developed in recent years. However, these processes take a very long time due to the difficulties caused by the growth of bacteria [7]. For these reasons, most of the research is focused on the hydrometallurgical process for recycling of valuable metals from lithium-ion batteries.

In this paper, leaching process of cathodic material was optimized in acid sulphate solution with the use of sulfur dioxide, as a reducing agent.

2. EXPERIMENTAL

Seventeen lithium-ion batteries with cathodes made of $LiCoO_2$ were collected and used in the experiments.After the application of pretreatment techniques,the cathode material was obtained and the chemical composition is presented in Table 1. Cobalt and lithium,as basic components of cathode material, were detected by various analytical methods. The presence of aluminum in the cathode material is probably a consequence of pretreatment on spent lithium-ion cells [8,9]. The

total cobalt content was determined using the inductively coupled plasma optical emission spectroscopy (ICP-OES), while the concentration of Co^{2+}in the initial sample of cathode leaching material was determined by UV-VIS spectrophotometric method. The values of the obtained cobalt concentrations, determined with UV-VISmethod, indicated that cobalt in solution was present in the stable ionic form of Co^{2+}, which is confirmed by other authors [10,11].

Table 1 -Chemical composition of the initial cathode material for leaching

Element	Mass content (wt.%)	Analyticmethod
Co	49.81	ICP-OES
Co (Co^{2+})	49.00	UV-VIS
Li	5.98	ICP-OES
Al	0.01	ICP-OES

3. RESULTS

3.1 Optimization of the leaching process

In order to optimize the leaching process of the cathode material in an acid sulphate medium, the influence on the leaching process of various process parameters (leaching agent concentrations, solid phase concentrations and temperature) was examined.

3.1.1 Influence of sulfuric acid concentration on the degree of cobalt leaching

In order to determine the optimal concentration of H_2SO_4 in the process of leaching of the cathode material, in a sulfur dioxide atmosphere, a series of experiments were performed with the different concentrations of H_2SO_4(0.5 mol/dm^3- 3 mol/dm^3). The experiments were performed at a temperature of 35°C, with a solid phase concentration 33 g/dm^3, and with a volume flow of 2 dm^3/min SO_2. Experiment time was 100 min.

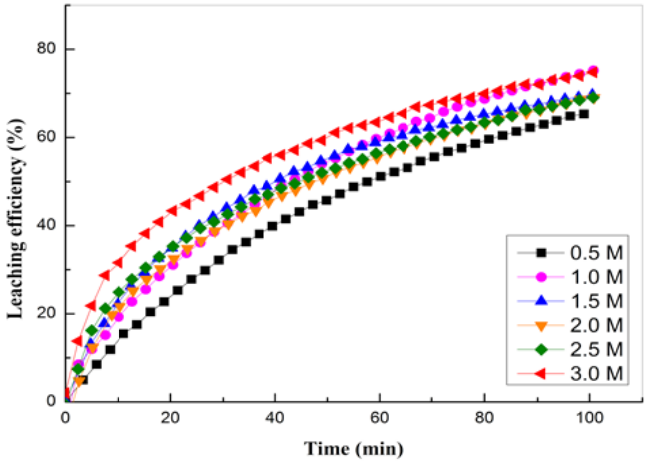

Figure 1 - Influence of H_2SO_4 concentration on the degree of cobalt leaching

The results of the research, shown in Figure 1, indicate that with an increase in the H_2SO_4concentration 0.5 mol/dm^3- 3 mol/dm^3, the degree of cobalt leaching increases from 65.3% to 73.9%. Considering the obtained results, the H_2SO_4concentration of 3 mol/dm^3 can be taken as optimal value and was used in further experimental studies.

3.1.2 Influence of solid phase concentration on the degree of cobalt leaching

The influence of solid phase concentration (in the range of 10 g/dm^3 to 67 g/dm^3) on the degree of cobalt leaching was examined under the following conditions: H_2SO_4 concentration was 3

mol/dm^3, volume flow sulfur dioxide was 2 dm^3/min, temperature was 35°C,and time of leaching was 100 min. The obtained results, shown in Figure 2, indicate that with the increase of the solid phase concentration, the degree of cobalt leaching decreases. The highest degree of cobalt leaching was recorded at a solid phase concentration of 10 g/dm^3. From the industrial point of view, in the process of material leaching, it is desirable to use a higher solid-liquid phase ratio, regardless of the achieved lower degree of metal leaching [12,13]. For this reason, a solid phase concentration of 33 g/dm^3 was taken as the optimal concentration and used in further experimental studies.

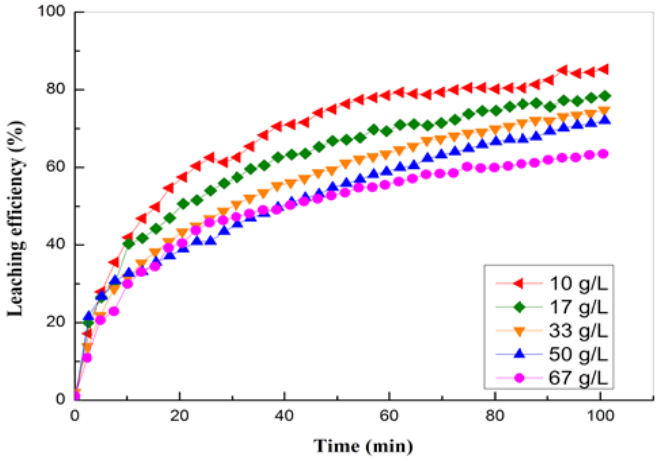

Figure 2 -Influence of solid phase concentration on the degree of cobalt leaching

3.1.3 Influence of temperature on the degree of cobalt leaching

In order to examine the kinetic laws of the process, the influence of the temperature of the cathode material on the degree of cobalt leaching was examined under the following conditions: acid concentration was 3 mol/dm^3, volume flow $SO_2$was 2 dm^3/min and solid phase concentration was 33 g/dm^3. The results of the research, shown in Figure 3, indicate that temperature has a positive effect on the degree of cobalt leaching. It was concluded that with an increase of the leaching temperature 35°C to 85°C, the degree of cobalt leaching increases from 74.8% to 99.4%.

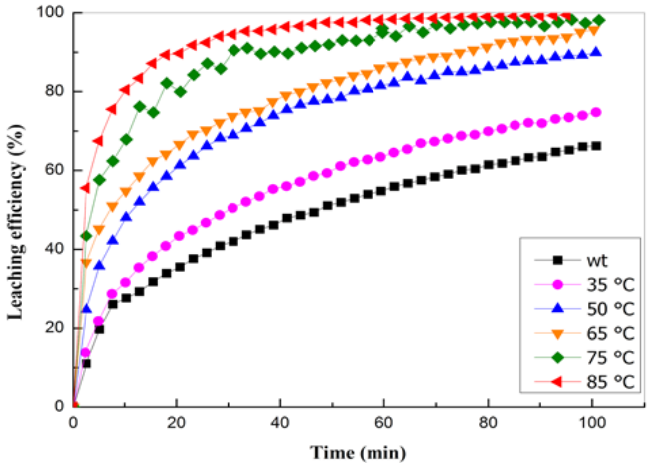

Figure 3 -Influence of temperature on the degree of cobalt leaching

4. CONCLUSION

Based on the results of leaching of the cathode material in a sulfur dioxide atmosphere, it can be concluded that the temperature and duration of the process have the greatest influence on the

leaching process. Also, the shape of the kinetic curves of leachingindicated that the concentration of sulfuric acid and the concentration of the solid phase, slightly influence the leaching of cobalt from the cathode material of spent lithium-ion batteries. The maximum degree of cobalt leaching (about 100%) was achieved at a sulfuric acid concentration of 3 mol/dm^3, a solid phase concentration of 33 g/dm^3, a volume flow of sulfur dioxide of 2 dm^3/min, temperature of 85°C and leaching process duration of 60 minutes.

ACKNOWLEDGEMENTS

The research presented in this paper was done with the financial support of the Ministry of Education, Science and Technological Development of the Republic of Serbia, within the funding of the scientific research work at the University of Belgrade, Technical Faculty in Bor, according to the contract number 451-03-9/2021-14/ 200131, and within the funding of the scientific research work at the Mining and Metallurgy Institute Bor, according to the contract number 451-03-9/2021-14/ 200052.

REFERENCES

[1] Y. Wang, N. An, L. Wen, L. Wang, X. Jiang, F. Hou, Y. Yin, J. Liang, J. Energy Chem., 55 (2021) 391-419.
[2] T. Huang, L. Liu, S. Zhang, Hydrometallurgy, 188 (2019) 101-111.
[3] Y. Guo, Y.L. Zhao, X. Lou, T. Zhou, Z. Wang, C. Fang, J. Guan, S. Chen, X. Xu, R.Q. Zhang, J. Hazard. Mater., 399 (2020) 123090.
[4] X. Chen, H. Ma, C. Luo, T. Zhou, J. Hazard. Mater., 326 (2017) 77-86.
[5] D. Wang, X. Zhang, H. Chen, J. Sun, Miner. Eng., 126 (2018) 28-35.
[6] Q. Meng, Y. Zhang, P. Dong, Waste Manage., 71 (2018) 372-380.
[7] J. Guan, Y. Li, Y. Guo, R. Su, G. Gao, H. Song, H. Yuan, B. Liang, Z. Guo, ACS Sustainable Chemistry & Engineering, 5 (2017) 1026-1032.
[8] J. Ren, R. Li, Y. Liu, Y. Cheng, D. Mu, R. Zheng, J. Liu, C. Dai, New J. Chem., 41 (2017) 10959-10965.
[9] C. Peng,K. Lahtinen, E. Medina, P. Kauranen, M. Karppinen, T. Kallio, B.P. Wilson, M. Lundström, J. Power Sources, 450 (2020) 227630.
[10] D.A. Ferreira, L.M.Z. Prados, D. Majuste, M.B. Mansur, J. Power Source, 187 (2009) 238-246.
[11] M.K. Jha, A. Kumari, A.K. Jha, V. Kumar, J. Hait, B.D. Pandey, Waste Manage., 33 (2013) 1890-1897.
[12] W. Gao, X. Zhang, X. Zheng, X. Lin, H. Cao, Y. Zhang, Z.H.I. Sun, Environmental Science & Technology, 51 (2017) 1662-1669.
[13] L.P. He, S.Y. Sun, X.F. Song, J.G. Yu, Waste Manage., 64 (2017) 171-181.

The 52nd International October Conference on Mining and Metallurgy
November 29th – 30th , 2021
www.ioc.tfbor.bg.ac.rs

OBTAINING MULTILAYER COPPER STRIPS BY ARB (ACCUMULATIVE ROLL BONDING) ROLLING PROCESS

Milijana Mitrović[1], Dragoslav Gusković[1], Saša Marjanović[1], BiserkaTrumić[2], Emina Požega[2], UrošStamenković[1],Jasmina Petrović[1]

[1]Technical Faculty Bor, University of Belgrade, V.J. 12, 19210 Bor, Serbia

[2]Mining and Metallurgy Institute Bor, Zelenibulevar 35, 19210 Bor, Serbia

Abstract

In this paper, the production of multilayer samples, by joining copper strips, by the rolling process at temperatures below the recrystallization temperature is presented.The newly obtained multilayer samples were then subjected to tensile testing and hardness measurement in order to determine their properties.The obtained results show that with increasing degree of reduction, the tensile strength and hardness of the samples increase.Up to the degree of reduction of 66.5%, the tensile strength and hardness of the samples increase slightly, while at a higher degree of reduction of 66.5%, the growth is much more pronounced.

Keywords:*Multilayer copper strips, ARB Roll Bonding, hardness, tensile strength.*

1. INTRODUCTION

The initial idea for this work was based on the knowledge about the application of ARB (Accumulative Roll Bonding) method for rolling sheets and strips (Figure 1) [1].This method achieves the required metal reduction with minimal stresses, by cutting the rolled sheets, joining and re-rolling, whereby this procedure can be repeated an unlimited number of times [2].There is a joining of metals by hot and cold rolling.Making the joint by hot rolling is a more efficient and widely used production method of rolled multilayer semi-finished products.The joint is made by hot rolling from pre-prepared strips packed and joined, and then heated to the temperature required for hot rolling.The application of hot rolling has its basic meaning in the setting to obtain products of smaller thickness than the initial large pieces without intermediate annealing and to facilitate joining, and the joint is achieved at a lower degree of deformation.Cold rolling technology, especially strips rolling, has a disadvantage in terms of the use of expensive equipment for both preparation and rolling.The requirements for large reduction in one pass impose the use of specialized rolling machines with large roller diameters, small rolling width and low rolling speed, as well as a preparation line within the rolling machine.In addition, solving the disadvantages of hot and cold rolling is done by combining procedures, in such a way that the joining is done by some other process, such as explosive joining, and by further hot or cold rolling pieces of the final dimensions are produced[3,4].

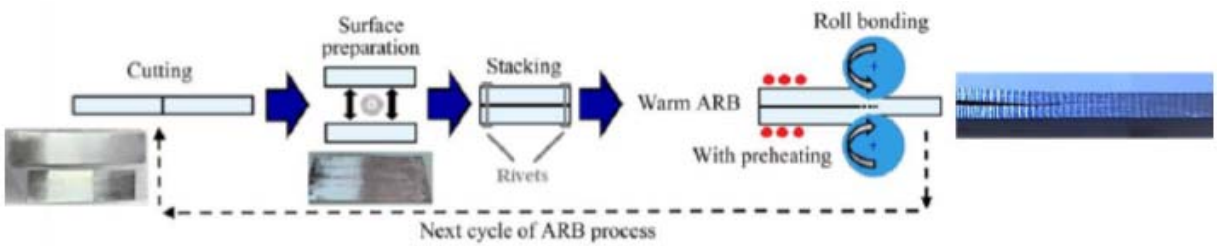

Figure 1. Schematic view of ARB (Accumulative Roll Bonding) rolling process

2. EXPERIMENTAL

As a starting material, dip-forming wire in the form of a strip with dimensions 100 x 7 x 1 mm was used, which was rolled on a quarto rolling machine with smooth rollers, diameter D =180 mm.

Rolling was done by cutting 200 strips 100 mm long, 7 mm wide and 1 mm thick.For degreasing, they were boiled in detergent for about 30 minutes, and then washed with a solution of nitric acid (1: 1 solution), distilled water and finally alcohol.After drying, two strips were joined together, whereby the joining was done by placing copper foil on the ends of the sample. Thus, two-layer samples (2 mm thick) were formed, ready for annealing.The samples were annealed at 400 ° C for 10 minutes to reduce the oxidation level of the sample surface.Annealing was performed by inserting the samples into a metal box filled with charcoal.After annealing, rolling was started on a quarto-rolling machine, whereby the obtained samples had a degree of reduction of ε_1 = 40%.Such samples were immediately deposited in a charcoal box, annealed at 400 ° C for about 10 minutes and re-rolled, with a reduction degree of ε_2 = 44.1%.The obtained sample consisted of two layers with a total reduction of ε_{uk} = 66.5%.After that, two two-layer samples were joined, of course, before their joining, the sample was washed and cleaned again, in order to remove impurities.Joining of these samples was done with copper foil at the ends of the sample. The samples were then annealed for 10 minutes at 400 ° C and then rolled. The degree of reduction after rolling is ε_3 = 48.5%.The obtained samples had four layers.The obtained samples were washed again for degreasing and cleaning, joined in pairs, annealed and rolled, however the process of joining these samples and obtaining eight layers in the sample was not successful.As a final result, a sample with four layers was obtained. The total degree of reduction in relation to the initial sample is ε_{uk} = 83%.The flow of the whole experiment is schematically shown in Figure 2.

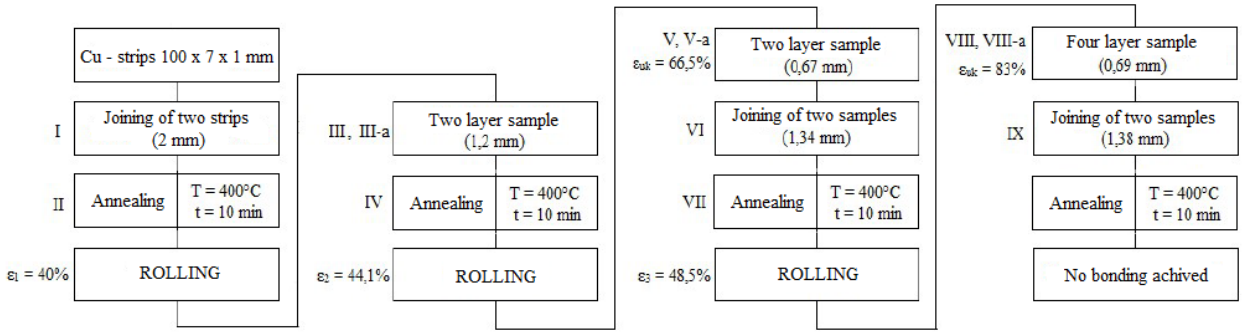

Figure2. Schematic view of the experiment flow

3. RESULTS AND DISCUSSION

Visual inspection of the samples has shown that quality bimetallic strips of small thickness below 0.7 mm can be obtained by rolling.

Flaking was not observed in any of the examined samples. The strips have smooth surfaces, even widths along the length, even thicknesses along the length, and the edges are smooth without cracks.

The results of the change in tensile strength and hardness of the samples depending on the degree of reduction are presented in Table 1 and Figures 3 and 4.

Table 1. Hardness and tensile strength values depending on the degree of reduction

Sample	Degree of reduction ε (%)	Medium hardness value (HV)	Tensile strength R_m (N/mm^2)
III	40	103	46,221
III - a	40	102	44,345
V	66,5	109	55,336
V - a	66,5	108	47,826
VIII	83	116	116,422
VIII - a	83	110	84,559

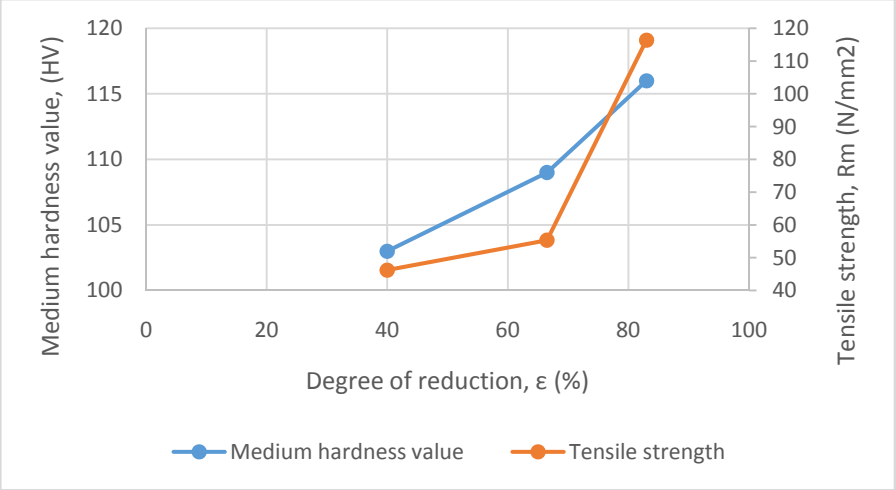

Figure3. Dependence of hardness and tensile strength of samples on the degree of reduction for the I series of samples

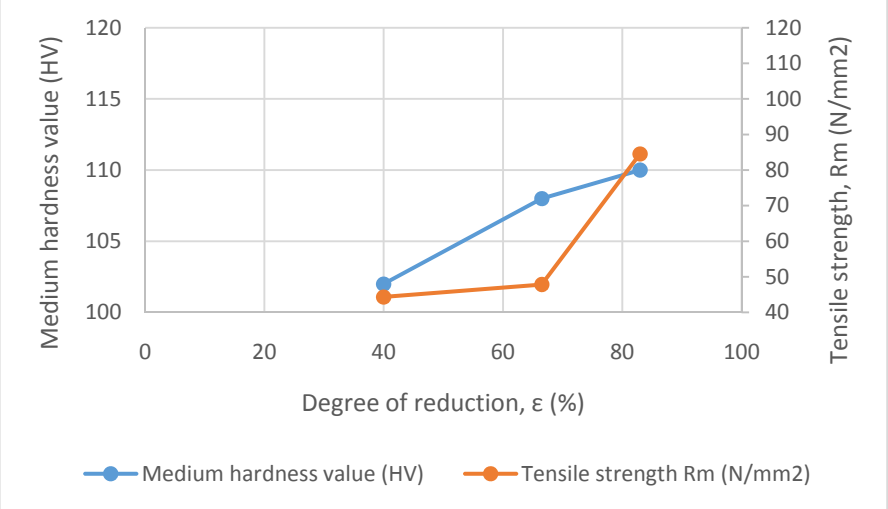

Figure4. Dependence of hardness and tensile strength of samples on the degree of reduction for the II series of samples

The diagrams show that as the total reduction increases, both the hardness and the tensile strength increase.

In the first series of samples, higher values of hardness and tensile strength were observed compared to the second series of samples.

The minimum hardness values, 102 HV and 103 HV, were obtained for samples deformed with a reduction degree of 40%, while the maximum values, 110 HV and 116 HV, were obtained at a

reduction degree of 83%.Tensile strength has values of 44 (N/mm^2) and 46 (N/mm^2) to a maximum of 116 (N/mm^2) and 84.5 (N/mm^2).

The measured values of hardness and tensile strength for the first series of samples are higher than the measured values of hardness and tensile strength for the second series of samples at given degrees of reduction.

4. CONCLUSION

Based on the obtained results, the following conclusions can be drawn:

- By rolling copper strips, samples less than 0.7 mm thick can be obtained, without flaking, the strips have smooth surfaces, uniform widths along the length, uniform thicknesses along the length, and the edges are smooth and without cracks.
- With increasing degree of reduction, the tensile strength and hardness of the samples increase. Up to the degree of deformation of 66.5%, the tensile strength and hardness of the samples increase slightly, while at a higher degree of reduction than 66.5%, the growth is much more pronounced.
- The measured values of hardness and tensile strength for the first series of samples are higher than the measured values of hardness and tensile strength for the second series of samples at given degrees of reduction.
- Higher values of hardness and tensile strength for samples rolled in the first series compared to the hardness and tensile strength of samples rolled in the second series, are probably due to either slightly shorter heating of samples in the furnace or longer retention of samples in the charcoal box after removal from the furnace and a longer time of transferring samples from the box to the rolling machine.

ACKNOWLEDGEMENTS

The research presented in this paper was done with the financial support of the Ministry of Education, Science and Technological Development of the Republic of Serbia, within the funding of the scientific research work at the University of Belgrade, Technical Faculty in Bor, according to the contract with registration number 451-03-9/2021-14/ 200131.

REFERENCES

[1] M. El Mehtedi, D. Lai, R. Almehtedi, M. Carta, P. Buonadonna, F. AymerichH, ESAFORM 2021. MS05 (Joining), 10.25518/esaform21.942.
[2] Q. Zhang, Mechanical Behavior of of Cu/Al multilayers fabricated by Accumulative Roll-Bonding (ARB) processing (Master Work), University of Nevada, Reno (2013).
[3] M. Miskovic, B. Miskovic, Teorijaplastičnepreradametala, Univerzitet u Beogradu, TMF Beograd, Beograd (1977).
[4] A. I. Celikov, TeorijaRascetaUsilij v ProkatnihStanah, Metallurgizdat, Moskva (1962).
[5] S. Zlatanovic, Uticajtermomehaničkihparametaraprerade na svojstvaviseslojnebakarnetrake
[6] (Diplomski rad), Univerzitet u Beogradu, TehnickiFakultet u Boru, Bor (2000).

THE INFLUENCE OF HIGH COMPACTION PRESSURE ON CORDIERITE-BASED CERAMICS

Nataša Đorđević[1], Slavica Mihajlović[1], Nina Obradović[2], Adriana Peleš[2], Suzana Filipović[2]

[1] Institute for Technology of Nuclear and Other Mineral Raw Materials, BulevarFransed'Eperea 86, 11000 Belgrade, Serbia

[2] Institute of Technical Sciences of SASA, KnezMihajlova 35/IV, 11000 Belgrade, Serbia

Abstract

Cordierite, $2MgO{\cdot}2Al_2O3{\cdot}5SiO_2$ is a high-temperature ceramic material. In order to improve its properties, titanium oxide was added to the starting mixture in an amount of 5%. Mechanical activation of samples was performed in a high-energy ball mill for 10 minutes. The compaction pressure was unusually high, 6 t cm^{-2}(588 MPa) in order to compare to previous research. Cordierite was sintered at the temperature of 1375°C. The phase composition of the activated and sintered samples was analyzed using X-ray diffraction. Scanning electron microscopy was used to analyze the microstructure of both compacted and sintered samples.

Keywords: *Mechanical activation, Cordierite, XRD, SEM.*

1. INTRODUCTION

Cordierite has a chemical composition of $2MgO\ 2Al_2O_3\ 5SiO_2$. The sintering temperature of this electronic ceramics in a narrow temperature range of 1350-1380°C. Its main characteristic is that it has a low coefficient of thermal expansion (20·10-7 ° C-1), so it is widely used in places where temperature shocks are frequent (with heat exchangers, as an electronics carrier, glaze for floor tiles, etc.). It also has a low dielectric constant (~ 5) as well as good thermotechnical, mechanical and chemical properties [1,2]. The widest application of this material is in places of sudden temperature change, [3-7], and they are also used as semiconductor carriers [8,9]. Mechanical activation of starting materials significantly reduces the sintering temperature [10]. The input of mechanical energy causes fragmentation, destruction of the crystal lattice, induced crystal defects, and an increase in the energy of the system. In addition to grinding or activating the system, additives further facilitate the sintering process. It is important to monitor the properties of the obtained materials, because additives should not affect their quality. After preparation (activation) of the starting substances, samples are prepared using compression pressure. The pressure applied to the sample preparation significantly affects the microstructure of the obtained product after the sintering process [11,13]. In this paper, the structure of the material was examined by X - ray diffraction and SEM analysis.

2. EXPERIMENTAL PROCEDURE

Material used in this study was: $Mg(OH)_2$, Al_2O_3, $SiO_2$and TiO_2(all p.a. purity). The mixture of $MgO{:}Al_2O_3{:}SiO_2$was 2:2:5 ratio with the addition of TiO_2 was 5.00 mass%. The mixture was mechanically activated in a high-energy planetary ball mill ZrO_2vessels with balls. The powder-to-balls mass ratio was 1:40. The milling process was performed in the air atmosphere for 10 minutes.

The X-ray powder diffraction patterns after milling and sintering were obtained using a Philips PW-1050 diffractometer with λCu-Kαradiation and a step/time scan mode of 0.05º $1s^{-1}$. The morphology of the obtained powders and sintered samples was characterized by Scanning Electron Microscopy (JEOL JSM-6390 LV). The powders were crushed and covered with gold in order to perform these measurements.

The pressure used in our experiments was 6 tcm^{-2}(588 MPa). The amount of the samples was 0.30 g. The pressure was performed in a double-sided tool 6 mm in diameter (Hydraulic press RING 14, VEB THURINGER).

The compacts were placed in an alumina boat and heated in a tube furnace (Lenton Thermal Design Type 1600), and then sintered isothermally at 1350ºC in air atmosphere for four hours; the heating rate was 10ºCmin^{-1}.

3. RESULTS AND DISCUSSION

Figure 1. shows the XRD patterns of the samples pressed under 6 tcm^{-2}, and sintered at 1350°C for four hours. The obtained peaks were identified using JCPDS cards (084-1220 for cordierite, 074-2220 for $Mg(OH)_2$, 083-2241 for TiO_2rutile, 074-0201 for SiO_2, 035-0310 for $(MgAl)SiO_3$). The XRD pattern shown in Figure 1. indicates the existence of a cordierite phase. No starting components (except TiO_2-rutile) have been detected. $(MgAl)SiO_3$phase is observed as a result of a reaction between the starting components, $Mg(OH)_2$and SiO_2.

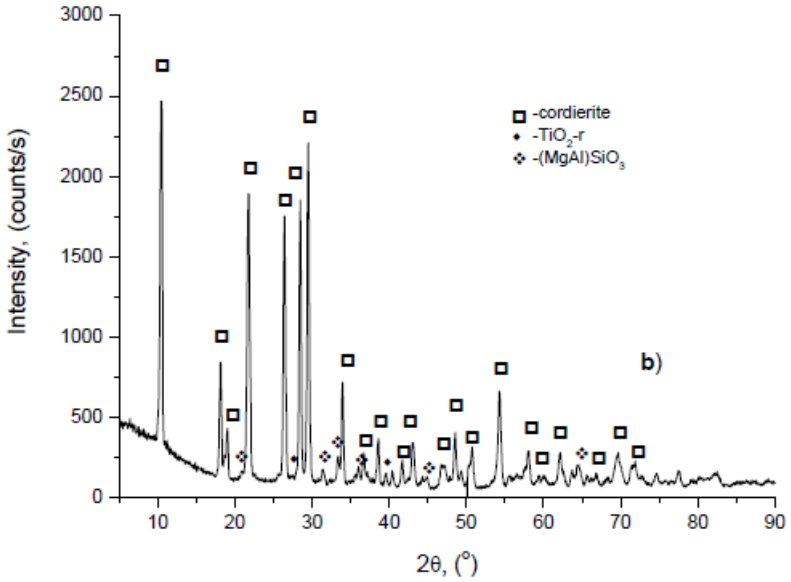

Figure 1. XRD patterns of the samples compacted at 6t/cm^2pressure and sintered at 1350°C for 4h.

At the Figure 2SEM images of the compacts obtained under 6 t/cm^2pressureare presented, a) before sintering, and b) sintered at 1350°C for 4h. It is clearly visible at Figure 2. a) that samples pressed under 6 tcm^{-2}have a denser structure and a great number of mutual contacts. The porosity is small and the shape of single particles is not visible; it can make conclusion that blocks of agglomerates are formed, due to big pressures. Figure 2 b) shows the sample after process of sintering. It is a stable structure with large surfaces and a closed porosity, typical of the final sintering stage, which is the obvious effect that high pressure applied contribute to the sintering process. High pressures allow for a great number of contacts between particles, leading to more compact samples without the small-grain structure.

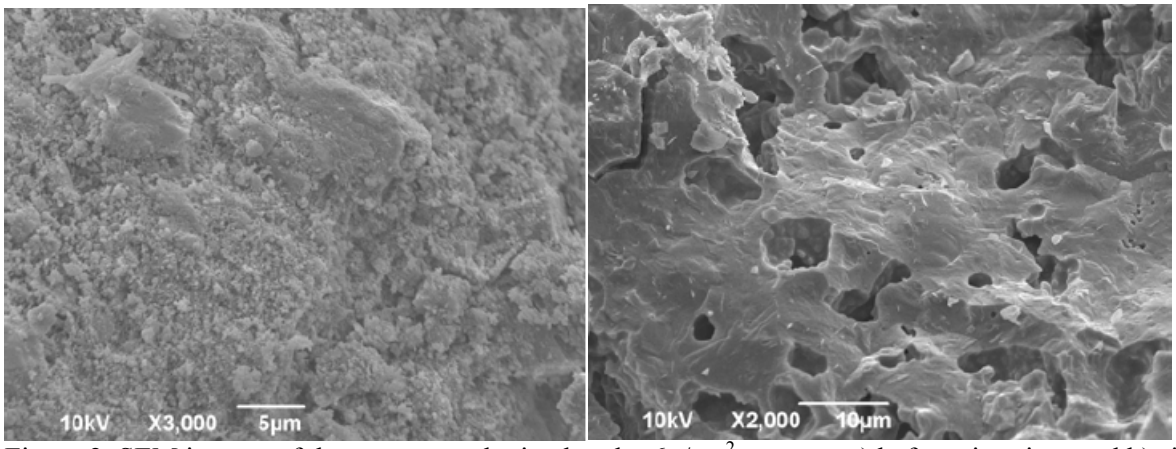

Figure 2. SEM images of the compacts obtained under 6 t/cm^{2}pressure, a) before sintering, and b) sintered at 1350°C for 4h.

4. CONCLUSIONS

The results of this study show that the applied high pressure has an impact on the final characteristics of the sintered material:

- According to the results presented in this study, the XRD analysis has shown phase composition in the sintered samples pressed under high pressure of 6 tcm^{-2}. The cordierite phase is the dominant phase; the starting components were completely used in the reaction yielding a new phase in the sample pressed under this high pressure.
- The SEM micrographs clearly indicate a microstructure as follows: with applied high-pressure value of 6 tcm^{-2}, a closed porosity and high-level homogeneous microstructures are obtained.

ACKNOWLEDGMENTS

The authors are grateful to the Ministry of Education, Science and Technological Development of the Republic of Serbia for their support in the research whose results are presented in the paper (451-03-9/2021-14/200023 and 451-03-9/2021-14/200026).

REFERENCES

[1] I. Kingon, R. F. Davis, Engineer Materials Handbook, Vol. 2. “Ceramics” edited by S. J. Schneider, Jr., ASM International Metals Park, OH, p. 1191.
[2] N. Obradovic, N. Djordjevic, S. Filipovic, N. Nikolic, D. Kosanovic, M. Mitric, S. Markovic, V. Pavlovic, Powder Technology 218 (2012) 157-161.
[3] V.J. Powers, C.H. Drummond, Ceram. Eng. Sci. Proc. 7 (1986) 969.
[4] Warsworth, R. Stevens, J. Eur. Ceram. Soc. 9 (1992) 153.
[5] M. Pinero, M. Atik, J. Zarzycki, J. Non-Cryst. Solids 147 –148 (1992) 1523.
[6] D. Kervadec, M. Coster, J.L. Chermant, Mater. Res. Bull 27 (1992) 967.
[7] N. Clausen, G. Petzow, J. Phys. (Paris), 47 (1986) 693.
[8] R. R. Tumala, J. Am. Ceram. Soc. 74 (1991) 895.
[9] S. H. Knickerbocker, A. H.Kumar, L. W. Herron Am. Ceram. Soc. Bull. 72 (1993) p 90.
[10] N. Djordjevic, N. Obradovic, S. Filipovic, J. Zivojinovic, M. Mitric, S. Markovic, Tehnika – Novi materijali 21 (2012) 3, 329.
[11] N. Obradovic, S. Stevanovic, M. Mitric, M. V. Nikolic, M. M. Ristic, Science of Sintering, 39 2007 p.241.

[12] N.Obradović,V.Blagojević,S.Filipović,N.Đorđević,D.Kosanović,S.Marković, M.Kachlik,K.Maca, V.Pavlović, Kinetics of thermally activated processes in cordierite-based ceramics, Journal of Thermal Analysis and Calorimetry138,2019, p2989–2998

[13] Obradović N, Đorđević N, Filipović S, Nikolić N, Kosanović D, Mitrić M, Marković S, Pavlović V. Influence of mechanochemical activation on the sintering of cordierite ceramics in the presence of Bi_2O_3as a functional additive. Powder Technol. 2182012, p.157–61.

The 52nd International October Conference on Mining and Metallurgy
November 29th – 30th , 2021
www.ioc.tfbor.bg.ac.rs

SEM AND X-RAY ANALYSES OF SINTERED MgO / Bi_2O_3BINARY SYSTEM

Nataša Đorđević[1], Slavica Mihajlović[1], Miroslav Sokić[1], Branislav Marković[1]

[1]Institute for Technology of Nuclear and Other Mineral Raw Materials, Franchetd'Esperey Blvd. 86, Belgrade, Serbia

Abstract

Magnesium oxide is a component of many ceramic materials. Bismuth oxide is added as an additive to ceramic materials in order to lower the sintering temperature. The influence of temperature was researched by sintering binary system: MgO/Bi_2O_3.The temperature of process was 820 °C and 1100 °C. Composition of this system was 80% of MgO and 20% Bi_2O_3. The effects of sintering, the composition and morphology were followed by X-ray diffraction and Scanning electron microscopy. It has been found that Bi_2O_3 forms intermediary unstable compound with MgO.

Keywords:*MgO, Bi_2O_3, sintering, SEM, x-ray analysis.*

1. INTRODUCTION

These studies were performed in order to determine the influence of bismuth oxide on the sintering process of ceramic materials and the possibility of reaction during sintering with magnesium oxide as one of the components of the system.

One of the most important ceramic materials whose composition includes magnesium oxide is cordierite. Its composition is $2MgO*2Al_2O_3*5SiO_2$. Since the temperature range of cordierite sintering is very narrow (sintered temperature is 1300 – 1400 °C), the techniques of lowering the temperature of its formation are very interesting for research.

As the melting point of bismuth oxide is 750 °C, adding the cordierite mixture during the sintering process is the expected result of lowering the sintering temperature due to the formation of a two-phase system. During sintering, it is possible to form intermediate compounds of additives with system components, which was the aim of this research.

2. EXPERIMENTAL

During this research following components were used: MgO (Euro Hemija, Beograd), Al_2O_3 (Aluminijumskikombinat, Podgorica), SiO_2 (Bela Reka) and Bi_2O_3, p.a. (Reahim, Rusia). Chemical composition of starting compounds is given in Table 1.

Following mixture was prepared: MgO/Bi_2O_3, in relation 80% of magnesium oxide and 10% of Bi_2O_3. Samples for sintering were prepared in the tablet shape, with radius 8mm and height 4mm, under the pressure of 1 t/cm^2. Sintering temperature of the sample MgO/Bi_2O_3 was 820 °C and 1100 °C.

X-ray powder diffraction (XRPD) technique was used for identification and definition of the unit-cell parameters. XRPD analysis was performed using the Philips PW1710 diffractometer; with Cu Kα radiation (40kV, 30mA), step scan 0.25s, 0.02° 2θ, *d* range from 5° to 85°2θ. The microstructures of the sintered samples were observed using scanning electron micrograph (SEM) with microsonde.

3. RESULTS AND DISCUSSION

Sample MgO/Bi_2O_3, sintered at 820°C (Fig.1.) showed very low level of crystallinity. Following compounds were detected: periclase (MgO), bizmite (α-Bi_2O_3) and silenite (γ-Bi_2O_3). Under these conditions, only Bi_2O_3 was phase transformed, other phases were not formed since this temperature was too low for any other transformations. In the sample MgO/Bi_2O_3 after sintering at 1100°C, periclase (MgO), mixture of bismuth oxide (α, β and γ Bi_2O_3) and unstable compound - $Bi_{12}MgO_{19}$ were found.

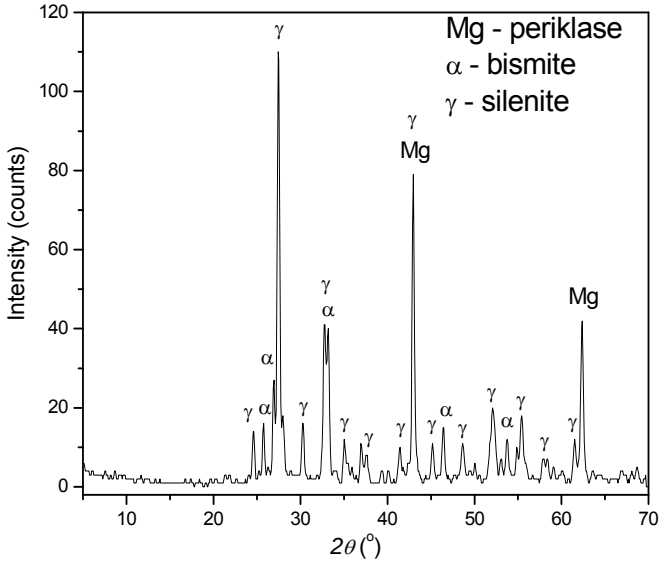

Figure 1. X-ray diffraction patterns of the sample MgO/Bi_2O_3 sintered at 820°C

SEM microphotograph of the sample MgO/Bi_2O_3, (Fig.2) sintered at 820°C, is shown in the Figure 3. The grains with flat surface could be notice. With the magnification of 2000X the pyramidal structure (5-10μm) and microstructure with spherical shape (dimension 100-400nm) are visible.

The microphotographs of the samples sintered at 1100°C are morphologically different from the sample sintered at 820°C. Small-grain structure of the crystal (visible with magnification of 25000X and pointed to initial sintering), by this microphotograph is well visible (Figure 4). The grains sizes ~100nm at 820 °C after sintering at 1100 °C have dimensions sized in μm. Pyramidal structure could not be founded in this sample.

Crystals are isometrics, enhydral. The grains are rounded, well developed, clearly visible, with diameter of ~ 1μm, symmetrically formed, flat surface boarded.

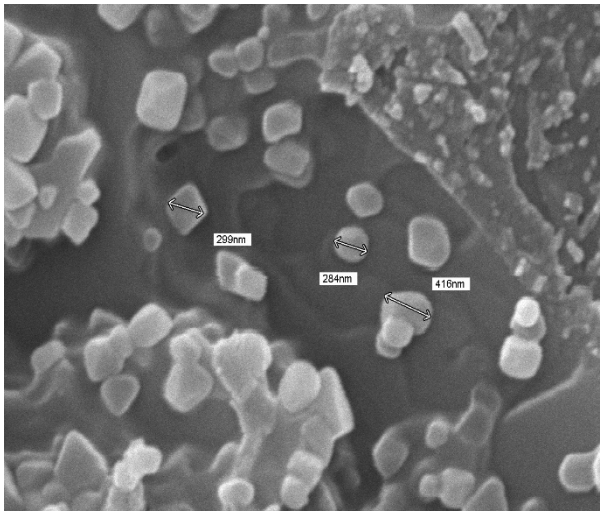

Figure 2. SEM microphotographs of the sample MgO/Bi_2O_3 sintered at 820°C (3000 X)

SEM microphotograph of the sample MgO/Bi_2O_3, (Fig.2) sintered at 820°C, is shown in theFigure 3. The grains with flat surface could be notice. With the magnification of 2000X the pyramidal structure (5-10μm) and microstructure with spherical shape (dimension 100-400nm) are visible.

The microphotographs of the samples sintered at 1100°C are morphologically different from the sample sintered at 820°C. Small-grain structure of the crystal (visible with magnification of 25000X and pointed to initial sintering), by this microphotograph is well visible (Figure 4). The grains sizes ~100nm at 820 °C after sintering at 1100 °C have dimensions sized in μm. Pyramidal structure could not be founded in this sample.

Crystals are isometrics, enhydral. The grains are rounded, well developed, clearly visible, with diameter of ~ 1μm, symmetrically formed, flat surface boarded.

4. CONCLUSIONS

In the aim of researching the reactions of cordierite synthesis, the binary systems were examined as follows: MgO/Bi_2O_3 sintered at 820ºC and 1100ºC. The results showed liquid phase in the system at 820ºC (the melting temperature of Bi_2O_3) and producing meta-stable compounds that form MgO with Bi_2O_3 at 1100ºC. This unstable compound transports through the liquid phase, which allowed (from the two aspects) the acceleration of the reaction in the more-component system.

ACKNOWLEDGEMENTS (optional)

The authors are grateful to the Ministry of Education, Science and Technological Development of the Republic of Serbia for their support in the research whose results are presented in the paper (451-03-9/2021-14/200023).

REFERENCES

[1] N. Djordjevic, Lj. Pavlovic, "The Influence of Activation and Relaxation Time on the Synthesis of Cordierite Ceramics", J. Serb. Chem. Soc, Vol. 71,No. 3, pp. 293-301, 2006.

[2] N. Obradović, N. Đorđević, S. Filipović, N. Nikolić, D. Kosanović, M. Mitrić, S. Marković, V. Pavlović, Influence of Mechanochemical Activation on the Sintering of Cordierite Ceramics in the Presence of Bi_2O_3 as a Functional Additive, Powder Technology 218 pp. 157–161, 2012.

[3] N. Obradovic, S. Stevanovic, M. Mitric, M. V. Nikolic, M. M. Ristic, Science of Sintering, 39 2007 p.241.

[4] N.Obradović,V.Blagojević,S.Filipović,N.Đorđević,D.Kosanović,S.Marković, M.Kachlik,K.Maca, V.Pavlović, Kinetics of thermally activated processes in cordierite-based ceramics, Journal of Thermal Analysis and Calorimetry138,2019p2989–2998

[5] Obradović N, Đorđević N, Filipović S, Nikolić N, Kosanović D, Mitrić M, Marković S, Pavlović V. Influence of mechanochemical activation on the sintering of cordierite ceramics in the presence of Bi_2O_3as a functional additive. Powder Technol. 2182012, p.157–61.

The 52nd International October Conference on Mining and Metallurgy
November 29th – 30th , 2021
www.ioc.tfbor.bg.ac.rs

COMPARATIVE RESULTS OF COPPER FLOTATION FROM SLAG BEFORE AND AFTER THE PROCESS OF MAGNETIC CONCENTRATION

Ivana Ilić[1], Jovica Sokolović[1], Maja Trumić[1], Zoran Stirbanović[1]

[1]Technical Faculty Bor, University of Belgrade, V.J. 12, 19210 Bor, Serbia

Abstract

Previousresearch on the possibility of valorization of usefulcomponents from smelterslaghasshown that copper and preciousmetals can be economicallyjustifiablyvalorized by flotation concentration. In addition to the basicusefulcomponents, smelterslagalsocontainsotherusefulcomponents (iron) whosevalorizationwouldimprove the economiceffects of processingthissecondaryrawmaterial. Thispaperpresents the results of testing the possibility of valorization of copper and iron from the newsmelterslag of Mining and SmeltingCombine Bor(RTB)Bor usingmagnetic and flotation concentration.

***Keywords**:smelter slag, magnetic concentration, flotation concentration.*

1. INTRODUCTION

Smelterslag as a by-product of pyrometallurgicalprocessing of copperconcentrate, in terms of the content of usefulcomponents (copper, iron, preciousmetals, etc.), represents a veryvaluable[1,2], and in terms of itsphysical and chemicalcharacteristics a verycomplex, technogenicsecondaryrawmaterial. From an environmentalpoint of view, smelterslag is also a potentiallyhazardous waste.

Smelting (copper) slag is a complexrawmaterial that consistsmainly of silicates, sulfides, oxides and some metalliccopper and iron, wherecopper mineralsortheirmixtures are present. The percentageshare of major oxides in slag is in the followinglimits: Fe_2O_3: 35–60%, SiO_2: 25–40%, CaO: 2–10%, Al_2O_3: 3–15%, CuO: 0,3–2,1%, MgO: 0,7–3,5%. Oxides of iron, SiO_2, Al_2O_3, CaOand MgOmakeup more than 95% of the total oxidespresent in the slag[3]. Various technologies and processessuch as flotation [3,4,5], magneticconcentration[6,7], leaching[8,9] and roasting[10] are used for valorization of usefulmetals from smelterslag. Due to the high content of magnetite in smeltingslag (35-60%), in recentyears more attentionhasbeenpaid to the valorization of ironusingmagneticconcentration. On the otherhand, magnetite, due to itsphysicalcharacteristics, negativelyaffects the characteristics of the pulp in the process of flotation concentration.

Thispaperpresents the results of testing the possibility of valorization of copper and iron from newsmelterslagusing the process of flotation, i.e.magnetic and flotation concentration.

2. EXPERIMENTAL

For the purposes of research in thispaper, sampling of hydro cycloneoverflows from the second stage of classification (OF II) was performed, which represents the entrance to the process of rough flotation of newsmelterslag in RTB Bor plants (now Serbia ZijinCopper) during 2017.

2.1 Magnetic separation

Laboratorytesting of the magneticconcentrationwasperformed on a Davismagneticanalyzer at differentmagneticfield intensity.

Considering the goal of the research, a chemical analysis of all obtained productswasperformed on the contents of iron (Fe), as well as copper (Cu) and sulfur (S).

2.2 Flotation concentration

Flotation concentrationexperimentswereperformedusing a laboratory flotation machinetype"DENVER DR 12", flotation cellvolume 2.6 l, at a constant rotor speed of 1700 rpm. Whenperforming flotation experiments, the followingreagentswere used: NaIPXcollector 600 g/t and D250 frother 10 g/t. The conditioning time was 10 minutes, while the total flotation time was20 minutes.Laboratorytesting of flotation concentrationwasperformed on the non-magneticfraction obtained at a previouslydefinedcurrent, i.e.magneticinduction, on which the bestresults of experimentalinvestigations of the magneticconcentration of iron are achieved.

3. RESULTS AND DISCUSSION

3.1 Results of granulometric and chemicalcomposition analysis

The results of the chemical analysis of the hydrocycloneoverflow of the secondstage of classification (OF II) are given in Table 1.

Table 1 - Results of chemical analysis of hydrocycloneoverflow (OF II) by sizeclasses[11]

Sizeclass d (mm)	Mass share W (%)	Cu (%)	Fe (%)	S (%)	R_{Cu} (%)	R_{Fe} (%)	R_S (%)
+0.150	0.35	0.46	22.19	2.09	0.13	0.19	0.55
-0.150+0.106	1.25	0.51	35.25	1.02	0.53	1.08	0.96
-0.106+0.075	5.85	0.49	38.49	0.81	2.37	5.54	3.56
-0.075+0.040	22.95	0.74	38.15	1.35	14.05	21.54	23.28
-0.040+0	69.60	1.44	41.84	1.37	82.92	71.65	71.65
Σ	100.00	1.21	40.65	1.33	100.00	100.00	100.00

From Table 1 can be concluded that the average copper content in the hydrocycloneoverflow (OF II) is 1.21% and is manytimeshigherthan the copper content in the primarycopper ores (about 0.30%), whichconfirms that the slag is high-valuesecondaryrawmaterial. The average iron content in the overflow of the secondstagehydrocyclone (OF II) is 40.65%, which indicates a significantshare of thiscomponent, so that the testedrawmaterialdeservesseriousresearch with the aim of valorization of copper and iron.

3.2 Results of magneticconcentration

Laboratorytesting of the magneticconcentrationwasperformed on the overflow of hydro cyclone II smelterslag with the aim of testing the possibility of ironvalorization and the introduction of the magneticconcentrationprocessbefore the flotation concentrationprocess. The results of the magneticconcentration are shown in Table 2.

Table 2 –Results of magneticconcentration[11]

Current intesity I (A)	Magnetic induction B (T) x 10^{-4}	Magneticfraction (MF)				Non-magneticfraction (NMF)			
		m (%)	Cu (%)	Fe (%)	S (%)	m (%)	Cu (%)	Fe (%)	S (%)
1	**1.79**	4.14	0.63	49.67	1.41	95.86	1.11	42.66	1.25
3	**4.63**	32.60	0.44	49.21	0.71	67.40	1.56	35.89	1.21
5	**7.15**	35.80	0.42	40.00	1.08	64.20	1.59	34.22	1.91
7	**9.55**	37.80	0.28	48.15	1.01	62.20	1.88	35.46	1.73

9	**11.02**	37.00	0.56	48.28	1.11	63.00	1.46	35.96	1.74

From the table 2 it can be concluded that the best separation of the testedsample (OF II) intomagnetic and non-magneticfractionwas achieved at a current of 7 A, or at an induction of a magneticfield of 9.55 x 10^{-4} T. Achieved results of mass recovery of a magnetic product of 37,80% with an iron content of 48.15% justify the introduction of the technologicalprocess of magnetic separation on the overflow of the seconddegree of hydrocyclone (OF II) before the process of flotation of smelterslag.The non-magneticfraction obtained by thisinduction of the magneticfield in the mass of 62.20% and with a copper content of 1.88% is as suchsuitable for furthertreatment with flotation concentration, in order to utilize the basicusefulcomponent, copper.

3.3 Results of flotation concentration

Withinthisphase of the research, two flotation experimentswereperformed. The firstexperimentinvolvedflotation of hydrocyclone II overflow to pH 7.83 (industrial conditions). In the secondexperiment, flotation of the non-magneticfraction obtained by the process of magneticconcentration at a current of 7 A, at a pH of 7.83 and using a 600 g/t NaIPXcollector and a 10 g/t D250 frother (industrial conditions) wasperformed. Figures 1 and 2 give comparativeresults.

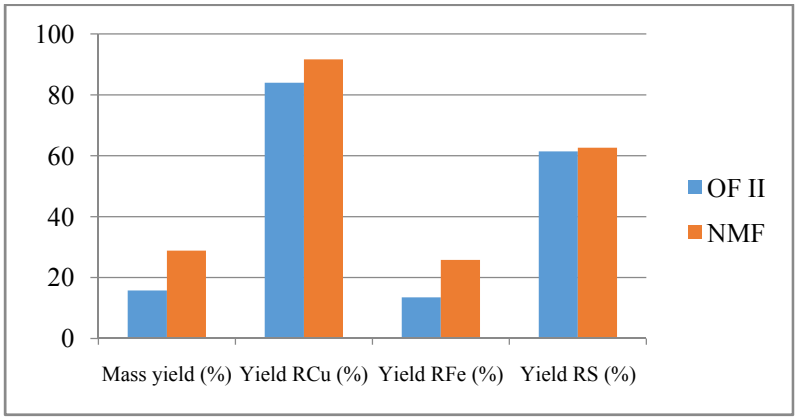

Figure 1 -Comparativeresults of mass and technologicalyield on the overflow of hydrocyclone (OF II) of smelterslag and on the non-magneticfraction (NMF)[11]

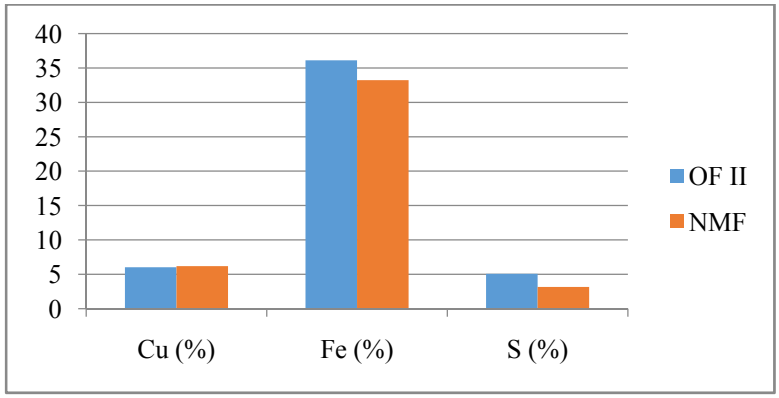

Figure 2 -Comparativeresults of Cu, Fe and S content on the overflow of hydrocyclone (OF II) of smelterslag and on the non-magneticfraction (NMF)[11]

Analyzing and comparing the results of flotation of the testedsample of smelterslag and flotation of non-magneticfraction (NMF) obtained at a current of 7 A, it can be concluded that

bettertechnologicalresults are achieved by flotation of non-magneticfraction (NMF) whichjustifies the introduction of magneticconcentrationbefore flotation.

By flotation of the non-magneticfraction (NMF) at pH 7.83, highertechnologicalyield of copper is achieved, whichamounts to 91.62%, while flotation of the overflowsample of hydrocyclone II of smelterslagachieveslowertechnological yield of copper by about 8% and amounts to 83.99%.The total mass yield obtained by flotation of the non-magneticfraction (NMF) at pH 7.83 is for 13.10% higher in relation to the flotation of the testedsmelterslagsample and it amounts to 28.85%.Comparing the quality of the concentrate, it can be concluded that the highestcopper content in the concentrate of 6.20% was obtained by floating a sample of non-magneticfraction (NMF) at pH 7.83. The highestsulfur content in the concentrate of 5.07% was obtained by flotation of the overflowsample of hydrocyclone II of smelterslag, in contrast to the flotation experiment of the non-magneticfraction obtained at a current of 7 A, where the sulfur content in the concentratewas 3.17%.

4. CONCLUSION

The results of the research of the possibility of valorization of iron from the overflow of hydrocyclone II smelterslagshowed that iron, under the examined conditions, can be successfullyseparated by magnetic separation. The best separation of the testedsampleintomagnetic (MF) and non-magneticfraction (NMF) is achieved at a current of 7 A, or at an induction of a magneticfield of 9.55 x 10^{-4} T. Achieved results of mass yield of the magnetic product of 37.80% with an iron content of 48.15% justify the introduction of a magneticconcentrationprocessbefore the flotation process.By flotation of the non-magneticfraction (NMF) at pH 7.83, a highertechnological yield of copper of 91.62% is achieved, compared to the flotation of the overflowsample of hydrocyclone II of smelterslag, whereby the technological yield of copper of 83.99% is obtained. Betterquality of the rough flotation concentrate and highercopper content in the concentratewas achieved by flotation of the sample of non-magneticfraction (NMF) and amounts to 6.20%. The obtained resultsfullyconfirm and justify the possibility of introducing the process of magneticconcentrationbefore the process of flotation of smelterslag.

ACKNOWLEDGEMENTS

The research presented in this paper was done with the financial support of the Ministry of Education, Science and Technological Development of the Republic of Serbia, within the funding of the scientific research work at the University of Belgrade, Technical Faculty in Bor, according to the contract with registration number 451-03-68/2020-14/ 200131.

REFERENCES

[1] B. Gorai, R. Jana, K. Premchand., Conservation and Recycling., 39 (2003) 299-313.
[2] H.Shen, E. Forssberg., Waste Management., 23 (10) (2003)933-949.
[3] A. Sarrafi, B. Rahmati, H.R. Hassani, H.H.A. Shirazi., Minerals Engineering., 17 (4) (2004)457-459.
[4] W.J. Bruckard, M. Somerville, F. Hao., Minerals Engineering., 17 (4) (2004) 495-504.
[5] Z.M. Stirbanovic, Z.S. Markovic., Separation Science and Technology., 46 (16) (2011) 2496-2500.
[6] K.Q. Li, S. Ping, H.Y. Wang, W. Ni., Intern. J. of Minerals, Metallurgy and Materials., 20 (11) (2013) 1035-1041.
[7] B. Kim, S. Jo, D. Shin, S. Jeong., Intern. J. of Mineral Processing., 124 (2013) 124-127.
[8] I. Mihajlovic, N. Strbac, P. Dordevic, A. Mitovski, D. Nikolic, Z. Zivkovic., Environment protection engineering., 38 (4) (2012) 171-184.
[9] Y. Li, I. Perederiyi, V. Papangelakis., J. of Hazardous Materials., 152 (2) (2008) 607-615.
[10] H.S. Altundogan, F. Tumen, Hydrometallurgy., 44 (1997) 261-267.
[11] I. Strainovic, Graduation thesis, Technical Faculty in Bor, Bor, 2018.

The 52nd International October Conference on Mining and Metallurgy
November 29th – 30th , 2021
www.ioc.tfbor.bg.ac.rs

FERROSILICON OBTAINING USING IRON-SILICATE –FAYALITE

Daniela Grigorova[1]

[1]University of Chemical Technology and Metallurgy, 1756 Sofia, 8 Kl. Ohridskyblvd., Bulgaria

Abstract

The use of by-products stimulates the circular economy by reducing the footprint on the environment and the use of natural raw materials. In the copper industry, iron-silicate fines, also called fayalite, are generated as a result of flotation processes in the production of copper concentrates. The bulk of this material is landfilled. The material contains about 46% iron and about 27% silicon dioxide. For the production of ferrosilicon FeSi, quartzite, carbon reducer, and iron chips are used as standard. In the present paper, an attempt has been made to partially replace quartzite and iron chips with iron silicate-fayalite. The quantitative ratio between the components for the production of ferrosilicon alloy was determined on the basis of the calculated material balance. The composition and amount of the alloy and slag were determined. The Gibbs energy for the different temperature retentions was calculated and an experimental equation for ΔG= f (T) in the temperature range 1250-1433K was derived. Ferrosilicon is used for oxidation, alloying, and modification in extractive metallurgy.

Keywords*: iron-silicate - fayalite, ferrosilicon, material balances, thermodynamics.*

1. INTRODUCTION

During copper production from smelting processes, iron silicate-fayaliteis generated. A small part of this material is treated as secondary material and is used in the cement industry, for road construction, in asphalt, and for the production of bricks. A significant part of it is stored in a specially prepared tailings storage area. Globally, the landfill of fayalite in annual terms is about 50 million tons, of which in Bulgaria alone- about 1 million tons [1].FerrosiliconalloysincludealargegroupofferroalloysfromtheFe-Sisystem and contains 20 to 90% silicon. For the production of FeSi, quartzite, and iron chips are used as standard [2-6]. Ferrosilicon is usually smelted in closed submerged arc furnaces with a power of 22 to 93 MVA. The composition of FeSi45 alloy by standard is: Si: 41-47%, Mn: 2,0%, Cr: 0,5%, P: 0,05%, S: 0,02%, Al: 2,0%. The density of the alloy is ~3,27g/cm^3, melting point 1330–1350°C. According to V. P.Elyutin [7], the beginning of the reduction for the production of FeSi45 is 1650K (1377°C). G.V. Karssanovachieves laboratory reduction at a temperature of 1500°C[2].The aim of the present work is to obtain a ferrosilicon alloy using iron silicate as an alternative raw material.

2. EXPERIMENTAL

The chemical composition of the initial charge materials used is presented in Table 1. Iron-silicate fines - fayalite contains iron oxide over 60% and 27% silicon dioxide. Particles with a size below 70 μm are about 80%, pycnometric density is3,6 t/m^3, bulk density - 2,4 t/m^3, humidity - 10%. The material is finely dispersed and in this form could not be used in metallurgy. Our research[8,9]has found an excellent opportunity for its agglomeration as by pelletization in a disk pelletizer so and by briquetting, including by extrusion briquettes.

In the balance calculations,distributions of the reduced elements and oxides between the metal, slag, and gas phases, which are well-known in practice, were used. The amount and chemical composition of the obtained alloy are presented in Table 2.

Table 1 - Chemical composition of charge materials,%

%	iron-silicate	quartzite	coke	A^C coke	electrode mass	A^E electrode mass
SiO_2	27,18	99,2	-	47,52	-	50
Fe_2O_3	Fe_2O_3 -11,26 FeO- 51, 55	0,17	-	9,67	-	14
Al_2O_3	3,76	0,31	-	30,78	-	23
CaO	2,32	0,14	-	6,3	-	8,1
MgO	1,19	0,19		2,4	-	3
P_2O_5		-		0,58	-	-
ZnO	1,69	-	-	-	-	-
PbO	0,53	-	-	-	-	-
Cu	0,47	-	-	-	-	
MnO	0,06	-	-	-	-	-
S	-	-	0,5	-	-	2
C	-	-	85	-	80	-
A^C	-	-	10,92	-	7	-
W	-	0,18	2,45	-	-	-
V^C	-	-	1,63	-	13	-

Table 2 - Quantity and chemical composition of the obtained alloy

elements	Fe	Si	Al	Ca	Mg	Cu	Total
kg	49,46	46,87	2,31	1,03	0,23	0,47	101,31
%	49,29	46,69	2,30	1,03	0,23	0.47	100,00

The composition of the resulting alloy (Table 2) meets the standard for ferrosilicon FeSi45. The amount and the chemical composition of the obtained slag are presented in Table 3.

Table 3 - Quantity and chemical composition of the obtained slag

oxides RxOy	FeO	SiO_2	Al_2O_3	CaO	MgO	Total
kg	0,624	2,001	1,863	1,439	1,124	7,051
%	8,85	28,38	26,41	20,41	15,94	100,00

Based on the stoichiometric calculations and distributions of the components, the quantitative distribution of the initial charge materials to the obtained products was determined. The material balance of the process for the production of ferrosilicon FeSi45 is presented in Table 4.

Table 4 - Material balance of ferrosilicon process

Input charge materials			Output products		
	mass (kg)	%		mass (kg)	%
quartzite	75,00	30,65	alloy FeSi45	95,67	39,10
coke	65,60	26,81	slag	7,05	2,88
iron-silicate	100,0	40,87	gas	135,88	55,53
electrode mass	2,70	1,10	red.elements	5,30	2,17
Fe furnace shell	1,40	0,57	unbound	0,80	0,32
Total	244,70	100,00	Total	244,70	100,00

In the heating process, the change of the electromotive force (EMF) on the principle of galvanic cell with solid electrolyte ZrO_2 (CaO) and a reference electrode Mo-MoO_2 was registered.

Thevalues of EMF and temperature as a function of time are presented in Figure1.Figure 2 shows the dependence of ΔG=f(T).

The Gibbs energy values at the respective temperatures were determined using the oxidation potential of the system.

$$E = \frac{R.T}{n.F}\left(\lg P''_{O_2} - \lg P'_{O_2}\right)$$

where E- measured EMF/V; R-gas constant 8,314/deg $K^{-1}mol^{-1}$; n-number of the electrons taking part in the reaction; F- Faraday constant $9{,}6489.10^4$ / $C.mol^{-1}$; lnP''_{O2} -oxygen pressure of the reference electrode; lnP'_{O2}- oxygen pressure of the system under investigation.

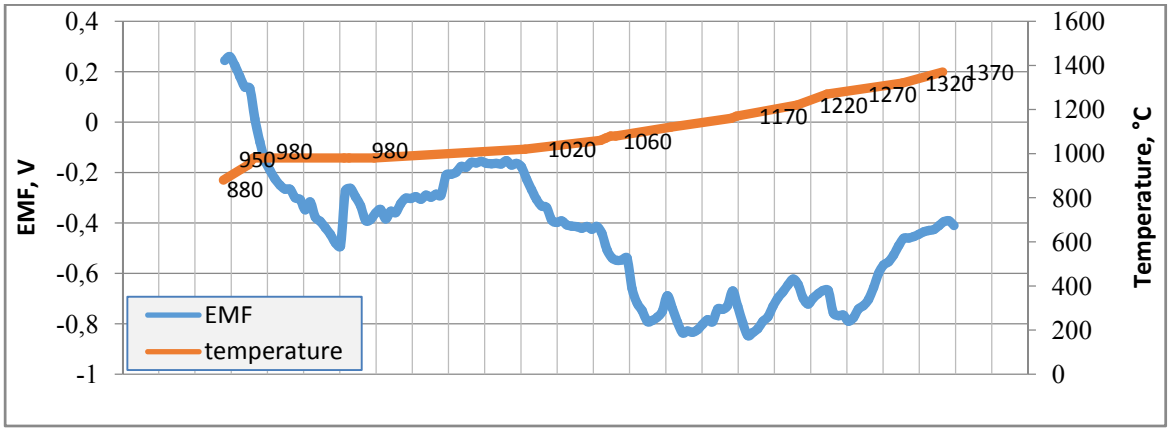

Figure 1 - EMF and temperature depending on time

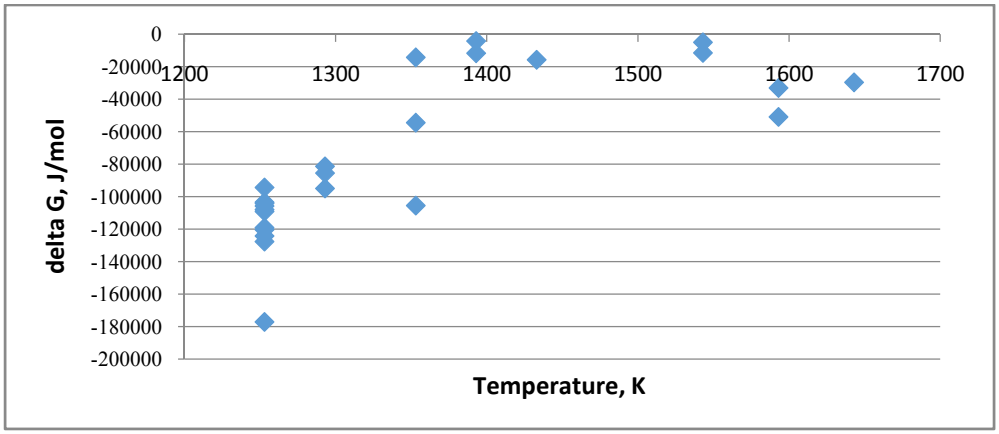

Figure 2 - Dependence of ΔG=f(T)

A dependenceΔG=f(T) for the temperature range 1253K to 1433K was derived:

ΔG= -886801+616,7. T, J/mol R^2=0,9308

This dependence is based on the average values of Gibbs energy obtained at the respective temperature retentions. During this time, the combustion of carbon took place, as well as the reduction of iron oxides.During this period the reactions took placeare

$3Fe_2SiO_4 + O_2 \rightarrow 2Fe_3O_4 + 3SiO_2$

ΔG=-471750+160,06.T J/mol (1080≤T≤1340K)[10]

$Fe_3O_4 + CO \rightarrow 3FeO + CO_2$

Equilibrium in this system is achieved at temperatures 1369 - 1661K.

3. CONCLUSION

A material balance was calculated, including a quantitative ratio between the components for the production of ferrosilicon FeSi45, using a by-product of copper production - iron silicate. Heating of the investigated charge was performed experimentally and EMF was registered. An equation for $\Delta G = f(T)$ in the temperature range 1250–1433 K was derived. The results of theoretical calculations show that it is possible to obtain FeSi45 according to the standard.

REFERENCES

[1] http://www.irt-bg.com
[2] Hr. Erinin, A. Avramov, Metallurgy of Ferroalloys, Technique, Sofia, 1979, p.138.
[3] A. Avramov, I. Ivanchev, Tsv. Tsanev, Iron Metallurgy, Technique, Sofia, 1994
[4] M. Gasik, Handbook of Ferroalloys, Theory and Technology, 2013, pp 179-220.
[5] Ya L.Liao, Xi J.Chai, J. T. Li, Fu Ch. Xu, Study on the reduction of ferrous compounds disseminated in fayalite, vitreous and magnetite in dumped copper slag by of carbonthermic method, Adv. Mat. Res., 233-235(2011), 684-688.
[6] Patent CN105886765A, Method for producing ferrosilicon, August 24, 2016.
[7] V.P. Elyutin, Yu.A. Pavlov, Production of ferroalloys, Metalurgizdat, Moscow, 1957.
[8] D. Grigorova, R. Paunova, G. Serafimov, D. Stoyanov, Influence on different basicity on thermodynamics of reduction of fayalite briquettes, ISC2015, July 13 – 14, Bor, Serbia, 2015.
[9] M. Mihovsky, V. Hadzhiyski, L. Todorov, D. Dimitrova, Plasma-induction technology for reduction processing of copper concentrate pellets, J. Chem. Technol. Metall., 41(1) (2006), 55-60.
[10] K.T. Jacob, G.M. Kale, and G.N.K. Iyengar, Chemical Potentials of Oxygen for FayaliteQuartz-Iron and Fayalite-Quartz-Magnetite Equilibria, Metall. Mater. Trans,20B, (1989), 679-685.

The 52nd International October Conference on Mining and Metallurgy
November 29th – 30th , 2021
www.ioc.tfbor.bg.ac.rs

THE CLAY PRELIMINARY TESTING FROM MUNICIPALITY AREA OF REKOVAC

Slavica Mihajlović[1], Marina Jovanović[2], Nataša Đorđević[1], Aleksandra Patarić[1], Milica Vlahović[3], Vladan Kašić[1]

[1]Institute for Technology of Nuclear and Other Mineral Raw Materials, Franchet d`Esperey 86, 11000 Belgrade, Serbia

[2]University of Zenica, Faculty of Metallurgy and Technology, Travnička cesta 1, 72000 Zenica, Bosnia and Herzegovina

[3]University of Belgrade, Institute of Chemistry, Technology and Metallurgy-National Institute of Republic of Serbia, Njegoševa 12, Karnegijeva 4, 11000 Belgrade, Serbia

Abstract

On the territory of Rekovac municipality, geological research has discovered clay deposit "Oparić". The sample was taken from the well core with 9 m depth, then stirred with water and sifted by wet process on a sieve with 0.063mm opening. It was obtained 71% of reflections (class + 0.063 mm) and 29% of sieves (class -0.063 mm).The chemical and X-ray analysis of the class -0.063mm was done. The results showed there is increased content of iron in the form of Fe_2O_3, which reduces the clay quality.Further research should focus on finding the iron removing possibility by magnetic concentration.

Keywords: *clay, chemical analysis, X-ray analysis.*

1. INTRODUCTION

Clay is plastic semi-bound sediment formed by diagenesis (binding) of sludge, pelitic material (grain size below 0.005 mm) transported by water and deposited in an aqueous medium.In addition to clays that become by transporting and depositing sludge material, there are also those that have become and remain at the site of decomposition of the primary material. These are residual or sedimentary clays [1]. Clays are rocks with different mineral and chemical composition.They are made of fine dispersed particles (finer than 2μm) which, in their natural state or mixed with water, give a plastic mass that retains its shape after drying, and gains the stone strength by baking.Unlike clays which are characterized by plastic properties, there are finely dispersed formations in nature without such properties, such as refractory and pottery clays. However, these clays also have a wide industrial application. Clay minerals represent a large group of related silicates.These minerals are usually deposited by surface decomposition of aluminosilicates in the parent rock or as sediments from surface waters. They are stable at low temperatures and low pressure. Clay minerals can also be products of hydrothermal solutions and hydrothermal transformation of suitable rocks.As clay constituents, minerals are usually found in aggregates with a predominance of one or more different minerals.Such aggregates are almost always fine-grained, so sometimes even microscopes cannot distinguish their individuals. In order to better and more detailed study of clay minerals, a special branch of mineralogy has been developed that deals with this, and that is clay mineralogy.Basically, clay consists of one or more main minerals (kaolinite, hydroliskuni-ilite, montmorionite and other aluminum silicates) and various impurities (quartz, zircon, apatite, garnets, iron carriers, etc.) [2]. Within silicates that are determined as clays, there are two distinguished groups: crystalline representatives (group of kaolin, pyrophyllite, montmorillonite, illite and halosite) and amorphous representatives

(allophane). All crystalline representatives are phyllosilicates. In addition to silicon, they contain aluminum and significant amounts of water.The composition differences of these minerals are mainly due to the different ratios of silicon and aluminum between the components. Impurity components appear only in traces and in small quantities [3].Phyllosilicates crystallize monoclinically and triclinically.Crystals are always plate-like, regardless of whether they are regular or not, due to a high developed base. They appear in the form of earthy, worm-shaped or irregular aggregates.The crystals show perfect fissility at the base. The sheets are flexible, but inelastic with Moss hardness 1 to 3, density 2g/cm^3 (for montmorillonite) to 2.6 g/cm^3 (for kaolin).They are in different colors: white, yellow (derived from iron), gray (from moisture or organic pigment), green, brown, etc.Phyllosilicates are characterized by having a more or less pronounced ability to adsorb many cations on the surface or between the crystal lattice layers.Clays are rocks that, depending on their purity, can have great use in various industries. Kaolinite clays are raw materials for the porcelain industry, montmorillonite for molds in the refractory industry, and impure clays are used in pottery. The clay has also use in the ceramics industry [4, 5, 6].

2. EXPERIMENTAL

2.1 Material and equipment

A sample of clay for testing was taken from the well core with 9 m depth at the Oparić site. The sample was stirred with water and sifted by wet process on a sieve with 0.063 mm opening. A mass fraction of reflections of 71% (class + 0.063 mm) and sieves of 29% (class -0.063 mm) was obtained.Having in mind that impurities in clay are concentrated in larger classes, the smaller class -0.063 mm was taken for further examination. This size is the most frequently required class for various applications. Chemical and X-ray diffraction (XRD) analysis were performed on the selected class.The atomic absorption spectrophotometer "Perkin Elmer" -Analyst 300 was used for chemical analysis. X-ray diffraction analysis was performed on an X-ray diffractometer device brand "PHILIPS", model PW-1710.

3. RESULTS AND DISCUSSION

3.1 The clay characterization from deposit "Oparić"

The chemical and XRD analysis was performed on the class -0.63+0.1 mm and the results are shown in Table 1 and Figure 1.

Table 1 - Chemical analysis of class -0.63 + 0.1 mm clay from deposit "Oparić"

Component	SiO_2	Al_2O_3	MgO	CaO	Fe_2O_3	Na_2O	K_2O	TiO_2	LoI*
%	56.00	14.72	0.462	6.29	7.93	0.803	2.63	0.335	10.78

*loss onignition (LoI)

The results of the chemical analysis show a high content of SiO_2 56% and CaO 6.29%, as well as a low content of Al_2O_3 14.72%. There is also an increase of iron content in form of Fe_2O_3 7.93%.This indicates that it is a poor quality raw material with limited use. Therefore, it is necessary to subject this raw material to certain preparation and refining processes.In order to determine which minerals are present in this sample, an X-ray analysis was performed and the obtained diffractogram is shown in Figure 1.

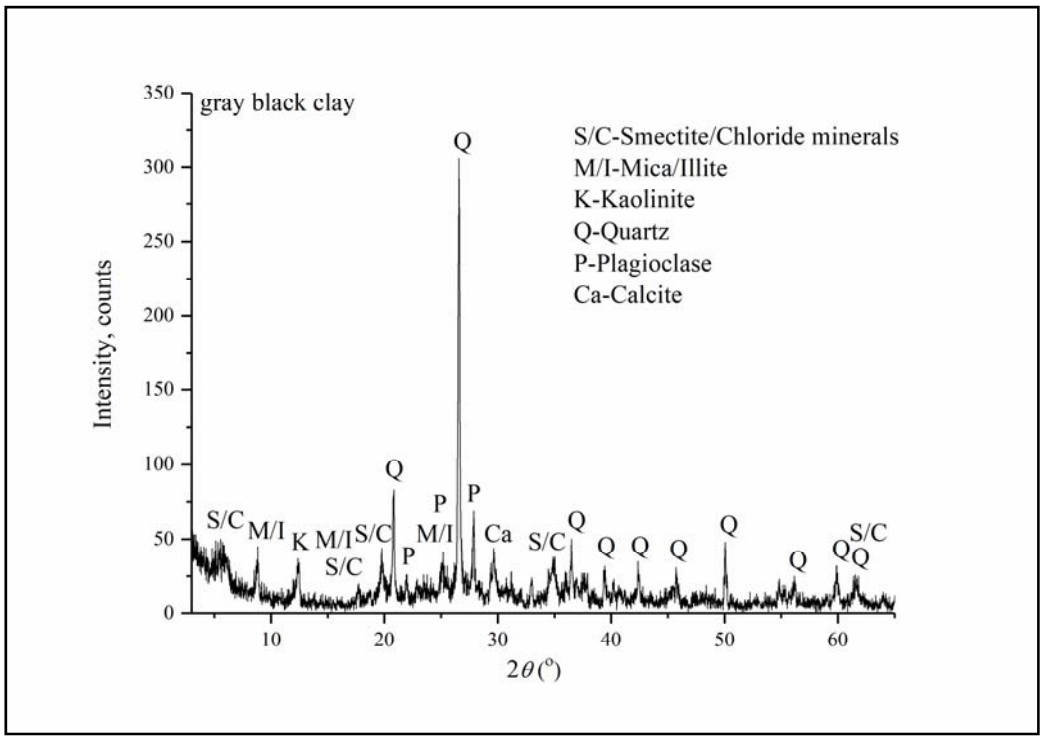

Figure 1 - Diffractogram of clay powder sample "Oparić"

In the analyzed sample the following mineral composition was determined: quartz, smectite/chlorite minerals, mica/illite, plagioclase, calcite.The clay minerals (smectites, kaolinite and illite), are the most represented mineral while quartz and plagioclase are less represented. Calcite is the least present.The results of chemical and mineralogical tests of the clay sample "Oparić" showed the presence of mixture of minerals: smectite, kaolinite and illite as well as the Fe_2O_3.The clay of this locality has a very limited use, due to the high iron content and low aluminum content.The subject of further research by the authors of this paper is to examine the possibility of smectite concentration and iron removal.The assumption is that iron can be removed by a high-gradient magnetic concentration process, but it is first necessary to determine in what form it is: is it an external Fe located between the layers of the crystal lattice of minerals or is it internally embedded in the crystal lattice of minerals.Magnetic concentration is possible to remove only Fe-bearing minerals that are physically trapped between the layers of the crystal lattice, while the removal of chemically bound Fe is impossible.

4. CONCLUSION

Based on preliminary clay quality tests of the "Oparić" site, it can be concluded that this raw material has limited application due to its chemical composition.Namely, in addition to the minerals kaolin, illite and smectite, this clay contains a high content of iron, which affects the poor clay quality and reduced its use.Iron can be removed by magnetic concentration, only if it is notchemically bound, but if Fe-bearing minerals are located between the layers of the crystal lattice of clay minerals.The removal of iron from the clay sample of the mentioned locality and the clay minerals concentration is the subject of further research by the authors of this paper.

ACKNOWLEDGEMENT

The authors wish to acknowledge the Ministry of Education, Science and Technological Development of the Republic of Serbia for financial support of the research which results are presented in the paper (contract 451-03-9/2021-14/200023 and 451-03-9/2021-14/200026).

REFERENCES

[1] S. Janković, B. Vakanjac, Ležišta nemetaličnih mineralnih sirovina, Građevinska knjiga, Beograd, 1969.
[2] V. Đorđević, P. Đorđević, D. Milovanović, Osnovi petrologije, Nauka, Beograd, 1991.
[3] M. Ilić, S. Karamata, Specijalna mineralogija (Deo I) Pregled petrogenih minerala, Građevinska knjiga, Beograd, 1963.
[4] http://www.gef.bg.ac.rs/wp-content/uploads/UPOTREBA-STENA.pdf
[5] M. Tecilazić-Stevanović, Osnovi tehnologije keramike, Tehnološko-metalurški fakultet Beograd, 1973.
[6] S. Popov, Lj. Kostić-Gvozdenović, Neorganskahemijskatehnologija, Univerzitet u Beogradu, Rudarsko-geološkifakultet u Beogradu, 1984.

The 52nd International October Conference on Mining and Metallurgy
November 29th – 30th, 2021
www.ioc.tfbor.bg.ac.rs

EXPERIMENTAL AND THERMODYNAMIC STUDY OF ISOTHERMAL SECTIONS AT 600 °C AND 400 °C OF TERNARY Bi-Cu-Ge SYSTEM

Milan Milosavljević[1], Milena Premović[1,2], Duško Minić[1], Dragan Mansijević[3], Aleksandar Đorđević[1], Milan Kolarević[4]

[1]University of Priština, Faculty of Technical Science, KnezaMilosa 7, 38220 Kos.Mitrovica, Serbia
[2]State Key Laboratory of Powder Metallurgy, Central South University Changsha, China
[3]University of Belgrade, Technical FacultyBor, V.J. 12, 19210, Bor, Serbia
[4]University of Kragujevac, Faculty of Mechanical Engineering, Kraljevo, Serbia

Abstract
Experimental and computation thermodynamic is very important for future development of materials and knowledge of phase diagram. Knowlegde of phase diagram without experimental confirmation is not worth a lot. In this study both calculation and experiments were performed for better knowledge of isothermal sections. Calculated phase diagrams were two isothermal sections at 600 °C and 400 °C. Calculations were done by using PANDAT software and thermodynamic data from literadute. Experimental were performed on 12 annealed alloys. Six alloys were prepared per isothermal section. Compositions od alloys and phases presented in microstructures were tested with SEM-EDS while determination of phases in samples were checked with XRD.Results of EDS were compared with calculated isothermal sections and good agreement were reached.

Keywords: *ternary Bi-Cu-Ge system, SEM-EDS analysis,XRD analysis, isothermal sections.*

1. INTRODUCTION

Germanium is important semiconductor and it is known that by addition of Bi to Ge-based materials their semiconducting properties can be improved [1]. Beside, it germanium based alloys are extensively used in electrical and electronic industry [2]. In this paper ternary Bi-Cu-Ge system is in focus. Cu is chosen as a alloying element due to the key properties of copper such as excellent electrical and heat conductivity, good erosion, corrosion and biofouling resistance, high strength, good machinability, non-magnetic, etc. [3,4]. In this work studied ternary alloys were from isothermal sections at 600 °C and 400 °C. Used experimental techniques included scanning electron microscopy (SEM) with energy dispersive spectrometry (EDS) and X-ray powder diffraction (XRD). The experimental results were compared with the calculated phase diagrams of the isothermal sections at 400 C and 600 °C. Reasonable agreement between the calculated phase diagrams and the experimental data was obtained. For studied ternary Bi-Cu-Ge system it was not necessary to introduce new ternary parameters.

2. EXPERIMENTAL

Ternary alloys for experimental tests are prepared from high pure Bi, Cu and Ge (99.999 at. %) elements, produced by Alfa Aesar, Germany. All samples are melted and re-melted five times in an induction furnace, to preserve homogeneity. Such samples are divided in two groups. One group is with 6 samples used for phase equilibriumat 600 °C. Second group of samples are used for phase equilibriumat 400 °C. The average mass of theeachternary alloy sample was about 4 g. Such prepared samples were tested by XRD and SEM-EDS.

Used device for SEM-EDS analysis was JEOL JSM-6460 scanning electron microscope paired with Oxford Instruments X-act energy dispersive X-Ray spectroscope. The used XRD device

was Bruker D2 PHASER powder diffractometer equipped with a dynamic scintillation detector and ceramic X-Ray Cu tube (KFL-Cu-2 K). XRD patterns were recorded in a 2θ range from 10 to 75° with a step size of 0.02° and then analyzed using the Topas 4.2 software and ICDD databases PDF2 (2020).

3. RESULTS AND DISCUSSION

3.1.Isothermal section at 600 °C

Six ternary samples annealed at 600 °C for five weeks were tested with SEM-EDS and XRD. Results of tests are presented in Table 1.

Table 1.Combined results of SEM-EDS and XRD analyzes of the selected alloys annealed at 600 °C.

No.	Composition of samples (at.%)	Determined phases		Compositions of phases (at.%)			Lattice parameters (Å)
		EDS	XRD	Bi	Cu	Ge	
1	89.13 Bi 0.86 Cu 10.01 Ge	L (Ge)	- (Ge)	93.52±0.5 0.01±0.3	1.58±0.2 0.19±0.1	4.90±0.1 99.80±0.7	- *a*=*b*=*c*=5.6531
2	36.75 Bi 25.64 Cu 37.61 Ge	L (Ge) η	- (Ge) η	93.88±0.2 0.03±0.3 0.09±0.6	2.29±0.8 0.08±0.3 75.73±0.1	3.83±0.3 99.89±0.4 24.18±0.6	- *a*=*b*=*c*=5.6547 a=5.2902, b=4.2003, c=4.5487
3	38.22 Bi 33.54 Cu 28.24 Ge	L (Ge) η	- (Ge) η	93.18±0.5 0.05±0.5 0.07±0.5	3.28±0.2 0.77±0.5 73.82±0.4	3.54±0.2 99.18±0.1 26.11±0.5	- *a*=*b*=*c*=5.6552 a=5.2892, b=4.2123, c=4.5531
4	36.75 Bi 51.04 Cu 12.21 Ge	L ε ξ	- ε ξ	93.52±0.1 0.55±0.7 0.37±0.2	5.72±0.7 76.47±0.5 83.40±0.2	0.76±0.4 22.98±0.3 16.23±0.1	- a=b=4.1673, c=7.5003 *a*=*b*=2.6022, *c*=4.2352
5	32.15 Bi 63.93 Cu 3.92 Ge	L (Cu)	- (Cu)	91.68±0.4 0.74±0.3	8.27±0.1 93.30±0.2	0.05±0.3 5.96±0.6	- *a*=*b*=*c*=3.6652
6	10.11 Bi 86.34 Cu 3.55 Ge	L (Cu)	- (Cu)	90.95± 0.7 0.56±0.2	8.63±0.5 96.33±0.4	0.42±0.2 3.11±0.1	- *a*=*b*=*c*=3.6611

With six samples four different phase regions are detected. In microstructure of sample 1, L and (Ge) phase are detected. Samples 2 and 3 detected same three phases L, (Ge) and intermetallic compound η. Sample 4 detected three phases L, ε and ξ. Samples 5 and 6 detected same two phases L and (Cu).

Experimental results given in Table 1 are compared with calculated isothermal section at 600 °C. Calculated phase diagram is performed by using Pandat software and thermodynamic dataset compiled. Calculated isothermal section with EDS results given in Table 1 are presented on Figure 1.

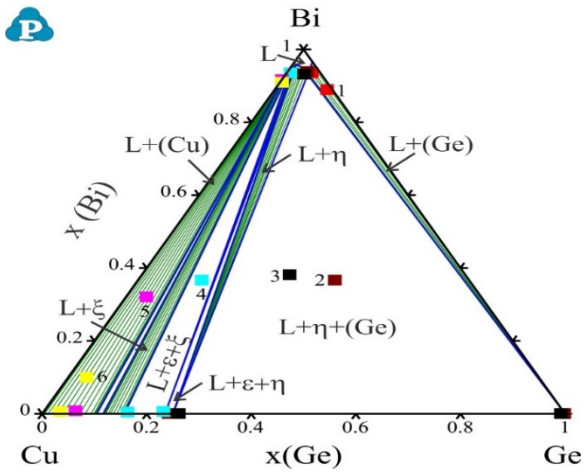

Figure 1. Calculated Bi-Cu-Ge isothermal section at 600 °C compared with EDS results given in Table 1.

On calculated isothermal section ten phase regions are visible. One region is L single phase region oriented to the Bi side, five are two-phase regions L+(Ge), L+η, L+ε, L+ξ and L+(Cu), four are three-phase regions L+η+(Ge), L+ε+η, L+ε+ξ and L+ξ+(Cu). From those ten calculated phase region four are experimentally confirmed with six samples.By comparison it is clear that experimental determined composition of phases is close with experimental composition of phases. As conclusion experiments can well follow calculated isothermal section at 600 °C.

3.2.Isothermal section at 400 °C

Six ternary samples marked with numbers from 7 to 12 are used for testing phaseequilibria at 400 °C. Samples were annealed at 400 °C for five weeks and tested with SEM-EDS and XRD. Results of tests are given in Table 2.

Table 2.Combined results of SEM-EDS and XRD analyzes of the selected alloys annealed at 400 °C.

No.	Composition of samples (at.%)	Determined phases		Compositions of phases (at.%)			Lattice parameters (Å)
		EDS	XRD	Bi	Cu	Ge	
7	47.04 Bi 11.38 Cu 41.58 Ge	L (Ge) η	- (Ge) η	99.18±0.1 0.20±0.5 0.34±0.4	0.81±0.1 1.62±0.4 73.53±0.3	0.01±0.4 98.18±0.5 26.13±0.1	- *a*=*b*=*c*=5.6579 *a*=5.2911, *b*=4.2087, *c*=4.5541
8	22.54 Bi 32.81 Cu 44.65 Ge	L (Ge) η	- (Ge) η	99.82±0.3 0.01±0.7 0.03±0.4	0.15±0.4 1.91±0.5 75.79±0.7	0.03±0.2 98.08±0.6 24.18±0.7	- *a*=*b*=*c*=5.6558 *a*=5.2972, *b*=4.2152, *c*=4.5598
9	36.93 Bi 40.21 Cu 22.86 Ge	L (Ge) η	- (Ge) η	99.01±0.2 0.12±0.5 0.54±0.6	0.68±0.1 1.05±0.3 72.92±0.7	0.31±0.6 98.83±0.4 26.54±0.4	- *a*=*b*=*c*=5.6560 *a*=5.2978, *b*=4.2155, *c*=4.5613
10	30.69 Bi 55.70 Cu 13.61 Ge	L η ξ	- η ξ	98.18±0.1 0.13±0.3 0.92±0.7	1.50±0.2 75.72±0.6 85.41±0.8	0.32±0.3 24.15±0.2 13.67±0.1	- *a*=5.2968, *b*=4.2052, *c*=4.5573 *a*=*b*=2.6125, *c*=4.2392
11	32.32 Bi 65.18 Cu 2.50 Ge	L (Cu)	- (Cu)	98.01±0.1 0.15±0.2	1.81±0.1 94.23±0.2	0.18±0.5 5.62±0.7	- *a*=*b*=*c*=3.6631
12	63.31 Bi 35.22 Cu 1.47 Ge	L (Cu)	- (Cu)	98.81±0.5 0.37±0.1	0.67±0.5 98.20±0.2	0.52±0.2 1.43±0.3	- *a*=*b*=*c*=3.6598

Three different phase regions are detected by six tested samples. In microstructure of samples 7, 8 and 9 three phases were detected. Detected phases are L, (Ge) and intermetallic compound η. Sample 10 detected three phases L, ηand ξ. Samples 11 and 12 detected same two phases L and (Cu). EDS results shows that L phase detected in all samples is rich with bismuth and can dissolve small amount of other two elements. Solid solution (Ge), detected in samples 7, 8 and 9 is rich with germanium with 98.08, 98.18 and 98.83 at. % and the rest is bismuth and copper.Intermetallic compound η is line compound with composition 75 at. % Cu and 25 at. % Ge, in our study detected η phase has variation in composition. Composition of η phase detected on samples annealed at 400 °C hasslightly different composition and it is in range from 72.92 to 75.79 at. % of Cu and 24.15 to 26.54 at. % Ge rest is a small amount of bismuth. According to the literature ξ phase have composition of Cu from 83.5 to the 90.2 at. % and rest is germanium, which is in range with composition of this phase detected in sample 10, 85.41 at. % of Cu.On samples 11 and 12 (Cu) solid solution is detected with composition of 94.23 to the 98.20 at. % of Cu which is in range with literature composition 88.3-100 at.% Cu.

Experimental results given in Table 2 are compared with calculated isothermal section at 400 °C. Calculated isothermal section with EDS results given in Table 2 are presented on Figure 2.

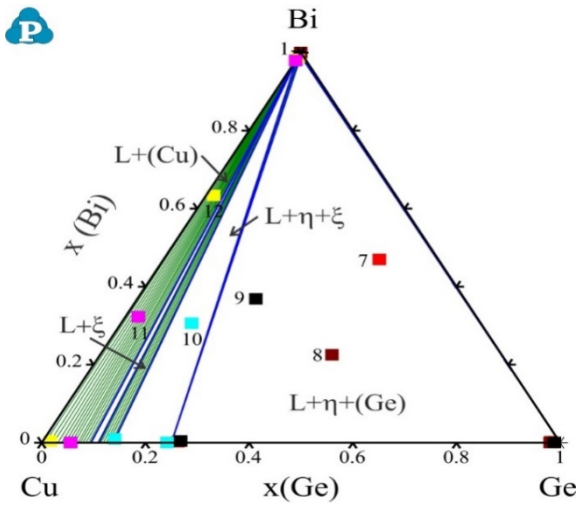

Figure 7. Calculated Bi-Cu-Ge isothermal section at 400 °C compared with EDS results given in Table 3.

On calculated isothermal section six phase regions are visible. Three are two-phase regions L+η, L+ξ and L+(Cu) and three are three-phase regions L+η+(Ge), L+η+ξandL+ξ+(Cu). From those six calculated phase region three are experimentally confirmed with six samples. Confirmed phase regions are L+η+(Ge) with samples 7, 8 and 9, L+η+ξ with sample 10 and L+(Cu) with sample 11 and 12. By comparison it is clear that experimental determined composition of phases is close with experimental composition of phases. As conclusion experiments can well follow calculated isothermal section at 400 °C.

4. CONCLUSION

The ternary Bi-Cu-Ge system was experimentally and analytically tested. Twelve samples were prepared and test by using SEM-EDS and XRD. Analytical by using Calphad approach two isothermal sections at 600 °C and 400 °C were calculated.The isothermal section at 600 °C was investigated with 6 ternary alloys and four different phase regions were detected. The isothermal section at 400 °C was investigated with 6 ternary alloys and three different phase regions were detected. In those samples ternary compounds and large solubility in intermetallic compound and solid solutions were not detected. In general, it can be concluded that phase equilibria of ternary Bi-Cu-Ge system presented in this paper is confirmed by experiments. Experiment agrees well with calculated phase diagrams and there is no necessity to introduce new ternary parameters for description of ternary Bi-Cu-Ge system.

ACKNOWLEDGEMENTS

This work has been supported by the National Nature Science Foundation of China (project No.51950410600) and the Ministry of Education, Science and Technological Development of the Republic of Serbia (Grant No. OI172037).

REFERENCES

[1] L. Tichy, H. Tichá, A. Pacesová, J. Petzlt, On the infrared spectra of Ge-Bi-Se(S) glasses, J. Non-Cryst. Solids, 128 (2) (1991) 191–196.
[2] S. Adachi, Properties of Semiconductor Alloys: Group-IV, III-V and II-VI, Semiconductors, Wiley, Hoboken, 2009.
[3] M. M. Vasić, A. S. Kalezić-Glišović, R. Milinčić, Lj. Radović, D. M. Minić, A. M. Maričić, D. M. Minić, J. Min. Metall. Sect. BMetall., 55 (1) B (2019) 85-93.
[4] M. Azimi, G. H. Akbari,J. Alloys Compd., 555 (2013) 112-116.

The 52nd International October Conference on Mining and Metallurgy
November 29th – 30th, 2021
www.ioc.tfbor.bg.ac.rs

STUDY OF TEMPERATURE PHASE TRANSFORMATION OF THETERNARY Bi-Cu-Ge SYSTEM

Aleksandar Đorđević[1], Duško Minić[1], Milena Premović[1,2], Dragan Mansijević[3], Milan Milosavljević[1], Vladica Ristić[4]

[1]University of Priština, Faculty of Technical Science, KnezaMilosa 7, 38220 Kos.Mitrovica, Serbia
[2]State Key Laboratory of Powder Metallurgy, Central South University Changsha, China
[3]University of Belgrade, Technical FacultyBor, V.J. 12, 19210, Bor, Serbia
[4]University Union – Nikola Tesla, Faculty of Engineering Management, Belgrade, Serbia

Abstract
Decades of scientific work dedicated to the investigation of phase diagrams gave significant benefit to industry and science. After all those years of phase diagram investigation still there is missing information about phase diagram of some ternary systems. One of those systems is Bi-Cu-Ge. It is known importance of Cu-based alloys and Ge-based alloys in electro industry. Since such combination is not tested before this work will provide information about phase diagram of the three vertical sections from ternary Bi-Cu-Ge system. From each vertical sections (Bi-CuGe, Cu-BiGe and Ge-BiCu), 4 alloys were prepared and tested by DTA. Experimentally obtained results were compared with corresponding vertical sections. Experimental temperatures of phase transformation shows close value with calculated one. Temperatures of liquidus curve and primary crystallization were determined.

Keywords:*ternary Bi-Cu-Ge system, DTA analysis, vertical sections.*

1. INTRODUCTION

In recent period ternary alloys based on Bi-Ge attracted attention. Our group tested ternary systemssuch as Bi-Ge-Zn,Ga,In,Sn,Ag,Sb [1-3]. On other side copper is recyclable without any loss of quality and can easily make alloys with a lot of elements beside it Cu and Cu-based alloys are wide used in building industry, electronic industry, transportation and many others. So, chosen system Bi-Cu-Ge is important due to the possible application in electronic industry and it is not tested before.In this work studied ternary alloys were from three vertical sections. Used experimental techniques included differential thermal analysis (DTA). The experimental results were compared with the calculated phase diagrams of the selected vertical sections.Reasonable agreement between the calculated phase diagrams and the experimental data was obtained.

2. EXPERIMENTAL

In total 12 ternary alloys were prepared by using high purity Bi, Cu and Ge produced by Alfa Aesar, Germany. Samples were measured in different molar ration and the total mass of each sample were 4 g. Weighed masses of the samples were arc-melted and re-melted six times under high-purity argon atmosphere. The average weight loss was about 0.5 mass %.

Such samples were tested by DTA method with DTG-60H (Shimadzu). Alumina crucibles were used and measurements were performed under flowing argon atmosphere. Samples weighing between 20 and 30 mg were investigated at a heating rate of 5 °C/min.

3. RESULTS AND DISCUSSION

Twelve ternary samples were selected for DTA tests. The samples were placed in alumina crucibles and characteristic temperatures were recorded under protective flowing Ar atmosphere. Weights of the analyzed alloy samples were between 30 and 40 mg and a reference material was an empty alumina crucible. Determination of phase transition temperatures was carried out according to recommendations from the literature [4,5].The liquidus and temperatures of monovariant phase transitions were determinedfrom peak maxima while the solidus temperatures and the temperatures of invariant reactions were determined from onset temperatures of the corresponding peaks.Such determined temperatures from DTA heating curves from 12 samples are summarized in Table 1.

Table 1. Phase transition temperatures of the studied alloys from the ternary Bi-Cu-Ge system determined by DTA at pressure p = 0.1 MPa.

Number	Composition (at. %)		Identified phase transition temperature in °C		
	Nominal	EDS	Ternary eutectic reaction	Ternary transition reaction	Liquidus
Vertical section Bi-CuGe					
1	$Bi_{20}Cu_{40}Ge_{40}$	$Bi_{20.15}Cu_{39.18}Ge_{40.67}$	279.47	613.53/636.21/701.3	849.09
2	$Bi_{30}Cu_{35}Ge_{35}$	$Bi_{29.11}Cu_{35.48}Ge_{35.41}$	269.09	610.34/629.30	933.10
3	$Bi_{50}Cu_{25}Ge_{25}$	$Bi_{49.81}Cu_{25.13}Ge_{25.06}$	275.24	610.19/634.16	979.54
4	$Bi_{70}Cu_{15}Ge_{15}$	$Bi_{70.02}Cu_{14.81}Ge_{15.17}$	278.22	-/622.34	918.92
Vertical section Cu-BiGe					
5	$Bi_{45}Cu_{10}Ge_{45}$	$Bi_{45.01}Cu_{9.81}Ge_{45.18}$	278.10	613.80/627.10	778.90
6	$Bi_{35}Cu_{30}Ge_{35}$	$Bi_{35.52}Cu_{29.61}Ge_{34.87}$	279.14	614.87/633.78	938.19
7	$Bi_{27.5}Cu_{45}Ge_{27.5}$	$Bi_{27.43}Cu_{44.87}Ge_{27.70}$	277.33	612.70/629.23	1035.74
8	$Bi_{20}Cu_{60}Ge_{20}$	$Bi_{19.73}Cu_{61.12}Ge_{19.15}$	277.02	681.20/727.20	1041.80
Vertical section Ge-BiCu					
9	$Bi_{45}Cu_{45}Ge_{10}$	$Bi_{45.08}Cu_{44.87}Ge_{10.05}$	278.31	548.90/723.90/765.61	1128.92
10	$Bi_{35}Cu_{35}Ge_{30}$	$Bi_{34.98}Cu_{35.09}Ge_{29.93}$	279.11	615.19/631.20	1024.90
11	$Bi_{20}Cu_{20}Ge_{60}$	$Bi_{19.35}Cu_{20.87}Ge_{59.78}$	280.10	615.70/631.67	768.62
12	$Bi_5Cu_5Ge_{90}$	$Bi_{4.35}Cu_{4.91}Ge_{90.74}$	277.78	615.30/628.10/733.10	915.90

From recorded DTA results in Table 1, it is visible that on three samples five peaks are detected, on eight samples four peaks and on sample $Bi_{70}Cu_{15}Ge_{15}$ three peaks. It can be notice that first detected peak ofeach sample have similar value of temperatures and it can be assumed that detected temperatures are related to the same transformation. Last detected temperature on all samples is liquidus temperature while peaks in-between are ternary transition reaction. Experimental temperatures from Table 1 are compared with calculated vertical sections. Calculated vertical sections are Bi-CuGe, Cu-BiGe and Ge-BiCu respectively presented on Figure 1.

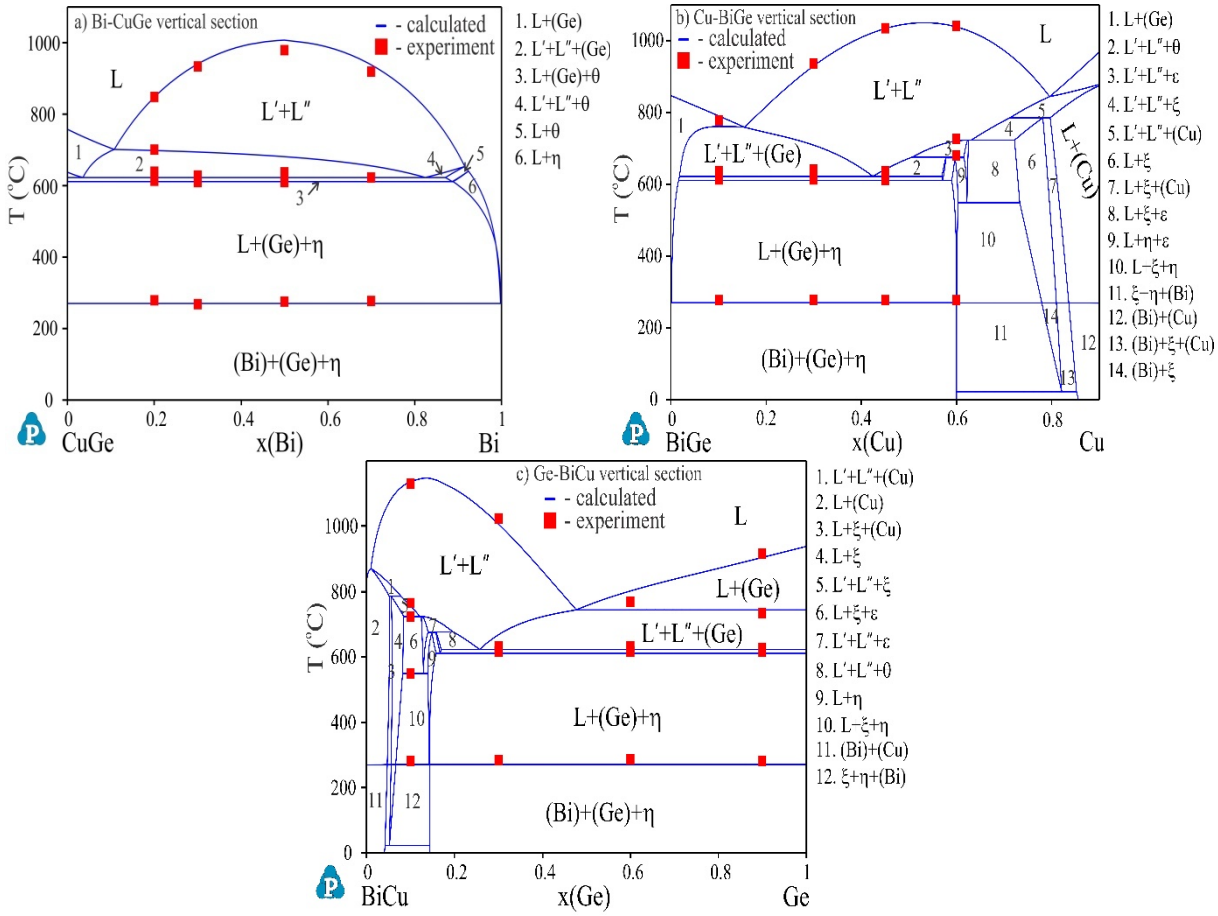

Figure 1. Calculated vertical sections of the ternary Bi-Cu-Ge system compared with DTA experimental results: a) Bi-CuGe, b) Cu-BiGe and c) Ge-BiCu.

From figure 1, good agreement with calculation and experimental resultscan be noticed.Figure 1a) presents calculated vertical section Bi-CuGe compared with experimental result of four samples 1-4. From calculation it is clear that first detected temperature of all samples is related to the same transformation which is related to the ternary eutectic reaction L→(Ge)+(Bi)+η. According to the calculation reaction appears at 271.07 °C, while experimental temperature is in range of 269.09 to the 279.47 °C, which are close to calculated value. Second detected temperature on samples 1, 2 and 3 is related to the θ→L+(Ge)+η calculated at 611.64 °C while experimental are 610.19 to the 613.53 °C which are close to each other. This transformation wasn't confirmed on sample 4 while according to the calculation it should be. Third detected temperatures on all samples is related to the L→L+(Ge)+θ with calculated temperature at 623.05 °C. Experimentally determined temperatures are 622.34, 629.30, 634.16 and 636.21 °C which are slightly higher than calculated one. On sample $Bi_{20.15}Cu_{39.18}Ge_{40.67}$ is also determined temperature of transformation L'+L"→L'+L"+(Ge) at 701.30 °C. Last temperature on all samples is liquidus temperature and all experimental temperatures agree well with calculated.

Tested samples from vertical section Cu-BiGe are marked with numbers 5, 6, 7 and 8. On each sample four temperatures were detected. By compering DTA results and calculated vertical section Figure 1b), it can be noticed that all four temperatures detected with samples 5, 6 and 7 corresponds to the same phase transformation on each sample. First temperatures are related to the ternary eutectic reaction L→(Ge)+(Bi)+η calculated at 271.07 °C. Experimentally detected temperatures of this reaction are 278.10, 279.14 and 277.33 °C which are close to calculated one. Second detected temperatures are 613.80, 614.87 and 612.70 °C which are related to the ternary phase transformation θ→L+(Ge)+η calculated at 611.64 °C. Third temperature on samples 5,

6and 7 are 627.10, 633.78 and 629.23 °C respectively. This temperatures are related to the L→L+(Ge)+θ phase transformation calculated temperature at 623.05 °C. Last temperatures on those samples are liquidus temperature. Sample 8, from same vertical section as samples 5 to 7, detected different phase transformations than samples 5 to 7. Fist temperature is related to the transformation of L+η→ξ+(Bi), second to the L+ε→L+ξ, third to the L'+L"→L'+L"+(Ge) and last one to the liquid temperature.

Four samples from vertical section Ge-BiCu are tested and marked with numbers 9 to 12. Sample 9 detected five phase transformations. First one is related to the L+η→ξ+(Bi) reaction calculated at 270.46 °C while experimental one is at 278.31 °C, next temperature is detected at 548.90 °C and it is corresponding to the L+ε→ξ+η reaction with calculated temperature at 549.31 °C. Third temperature detected with sample 9 is at 723.90 °C while calculated is at 723.67 °C, this temperature corresponds to the reaction L'→L"+ξ+ε. Next temperature detected at 765.61 °C is related to the solidification of ξ phase while end temperature is liquidus. Samples 10 and 11 detected temperatures of same transformations. First at both samples is relate to the ternary eutectic reaction L→(Ge)+(Bi)+η calculated at 271.07 °C while experimental are 279.11 and 280.10 °C. Second temperature is related to the reaction θ→L+(Ge)+η calculated at 611.64 °C while experimental are 615.19 and 615.70 °C. Third detected temperatures on samples are 631.20 and 631.67 °C which are related to the L'→L"+(Ge)+θ with calculated temperature at 623.05 °C. Last temperatures are liquid. Sample 12 detected five temperatures. First three one are related to the L→(Ge)+(Bi)+η calculated at 271.07 °C, θ→L+(Ge)+η calculated at 611.64 °C and L'→L"+(Ge)+θ calculated at 623.05 °C reactions, experimentally detected at 277.78, 615.30 and 628.10 °C, respectively. Forth temperature is at 733.10 related to the transformation of L+(Ge) into L'+L"+(Ge) while last one is liquid temperature.

As general conclusion after comparison of experimental temperatures and calculated vertical sections good agreement with temperatures is reached in most cases.

4. CONCLUSION

The ternary Bi-Cu-Ge system was experimentally tested. Twelve ternary samples were prepared and test by using DTA.Three vertical sections were calculated from each corner Bi, Cu and Ge. Each vertical section was tested with four samples by DTA. DTA test shows temperatures of phase transformation which were in good agreement with calculated temperatures.In general it can be concluded that phase equilibria of ternary Bi-Cu-Ge system presented in this paper is confirmed by experiments

ACKNOWLEDGEMENTS

This work has been supported by the National Nature Science Foundation of China (project No.51950410600) and the Ministry of Education, Science and Technological Development of the Republic of Serbia (Grant No. OI172037).

REFERENCES

[1] A. Djordjevic, M.Premovic, D. Minic, V. Cosovic, D. Manasijevic, J. Chem. Thermodynamics 142 (2020) 106000.
[2] A. Djordjević, D. Minić, M.Premović, D. Manasijević, V. Ćosović, Inter. J.Thermophysics (2019) 29-40.
[3] P. Fima, A. Gazda, J. Therm. Anal. Calorim., 112 (2013) 731–737.
[4] W.J. Boettinger, U.R. Kattner, K.W. Moon, J.H. Perepezko, in DTA and Heat-Flux DSC Measurements of Alloy Melting and Freezing (NIST recommended practice guide, Special publication 960-15, NIST, (2006).

The 52nd International October Conference on Mining and Metallurgy
November 29th – 30th , 2021
www.ioc.tfbor.bg.ac.rs

RECYCLED COARSE AGGREGATE AND FLY ASH EFFECT ON COMPRESSIVE STRENGTH OF SELF-COMPACTING CONCRETE

Aleksandar Savić[1], Ivana Jelić[2], Marija Šljivić-Ivanović[2], Slavko Dimović[2], Nikola Pudar[3], Aleksandar Pfandler[4]

[1]Faculty of Civil Engineering, University of Belgrade, B.K.A. 73, 11000 Belgrade, Serbia

[2]Vinca Institute of Nuclear Sciences, University of Belgrade, M.P.A. 12-14, 11351Belgrade, Serbia

[3]First Technical High School, R.D. 8, Kragujevac, Serbia

[4]Energoprojekt (Head of concrete laboratory, retired), B.M.P. 12, Belgrade, Serbia

Abstract

The paper presents experimental results of the tests conducted on Self-Compacting Concrete (SCC) with recycled coarse aggregate, and fly ash as filler component. A fine fraction of aggregate originated from a riverbed, while coarse aggregate was obtained either from a riverbed or by crushing laboratory concrete cubes as recycled concrete aggregate. The larger coarse aggregate grains than typical for SCC were used, to highlight the possibility of application in structure elements with sparse reinforcement bars. Four mixtures of concrete were made, in order to compressive strength as the dominant property of any concrete. All of the fresh concrete mixtures displayed proper behavior for this kind of concrete, whereas recycled concrete aggregate induced several challenges. Hardened concrete mixtures showed that beyond the use of natural coarse aggregate, there is the possibility to obtain proper mechanical behavior needed for structural concrete, with moderate amounts of cement. Such an approach paves a way for a cleaner and more sustainable civil engineering practice.

***Keywords**: self-compacting concrete, recycled aggregate, fly ash, sustainable development.*

1. INTRODUCTION

Concrete is the most used material in the world for decades, after water. The estimated amount of annual production of concrete worldwide is estimated to be more than three tons per inhabitant of the planet and continues to grow [1]. Consequently, concrete production is considered to be the highest issue in terms of energy efficiency and climate change. However, its accelerating production also acts upon the consumption of natural resources, i.e. aggregates. One cubic meter of concrete contains nearly one cubic meter of aggregates, and the growing trend of aggregates excessive consumption raises the issue of depletion of natural resources of coarse aggregates and the need to find new opportunities to obtain their replacements. As a sustainable solution to this problem, as well as the problem of construction and demolition waste generation, the process of waste construction materials recycling, primarily concrete, has been imposed [1]. Based on these facts, the recycled aggregate is getting growingly applied in concrete production.

Likewise, the reuse of industrial waste and by-products (e.g. fly ash, sludge, etc.) in concrete production represents the appropriate way for developing sustainable construction. Fly ash represents a fine powder collected on electrostatic precipitators from flue gases in thermal power plants [2]. As a waste, it is deposited in landfills that are typically located near thermal power plants, representing a global concern for which the solutions are constantly pursued [3]. Its use reduces the consumption of non-renewable natural resources and has economic significance. Most commonly, it is used as a supplementary cementitious material in the production of

Portland cement concrete due to its pozzolanic properties. The reuse of fly ash decreases its negative impact on the environment, also reducing its quantities in landfills.

The development of Self-Compacting Concrete (SCC) is an additional way to boost the sustainability of construction, due to the reduction of energy use, i.e. energy required for its preparation. It simplifies implementation by reducing the engagement of highly skilled workers and machines (vibrators). In addition to the benefits obtained in terms of safety of the working environment, noise reduction, savings on energy, human resources, and execution time, there are also benefits in terms of durability. Namely, the influence of human error is eliminated from this phase of concrete works on site. The utilization of recycled concrete aggregate and fly ash in SCC also has the potential to reduce both the environmental impact and financial cost associated with the increasing demand for this construction material. The usage of SCC obtained by fly ash and recycled aggregate leads to a significant reduction in natural resources consumption and waste disposal, especially when the concrete compositions are optimized [4-5].

The aim of this study was to investigate the impact of used recycled aggregate and fly ash on the properties of SCC. The usage of the fourth fraction of aggregate (16 – 31.5mm, the grain size uncommon for SCC) was hereby promoted, in such cases whenever there are no restrictions for its application. Within this experimental work, four series of SCC were made. All series were prepared with the addition of fly ash. The first and the third series were made with natural aggregate. The second and the fourth series were made with recycled aggregate. The third and the fourth series were prepared with reduced cement content and increased content of fly ash in order to increase the energy efficiency of the produced SCC additionally.

2. EXPERIMENTAL

For the production of SCC samples, the natural aggregate was used in the common fractions: I (0/4), II (4/8), III (8/16), and IV (16/31.5) declared by origin as “Dunavac”, as well as the recycled aggregate, i.e. crashed control concrete cubes, sieved into the IV (16/31.5) fraction.

Densities of the natural river aggregate were 1.60 t/m^{3}for the fraction I (0/4), 1.49 t/m^3 for the fraction II (4/8), 1.45 t/m^{3}for the fraction III (8/16), and 1.47 t/m^{3}for the fraction IV (16/31.5) in loose state, and 1.74 t/m^3, 1.64 t/m^3, 1.63 t/m^3 and 1.56 t/m^3 in compacted state, respectively.For the only one used recycled aggregate fraction IV (16/31.5), the loose and compacted state densities amounted to 1.31 t/m^{3}and 1.46 t/m^3, respectively.

The pure cement without additions CEM I was used in all of the mixtures. The fly ash used in this study was generated and stored within the complex of the thermal power plant Nikola Tesla B, Obrenovac, Serbia. Its chemical composition was previously found to be in accordance with conditions prescribed by the standards and recommendations [3,6-7]. Fly ash was used without prior activation, as the only filler component.

The amount of the polycarboxylate based superplasticizer TKK CementolHiperplast 463 was the same 6 kg/ m^3 in all of the mixtures.

The defined compositions of the SCC series are listed in Table 1.

The samples were molded and cured for 1 day in the air, covered with a wet cloth. After demolding, the samples were cured in 20˚C water for 28 days and removed from water a little prior to testing.

Table 1 – Compositions of the series

	Quantities [kg/m^3]			
Component	I	II	III	IV
Cement	300.0	300.0	270.0	270.0
Water	155.8	155.8	155.8	155.8
Additional absorption water	11.5	49.2	11.5	49.2
Fly ash	150.0	150.0	180.0	180.0
Natural aggregate, I fraction (0<d<4mm)	657.0	657.0	657.0	657.0
Natural aggregate, II fraction (4<d<8mm)	274.0	274.0	274.0	274.0
Natural aggregate, III fraction (8<d<16mm)	402.0	402.0	402.0	402.0
Natural aggregate, IV fraction (16<d<31.5mm)	492.0	-	492.0	-
Recycled aggregate, IV fraction (16<d<31.5mm)	-	492.0	-	492.0

3. RESULTS AND DISCUSSION

All of the fresh concrete mixtures displayed proper behavior for this kind of concrete, with slump-flow diameters ranging between 650 and 800 mm; whereas recycled concrete aggregate induced several challenges. For instance, the amount of water had to be carefully waged, based on absorption values. Therefore, the consistency of the series with the recycled coarse aggregate was more fluid immediately after mixing. Due to the absorption process, the consistency of the series with recycled concrete was more rapidly changing in time, in comparison to the series without recycled concrete aggregate.

The compressive strength tests were performed according to the standard SRPS EN 12390-3:2010 on triplet 10 cm cubic samples [8]. The test was performed with a gradual load increase until the sample failure, Amsler, with a range of 2500 kN. The loading rate was 0.6 ± 0.4 MPa/s.The results are presented in Figure 1. The test was conducted at the age of concrete of 28 days.

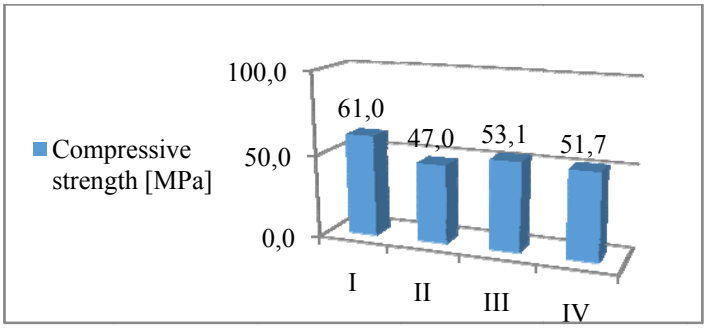

Figure 1. Compressive strength results at the age of 28 days

For similar values of the water to cement ratio, the studies showed that the compressive strength does not differ significantly in SCC and Normally Vibrated Concrete (NVC). However, the choice of aggregates (riverbed, crushed, recycled) has a much greater influence on compressive strengths in NVC than in SCC due to substantial homogeneous matrix in SCC and lower content of coarse aggregate, which reduces its impact [9]. Therefore, the results obtained on the tested series showed this trend, meaning that the differences in the results would be much higher if the NVC was made with the same aggregate composition and water to cement ratio.As far as the compressive strength of concrete is concerned, a noticeable decrease was recorded in the cases of samples with recycled aggregate and fly ash with regard to the first, referenced series, made with natural aggregate.The addition of fly ash mixed with recycled aggregate showed a positive effect by the increase in compressive strength.

4. CONCLUSION

The experimental results of the compressive strength test conducted on SCC with recycled coarse aggregate, and fly ash as filler component, were discussed. Although all of the mixtures were characterized as SCC with a slump-flow diameter of more than 650 mm, the introduction of recycled concrete aggregate induced challenges regarding the consistency as expected. The consistency of the series with the recycled coarse aggregate was both more fluid and more rapidly thickening, in comparison to the series without recycled concrete aggregate. Fly ash was used in the SCC mixtures as the solitary filler and without prior activation. The compressive tests were obtained at the age of 28 days, and a further increase of compressive strength was expected due to the presence of fly ash. Although the reference series showed the highest compressive strength, the coarse recycled aggregate had a moderate influence on a drop in strength. The series with a lower amount of cement and with fly ash had higher values of strength than the reference altered with recycled aggregate, most probably due to the positive influence of fly ash. Also, the differences of the SCC series made with and without the recycled coarse aggregate were almost neglectable (2.6%).

The aggregate fraction IV (16/31.5 mm) was used to highlight the possibility of SCC application in structure elements with sparse reinforcement bars, and where the large quantities of concrete have to be used without a need for vibration. The sustainability aspect of SCC was improved through the use of recycled concrete aggregate and fly ash, with respect to the reduction in cement and natural aggregate for concrete, which illustrates the potential of concrete to improve in light of its environmental and sustainability impacts.

ACKNOWLEDGEMENTS

The research presented in this paper was done with the financial support of the Ministry of Education, Science and Technological Development of the Republic of Serbia, within the funding of scientific research work at the University of Belgrade, Faculty of Civil Engineering (No. 200092) and the University of Belgrade, Vinca Institute of Nuclear Sciences (Contract No. 451-03-9/2021-14/200017).

REFERENCES

[1] C. Lian, Y. Zhuge, Constr. Build. Mater., 24 (12)(2002) 2664-2671.
[2] M. Muravljov, Construction materials,Construction book, Belgrade, 2011.
[3] A. Savic, D. Antonijevic, I. Jelic, D. Zakic, Energy Build., 229 (110511)(2020) 1-7.
[4] C.K. Sarath, P.S. Bendapudi, Int. J. Earth Sci. Eng., 4 (6)(2011) 1017-1023.
[5] M. Vasić, Physical and Mechanical Properties of Green Self-Compacting Concrete Designed by the Method of Maximum Density of Grain Packaging, Faculty of Civil Engineering, University of Belgrade, Belgrade, 2019.
[6] SRPS EN 450-1:201, Fly ash for Concrete – Part 1: Definition, specifications, and conformity criteria.
[7] ASTM C618-19: Standard Specification for Coal Fly Ash and Raw or Calcined Natural Pozzolan for Use in Concrete.
[8] SRPS EN 12390-3:2010, Testing hardened concrete – Part 3: Compressive strength of test specimen.
[9] R. Martínez-García, P. Jagadesh, G. Búrdalo-Salcedo, C. Palencia, M. Fernández-Raga, F.J. Fraile-Fernández, Materials, 14 (13)(2021) 3480-3492.

FORECAST RESOURCES OF ZEOLITHIC TUFFS OF SERBIA

Vladan Kašić[1], Dragana Životić[2], Vladimir Simić[2], Ana Radosavljević-Mihajlović[1], Jovica Stojanović[1], Slavica Mihajlović[1], Melina Vukadinović[1]

[1]Institute for Technology of Nuclear and Other Raw Mineral Materials, Applied Mineralogy Unit, P.O. Box 390, Franschet d'Esperey 86, 11000 Belgrade, Serbia

[2] Faculty of Mining and Geology, Djusina 7, University of Belgrade, 11000 Belgrade, Serbia

Abstract

*Our zeolite tuff deposits (Zlatokop, Igroš, Jablanica 1, Beočin, Toponica and Slanci), which were the subject of detailed research, spatially and genetically are connected to volcanic*volcaniclastic*rocks of marine environment of Senonian and Neogene age, as well as lake sediments of Neogene age. Zeolitic tuff deposits were formed as a product of devitrification of volcanic glass. More will be said here about the prognostic resources of our zeolite tuffs, both in relation to the registered phenomena so far, and to possible areas in terms of finding new quantities of this economically very interesting mineral raw material.*

***Keywords**: zeolitic tuff, clinoptilolite-heulandite group, Serbia deposit.*

1. INTRODUCTION

During the geological development of the earth's crust, favorable geological conditions for the creation of higher concentrations of zeolite minerals and the formation of zeolite mineral deposits have been renewed several times. In Serbia, this occurred during the Upper Cretaceous, Paleogene and Neogene, and are related to the effusive activities of Dacite, Dacito-andesitic and andesitic magmas. The most economically significant deposits of zeolite tuffs in our country were created during the Neogene by intensive Young Alpine tectonic-magmatic multiphase activity. Potentially the most promising are: the Vranje, Toplica, Kruševac, Krivorec, Sokobanj, Bogovina, West Moravian and Ibar basins, the eastern part of the Great Moravian trench as well as the Fruška Gora area.

2. MINERAGENETIC SKETCH OF SERBIA

The following regional geotectonic units face each other on the territory of today's Serbia: theDinarides, the Carpatho-Balkanids and the Serbian-Macedonian mass, and the Pannonian and Dacian basins are also present. In addition to the mentioned geotectonic units, geological processes that took place during the Cenozoic era - in the zone of neo-Alpine (Cenozoic) tectonic-magmatic activation (TMA) are of special importance in the formation and spatial distribution of many important non-metallic raw materials in Serbia.

The zone of the Cenozoic TMA extends in the middle of the Balkan Peninsula and diagonally intersects all its main geotectonic units. According to Grubić (1974) [2], it is characterized by Tertiary minerageny - intrusive and volcanic igneous activity, specific molasses Neogene lake basins and intense neotectonic movements, which caused significant ups and downs (up to 2 km) of large blocks limited by renewed old and new faults. Since this zone is young, formed in the final stages of the alpine geotectonic cycle, it cannot genetically be included in any of the older geotectonic units it intersects, but represents a separate mineragenetic unit of Serbia [1]. Numerous and economically very important deposits of non-metallic mineral raw materials are

located in the Cenozoic TMA zone. Their formation is conditioned by tectonic-magmatic activity, which began at the end of the Oligocene and was renewed with varying intensity throughout the Neogene. Simultaneously with this activity, many sedimentation basins were formed in which there are economically very interesting volcanogenic-sedimentary formations.

Volcanogenic-sedimentary (and hydrothermal-sedimentary) processes that were manifested in many Neogene basins have enabled the formation of numerous deposits of useful raw materials (bentonites, diatomites, magnesite, dolomites), among which vitroclastic tuffs (pozzolans) and zeolites (zeolites) occupy a significant place. In most cases, volcanic pyroclastic material is interstratified in the form of layers of different thickness among the sediments of Neogene lake basins. In addition, our Neogene tuffs have Dacite, Dacite-andesitic and andesitic composition of their equivalent magmas. They mainly belong to vitroclastic and vitrocrystalloclastic types with a volcanic glass content of 60-90% - all of which were very favorable preconditions for their later zeolitization [4].

The area of Fruška Gora belongs to the Pannonian Basin, the formation of which was conditioned by intense neo-alpine tectonic movements, and from the beginning of the Neogene it was covered by the Paratethys Sea, from which only the Horst Mountains protruded [6]. Along the southern rim of Paratethys, in connection with the same tectonic movements, smaller or larger intermountain depressions were created, which in the form of individual bays of the Pannonian Sea or separate lakes, stretched over the sunken parts of older geotectonic units. Within the Neogene (Miocene and Pliocene) sediments, which are spread on the surface around the Horst mountains, along the southern periphery of the basin and in the surrounding intermountain depressions, there are numerous economically very important deposits of non-metallic minerals: rock salt (Tuzla), cement marls, expanding, ceramic, refractory and brick clays, limestones, etc. On the northern slopes of Fruška Gora, zeolite tuffs (Općište-Beočin deposit) of Dacite composition are present, which appear as interstratified parties in the Middle Miocene series. Also, in the north of Vojvodina, in northern Bačka, deep drilling as part of the exploration of oil deposits, the presence of zeolite tuffs was ascertained. However, considering the great depth (950 to 980 m) at which the presence of zeolite minerals within the Neogene volcaniclastic deposits on the territory of Vojvodina was stated, it can be said that these phenomena of zeolitized pyroclastics cannot have any greater economic significance.

Lake Miocene formations are also located east of Belgrade in DunavskiKljuc, in the area of VelikoSelo and Slanci, where lake pelites represent typical lake formations consisting of well-layered marly clays and marls, laminated bituminous shales, with frequent occurrences of dacite tuffs and tuff. According to the manner of occurrence (exclusively interlayers) and chemical composition, tuffs from Slanci coincide with synchronous Dacite tuffs on Fruškagora and Posavo-Tamnava, central Šumadija and Pomoravlje.

In addition to the Neogene basins (valleys) that territorially belong to the southern edges of the Pannonian Basin, potentially promising areas in terms of the existence and finding of deposits and occurrences of zeolite tuffs are ore-bearing formations of our Neogene volcanic-sedimentary lake basins within the Serbian-Macedonian province. In the first place, it is the area of the Vranje valley with already known deposits and phenomena (Zlatokop, Katalenac, Mečkovac, etc.).In addition to the Vranje basin, the Toplica, Kruševac (Igroš, Jablanica I), Krivareka(Toponica), Sokobanja, Bogovina, West Moravian and Jarandol basins, as well as the eastern part of the Great Moravian trench (Sokobanja and Bogovina basin) are potentially the most interesting and significant.

3. FORECAST RESOURCES OF ZEOLITE TUFFS IN SERBIA

The most important parameters of the zeolite tuff deposits of Serbia explored so far (Table 1) [5] show us that, in terms of proven reserves, they are relatively small deposits on a global scale. The predominant zeolite mineral in our zeolite tuff deposits is clinoptilolite, while only in some cases it is mordenite. Geological and technological knowledge about some phenomena of zeolite tuffs (Katalenac, DugeNjive and Mečkovac-Vranjskakotlina) are insufficiently known, primarily because they have been considered as tuffs (raw materials for the cement industry), while their zeolite characteristics have remained only indicative. and insufficiently examined. Figure 1 [3]shows a prognostic mineragenetic map of Serbia with potentially the most important Neogene basins for finding deposits and occurrences of zeolite tuffs.

Table 1. Basic parameters of zeolite deposits in Serbia (according to Simić et al., 2014)

Tray	Depth zeolite (m)	Zeolite layer thickness (m)	Potential reserve (mil t)	Reserves (mil t)	CEC (meq / 100g)	Method of exploitation
Općište-Beočin	2-28	14.2	2	0.26 0.15	157 108	Surface mine
Igroš	5-20	1.5	0.1	0.05	145	Surface mine
Jablanica 1	0-15	18.5	2.2	0.20	168	Surface mine
Toponica	2-25	2.4	0.5	0.50	140	Pit exploitation
Zlatokop	20-30	2	1.3	0.67	164	Pit exploitation
Katalenac	On the surface	110	3.4		70	Surface mine
Duge njive	On the surface	> 50	1.1			Surface mine
Mečkovac	On the surface	38	1.0			Surface mine

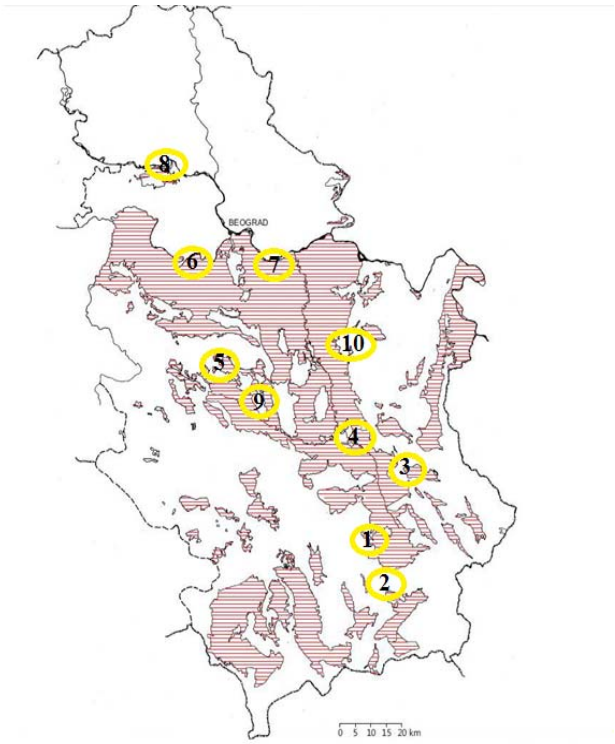

Figure 1. Forecast mineragenetic map of Serbia with potentially the most important Neogene basins for finding deposits and occurrences of zeolite tuffs (1. Vranje basin; 2. Krivorec basin; 3. Toplica basin; 4. Krusevac basin; 5. Valjevo-Mionica basin; 6. Posavina region -Tamnava basin, 7. Slanci basin, 8. Fruška Gora area, 9. West Moravian basin, 10. Eastern part of the Great Moravian trench (Sokobanja and Bogovina basin))

4. CONCLUSION

Based on all the above, it can be said that Serbia is a potential country in terms of the existence and discovery of zeolite tuffs, and thus the further development of the zeolite industry, ie their application in various fields. For that, it is necessary to continue detailed monitoring and study of geological and technological properties of our zeolite tuffs and their more complete characterization. Future research in the coming period in the aforementioned areas will almost certainly reveal some new sites with zeolite tuffs as the predominant and economically very interesting mineral raw material.

ACKNOWLEDGEMENTS (optional)

The authors wish to acknowledge the Ministry of Education, Science and Technological Development of the Republic of Serbia for financial support of the research which results are presented in the paper (contract 451-03-9/2021-14/200023).

REFERENCES

[1] Vakanjac B., Geology of non-metallic mineral raw materials, Faculty of Mining and Geology, Belgrade, (1992), 323 p.

[2] Grubić A., Serbian-Macedonian Mineragenetic Province in the Light of Neo-Alpine Activation, in Vol. Metalogenie i and concept of geotectonic development of Yugoslavia R. Geology Faculty, Belgrade, (1974), s. 261-263.

[3] Kašić, V., Mineragenic of zeolite tuffs of Srbia, Doctors disertation, RGF, Belgrade, (2017), 168 p.

[4] Kašić V., Simić V., Životić D., Radosavljević-Mihajlović A., Stojanović J., Mineralogical and crystallochemical properties of HEU-type minerals and deposits of zeolite tuffs in Serbia, Hemijska Industrija 71 (1), Belgrade, (2017)), p. 49-60.

[5] Simić V., Životić D., Andrić N., Radosavljević-Mihajlović A., Kašić V., Zeolite deposits and occurrences in Serbia - an overview, 9 International Conference on Occurrence, Properties and Utilization of Natural Zeolites, Belgrade , (2014), p. 217-219.

[6] Toljić M., Matenco L., Ducea MN, Stojadinović U., Milivojević J., Đerić N., The evolution of a key segment in the Europe-Adria collision: The Fruška Gora of northern Serbia. Global Planetary Change, 103, (2013), p. 39–62.

GEOLOGICAL AND MINERAL CHARACTERISTICS OF ZEOLITHIC TUFF TOPONICA DEPOSITS NEAR KOSOVSKA KAMENICA

Vladan Kašić[1], Ana Radosavljević-Mihajlović[1], Slobodan Radosavljević[1], Jovica Stojanović[1], Slavica Mihajlović[1], Melina Vukadinović[1]

[1]Institute for Technology of Nuclear and Other Raw Mineral Materials, Applied Mineralogy Unit, P.O. Box 390, Franschet d'Esperey 86, 11000 Belgrade, Serbia

Abstract

Zeolites are a group of natural and artificial inorganic compounds, which have specific physicochemical properties appropriate for industrial application. These minerals make a specific group of alumosilicates within tectosilicates because of their origin, chemical compositions, structural characteristics and application. This paper presents the results of mineralogical and crystallographic examination of zeolite tuff samples from the Toponica deposit. The deposit of zeolite tuff "Toponica" is located in the extreme eastern part of Kosmet near Kosovska Kamenica. The immediate geological structure of the zeolite tuff deposit consists of the Lower Miocene (M) clayey sandstone, the horizon of the white zeolite tuff and the reclassified Miocene clays, clays and gravel. The basic mineral composition is the mineral clinoptilolite-Ca from the heylandite series.

***Keywords**: Toponica, zeolitic tuff, clinoptilolite-heulandite group.*

1. INTRODUCTION

Studies have shown that zeolite deposits according to genetic characteristics belong to diagenetic deposits (volcanic-sedimentary) and hydrothermal-metasomatic deposits (with volcanic formations) [1-3]. In the deposits of marine and lake sediments, zeolites are mainly formed in the reaction of water with solid materials. The most present solid material (reactant) is volcanic glass, and the second reactant can be amorphous phase, poorly crystallized clays, montmorillonite, minerals of the plagioclase group, nepheline, quartz or silicon of biogenic origin. Clay minerals and zeolite minerals can be formed from the same material, and whether one or another mineral will crystallize will depend on the physico-chemical conditions of the given environment.

Thanks to the dimensions of their channels, zeolites absorb only those molecules whose sizes correspond to the dimensions of cavities, which is why they are called molecular sieves. Adsorption and molecular sieves are used in numerous processes of extracting harmful or useful components from gaseous phases, for the purpose of separation, purification and drying of gases.

Numerous technological processes are based on the properties of ion exchange, and have found application in the extraction of harmful components from wastewater or natural waters, in the processes of drinking water purification. The reactivity of the molecules increases, as a result of which zeolites exhibit intense catalytic activity. Based on that, they have found application in reactions in the processing of natural gas, petroleum raw materials, obtaining various products in the processes of organic synthesis [5].

2. METHODS

For mineralogical and crystallographic analyzes, flat samples were used and prepared under the same conditions up to grain size + 100% -63μm. A polarizing microscope ("JENAPOL-U" Zeiss-Jena), in transmitted light, by the immersion method, was used for mineralogical analysis.

A scanning electron microscope (SEM-PHILIPS ™ XL20) with an EDS component (Energy Dispersion X-ray, EDX) was used to observe the morphological properties and determine the chemical composition of the zeolite tuff. X-ray analysis was performed on an automatic diffractometer "PW-1710", using Cu tubes at a voltage of 40 kV and a current of 30 mA for powder.

3. RESULTS AND DISCUSSION

3.1 Geology of the Toponica deposit

The deposit of zeolite tuff "Toponica" is located in the extreme eastern part of Kosovo, near Kosovska Kamenica. Regionally, the examined area belongs to the tectonic unit of the Serbian-Macedonian metallogenetic province. This area is characterized by intense magmatic activity from the Paleozoic to the Tertiary, when the largest complexes of dacito-andesitic rocks of Novo Brdo and the surrounding area were cast.

The geological structure of the wider area of zeolite tuff deposits consists of: crystalline shales and migmatites, garnets, pegamites and aplites, Tertiary sediments of the Miocene, andesites, dacites and their tuffs, Pliocene deposits and Quaternary formations. Granites, pegmatites and aplites are imprinted in a series of crystalline shales, pegmatites appear in the form of hemispherical bodies, elongated lenses and stripes [4]. Andesite-Dacite tuffs formed in closed basins, they are related to the last phase of Dacite-Andesite magmatism in the torton: ash, lapil and other volcanic material was deposited over the sandstone.

The geological structure of the Zeolite tuff deposit "Toponica" consists of: lowland Miocene gray-blue clay sandstones, partly gray-green, then the horizon of white zeolite tuffs and upland Miocene sediments - clays, gravel, clay sand and gray-green sandy clay. The bottom sediments are built from gray-blue to gray-green sandstones. Zeolite tuff occurs in the form of a lens, which is interrupted in several places and intersected by cracks, where the thickness of the zeolite tuff is from 0.2 to 4.9 m.

3.2 Mineralogical and chemical analyzes of zeolite tuff

The tuff is white with yellow limonite scars on the surfaces of the cracks. It is crystalline in structure [6]. The examined tuffs show a pronounced zeolitization process and basically have a holocrystalline crystalline porphyry to vitrophyre texture, Figure 1.

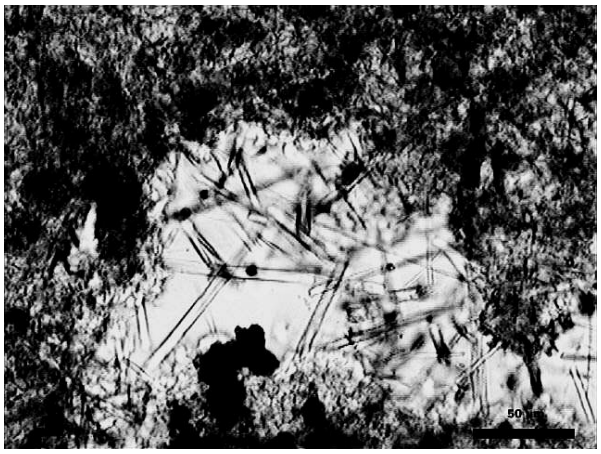

Figure 1. Elongated crystals of zeolite minerals in a zeolite tuff sample.

Clinoptilolite in sedimentary rocks mainly occurs in the form of euhedral plates, of several microns in length and thickness of 1-2μ [4]. The morphological forms of clinoptilolite presented in Figure 2 (ad) have characteristic monoclinic forms, with pronounced anhedral forms.

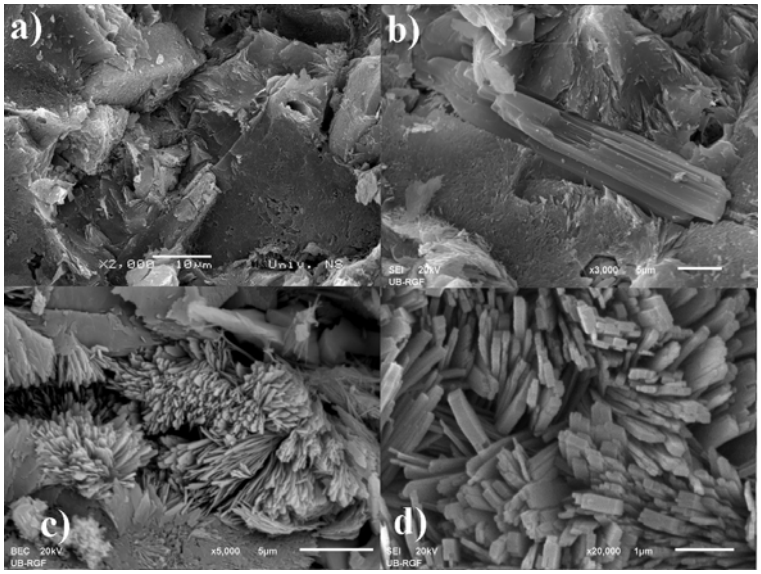

Figure 2. SEM micrographs of zeolite tuff.

Quantitative chemical analysis determined the chemical composition of the starting zeolite tuff, and is presented in Table 1. Atomic ratios (Si/Al), as well as the ratio of divalent and monovalent cations, were obtained based on quantitative chemical analysis. The cation exchange capacity of Zeolite tuff samples of Toponica (MmolM/ 100g) is 140 meq / 100g.

Table 1. Chemical composition of zeolite tuff of the Toponica deposit and ratio of present inorganic cations in hoylandites (two medium samples)

Oxide (%)	Trial 1	Trial 2	Sad.element (%)	Trial 1	Trial 2
SiO_2	67.5	60	Si	31.5	28.04
Al_2O_3	12	13.46	Al	6.3	7.1
Fe_2O_3	1	1	Fe	0.35	0.35
CaO	4.9	5.74	Ca	3.5	4.1
MgO	0.34	2.41	Mg	0.2	1.45
Na_2O	1.13	0.25	Na	0.83	0.18
K_2O	1.01	0.44	K	0.83	0.36
G. annealing	12.65	17	-	-	-
SiO_2/ Al_2O_3	5.62	4.46	Si / Al	5.00	3.95
$Na_2O/Na_2O + K_2O$	0.53	0.36	$Na^+/ Na^+ + K^+$	0.50	0.33
$CaO/CaO + MgO$	0.93	0.70	$Ca^{2+}/ Ca^{2+} + Mg^{2+}$	0.94	0.74

3.3 Structural analysis of Ca-clinoptilolite in zeolite tuff

The mineral composition of the tested sample of zeolite tuff from the Toponica deposit corresponds to microscopic examinations. The following are present in the sample: the mineral clinoptilolite, quartz, minerals of the mica group, minerals of feldspar (mainly plagioclase), Figure 3. Other minerals determined by the microscopic method were not detected because they are below the detection threshold.

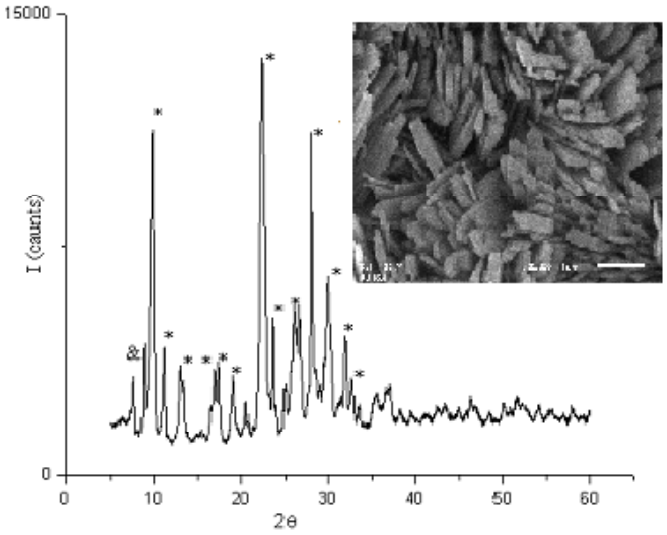

Figure 3 - X-ray diagram of clinoptilolite-Ca powder of zeolite tuff Toponica (symbol * represents the mineral clinoptilolite; symbol & represents a mineral from the mica group).

4. CONCLUSION

Based on the presented results, the zeolite tuff of the Toponica deposit contains a mineral from the heilanidite series, clinoptilolite, as the basic mineral component. The basic offline cation is calcium. The cation exchange capacity is 140 meq / 100g, which makes this mineral raw material extremely high quality and suitable for use in various industries.

ACKNOWLEDGEMENTS

The authors wish to acknowledge the Ministry of Education, Science and Technological Development of the Republic of Serbia for financial support of the research which results are presented in the paper (contract 451-03-9/2021-14/200023).

REFERENCES

[1] Armbruster, T., Clinoptilolite-heulandite: applications and basic research. Studies in Surface Science and Catalysis 135, Zeolites and Mesoporous Materials at the Dawn of the 21st Century A. Galarnau, F. Di Renzo, F. Faujula and J. Vedrine (Editors), (2001).

[2] Barrer, RM Zeolites and Clay Minerals as Sorbent and Molecular Sieves, Academi Press, New York, (1978).

[3] Hay RL, Geologic Occurrence of Zeolites, Natural Zeolites, Occurence, Properties, Use LB Sand and FA Mumpton, (Jun 1976), Pergamon Press.

[4] Kašić, V., Minerageny of zeolite tuffs of Serbia, Doctoral dissertation, RGF, Beograd, (2017), 168.

[5] McBride, MB, Surface Chemistry of Soil Minerals, Minerals in Soil Environments, Dixon JB, Weeds SB, Ed., SSSA, Madison, (1989).

[6] Radosavljević-Mihajlović, A., Stojanović, J., Kašić, V.,Comparative mineralogical, crystallochemical and thermal properties of deposits of zeolite tuffs of Serbia rich in HEU-type minerals, Geoinstitut papers, Vol.40., (2005), 191 -200.

The 52nd International October Conference on Mining and Metallurgy
November 29th – 30th , 2021
www.ioc.tfbor.bg.ac.rs

METHOD FOR UTILIZATION OF THE SULFURIC ACID OBTAINED DURING AUTOCLAVE DISSOLUTION OF PYRITE CONCENTRATE

Konstantin Petkov[1], Vladislava Stefanova[1], Peter Iliev[1]

[1]University of Chemical Technology and Metallurgy – Sofia, Sveti Kliment Ohridski 8,1756 Sofia, Bulgaria

Abstract

At high-temperature pressure oxidation of pyrite concentrate in an autoclave, solutions with a high concentration of ferric ions and a free sulfuric acid(>60 gL^{-1})were produced.After a partial neutralization of these solutions with a waste from cutting of marble plates containing ~95 % $CaCO_3$, a gypsum waste with 0.05% Fe has been obtained.

The objective of this study isto determine the optimal technological parameters of the conversion process of the gypsum waste to ammonium sulfate, a commercial product that can be used in agriculture as artificial fertilizer. Based on the experimental results a counter-current scheme of the conversion process is proposed.

Keywords: *acidic ferric-sulfate solutions, neutralization, gypsum waste, conversionprocess.*

1. INTRODUCTION

In recent years, due to the depletion and sharp deterioration of the quality of gold-bearing raw materials, a new strategy for expanding the raw material base has been observed in the gold industry [1]. In practice, this imposes the processing of gold-bearing ores and concentrates with lower quality [2].

During the dissolution of pyrite, gold-containing concentrate in a TL20 laboratory autoclave, the possibility of complete gold recovery has been established. A disadvantage of the developed method was the productionof solutions with high concentration of iron (60.2 $g.L^{-1}$) and sulfuric acid (61.5 $g.L^{-1}$).In our previous studies, the possibility of crystallization of Ammonium Ferric Dodecahydrate and Ferric Sulfate Hydrate from these solutions was proved [3, 4].

The problem of sulfuric acid recovery still remains unresolved. Complete neutralization of H_2SO_4 results in obtaining of gypsum heavily contaminated with iron and other non-ferrous metals. It is a waste product and is deposited in tailings ponds or mountainous terrain, which leads to environmental pollution. In [5], a partial neutralization of sulfuric acids with a high concentration of Fe^{3+} ion solutions has been proposed. The resulting gypsum was with high purity.

The objective of this study is to develop atechnologicalscheme of the conversion process of gypsum, obtained during a partial neutralization with marble waste, to ammonium sulfate - a commercial product than can be used as artificial fertilizer.

2. EXPERIMENTAL

2.1 Materials and research methodology

Chemical analysis of the solution obtained after autoclave dissolution of pyrite concentrate is given in Table 1. Waste from cutting marble plates was used for partial neutralization of the sulfuric acid.The chemical silicate analysis of the neutralization reagent is presented in Table 2.

The mineralogical assays of representative sample have been analyzed in the Central Scientific Laboratory in the UCTM. It is evident that marble waste is characterized with high $CaCO_3$ content (above 94 %).

Table 1 - Chemical composition of thesolution, g/L

Fe^{3+}	Fe^{2+}	Na	K	Mg	Mn	Mo	Ni	Pb
58,54	1,40	0,1	0,1	<0,01	0,016	0,025	0,076	0,040
Co	**Sb**	**Sn**	**P**	**Al**	**Bi**	**Ca**	**As**	**H_2SO_4**
0,008	<0,01	0,064	<0,01	0,9	0,018	0,20	0,11	61,5

Table 2 - Chemical silicate analysis of marble-cutting waste, fine fraction (MFF), % w/w

CaO ($CaCO_3$)	MgO ($MgCO_3$)	SiO_2	TiO_2	Al_2O_3	Fe_2O_3	Others
52,75 (94,15)	1,70 (3,55)	0,81	1,08	0,06	0,01	0,34

Mastersizer 2000, Malvern Instruments has been used for determination of particle size analysis of marble waste. The particle size distribution of MFF calculated on the basis of the performed analysis is presented in Table 3.

Table 3 - Size distribution in marble-cutting waste, fine fraction (MFF)

Size of fraction	<10 µm	-20+10 µm	-30+20 µm	-40+30 µm	-50+40 µm	-70+50 µm	-100+70 µm
Share in %	49,6	37,6	11,0	1,6	0,2	0,0	0,0

It can be seen from the table that marble waste is characterized by with a substantial share (87.2%) of fine particles with a size of <20µm. Taking into account the high content of $CaCO_3$ in this waste (>94%), it can be expected that it will be very suitable as a reagent for the process of neutralization of the free sulfuric acid.

To obtain of larger quantities of gypsum neededfor the conversion process, three parallel experiments were performed with 500 ml of solution each. The neutralization conditions were as follows: MFF suspension (20%), T = 50°C and time - 60 min. The resulting precipitates were washed with 7% H_2SO_4 solution and dried at temperature 65 °C. The final iron content in the resulting gypsum is 0.05%.Othersmaterials needed for the conversion process were: 33% saturated solution of ammonium carbonate (AC) and ammonium sulfate (AS).

The methodology of the conducted experiments is shown schematically in Figure 1. It involves two main processes: a partial neutralization of the free sulfuric acid with MFF (reaction 1) and conversion of the resulting gypsum to ammonium sulfate by the Merseberg reaction (2):

$$H_2SO_4 + CaCO_3 + H_2O = CaSO_4.2H_2O \quad (1)$$

$$CaSO_4.2H_2O + (NH_4)_2CO_3 = CaCO_3 + (NH_4)_2SO_4 + 2H_2O \quad (2)$$

The degree of conversion (α) was calculated by the following formula:

$$\alpha = \left\{ \frac{[(M_{gypsum}.\%S_{SO4,gypsum}) - (M_{sludge}.\%S_{SO4,sludge}}{M_{gypsum}.\%S_{SO4,gypsum}} \right\}.100, \%$$

where: M_{gypsum}; M_{sludge}– the mass of gypsum and the sludge, respectively, g;
$\%S_{SO4,gypsum}$; $\%S_{SO4,sludge}$ – percentage of sulfur (as SO_4) in gypsum and the resulting sludge.

The conversion process was studied with gypsum sample (10 g) obtained after neutralization with MFF and with chemical reagent $CaSO_4.2H_2O$. The experiments were conducted with 50% excess of $(NH_4)_2CO_3$, temperature ~35 °C and conversion time 30 minutes.The effect of the concentration of $(NH_4)_2SO_4$on the degree of conversion is shown on Figure 2.

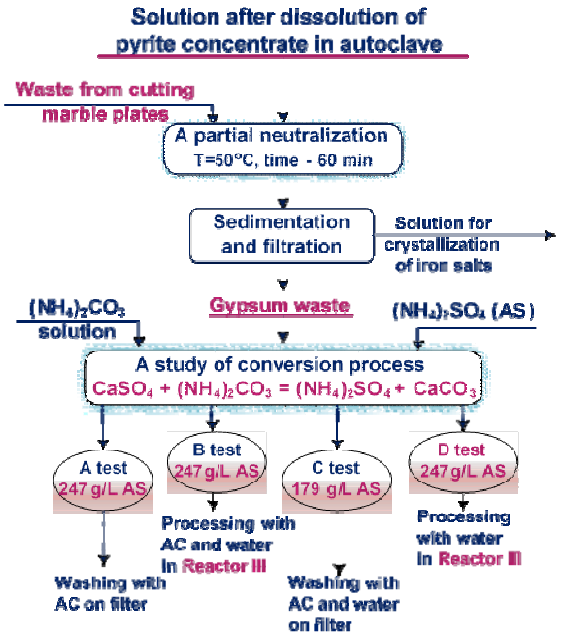

Figure 1 - Schematic diagram for conducting of the experiments

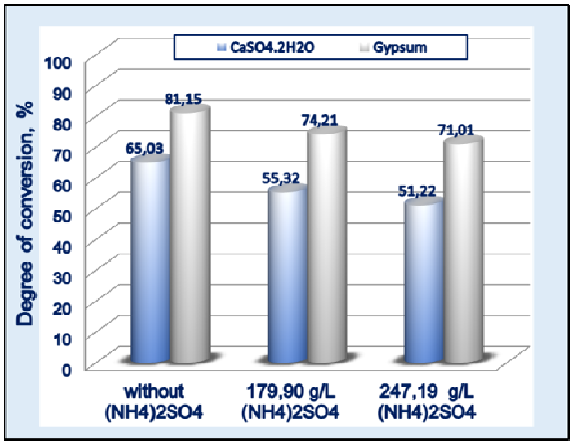

Figure 2 – Effect of$(NH_4)_2SO_4$ concentration in the solution on the degree of conversion ofgypsum waste and chemical reagent. (Reactor I)

3. RESULTS AND DISCUSSION

The results of the conducted experimental tests are summarized in Table 4.

Table2 - Chemical composition of the obtained filtrate and sludge

	Parameter	Test A	Test B	Test C	Test D
RI	$(NH_4)_2SO_4$, $g.L^{-1}$	247* **341,56**	247* **314,43**	179* **271,13**	247* **367,85**
	$(NH_4)_2CO_3$, $g.L^{-1}$	6,72	6,72	4,80	6,72
RII	$(NH_4)_2SO_4$, $g.L^{-1}$	148,94	157,77	76,65	78,99
	$(NH_4)_2CO_3$, $g.L^{-1}$	72,0	172,0	249,76	239,12
	Washingof the sludge with 33% $(NH_4)_2CO_3$solution on the filter	yes	-	-	-
RIII	Processing of the sludge with 33% solution of AC and water in Reactor III	-	yes	-	-
	Washing of the sludge with 33% solution of ACand water on filter	-	-	yes	-
RIII	Processing of the sludge with water in Reactor III	-	-	-	yes
Content of S_{SO4}, in carbonate sludge, %		**6,16**	**0,55**	**2,58**	**1,24**
Degree of conversion, %		**93,91**	**99,0**	**97,24**	**97,78**

*) initial concentration of $(NH_4)_2SO_4$

Obviously, the best results were obtained in test No.4.The solution has the highest concentration of $(NH_4)_2SO_4$ (367.85 $g.L^{-1}$). The content of S_{SO4} in the resulting precipitate is relatively low (1.24%) and it can be used directly for the neutralization process of the sulfuric acid solutions, obtained during autoclave dissolution of pyrite concentrate.

Based on the conducted research, a counter-current scheme for conversion of the gypsum to ammonium sulfate has been proposed. It is schematically shown in Figure 3.

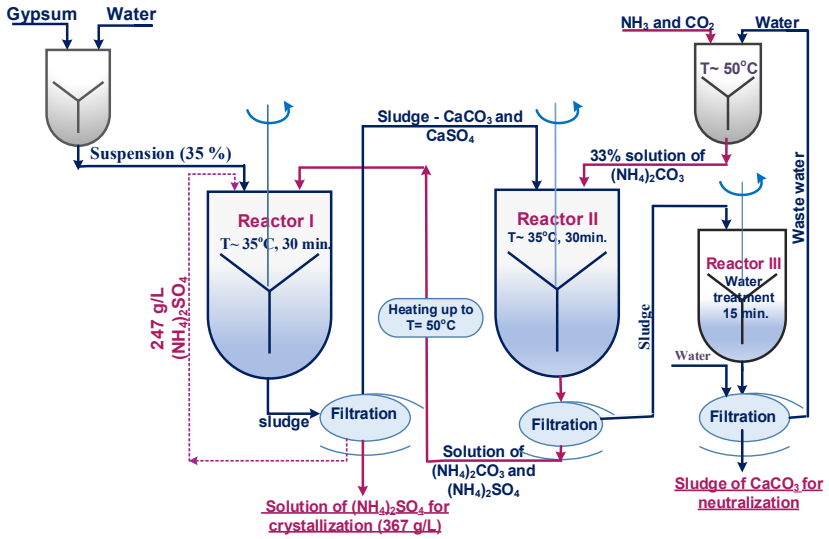

Figure 3. Principal counter-current scheme of the conversion process of gypsum waste to concentrated ammonium sulfate solution

4. CONCLUSION

Optimal parameters for the conversion process have been determined: 50% excess of $(NH_4)_2CO_3$, T=35 ^oC; reaction time = 30 min. The conversion in I reactor was conducted in the present of $(NH_4)_2SO_4$ (247 g/l). The obtained precipitate was treated with water in reactor III.

The products of the conversion process were: concentrated ammonium sulfate solution (367 g/L) and $CaCO_3$ precipitate. The solution is being sent for a crystallization of $(NH_4)_2SO_4$ – an artificial fertilizer, which can be used in agriculture. The obtained precipitate of $CaCO_3$contains 1,24% sulfate sulfur (S_{SO4}) and it is returned for the neutralization of the initial ferric sulfate solutions. The achieved maximum degree of conversion of the gypsum to ammonium sulfate is 97,78%. Based on the experimental results, the counter-current scheme of the conversion process is proposed.

REFERENCES

[1] World Economic Outlook. Global Manufacturing Downturn, Rising Trade Barriers, International Monetary Fund, Oct. 2019, http://books.google.bg/books
[2] A. Ivanik,D.Yukhin., J.Indust. Pollution Control 33(1), 2017, p.891-897
[3] L. Stamenov, V. Stefanova, K. Petkov, P. Iliev, Russ. J. of App. Chem., 89, 8, 2016, p 1341-1346
[4] L. Stamenov, V. Stefanova, B. Lucheva, S. Atanasova-Vladimirova, J. Chem. Tech. and Met., 54, 2, 2019, p.379-386.
[5] M.Danovska, M.Golomeova, D.Karanfilov, A.Zendelska, V. Balkan Mine W. Symposium, Ohrid, 2013

The 52nd International October Conference on Mining and Metallurgy
November 29th – 30th , 2021
www.ioc.tfbor.bg.ac.rs

MONITORING OF pH VALUE AND CONCENTRATION OF COPPERIN RIVERSDOWNSTREAM FROM BOR MINE IN PERIOD 2015-2021

Stefan Đorđievski[1], Daizo Ishiyama[2], Yasumasa Ogawa[2], Zoran Stevanović[1], Olaotse Osenyeng[2], Dragana Adamović[1], Vanja Trifunović[1]

[1]Mining and Metallurgy Institute Bor, ZeleniBulevar 35, 19210Bor, Serbia

[2]Akita University, Tegatagakuen-Machi 1-1, 010-8502 Akita, Japan

Abstract

This paper presents the results of the monitoring of pH value and concentrations of the dissolved and particulate forms of copper in the period from 2015 to 2021 in wastewaters that form Bor River, and in the water ofBor River, Krivelj River, Bela River, and Timok River which are under the influence of mining and metallurgical activities in Bor. Copper was mainly present in dissolved form in acidic river water, whereas in neutral and alkaline river water, copper was present relatively equally in both dissolved and particulate form. According to the pH values and copper concentrations, the water quality of Bor River and Bela River did not improve during the studied period. On the other hand, the water quality of Krivelj River significantly improved, possibly due to the changes caused by the construction of the new flotation tailing pond "VelikiKrivelj Zero Field". The quality of Bor River, Bela River, and TimokRiver was largely controlled by the temporal influxes of highly acidic and copper-rich wastewater from metallurgical facilities in Bor.

***Keywords**: Bor mine, copper, acid mine drainage, river water.*

1. INTRODUCTION

Copper mining and metallurgical activities in Bor, Serbia, have caused significant environmental pollution of river water.Several projects were conducted to evaluate the quality of river water downstream from Bor mining and metallurgical facilities, and the results are published in scientific journals or as technical reports as separate studies [1-8].Although the water quality wasmonitored by the Serbian Government at one point at Bela River and one point at Timok River from 1990 to 2014 [3,7], systematic monitoring of river water quality downstream from Bor mining and metallurgical facilities have not been conducted recently.

Processing of copper sulfide ores in Bor generates acidic copper-rich wastewaters.Therefore, the pH values and copper concentrations are the two most important parametersfor the quality assessment of the river waters. This paper presents the results of the monitoring of the pH values and concentrations of the dissolved and particulate forms of copper in the period from 2015 to 2021 in wastewaters that affectBor River and in the water ofBor River, Krivelj River, Bela River, and Timok River.

2. EXPERIMENTAL

Rivers that are the focus of this study are located in eastern Serbia (Figure 1). Bor River is formed by mixing of overburden drainage waters, municipal wastewater from Bor City, and metallurgical wastewater. Bela River is formed by the merging of Bor River and Krivelj River.Bela River flows into the Timok River, and Timok River flows into the Danube River.

Unfiltered and filtered water samples were collected in 50 mL polypropylene bottles. Filtration was carried out using cellulose acetate filters with pore size 0.2μmor 0.45μm to investigate the

distribution of dissolved and particulate forms of copper. Samples were acidified with nitric acid after the sampling so that the final concentration of nitric acid in samples was 5 %. The pH valueswere measured in the field using IM-23P pH meter, and copper concentrationswere measured using ICP-MS in several laboratories depending on the sampling season: Actlabs in Canada (for samples collected in August 2015), Akita University in Japan (September2016, February 2017, August 2017, and September 2019), and Mining and Metallurgy Institute Bor in Serbia (February 2020, August 2020, and September 2021).

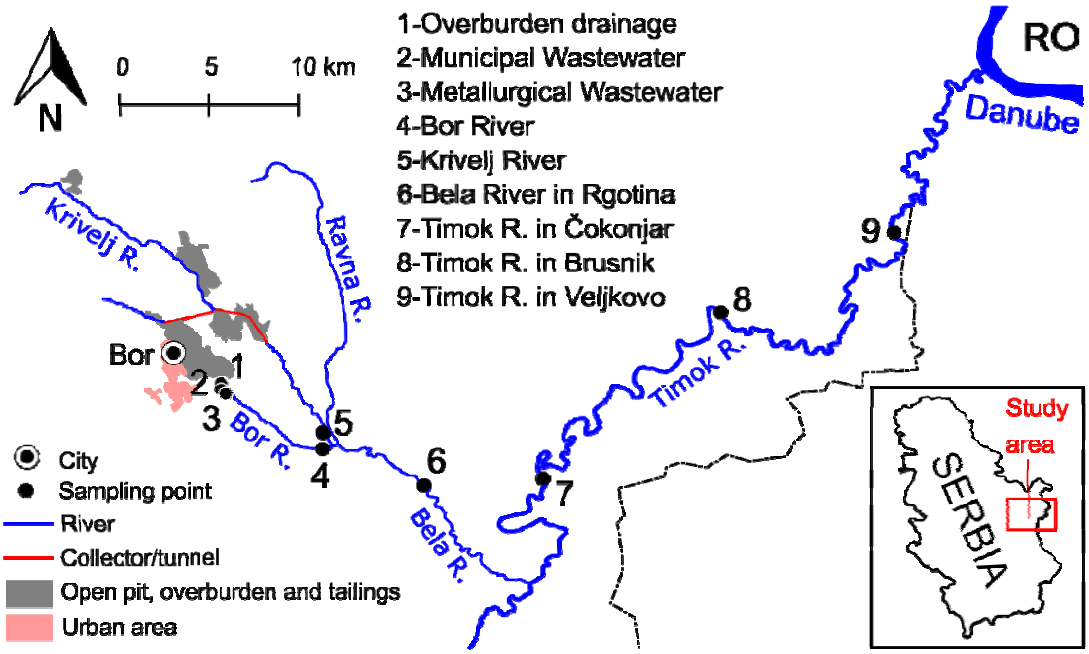

Figure 1Map of the study area with locations of the sampling points

3. RESULTS AND DISCUSSION

Metallurgical wastewater was the most acidic, with pH values ranging from 1.2 in August 2017 to 2.6in August 2015 (Figure 2). Overburden drainage had a moderately acidic signature, with pH values ranging from 4.4 in September 2021 to 6.0 in February 2020. Municipal wastewater was neutral to moderately alkaline during the studied period, with pH ranging from 6.8 in September 2021 to 8.6 in August 2015. The highest concentrationof copper was observed in metallurgical wastewater, reaching 275 mg/L in September 2020. Copper was always present in dissolved form in metallurgical wastewater during the studied period due to the very acidic pH value. In overburden drainage, copper was equally present, however relatively, in dissolved and particulate forms, while in municipal wastewater copper was dominantly present in particulate form, possibly due to the sorption of copper onto the suspended fecal material.

In Bor River, pH value was mostly acidic, and copper was present dominantly in dissolved form with relatively high concentration, except in August 2017 when the pH value was near-neutral, and copper was present in particulate form with 10 to 30 times lower concentration than usual. On the same sampling day in August 2017, the pH value of Bela River was acidic, and copper concentration reached 131 mg/L. The possible cause of these fluctuations is the temporal influx of a large quantity of highly acidic and copper-rich metallurgical wastewater.

The concentration of copper in the water of Krivelj River decreased gradually during the studied period from 31.5 mg/L in August 2015 to below 0.2 mg/L in February 2020 and onwards. The increase in pH value followed the decrease of copper concentration in Krivelj River.As the pH value increased, the form of copper in river water changed from dissolved to particulate. These results have shown that the water quality of Krivelj River improved over time.

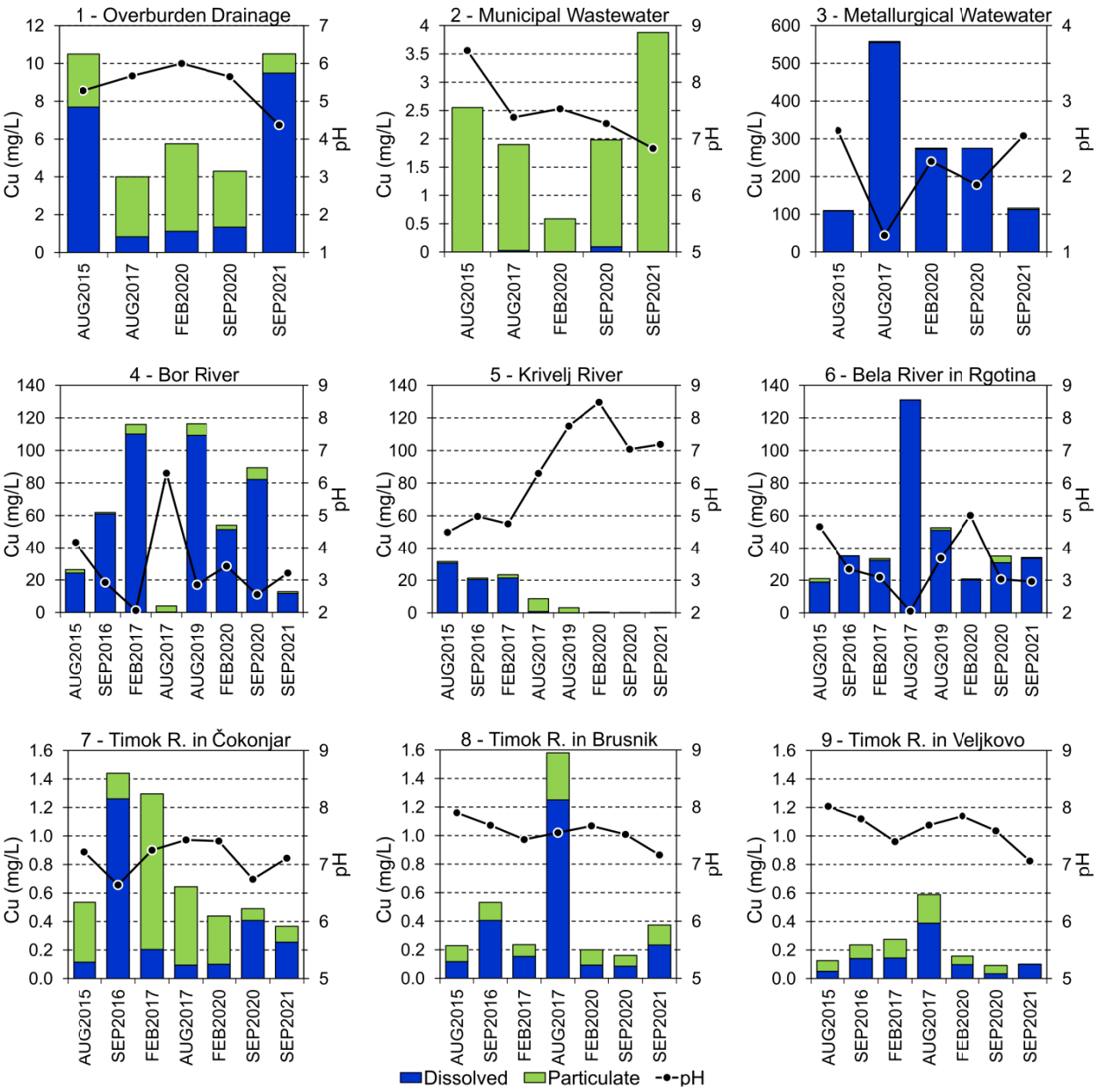

Figure 2Variations of pH and concentrations of dissolved and particulate forms of copper in wastewater and river water downstream from mining and metallurgical facilities in Bor in the period 2015-2021

Timok River, with its larger discharge, diluted the copper-rich and acidic water of Bela River.Therefore, after the confluence with Bela River, the copper concentration in Timok River was lower, and the pH value wasmore alkaline than those in the water of Bela River. As a result of near-neutral pH value, copper in Timok River was relatively equally present in dissolved and particulate forms. However, a higher percentage of the particulate form of copper was present in Timok River near Čokonjar Village because this point is close to the confluence with Bela River. Theprecipitation of particulate forms of copper on the river bed contributed to the decrease of total copper concentrations in the water of Timok River toward the Danube River.

The variations of pH values and copper concentrations during the summer and winterperiods did not show any significant trend, although it could be expected that the copper concentration inTimok River inthe winter season should be lower due to the dilution by a significantly higher

discharge of the unpolluted river water. A large fraction ofthe particulate form of copper was recorded in February2017 and February 2020, in the water of Timok River near Čokonjar, which could be caused by the resuspension of the particulate forms of copper that was precipitated in summer on the river bed.

4. CONCLUSION

In acidic river water, copper was present in dissolved form, whilein near-neutral and alkaline river water copper was relatively evenly present in dissolved and particulate form. Although the pH value of municipal wastewater was similar to the pH value of Timok River, copper was dominantly present in particulate form in thiswastewater, possibly due to the sorption of copper onto the suspended fecal material.Inthe water of Krivelj River,the concentration of copper decreased, and pH value became near-neutral, which is a significant improvement caused by the construction of the new flotation tailing pond "VelikiKrivelj Zero Field" in the watershed of Krivelj River. On the other hand, the concertation of copper and the pH value in the water of Bor River and Bela River did not improve during the studied period. The quality of BorRiver, and consequently the quality of Bela River and Timok River,was largely controlled by the temporal influxes of wastewater from metallurgical facilities in Bor.

ACKNOWLEDGEMENTS

This work was financially supported by the Ministry of Education, Science and Technological Development of the Republic of Serbia, Grant No. 451-03-9/2021-14/200052 and project "Research on the Integration System of Spatial Environment Analysesand Advanced Metal Recovery to Ensure Sustainable ResourceDevelopment"that belongs to SATREPS program, supportedby the Japan International Cooperation Agency (JICA) and JapanScience and Technology (JST).

REFERENCES

[1] D. Adamovic, D. Ishiyama, S. Đorđievski, Y. Ogawa, Z. Stevanovic, H. Kawaraya, H. Sato, Lj. Obradović, V. Marinković, J. Petrović, V. Gardić, Res. Geol.(2021) 123–143.
[2] S.Đorđievski, D. Ishiyama, Y. Ogawa, Z.Stevanović, Environ. Sci. Pollut. Res. (2018) (25) 25005–25019.
[3] D.MilijaševićJoksimović, B.Gavrilović, S.LovićObradović, J. Geogr. Inst. Cvijic. 68(3) (2018) 333–344.
[4] S. Šerbula, V. Stanković, D. Živković, Ž. Kamberović, M. Gorgievski, T. Kalinović, Mine Water Environ. 35 (2016) 480–485.
[5] V. R. Gardić, J. V. Petrović, L. V. Đurđevac-Ignjatoviić, S. R. Kolaković, S. R. Vujović Hem. Ind. 69(2)(2015) 165–174.
[6] D. Ishiyama, H. Kawaraya, H. Sato, L. Obradović, B. Blagojević, J. Petrovic, V. Gardić, Z.Stevanovic, A. Shibayama, N. Masuda, Y. Takasaki, Scientific and Technical Reports of Graduate School of Engineering and Resource Science, Akita University 33 (2012) 41–49.
[7] J. Brankov, D. Milijašević, A. Milanović, Arch. Environ. Prot. 38 (1)(2012) 49–61.
[8] M. Korać, Ž. Kamberović, Metalurgija 13 (1)(2007) 41–51.

CHEMICAL COMPOSITION OFPARTICULATE MATTER IN THE INDOOR AIRAT THE TECHNICAL FACULTY IN BOR (SERBIA)

VišaTasić[1], Mira Cocić[2], Bojan Radović[1], Tatjana Apostolovski-Trujić[1]

[1]Mining and Metallurgy Institute Bor, Zeleni bulevar 35, 19210 Bor, Serbia

[2]Technical Faculty Bor, University of Belgrade, V.J. 12, 19210 Bor, Serbia

Abstract

This paper presents part of the research results of human's exposure to air pollution with suspended particles in selected educational and residential buildings in the town of Bor.In recent years, special attention has been paid to indoor air quality, because people spend a large part of their time during the day in closed micro-environments. Mass concentrations of 24 chemical elements were determined from PM_{10} samples collected in the selected classroom at the Technical Faculty in Bor during March 2018. Major elements (Fe, Al, Na, Mg, Ca, K) and trace elements (As, Cd, Pb, Ni, Zn, Cu, Ti, Co, V, among others) were analyzed by Inductively Coupled Plasma Optical Emission Spectrometry (ICP OES) and Inductively Coupled Plasma Mass Spectrometry (ICP MS), respectively. The phase composition of the total suspended particulatematter (TSPM) samples was determined by X-ray powder diffraction (XRPD)analysis.XRPD analysis of the SPM samples identified: calcite ($CaCO_3$), quartz (SiO_2), gypsum ($CaSO_4x2H_2O$), dolomite ($CaMg(CO_3)_2$) andplagioclase (albite – $NaAlSi_3O_8$).

***Keywords**: indoor air pollution,particulate matter,copper smelter, arsenic.*

1. INTRODUCTION

This work aims to present a part of the results of an ongoing study on human's exposure to suspended particulate matter in the indoor air in the town of Bor. The Bor town is situated in the eastern part of the Republic of Serbia. It has been a major center for mining and processing of copper and other precious metals for more than 100 years. So that, the town of Bor is assumed as a good representative of an urban-industrial environment in the Republic of Serbia, due to the sulfur oxides and particulate matter emissions from the copper smelter, situated next to the town.The amount of harmful substances contained in the copper smelter waste gases depends on many factors, such as: the choice of technological procedure for processing copper ore, the composition of the input raw material, temperature and duration of the process, type and amount of process gases and the like. Numerous exposure studies have associated the level of outdoor particulate matter with mortality and morbidity [1,2,3,4]. Thus the relationships between outdoor air pollution and health are beyond doubt. The influence of indoor air pollution on health is complex and still unexplored in detail so that more researchers explores this topic these years. In the indoor environment, in which people spend most of their time, both indoor and outdoor sources contribute to changes in PM levels. PM in indoor air originates from outdoor infiltration and additional indoor sources such as cooking and heating devices, tobacco smoking, etc. For health impact assessment studies, it is very important to determine PM mass concentration, PM particle size distribution, and chemical composition of PM in indoor microenvironments.

2. EXPERIMENTAL

The collecting of PM samples was carried out in the selected classroom at the Technical Faculty in Bor, from March5th to March 19th in 2018 (as shown in Figure 1). There was a maximum of 20 people in the selected classroom during lectures and exercises (period from 8 am to 6 pm).

The window area in the classroom is 4 m^2 and the volume of the classroom is 50 m^3.A sampling of the $PM_{10}$and TSPM was performed with reference samplers Sven/Leckel LVS3 [5] simultaneously, indoors and in ambient air in the immediate vicinity of the classroom.Quartz fiber filters (Whatman QMA, 47 mm) were used throughout this study. Before and after sampling, the filter mass was measured in accordance with the procedure prescribed by the standard SRPS EN12341: 2015 [6]. Based on the difference between the masses of exposed and unexposed filters and the known airflow through the sampler, the mass concentrations of suspended particles of the PM_{10}fraction were calculated.

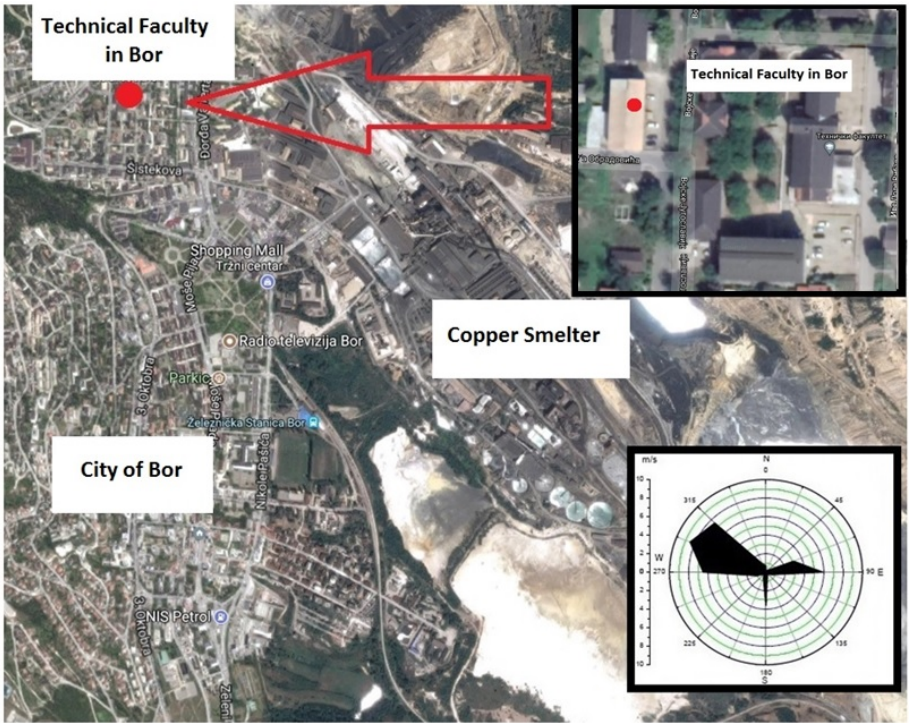

Figure 1 - Position of the Technical Faculty in Bor and the selected classroom in relation to the copper smelter

After measuring the mass of the exposed filters, they were further prepared for chemical analyzes in accordance with the procedure of SRPS EN14902: 2008 [7]. Major elements (Fe, Al, Na, Mg, Ca, K) and trace elements (As, Cd, Pb, Ni, Zn, Cu, Ti, Co, V, among others) were analyzed by Inductively Coupled Plasma Optical Emission Spectrometry (ICP OES) and Inductively Coupled Plasma Mass Spectrometry (ICP MS), respectively. The loaded filters, after gravimetric measurements, were prepared for chemical analyses following the procedure from CEN/TC 264 N779 (EU, 2008). Urban particulate matter Certified Reference Material 1648a [8] was analyzed for quality control and verification of the applied procedures for microwave digestion and trace element analysis. Recoveries were in the range from 80 to 120% for all measured elements.In this way, the mass concentrations of 24 chemical elements from the PM_{10} samples were determined.

The phase composition of the compositeTSPM samplewas determined by x-ray powder diffraction analysis (XRPD). Diffractograms were obtained using the Siemens D500 diffractometer with CuKα radiation (λ = 1.54184 Å) and Ni-filters at a current of 20 mA and a voltage of 35 kV in the range of 5 - 85 o2θ, with a step of 0.02° and an exposure of 0.5 s per step. The relationship between phases is determined by the Powder Cell (PCW) software using structural models of: calcite [9], quartz [10], gypsum [11], dolomite [12] and plagioclase [13].

3. RESULTS AND DISCUSSION

The indoor average daily concentration of PM_{10}in the classroom in the observed period was 28.2 μg/m^3. Similarly, the outdoor average daily concentration of PM_{10} was 46.1 μg/m^3. The obtained results indicate that the average concentrations of PM_{10} particles measured in the classroom were on average 1.6 times lower than those measured in the ambient air.According to national legislation[14], aiming to protect human health, annual limits for Pb, Cd, Ni, and As contents in $PM_{10}$are 500, 5, 20, and 6 ng/m^3, respectively. According to data shown in Table 1, average levels of As in PM_{10} in the classroom, as well as in the ambient air, were above the prescribed annual limitin the studied period.Based on the results shown in Table 1, it can be noticed that there are no significant additional sources of suspended particles PM_{10} in the classroom, so that mostly particles enter the classroom by infiltration from the external environment.

Table 1 - Summary of the chemical composition of PM_{10} (ng/m^3)

	TF Bor PM10-in	TF Bor PM10-out	MES Bor PM_{10}-in [15]		TF Bor PM10-in	TF Bor PM10-out	MES Bor PM_{10}-in [15]
As	17.0	49.9	1.9	Ca	455.3	896.7	541.4
Cd	1.4	2.1	0.3	Al	189.7	600.2	78.2
Mn	2.4	13.1	7.6	Mg	656	687.6	243.4
Pb	43.7	87.7	16.1	Na	55.1	77.2	303.3
Cu	179	574.5	39.1	K	1004	964.1	502.7
Zn	44.9	100.9	45.6	Co	1.1	0.9	0.2
Ni	0.1	1.9	4.3	Zr	0.9	0.8	2.4
Cr	0.2	1.2	21.6	V	1.8	1.6	0.8
Ti	10.0	21.9	23.4	Ce	0.5	2.2	
Sr	13.0	11.5	4.2	Se	5.8	6.1	1.5
S	905	1134.5	1691.7	Rb	1.2	1.5	0.6
Fe	803.9	915.2	414.2	Ag	1.1	3.1	1.9

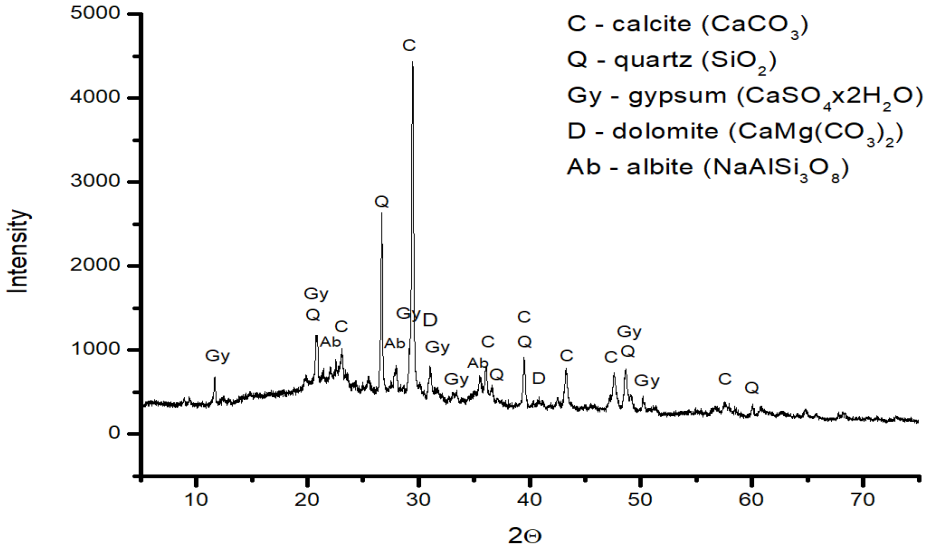

Figure 2 - X-ray powder diffraction diagram of TSPM samples collected in the classroom

The results from the reference [15], where the content of PM_{10} in the high school classroom in Bor was presented for the winter period in 2019 (Table 1) shows that the contents of As, Cd, Pb,

and Cu in PM_{10} were significantly lower in comparison with these obtained for the classroom at the Technical Faculty.This school is not located at the dominant wind direction in relation to the copper smelter, so the impact of pollutant emissions from the smelter is weaker.

Phase identification of TSPM samples was determined using XRPD analysis. The main peaks occur between 10 and 50^o 2θ as shown in Figure 2.XRPD analysis of TSPM samples identified: silicate minerals (quartz and plagioclase (albite)), carbonate minerals (calcite and dolomite) and gypsum as a representative of hydrated sulfates. The most dominant minerals are calcite, followed by quartz, dolomite, gypsum and plagioclase (albite).

4. CONCLUSION

The results of the examination of the content of suspended particles of the PM_{10} fraction in the classroom at the Technical Faculty in Bor show that a significant part of the air pollution from the external environment reaches the classroom. Of particular concern is the fact that the detected average arsenic content in PM_{10} is almost three times higher than the annual limit value. The analyses of the PM_{10} content show that there are no significant additional sources of suspended particles PM_{10} in the classroom, so that mostly particles enter the classroom by infiltration from the external environment.This fact indicates the need to take additional measures to reduce the infiltration of particles from the external environment.

ACKNOWLEDGEMENTS

This work was financially supported by the Ministry of Education, Science and Technological Development of the Republic of Serbia, Grant No. 451-03-9/2021-14/ 200052 and 451-03-9/2021- 14/200131.

REFERENCES

[1] Anderson H.R., Bremner S.A., Atkinson R.W., Harrison R.M., Walters S., Occup Environ Med, 58 (2001) 504–510.
[2] Atkinson R.W., Fuller G.W., Anderson H.R., Harrison R.M., Armstrong B., Epidemiology 21 (2010) 501–511.
[3] Pope III C.A., Dockery D.W., Journal of the Air and Waste Management Association, 56 (2006) 709-742.
[4] Pope III CA, Burnett RT, Thun MJ, et al., J Am Med Assoc, 287 (2002) 1132–1141.
[5] https://www.et.co.uk/products/air-quality-monitoring/particulate-monitoring/kfg-lvs-3-single-filter-gravimetric-sampler[accessed 12 September 2021]
[6] SRPS EN 12341:2015, https://iss.rs/sr_Cyrl/project/show/iss:proj:49389
[7] SRPS EN 14902:2008, https://iss.rs/sr_Cyrl/project/show/iss:proj:18667
[8] http://www.speciation.net/Database/Materials/National-Institute-of-Standards-and-Technology-NIST/SRM-1648a--Urban-Particulate-Matter-;i790 [accessed 12 June 2021]
[9] Chessin H., HamiltonW.C., Acta Crystallographica, ACCRA 18 (1965) 689-693.
[10] Zachariasen W. H.,Plettinger H. A., Acta Cryst. 18, (1965) 710.
[11] Cole W.F., LancuckiC.J, Acta Crystallographica B, ACBCA 30 (1974) 921-929.
[12] Althoff P. L., American Mineralogist AMMIA 62 (1977) 772-783.
[13] Horst W., Tagai T., Korekawa M., Jagodzinski H., Z. Kristallogr. 157 (1981) 233.
[14] https://www.paragraf.rs/propisi/uredba-uslovima-monitoring-zahtevima-kvaliteta-vazduha.html [accessed 12 June 2021] (in Serbian)
[15] https://www.vin.bg.ac.rs/webiopatr/#Publications.[accessed 12 June 2021]

The 52nd International October Conference on Mining and Metallurgy
November 29th – 30th , 2021
www.ioc.tfbor.bg.ac.rs

DEFINING STRUCTURAL CORRELATION USING OF TOTALHORIZONTAL GRADIENT

Snežana Ignjatović[1], Ivana Vasiljević[1], Milanka Negovanović[1]

[1]Faculty of Mining and Geology, University of Belgrade, Đušina 7, 11000 Beograd, Serbia

Abstract

Gravity data can help to define the structural correlation along significant vertical shifts. The different procedures of mathematical transformations on gravity data are applied to define structural correlations. The paper presents the results obtained using the procedure total horizontal gradient on gravity data. The application of the total horizontal gradient helped to detect contacts with a large dip angle (vertical or subvertical contacts), which can be interpreted as faults. The study area located in the wider area of the Vranje basin was taken as field example. The positions of the main neotectonics faults detected during geological survey in the vicinity of the Vranje basin correspond to the contacts acquired by applying the total horizontal gradient.

Keywords: *gravity data, gradient, vertical contact.*

1. INTRODUCTION

Gravity data can be used to define the structural correlation in the survey area. Vertical or subvertical contacts of two environments of different density may indicate abrupt changes in anomaly values, and these contacts may be interpreted as faults [1].

By applying certain procedures of mathematical transformations to gravity data, structural correlation can be identified in study area. A mathematical transformation that gives good results is the procedure total horizontal gradient, which is applied to the Bouguer anomaly data.

The paper presents the theoretical basis of the procedure total horizontal gradient, and its practical application. As practical example we used data from gravity measurements in the wider vicinity of the Vranje basin.

Gravity survey data from the former Yugoslavia were used to create the Bouguer anomaly map [2].

The Golden Software Surfer geophysical software package were applied during the processing and analysis of gravity data.

2. THEORETICAL BACKGROUND

The procedure total horizontal gradient (THDR) is used to differentiate the boundaries of near-surface causes of gravity anomalies, as well as to identify the position of contacts with alarge dip angle, which may correspond to a fault, the front of thrust, etc. The total horizontal gradient is defined as[3]:

$$\mathrm{THDR} = \sqrt{\left(\partial \mathrm{f}/\partial \mathrm{x}\right)^2 + \left(\partial \mathrm{f}/\partial \mathrm{y}\right)^2} \qquad (1)$$

where f – gravity field (in papireBouguer anomaly), $\partial \mathrm{f}/\partial \mathrm{x}$, $\partial \mathrm{f}/\partial \mathrm{y}$- are first-order derivative of the gravity field in x and ydirections.

The maximum values of THDR are above the edge of the source of the anomaly, and zero value is above the center of gravity of the body, which is the source of the anomaly. On the map of total horizontal gradient, the contacts are detected as the elongated maximum [4,5].

3. FIELD EXAMPLE

By applying the procedure, the total horizontal gradient on the data of Bouguer anomalies can be detected by contacts, which have a large dip angle, and which can be interpreted as faults. The wider area around the Vranje basin was chosen as the test area.

The positions of the main faults for the study area in this paper were taken from the neotectonics map [6]. The dominate directions of neotectonics faults in the study field are NE-SW and SE-NW.

The boundaries of the exploration area in the Gauss-Krüger coordinate system are [7550 km - 7600 km] and [4700 km - 4730 km].

To create the Bouguer anomaly map, which is the basis for further processing, gravity survey data from the former Yugoslavia were used [2]. The Bouguer anomaly map was done using a density value of 2.67 t/m3 and by converting the Bouguer anomaly data to a 500 m grid.

To eliminate or reduce errors and disturbances in the measured signal, data filtering was performed. The filtered map of Bouguer anomaly is shown in Figure 1.

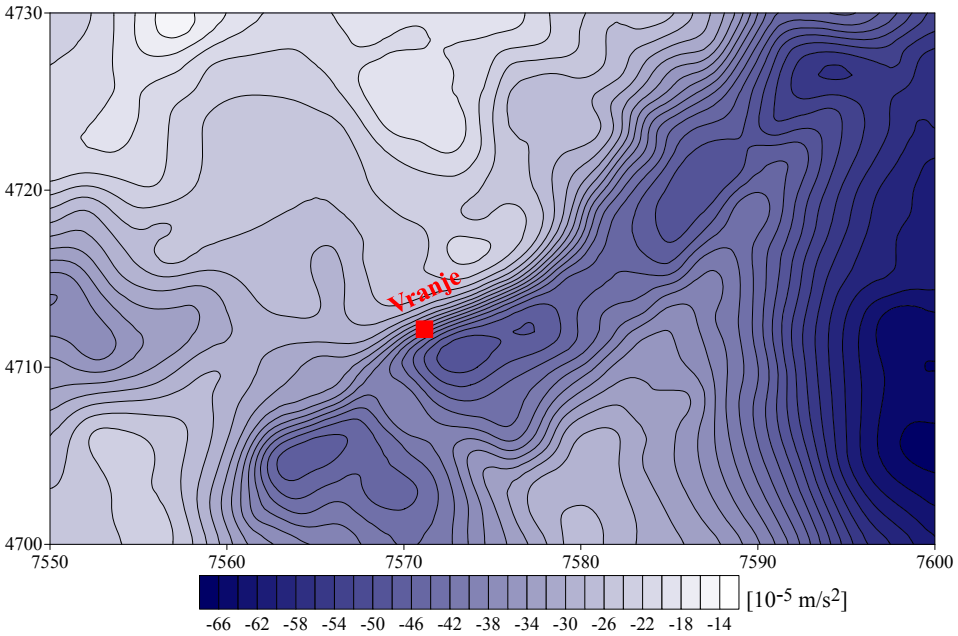

Figure 1. Filtered map of Bouguer anomaly

On the map of Bouguer anomaly (Figure 1), sudden changes in the values of anomaly are observed, which may indicate the existence of vertical or subvertical contacts of two environments of different densities.

To detect contact with a large dip angle (vertical or subvertical contacts), the total horizontal gradient on Bouguer anomaly was applied (Figure 2). The contacts are identified as the elongated maximum on the map of total horizontal gradient [4.5]. The contacts in Figure 2 are drawn in black lines. These contacts have a dominant direction NE-SW and SE-NW.

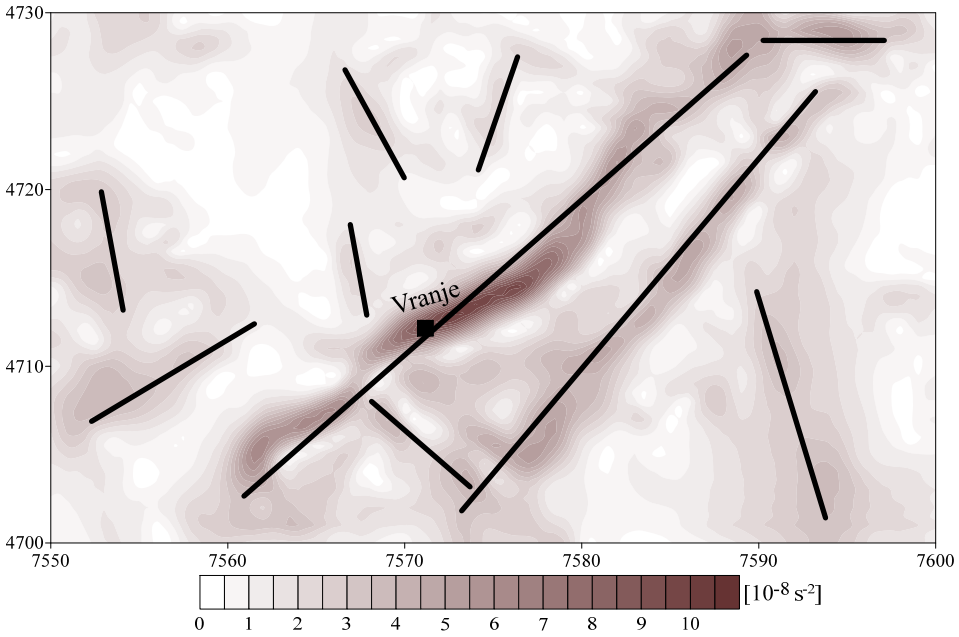

Figure 2. The map of total horizontal gradient (black lines - interpretation contacts)

To accomplish a detailed interpretation of the data it was necessary to compare the contacts detected based on the total horizontal gradient, with faults detected during geological surveys for a given exploration area. The positions of the main neotectonics faults are shown in Figure 3 and were obtained from the neotectonics map of Serbia [6].

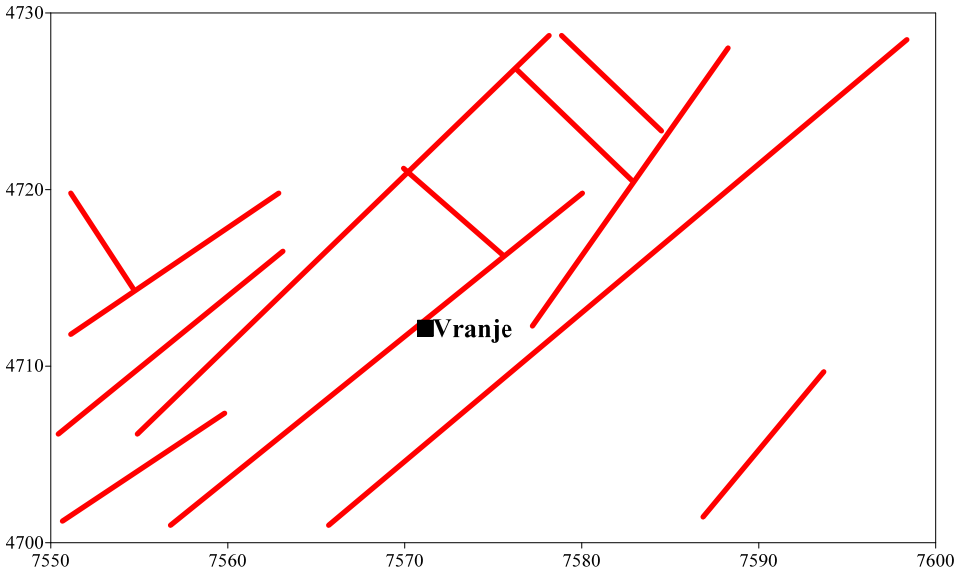

Figure 3. The positions of the main neotectonics faults (faults – red lines)

Figure 4 shows the contacts defined by the total horizontal gradient (black lines) and faults defined during geological research (red lines), which were taken from the neotectonics map [6].

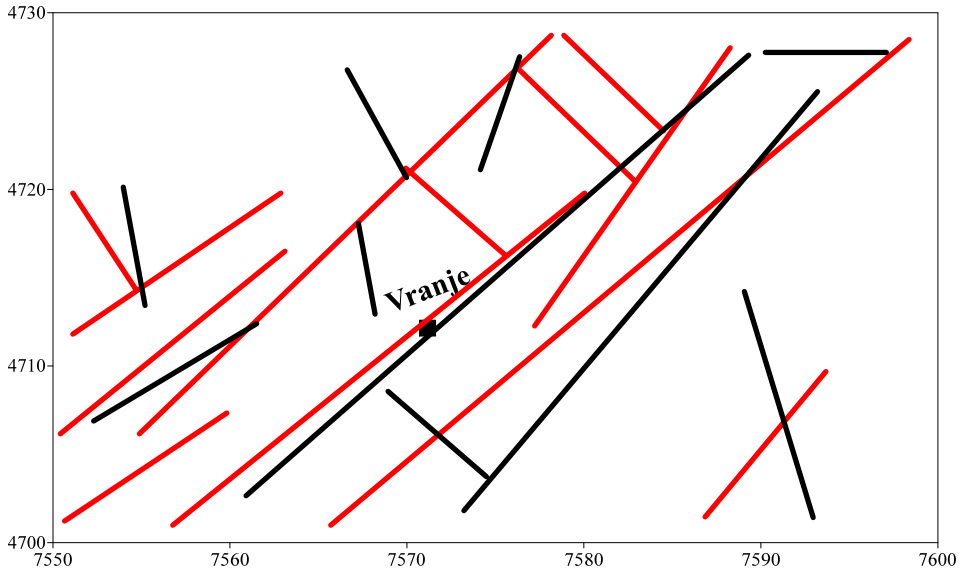

Figure 4. Map of contacts obtained using the total horizontal gradient (black lines) and faults defined during geological research (red lines)

The analysis of Figure 4 shows that there is a pretty good match between the faults distinct during the geological surveys taken from the neotectonics map of Serbia and the contacts defined by the total horizontal gradient, as it can be seen in the central part of the map (Figure 4). Contacts/faults general direction is NE-SW and SE-NW.

4. CONCLUSION

Different procedures of mathematical transformations on gravity data can help to successfully distinguish contacts in the exploration area, which can correspond to faults with a large dip angle. The paper shows that applying a mathematical transformation of the total horizontal gradient to gravity data, facilitate detection of vertical and subvertical contacts. These contacts can be interpretated as faults.

REFERENCES

[1] Vasiljević I, Ignjatović S. *Osnovigravimetrije - praktikum*, Univerzitet u Beogradu - Rudarsko-geološkifakultet, Beograd, 2016.

[2] Bilibajkić P, Mladenović M, Mujagić S, Rimac L. *Tumač za gravimetrijskukartu SFR Jugoslavije – Bugeoveanomalije 1:500 000*, Saveznigeološkizavod, Beograd, 1979.

[3] Cooper GRJ, Cowan DRD. Edgeenhancementofpotential-field data usingnormalizedstatistics. *Geophysics*, 2008, Vol. 73, No. 3, pp. H1-H4.

[4] Miller GH, SinghV. Potential field tilt-a new concept for location of potential field sources, *Journal of Applied Geophysics* 32, 1994, pp. 213-217.

[5] GETECH. *Advanced Processing and Interpretation of Gravity and Magnetic Data*, GetechKitson House Elmete Hall Leeds, UK, 2007.

[6] Marović M. Toljić M, RundićLj, Milivojević J, *Neoalpine Tectonics of Serbia*, Serbian Geological Society, Beograd, 2001.

The 52nd International October Conference on Mining and Metallurgy
November 29th – 30th , 2021
www.ioc.tfbor.bg.ac.rs

INCREASING THE CAPACITY OF THE COPPER SMELTING COMPANY IN THE COMPANY "SERBIA ZIJIN COPPER" - CHALLENGES AND CONSEQUENCES TO THE ENVIRONMENT

VelizarStanković[1], Miloš Janošević[2]

[1]Technical Faculty Bor, University of Belgrade, V.J. 12, 19210 Bor, Serbia

[2]Serbia Zijin Copper Co., ĐorđaVajferta 29, 19210 Bor, Serbia

Abstract

Through this paper a critical review will be given on the ENVIRONMENTAL IMPACT ASSESSMENT STUDY, presented to the public discussion, in the frame of Serbia Zijin Copper Co. intention of increasing a production capacity of copper in the existing Flash copper smelter and the auxiliary installations, from its nominal capacity of 80.000 tCu/year on a significantly enlarged one.

***Keywords**: environment, Flash copper smelter.*

1. INTRODUCTION

Serbia Zijin Copper Co., as a buyer of the RTB Bor Copper Co., has ordered a study of the environmental impact assessment (Study) [1,2], to increase a copper production capacity in the New Copper Smelter Plant. The Study was made by the TMF University of Belgrade, while the Ministry of Environmental Protection Serbia has offered it to the public discussion, according to the regulations. Remarks and comments, made through the public discussion, expressed some reserves about the Study in a view of the Smelter capacity enlargement and its effect on the environment while working. The further text is a critical analysis of the processes that would take place within the FSF with increased copper production, as well as the consequences that affect the environment in those circumstances.

2. INCREASING THE CAPACITY FOR COPPER PRODUCTION AND THE PROBLEMS THAT WOULD ARISE DUE TO THE RECONSTRUCTION OF THE SMELTER

Nominal production capacity of the New Copper Smelter has been designed and constructed based on the needs of the Serbian economy for copper, as well as the ore potential of copper mines and ore bodies that will be exploited in the future. To meet the nominal capacity, about 380.000 t/year of copper concentrate (21% Cu) should be produced, which is close to the copper concentrators capacity currently operating. Serbia Zijin Copper Co., as the new owner of all copper mines and other mining and metallurgical facilities bayed from the RTB Bor, driven by

profit, want to increase an annual copper production on 200.000 tones [1,2], meaning that more than 1·106 t/year of copper concentrate has to be processed in the same FSF changing or adjusting auxiliary facilities and installations, as sulphuric acid plants, concentrate drying and feeding installations, copper mate converters, off-gases purification, slag cooling and reflotation facilities, etc. So ambitious increase in production capacity of 2.5 times compared to the nominal one, requires a careful reconstruction of the installed FSF and all the installations coming before and after it in the technology chain of copper extraction from concentrate [2]. All these will cause a series of issues they have to concern the owner, and could interfere with the process itself, causing the threats to the environment and people living in Bor nearby the copper smelting plant. Among them, the most important one is how so big step towards production increase would reflect the environmental pollution and the people community living next to the Smelter.

The first issue that will arise is the shortage of concentrate from domestic sources, by almost two-thirds of the required annual amount. Domestic copper concentrates have a well-defined chemical and mineralogical composition ensuring stable process parameters. The missing amount of concentrate must be imported from the world market. Some of these concentrates are known as „dirty“ ones. Imported concentrates might differ from the domestic ones, containing some hazardous metals („dirty“ concentrates) that could affect the melting process polluting the melt and, what is more important, affecting the composition of off-gases especially if they are more volatile than copper. In that case, an increased amount of dust will be produced, in which hazardous metals will be presented either as metal oxides or fine metallic powder. Off-gases need to be purified from to eliminate fully the finest particles from the gas phase. Even that to reach a very high purification degree of FSF gases, an unknown amount of hazardous metallic compounds will go out, polluting the atmosphere around the smelter.

As is given through the conceptual solutions [2] and the Study [1], increasing capacity for 2.5 times, in relation to the existing copper production, should be carried out in the existing FSF reacting volume. The only changes relate to the installation of an adequate doser able to fulfil the new feeding capacity request and to a burner that will decrease problems at the uptakes lagging [1]. The reaction chamber height will only be increased by 40 cm, while the other dimensions of the FSF will remain the same. Increasing the production capacity of copper 2.5 times in the same FSF slightly adjusted for the new conditions will negatively be reflected on the copper smelting process in several ways. Even in the current work of the FSF, off-gases velocity in the settler gas space causes an elevated entrainment of melt droplets forming agglomerates at the end of up-take and on tubes in the boiler, causing breaks in the production, in order to remove the slag deposits from the up-take walls [1].

Increase in the concentrate charging, which would correspond to 2.5 times higher mass flux of the dispersed phase in the reaction chambre will cause the change in several working parameters of the process in the FSF:

- The residence time of the concentrate particles will be shortened, making questionable the completion of chemical reactions occurring in it;
- The flow rate of waste gases through the FSF will increase almost 3 times, due to an increased input of concentrate that will be burned, increasing the volume of chemically generated gases. Chemical reaction heat will raise the temperature inside the FSF;

- Linear gas velocity through the settler gas chamber will be increased, reaching > 21 m/s, leading to elevated entrainment of particles and droplets with the gas phase;

- Increased concentration of dispersed particles in the gas phase will contribute to significant slagging at the up-take end, as well as at the boiler, changing its heat transfer regime. Moreover, the planned burner at the end of the up-take to reduce the slagging effect could move the solidification front towards the boiler interior, while the problem with slagging deposits would remain and would be even enlarged;

- Increased mass flux of the dispersed phase will affect in worsening the melt phases settling leading to an increase of copper content in the slag and a higher concentration of iron oxides in the mate. In both cases, the work of the converters and the slag flotation will be disrupted;

- Increased flow-rate of the melt through the settler, besides bad separation of the phases, will disturb the regime of slag and mate discharging;

- Return of the dust to the FSF will additionally burden it and its work would deteriorate.

3. CONCLUSION

In conclusion, it would be more sustainable for the local environment, but also for the owner, to forget about the considered drastic increase in the production capacity of 200,000 t Cu /year and to give it up. Instead, one should validly and analytically reconsider whether and to what extent is possible to increase the capacity of the existing FSF and the accompanying facilities above the nominal one of 80,000 t Cu/year and to rely exclusively on domestic concentrates of defined quality, without buying any of dubious origin on the world market. In that way, any hazardous impact of the copper smelting plant on the environment will be minimized.

As for the environmental impact of the Smelter working with the enlarged production capacity, its footprint will be more expressive in the new circumstances than it currently is. Whether linearly with the new capacity, or following another functionallity, will depend not only on the concentrate origin, but also from many other facts. In any case, the city of Bor and its surrounding will remain a polluted area- a hot spot on the map of Eastern Serbia. Most probably the new spot will be bigger in size.

REFERENCES

[1] Studija o proceniuticajanaživotnusredinuprojekta: Povećanjekapacitetatopionice bakra u okvirukompleksa „Serbia Zijin Copper" DOO; Bor, July 2021

[2] IdejnorešenjeProjekatpovećanjakapacitetatopionice bakra u okvirukompleksa Serbia Zijin Bor Copper d.o.o. Bor; TMF Belgrade, February 2020

CHARACTERIZATION OF PELLET SAMPLES OBTAINED BY PELETIZATION OF LIMESTONE AND SEAWEED

Vladimir Jovanović[1], Dejan Todorović[1], Branislav Ivošević[1], Dragan Radulović,[1] Sonja Milićević[1], Dragana Nišić[2]

[1]Institute for Technology of Nuclear and Other Mineral Raw Materials, Franšed'Eperea 86, 11000 Beograd, Serbia
[2]Faculty of Mining and Geology, Đušina 7, Beograd, Serbia

Abstract

This paper presents the results of physico-chemical characterization of both the initial samples of lithotamnian limestone and seaweed (Ascophyllum Nodosum), and the products of aggregation of their mixtures in different ratios by the pelletization process. The initial samples were waste limestone from filter plants and dried seaweed. The final product of the pelletization process should serve the needs of agriculture as a means of biostimulation and can also be used in raising the pH levels of acidic soils. Several different pellet formulations were obtained by the process of discontinuous pelletization, and also by using a simulation of the continuous pelletization process on a pelletization plate.Tests of the mechanical properties of the pellets showed that the best results are shown by the pellets of the 4K sample, which were obtained by a continuous pelletization process with a mutual ratio of seaweed and limestone of 70:30%.

***Keywords**:litotamnian, limestone, seaweed, pelletization.*

1. INTRODUCTION

One of the most important parameters of soil fertility is substitution acidity. Over 60% of arable land worldwide can be classified as acidic. This is a consequence of the geological substrate and other natural factors, but also of industrial development and irresponsible attitude towards the environment[1].In Serbia, 13% of the soil is extremely acidic (pH ‹4), 17% very acidic (pH = 4-4.5), 30% medium (pH = 4.5-5.5), and 22% slightly acidic (pH = 5.5-6.5), while only 18% with a neutral and alkaline reaction [2].Acidic or alkaline properties of the soil have a decisive influence on the dynamics of nutrients and heavy metals in the soil. In an acidic environment, larger amounts of heavy metals are released into the soil solution.The use of limestone is very wide, on all acidic soils. The goal is to achieve the optimal pH value of the soil [3]. As powdered limestone from various filter plants is mainly used, the biggest problem in its application is scattering during transport and handling. This dust is also dispersed from the ground by the wind. On the other hand, limestone should be small enough to dissolve and evenly distribute in the soil under the influence of the weather.In order to reconcile these two demands, it is necessary to consolidate small classes of limestone. This is most often achieved by pelletization processes. Thus, a material of appropriate size is obtained, suitable for transport, manipulation and application, and at the same time small enough to dissolve under the action of weathering and moisture from the soil [4].The advantage of using pelleted or briquetted limestone versus the crushed limestone dust is related to easier application and lower consumption of pellets (ratio is 1:10) [5].Seaweed has recently been proven to be an excellent biostimulant and its use in various areas of agriculture is on the rise. It can be used in various fields of agronomy and horticulure, fruit and vegetable growing, production of certain types of organic fertilizers and also in the production of animal feed.The seaweed is obtained from the sea, using the so-called mowing proccess and can be used in various forms. They can be used dried and micronized to various sizes, they can also be used in the form of an extract or be used as sludge residue – which is a by-

product. Having in mind the individual properties of limestone and seaweed, the idea came to make pellets by mixing these two raw materials in different proportions. As both starting samples are fine-grained (<100 microns), they represent an excellent input for the pelletization aggregation process, and as seaweed in contact with water release their sticky ingredients (alginates) during homogenization, it is not necessary to add binders.Pelletization experiments in discontinuous and simulated continuous process were performed. After that, the obtained green pellets were dried at room temperature for 24 h, and then the characterization was performed (pressure resistance test, impact resistance test, abrasion resistance test and complete disintegration in water). After characterization, the obtained results were presented in parallel and based on that conclusions.

2. EXPERIMENTAL

2.1 Baseline samples

The lithotamnian limestone of the Dobrilovići deposit is made of calcite, quartz, clay minerals, and limonite [6]. The most common mineral, calcite, is of organogenic origin, it mainly appears as cryptocrystalline. Fragments of fossil remains appear.

Micronized seaweed (ascophyllum nodosum), is native to the North Sea. It contains natural plant hormones and various natural nutrients, trace minerals, microelements, carbohydrates, such as alginic acids, polysaccharide, etc. [7].

2.2 Determination of chemical composition of starting samples

Tables 1 and 2 show the chemical compositions of the starting samples of lithotamnian limestone and seaweed.

Table 1. Chemical composition of the initial limestone sample

Element	CaO	SiO_2	Al_2O_3	MgO	Na_2O	K_2O	Fe_2O_3	MnO	P_2O_5	TiO_2	G.Ž.
Content %	52.55	3.87	0.50	0.41	0.204	0.104	0.461	0.07	0.032	---	41.81

Table 2. Chemical composition of the initial sample of seaweed

Element	C	O	Na	Mg	Al	Si	S	Cl	K	Ca	Fe
Content %	37,92	26,23	13,52	0,61	0,23	0,37	1,75	14,99	2,54	0,98	0,86

2.3 Pelletization

For the pelletization of limestone, a laboratory pelletizing plate of the "Unalmuhendislikvemakinasanay" brand was used. For homogenization of limestone samples with seaweed, a mixer "Toni Technik" was used. In order to simulate the continuous dosing of the homogenized material on the pelletizing plate, the laboratory vibrating feeder "Retsch" was used.Homogenization of limestone and the required proportion of seaweed was performed, with the addition of water, after which the entire sample was homogenized and added to the pelletizing plate, on which the required minimum amount of additional water was added. The inclination of the plate (60^o) and the number of revolutions (50 min^{-1}) were constant, while the amount of binder was changed. The formed "green" pellets were stored for 24 h at room temperature.In the process of simulation of the continuous pelletization, the homogenization of limestone and the required proportion of seaweed was performed without the addition of water, after which the homogenized sample was continuously added to the pelletizing plate with a vibrating feeder, to which the required amount of water was added. All other pelletization conditions were identical to the discontinuous pelletization process.This way, the following samples were obtained (according to the % ratio of seaweed and limestone):

• Sample 1L: 50: 50%;• Sample 2K: 50: 50%;• Sample 3L: 70: 30%;• Sample 4K: 70: 30%

2.4 Determination of mechanical properties of pellets

Impact resistance of pellets is tested by dropping a group (set) of pellets with a total mass of 100g 25 times, from a height of 457 mm on a steel plate 9 mm thick, after which the sample is sieved on a sieve with a mesh size of 2 mm and the sieve mass is measured, which should not exceed 5% (rarely 10%) of the total sample mass [8].

The resistance of pellets to pressure was tested on a group (set) of 10 pellets on a standard hydraulic laboratory press, in order to determine the maximum pressure that the pellet can withstand without breaking. The results obtained by the Mars Minerals company, which has been dealing with agglomeration of limestone for many years, show that pellets should withstand a minimum of 0.5 kg/pellet, which is considered satisfactory for further manipulation [8].

The resistance of pellets to abrasion is tested by sieving a group of pellets weighing 100 g on a mechanical laboratory sieving device with a sieve with a mesh size of 2 mm, in a time of 5 min. After that, the mass share of class -2 mm is determined, which should not exceed 5% of the total mass of the sample [8].

The time of disintegration of pellets in water is examined by immersing the pellets from each group in water, at room temperature, measuring the time required for complete disintegration of the pellets. Disintegration is determined visually.

3. RESULTS AND DISCUSSION

Table 3 shows the summary results of testing the mechanical properties of limestone and seaweed pellets, obtained by the discontinuous process and the simulated continuous pelletization process.

Table 3. Aggregate test results of "green" pellets;

Sample		Resistance to			Time to desintegration
		impact	pressure	abrasion	
No.	seawead ratio : CaO, %	-2 mm, %	kg/pelet	-2 mm, %	s
1L	50 : 50	19,40	2,65	4,8	25,5
2K	50 : 50	70,24	2,67	0,84	28,9
3L	70 : 30	19,00	9,63	3,0	5,6
4K	70 : 30	5,06	3,51	4,22	7,4
Required value		Max. 5 - 10	Min. 0,5	Max. 3 to 5	As long as possible

Based on the results of testing the mechanical properties of "green" pellets obtained by laboratory procedures, we can conclude that they have satisfactory resistance to pressure and abrasion, and relatively poor disintegration in water and poor properties related to impact, regardless of the mass ratio of components. As for the pellets obtained by the continuous pelletization process, it can be observed that they have satisfactory resistance to pressure and abrasion and relatively poor resistance to disintegration in water, regardless of the mass ratio of the components. When it comes to the impact resistance of continuously obtained pellets, it can be seen that there is a drastic difference between the 2K and 4K samples. Namely, the sample with a higher seaweed content has a completely satisfactory impact resistance, while the sample

with an equal share of seaweed and limestone has an unacceptably poor impact resistance. If you choose between the analyzed pellets, then it can be seen that the most favorable results are obtained with the ratio of seaweed and limestone of 50:50%. Due to the relatively poor resistance to disintegration in water, the practical usability of the "green" pellets obtained in this way is quite limited.

4. CONCLUSION

Pelletization experiments of lithotamnian limestone dust and seaweed, size 100% -100 μm, were performed on a pelletizing plate by discontinuous and continuous procedure. The pellets obtained in this way were tested for impact resistance, pressure resistance, abrasion resistance and time required for disintegration of pellets in water.Tests of mechanical properties of pellets showed that the obtained pellets do not fully meet the usual standards for pellets used in agriculture (for calcification of acid soils), and that among the tested results show the best pellets of sample 4K, obtained by continuous pelletization with the ratio of seaweed and limestone 70: 30%.Namely, the impact resistance of 4K pellets was 5.6% (class -2mm, and the maximum allowable value is up to 10%), the pressure resistance was 3.51 kg/pellet (minimum required 0.5 kg/pellet), while the resistance to abrasion was 4.22% (maximum up to 5%), and the time of disintegration in water was very short and amounted to 74 s.The obtained results show that green pellets need to be dried in order to improve their mechanical properties, but this leads to a significant increase in pelletization costs. It is also necessary to expand the tests with other mutual relations of the input components, in order to obtain the optimal ratio for the required quality of the obtained pellets.

ACKNOWLEDGEMENTS

The research presented in this paper was done with financial support of the Ministry of Education, Science and Technological Development of the Republic of Serbia, within the funding of the scientific research work, according to the contracts with registration numbers 451-03-68/2021-14/200023.

REFERENCES

[1] H R von Uexküll, E. Mutert: Global extent, development and economic impact of acid soils**,** Plant and Soil, Volume 171, Issue 1, 1-15, 1995.

[2] D. Vidojević, Report of the state of land in Serbia, Ministry of Environmental Protection and physical Planing, Belgrade, 2009.

[3] B. C. Nyle: The Nature and Properties of Soils, 10th edition, p. 232-235, Macmillan Publisher, 2000.

[4] V. D. Jovanović, D. N. Knežević, Ž. T. Sekulić, M. M. Kragović, J. N. Stojanović, S. R. Mihajlović, D. D. Nišić, D. S. Radulović, B. B. Ivošević, M. M. Petrov, Effects of bentonite binder dosage on the properties of green limestone pellets, Chem. Ind. DOI: 10.2298/HEMIND160210023J, 2016.

[5] Breaton stone, The Complete guide to agricultural lime, **Error! Hyperlink reference not valid.**

[6] Ž.Sekulić, S.Mihailović, V.Kašić, V.Ćosić, Calcification of acid soils using lithotamnian limestone, Symposium: Natural mineral raw materials and the possibility of their use in agricultural production and food industry, Ed:Union of engineers and tehnicians and Geoinstitute, Belgrade, 113-123, 2006.

[7] Norrie, J. and D.A. Hiltz. 1999. Agricultural applications using Ascophyllum seaweed products. Agro-Food Industry High-Tech. 2:15-18.

[8] K.B. Albert, D. Langford: Pelletizing limestone fines, Mars Mineral, Pennsylvania, 12-29, 1998.

The 52nd International October Conference on Mining and Metallurgy
November 29th – 30th , 2021
www.ioc.tfbor.bg.ac.rs

HYDROMETALLURGICAL TREATMENT OF ELECTIRIC ARC FURNACE DUST IN AIM OF ZINC SEPARATION

Vanja Trifunović[1], Ljiljana Avramović[1], Radojka Jonović[1], Snežana Milić[2], Stefan Đorđievski[1], Marko Jonović[3]

[1]Mining and Metallurgy Institute Bor, Zelenibulevar 35, 19210 Bor, Serbia

[2]University in Belgrade, Technical Faculty in Bor, VojskeJugoslavije 12, 19210Bor, Serbia

[3]Institute of Chemistry, Technology and Metallurgy, Njegoševa 12, 11000Belgrade, Serbia

Abstract

During the steel production from secondary raw materials in the electric arc furnace, generation of the main intermediate of the process- dust from the electric arc furnace (EAF dust) occurs. This dust contains significant amounts of Zn and Fe, as well as Pb, Ca, Mn, Ni, Cu, Cd, Mg, Si, Cr, F, Cl and other elements and is considered hazardous industrial solid waste since it contains heavy metals. In order to separate Zn as a valuable component, hydrometallurgical treatment of EAF dust was investigated.The treatment consists of two stages: 1st stageis water leaching of EAF dust performed in order to remove water-soluble compounds, and 2nd stage is acid leaching in order to leach ZnO from EAF dust and obtain a $ZnSO_4$solution. With optimal parameters of the water leaching process of EAF dust, the achieved leachingrates of water-soluble compounds are as follows: 80.84% Cl, 60.63% K, 52.95% Na, 18.23% Ca, while with acid leaching of the solid residue obtained after water leaching at optimal parameters achieved leaching rate of Zn is 82.34%. In addition to the economic aspect of this treatment where the separation of Zn from EAF dust is performed, the treatment also has an ecological aspect because the transformation of hazardous waste into non-hazardous waste is performed, which has a positive effect on the environment.

***Keywords**: EAF dust, hydrometallurgical treatment, Zn separation, environment protection.*

1. INTRODUCTION

The total world steel production in 2019 amounted to 1869 million tons, of which the steel production in the electric arc furnace amounted to more than 30% of the world steel production [1-3]. Steel production from secondary raw materials, so-called scrap iron, is performed in an electric arc furnace (EAF) at a temperature of 1600°C, where during the melting of the batch the elements from the iron melt evaporate, which leads to the formation of the main intermediate of the process - electric arc furnace dust (EAF dust) [3-7]. In general, about 10-20 kg of EAF dust is generated during the production of 1 ton of crude steel[5, 8-10].Electric arc furnace dust contains significant amounts of zinc and solid iron oxides, as well as variable amounts of Pb, Ca, Mn, Ni, Cu, Cd, Mg, Si, Cr, F, Cl, etc. [1, 8-10]. The Zn content in EAF dust varies between 2 and 40% [2, 5, 6, 8-10]. Due to the fact that EAF dust is formed under oxidation conditions, most metals are present in the form of metal oxides. Zinc occurs in the form of ZnO and $ZnFe_2O_4$, while iron mainly occurs in the oxide form as Fe_3O_4 and Fe_2O_3 [3, 5, 8, 9]. The presence of heavy metals such as Pb and Cd in EAF dust can pose a threat to the environment and human health, and for this reason EAF dust is considered officially hazardous industrial solid waste in many countries [4, 5, 6, 9, 8, 10, 11].

In this paper, a laboratory experimental study of hydrometallurgical treatment of EAF dust originating from a steel plant in the Republic of Serbia was performed. Chemical characterization of EAF dust, laboratory experimental tests of EAF dust water leaching process

in order to remove chlorides and other water-soluble compounds, as well as tests of acid leaching process of solid residue obtained after water leaching in order to separate zinc were performed.

2. EXPERIMENTAL

Chemical characterization was performed on a reference sample of EAF dust by the following methods: Atomic Absorption Spectrophotometry (AAS), Volumetry (V), Inductively Coupled Plasma Atomic Emission Spectroscopy (ICP-AES), Spectrophotometry(SF), Carbon/Sulfur Analyzer (ACS).

Laboratory experimental investigations of hydrometallurgical treatment of EAF dust include water leaching and acid leaching processes. The parameters of the water and acid leaching processesat ambient temperature were investigated. All leaching experiments were performed on an initial EAF dust sample in an amount of 100 g, in a glass reactor with volume of 1 L, equipped with a stirrer with speed control and a device for automatic temperature control. For acid leaching experiments with the addition of oxidants, O_2 from a pressurized bottle was used.

3. RESULTS AND DISCUSSION

The chemical composition of the initial EAF dust sample is presented in Table 1.

Table 1 - Chemical composition of the initial EAF dust sample

Element	Zn	Fe	Mn	Cu	Pb	Co	K	Ni	Cr	Ca	Cd
Content (%)	32.44	18.92	1.81	0.19	1.39	0.0017	0.87	0.036	0.25	3.85	0.04
Element	Cl	Mo	S	P	As	Sb	Sn	Al	Si	Na	Mg
Content (%)	2.85	<0.005	0.51	0.15	0.0041	0.022	0.037	0.73	1.0	1.28	0.93

3.1.Water leaching of EAF dust

The following parameters of the EAF dust water leaching process were investigated: pulp density 5-20%, ambient temperature-80ºC and pH correction to <11. Process parameters such as the leaching process duration of 60 min and the mixing speed of 750 rpm remain constant in all experiments.

The 1ststage of hydrometallurgical treatment of EAF dust was performed in order to remove chlorides and other water-soluble compounds from EAF dust, such as Ca, Mg, K, and Na. The effects of water leaching EAF dust are a reduction in the consumption of sulfuric acid and chlorine ions in the second stage of leaching. The test results of the water leaching process confirm the removal of chloride from EAF dust, as well as other water-soluble elements. The leaching rates of chlorides and soluble compounds from EAF dust in water are shown in Figure 1 and amount to 80.84% Cl, 60.63% K, 52.95% Na, 18.23% Ca, 0.14% Zn and <0.0006% Pb.

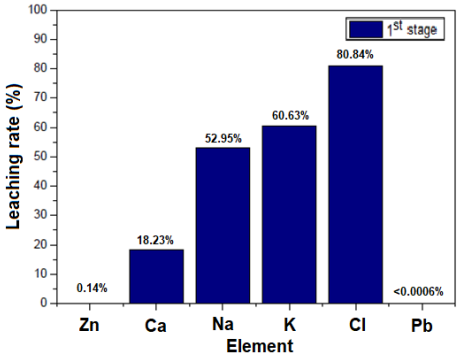

Figure 1 - Leaching rates of chlorides and water-soluble compounds

In water leaching experiments without pH correction, the pH of the suspension is above 11 at the end of leaching, which causes an increase in the concentration of Pb and Zn in the pregnant leaching solution. In order to prevent leaching of Pb and Zn with water, the pH of the suspension was corrected to <11 by adding concentrated HNO_3. The mass of the solid residue after water leaching without heating is reduced by about 10% compared to the initial mass of the EAF dust sample. The same percentage of weight reduction was shown in the experiment performed at a temperature of 80ºC, which means that the increased temperature is not necessary during water leaching process. Also, no significant influence of pulp density on the metal concentration in the solution after leaching was observed, so that the pulp density of 20% was taken as the optimal parameter.

3.2.Acid leaching of the solid residue

After the 1st stage of hydrometallurgical treatment of EAF dust, the obtained solid residue was leached in the 2nd stage with sulfuric acid at ambient temperature in order to leach ZnO from EAF dust and obtain a solution of $ZnSO_4$. The following process parameters were examined: H_2SO_4 concentration (0.25M, 0.5M, 0.75M, 1.0M and 1.5M), leaching process time (10 and 20 min), as well as oxidant addition (O_2), while a pulp density of 20% and a stirring speed of 750 rpm were constant.

Leaching rate of the tested elements depending on the concentration of H_2SO_4 without addition of oxidant is presented in Figure 2. From the obtained results it can be concluded that the leaching rate of Zn increases with increasing H_2SO_4 concentration for both tested leaching times (10 and 20 min). The highest Zn leaching rate of 71.63% was achieved by leaching with 1.5M H_2SO_4 over a time of 10 min. Leaching rate of Cu and Fe increases significantly at H_2SO_4 concentrations above 0.75M H_2SO_4. With increasing concentration of H_2SO_4, the leaching rate of Ca and Ni does not change significantly. Leaching rate of Cd leaching increases with increasing H_2SO_4 concentration from 0.25M to 0.75M. With a further increase in the concentration of H_2SO_4 from 0.75M to 1.5M, no significant change in the leaching rate of Cd was observed.

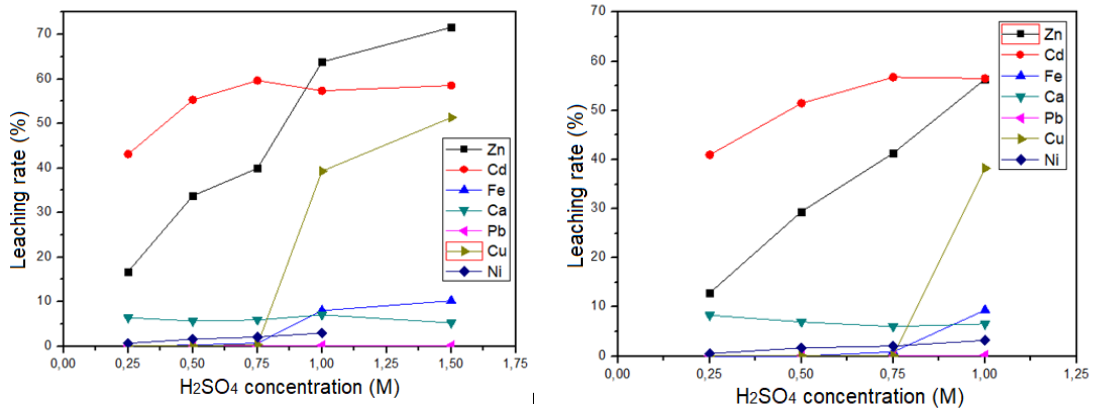

a) Leaching time 10 min b) Leaching time 20 min

Figure 2 - Leaching rate depending on the concentration of H_2SO_4 at a leaching time of 10 min and 20 min (leaching reagent 0.25-1.5M H_2SO_4, pulp density 20%, mixing speed 750 rpm, ambient temperature, without oxidant addition)

Investigation resultsof the addition of O_2influence as an oxidant on Zn leaching showed that the Zn leaching rate significantly increases with the addition of oxidant during the acid leaching process. The achieved Zn leaching rate with the addition of oxidant is 10% higher than the leaching rate without the addition of oxidant at the same tested process parameters (leaching with

1.5M H_2SO_4, pulp density of 20%, leaching time 10 min, mixing speed 750 rpm, ambient temperature) and amounts to 82.34%.

After acid leaching, the obtained solid residue showed the characteristics of non-hazardous waste based on TCLP and LP tests.

4. CONCLUSION

In order to separate Zn from EAF dust as a valuable component, hydrometallurgical treatment of EAF dust was investigated. The treatment consists of two stages: 1st stage of leaching with water was performed in order to remove water-soluble compounds, and 2nd rate of leaching with sulfuric acid in order to leach ZnO from EAF dust and obtain a solution of $ZnSO_4$. The achieved leaching rates of water-soluble compounds from EAF dust are 80.84% Cl, 60.63% K, 52.95% Na, and 18.23% Ca at the following optimal process parameters: pulp density 20%, ambient temperature, time 60 min, stirring speed 750 rpm and pH correction to pH <11.

The best results of acid leaching were achieved by leaching the solid residue obtained after water leaching EAF dust at the following parameters: 1.5M H_2SO_4 with the addition of O_2 as oxidant, pulp density 20%, leaching time 10 min, stirring speed 750 rpm at ambient temperature. Leaching rate of Zn at these leaching parameters is 82.34%. Apart from the economic one, the investigated treatment has also ecological significance because it transforms the starting material which represents hazardous industrial solid waste into non-hazardous waste, which can be disposed of at a non-hazardous waste landfill without risk to the environment.

ACKNOWLEDGEMENTS

This work was supported by the Ministry of Education, Science and Technological Development of the Republic of Serbia, Grant No. 451-03-9/2021-14/200052.

REFERENCES

[1] V. Montenegro, S. Agatzini-Leonardou, P. Oustadakis and P. Tsakiridis, Waste Biomass Valorization, 7 (6) (2016) 1531–1548.
[2] M. Čerňan, Z. Müller, J. Tlustý, V. Valouch, Int. J. Electr. Power Energy Syst. 129 (2021) 106831.
[3] F. Kukurugya, T. Vindt, T. Havlík, Hydrometal. 154 (2015) 20–32.
[4] W. J. Bruckarda, K. J. Daveya, T. Rodopoulosa, J. T. Woodcocka, J. Italiano, Int. J. Miner. Process. 75 (2005) 1 – 20.
[5] J. Wang, Y. Zhang, K. Cui, T. Fu, J. Gao, S. Hussain, T. S. AlGarni, J. Cleaner Prod. 298 (2021) 126788.
[6] V. S. Silvaa, J. S. Silvaa, B. dos S. Costaa, C. Labesb, R. M. P. B. Oliveira, J. Mater. Res. Technol. 8(6) (2019) 5504–5514.
[7] G. Laforest, J. Duchesne, J. Hazard. Mater. B135 (2006) 156–164.
[8] P. K Hazaveh, S. Karimia, F. Rashchia, S. Sheibania, Ecotoxicol. Environ. Saf. 202 (2020) 110893
[9] C. A. Pickles, Miner. Eng. 22 (2009) 977–985.
[10] T. Havlika, M. Turzakovaa, S. Stopic, B. Friedrich, Hydrometal. 77 (2005) 41–50.
[11] https://www.scribd.com/doc/26038172/Evropski-katalog-otpada

The 52nd International October Conference on Mining and Metallurgy
November 29th – 30th , 2021
www.ioc.tfbor.bg.ac.rs

EVALUATION OF ADSORPTION PERFORMANCE OF PHOSPHATES REMOVAL USING CELL-MG HYBRID ADSORBENT

Jovana Bošnjaković[1], Nataša Knežević[2], Natalija Čutović[2], Mladen Bugarčić[3], Aleksandar Jovanović[2], ZlateVeličković[4], Srećko Manasijević[1]

[1]Research and Development Institute Lola L.T.D., K. V. 70A, 11030 Belgrade, Serbia

[2]Faculty of Technology and Metallurgy, University of Belgrade, K. 4, 11000 Belgrade, Serbia

[3]Institute for Technology of Nuclear and Other Raw Materials, B. F. d'E. 86, 11000Belgrade, Serbia

[4]University of Defense, Military Academy,G. P. J. Š. 33, Belgrade 11040, Serbia

Abstract

Due to the high accumulation of nutrients in water (primarily phosphates) because of increased use of fertilizers and plant protection products, it is necessary to apply various techniques for their detection, and then removal. Adsorption is one of the promising techniques to removing them. Magnetite (MG) modified cellulose membrane (Cell-MG), obtained by reaction of 3-aminosilane and subsequently with diethylenetriaminepentaacetic acid dianhydride functionalized waste Cell fibers (Cell-NH_2 and Cell-DTPA, respectively), and amino-modified diatomite was used for phosphate ionsremovalfrom water. Cell-MG membrane was structurally and morphologically characterized using SEM and TEM techniques. The influences of operational parameters, i.e. pH, contact time, temperature, and the mass of adsorbent on adsorption and kinetics were studied in a batch system. The calculated capacities of 79.08 mg g^{-1} at 45°Cfor phosphate ions were obtained from non-linear Langmuir model fitting. The reusability of adsorbent and results from wastewater purification showed that Cell-MG could be used as general-purpose adsorbent. Based on the kinetic studies the adsorption process followsthe pseudo second-order model. Thermodynamic parameters showed that the adsorption process is endothermic and spontaneous.

***Keywords**: phosphates, adsorption isotherm, kinetics, activation energy.*

1. INTRODUCTION

Nowadays, there is a great demand for an efficient adsorbent that is able to simultaneously remove both anions and cations, as well as organic pollutants from water. The presence of different anions in wastewater poses a great danger to the environment. The adsorption process, as a promising, cheap and efficient technique, is most often used in the removal of pollutants (in this case PO_4^{3-}ions) from aqueous solutions [1,2].

Cellulose, a natural, widespread, fibrous and eco-friendly polymer can be used as a sorbent in various forms in order to eliminate pollutants from water. It can be used as a sorbent in natural and modified form, but due to its small sorption capacity, its modification is desirable [3]. Due to easy chemical modification, non-toxicity, good mechanical properties, cellulose shows potential as a sorbent [3]. Iron oxides, magnetite and hematite, have given good results in the removal of oxyanions and cations. The incorporation of hematite and magnetite into waste cellulose, as an adsorbent, improves the sorption capacity due to the improvement of magnetic properties.

The aim of this study was to remove PO_4^{3-} ions using modified Cell-MG membranes. The membrane was obtained by combining modified cellulose with 3-aminopropyltriethoxysilane (Cell-NH_2) and diethylenetriaminepentacetic acid dianhydride (Cell-DTPA) with magnetite and hematite, using it to remove ions.

2. EXPERIMENTAL

Cell-MG hybrid membranes and D-APTES (Diatomite modified with 3-aminopropylsilane, i.e. APTES) were prepared by the procedure described in Perendija*et al*. [4]. Magnetite was synthesized according to the method described in the literature [5].

3. RESULTS AND DISCUSSION

3.1 SURFACE MORPHOLOGY ANALYSIS

The results of the morphological analysis of the Cell-MG membrane and Fe_3O_4 particles, using SEM and TEM techniques, respectively, are given on Figures 1 and 2[4].

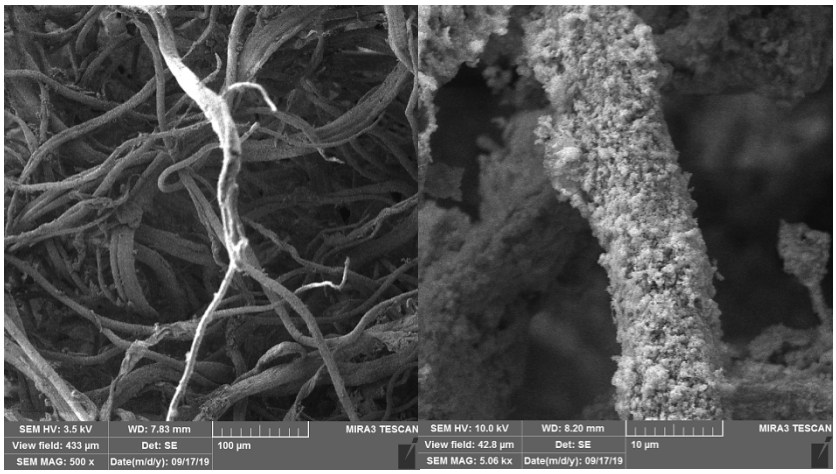

Figure 1.SEM images of Cell based membrane (left) and Cell-MG hybrid membrane (right)

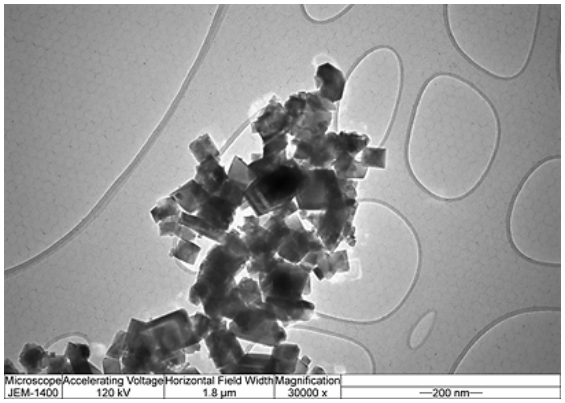

Figure 2.TEM image of Fe_3O_4 particles

The applied optimized procedure, which is used for the deposition of MG on the Cell-COOH membrane, provides a uniform distribution of MG nanoparticles, which contributes to increasing the surface area of the adsorbent and the active Fe-OH site capable of removing pollutants. As can be seen in Figure 1, there are no changes in the structure of cellulose fibers, while the surface morphology of the hybrid adsorbent is significantly changed due to the precipitation of MG. 7.8% by weight of iron and ~ 10.8% by weight of 14% were evenly distributed in the Cell-MG hybrid membrane [4].

3.2 ADSORPTION STUDY

Adsorption capacities were determined at the optimal pH value of 6, C_i = 9.1 mg L^{-1}, t = 90 min. Adsorption results are presented using Langmuir, Freundlich and Dubinin-Radushkevich adsorption isotherms.

Table 1. The results of non-linear fitting using Langmuir isotherm model for PO_4^{3-}adsorption onto Cell-MG hybrid membrane

Ion	*Temperature*	q_m(mg g^{-1})	K(dm^3 mg^{-1})	K_L(dm^3 mol^{-1})	R^2
PO_4^{3-}	25□	69.51	0.406	38524,623	0.989
	35□	71.51	0.546	51903,707	0.996
	45□	79.08	0.799	75946,905	0.992

Table 2.Non-linear Freundlich and Dubinin-Radushkevich isotherm parameters for PO_4^{3-}on Cell-MG membrane

	Parameters	*25°C*	*35°C*	*45°C*
Freundlich isotherm	K_F(mg g^{-1})(dm^3mg^{-1})$^{1/n}$	46.21	70.58	126.5
	1/n	1.309	1.313	1.299
	R^2	0.989	0.991	0.994
Dubinin-Radushkevich isotherm	q_m (mg g^{-1})	57.18	65.42	79.66
	K_{ad} (mol^2 KJ^{-2})	7.420	7.280	7.080
	E_a (KJ mol^{-1})	8.212	8.287	8.401
	R^2	0.898	0.917	0.943

The good adsorption capacities (q_m), obtained using the Langmuir isothermal model (Table I), are slightly increased with temperature increase, which indicates the chemical type of the binding of PO_4^{3-} ions. Also, the high values of the Langmuir constant (K_L) reflect the pronounced sorption affinity of the adsorbate towards the adsorbent surface. This means that the adsorption produced is caused by the high affinity of the adsorbent surface for ions by creating a weak interaction with the surface functionality.

3.3 THERMODYNAMIC PARAMETERS OF ADSORPTION

Table 3. Calculated Gibbs free energy, enthalpy and entropy for the PO_4^{3-} adsorption on Cell-MG hybrid membrane

Ion	ΔG° (kJ mol^{-1})			ΔH°	ΔS°	R^2
PO_4^{3-}	298 K	308 K	318 K	(kJ mol^{-1})	(J mol^{-1} K^{-1})	
	-36.13	-38.11	-40.35	26.72	210.7	0.992

A gradual increase in ΔG° in relation to the increase in temperature indicates more favourable processes of desolvation and diffusion at a higher temperature. Based on the literature values for ΔG° and the obtained values of ΔG° in the range -36.13 to -40.35 kJ mol^{-1}, a spontaneous process is clearly indicated, in which both physisorption and hemisorption processes participate.

A high ΔS° indicates increased randomness at the adsorbent/solution interface. The progress of the adsorption process is accompanied by the formation of a surface structure with the adsorbed pesticide by the formation of different interactions.

3.4 ADSORPTION KINETICS

Table 4. Pseudo-first, pseudo-second and second order reaction kinetic parameters for the PO_4^{3-}adsorption using Cell-MG adsorbent

Ion/order of kinetic law		*Pseudo-first*	*Pseudo-second*	*Second order*
PO_4^{3-}	q_e	51.67	66.44	66.44
	k (k_1, k_2)	0.062	0.003	0.008
	R^2	0.930	0.984	0.934

Determination of PSO rate constants at 25, 35, and 45 °C provides data for determining activation energy. The obtained value of 14,797 KJ mol^{-1}indicates the importance of the structural characteristics of the studied pollutants and adsorbent: geometry, spatial arrangement, atomic/surface functionalities charges,dipolarity/polarity, and proton donating/accepting properties that contribute to the efficiency of molecule diffusivity, the extent of solvent-sorbate and sorbate-surface functionalities interactions.

4. CONCLUSION

Magnetite-synthesized (MG) modified cross-linked carboxy functionalized cellulose membrane showed good efficacy for removing phosphate ions from water. The obtained results indicate that both the properties of phosphate ions and hybrid membrane adsorbent affect the manner and extent of sorbate-surface functionalities interactions. Based on kinetic and thermodynamic studies, it was confirmed that Cell-MG membranes as adsorbents have a high potential. The obtained results and applied methods are in line with the current trend in environmental protection where understanding the molecular interaction helps to design a new adsorbent with better performance.

ACKNOWLEDGEMENTS

This work was supported by the Ministry of Education, Science and Technological Development of the Republic of Serbia (Contract Nos. 451-03-9/2021-14/200066; 451-03-9/2021-14/200023; 451-03-9/2021-14/200135; 213-1/21-08-03-2021).

REFERENCES

[1] T. Sumathi, G. Alagumuthu, International Journal of Chemical Engineering, 2014, pp 1-7.
[2] A.E. Burakov, E.V. Galunin, I.V. Burakova, A.E. Kucherova, S. Agarwal, A.G. Tkachev, V.K.Gupta, Ecotoxicology and Environmental Safety, 2018, pp 702-712.
[3] Suhas, V.K. Gupta, P.J.M. Carrott, R. Singh, M. Chaudhary, S.Chaudhary, S.Kushwaha, Bioresource Technology, 2016, 1066-1076.
[4] J. Perendija, Z.S. Veličković, I. Cvijetić, J.D. Rusmirović, V. Ugrinović, A.D. Marinković, A. Onjia, Cellulose., 27 (2020) 8215–8235.
[5] U. Schwertmann, R.M. Cornell, Iron Oxides in the Laboratory (Second Edition), WILEYVCH Verlag GmbH, Weinheim, 2001.

The 52nd International October Conference on Mining and Metallurgy
November 29th – 30th , 2021
www.ioc.tfbor.bg.ac.rs

POSSIBILITY OF USING LIMESTONE FROM "PJEŠIVAČKI DO"-DANILOVGRAD DEPOSIT AS FILLER IN VARIOUS INDUSTRY BRANCHES

Dragan Radulović[1], Ljubiša Andrić[1], Darko Božović[2], Vlada Jovanović[1], Branislav Ivošević[1], Dejan Todorović[1],

[1]Institute forTechnology of Nuclear and Other Mineral Raw Materials, Franšed'Eperea 86, 11000 Beograd, Serbia

[2]Geological Survey, Podgorica, Montenegro

Abstract

This paper presents results of investigations of the possibility of using "Pješivački Do"-Danilovgradlimestone as filler in various industry branches. Micronization methods, granulometric composition, oil and water absorption and degree of whiteness were investigated, and chemical and thermal analyses (DT/TG) were performed.Physico-chemical properties of this limestone classify it among high quality carbonate raw materials with high $CaCO_3$ content of 98.65%, as well as low $MgCO_3$ content of 0.95% and low silicate content (SiO_2 0.23%). Its quality satisfies requirements of standards on using of calcium carbonate as filler in industry of paints and coatings; paper industry; rubber and PVC industry; in production of cattle feed; glass industry; production of mineral fertilizers and sugar industry. Due to the low degree of whiteness (87,6%) Pješivački Do"limestone cannot be used in pharmaceutical and cosmetics industry. Due to relatively high content of Cr (10 ppm) as heavy metal, content of S (0,19%), as well as biogenic elements P_2O_5 (0.030%), "Pješivački Do" limestone cannot be used in, foundry industry and metallurgy and for neutralization of acidic soils.

***Keywords**: limestone, filler, industrial use, standards.*

1. INTRODUCTION

The limestone is a sedimentary rock comprising predominantly carbonate minerals (i.e. calcium carbonate, $CaCO_3$) in the quantity surpassing 50%.Calcite, aragonite and/or vaterite mineral phases are carbonates usuallyappearing in the limestone. However, thecalcite[1-3]is the only crystal form with real significance. Being one of the most common minerals on Earth, the calcite ($CaCO_3$) occupies about 4% of the *Earth's crust* [4] mass. Calcite is an important resource and subject of investigations in various scientific fields: mineralogy, chemistry, physics, materials science [1, 5-7].Republic of Montenegro has big reserves of limestone [3, 8]. Even though deposits are huge, limestone is mainly used in construction as construction stone, and to some extent as architecturalstone[3, 8]. Since calcium carbonate as filler is much more expensive than construction stone, relevant institutions of Montenegro initiated investigations of the possibility of using limestone as filler[3, 8]. On the basis of the obtained results it was evaluated whether it can be used as filler in accordance with standards (SRPS) in various industry branches[3, 8]."Pješivački Do"-Danilovgrad deposit consists of carbonate sediments, mostly limestone ones, and less dolomitic sediments. Out of total reserves of 5,000,000 t of limestone, it is mainly used in construction as construction stone. The aim of the investigations presented in this paper was to determine the possibility of using this material, to obtain filler for application, in various industry branches.

2. EXPERIMENTAL

2.1 Materials and methods

Starting limestone sample used in investigations was from "Pješivački Do"-Danilovgrad deposit. First, its specific volumetric weight (density) and granulometric composition were determined. Its density was measured by pycnometer with xylol as fluid, granulometric composition was determined by Tyler screen. Granulometric composition of the micronized sample was determined bysieve size 63 μm, classification on Cyclosizer and Bach elutriator. Limestone filler quality was determined by chemical analysis. Thermal (DT/TG) analysis of the sample was performed using Netzsch-Simultaneous Thermal Analysis- STA 409 EP device, with heating speed of $\Delta T = 10\ ^{\circ}C/min$, in temperature interval from 20 to 1000 $^{\circ}C$. Degree of whiteness was determined by whiteness meter, according to MgO 100%standard.

2.2 Investigation of physical properties of starting sample

Specific volumetric weight of the starting sample is $\gamma = 2{,}632\ g/cm^3$, ggk of the sample is 16.67 mm, and $d_{50} = 6.98$ mm.

2.3 Technological investigations

For investigations of the possibility of using limestone as filler in various industry branches limestone was micronized, and thus obtained product were subjected to the following physico-chemical characterization:

- chemical analysis, thermal (DT/TG) analysis, determination of granulometric composition, degree of whiteness and absorption of oil and water.

2.3.1 Characterization of micronized product

Granulometric composition of the micronized products showed that ggk is 33 μm, and that the finest class -5.7 μm content is 58.84%, whiteness is 87.60%, oil absorption 13.90% and water absorption 15.50%.

2.3.2 Thermal (DT/TG) analysis

Results of thermal (DTA/TG) analysis of the micronized "Pješivački Do" limestone are presented as a diagram in Figure 1.

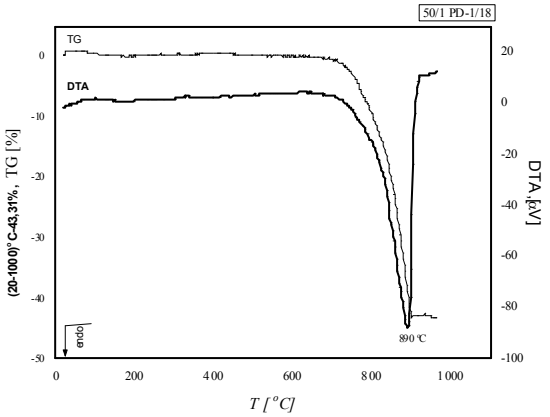

Figure 1. DTA/TG diagram of "Pješivački Do" limestone sample

DTA diagram (Figure 1.) shows endothermic peak with maximum at 890^0C, which is attributed to phase transformation of calcite ($CaCO_3$) into CaO, which is followed by mass loss of 43.31% in temperature range from 650 ^0C to 900 ^0C (TG diagram, Figure 1.).

2.3.3 Chemical analysis

Results of chemical analysis of the micronized limestone with contents of main components and damaging components are presented in Table 1 and Table 2.

Table 1. Chemical composition of main components of limestone sample

Comp.	CaO	$CaCO_3$	CO_2	$MgCO_3$	Fe_2O_3	Al_2O_3	SiO_2	K_2O	Na_2O	TiO_2	P_2O_5	LOI
Cont., %	55,24	98,65	43,41	0,95	0,053	0,026	0,23	0,012	0,064	<0,02	<0,030	43,80

Table 2. Chemical composition of damaging components of limestone sample

Comp.	Pb	Cu	Mn	S	Ni	Cr	Mo	Co	Cd	pH	Fe solu.	As	Hg
Cont., %	<10ppm	<0,5ppm	6,99ppm	0,19	<2ppm	10ppm	<50 ppm	<10ppm	<0,5ppm	9,35	0,0430	/	1,2ppm

Results of physico-chemical characterization of "Pješivački Do" limestone sample and the required filler quality (Standards) lead to conclusion that this limestone is of good quality. Namely, its $CaCO_3$ content is high- 98.65%, and $MgCO_3$(0.95%) and silicates ($SiO_2$0.23%) content low. However, an increased content of Cr (10ppm) as heavy metal in the sample was found.

3. RESULTS AND DISCUSSION

Limestone filler quality for each industry branch is defined by appropriate standards or requirements of manufacturers who use limestone as raw material in their production cycle. Limestone quality requirements are defined as content of useful and damaging components, i.e. as chemical composition, as well as the necessary size class.

3.1 Evaluation of "Pješivački Do" limestonefiller quality based on chemical composition

According to the results presentedabove, limestone from "Pješivački Do" – Danilovgrad deposit can be used in the following industries:

- in industry of paints and coatings; it is among high quality raw materials in accordance with market and standardrequirements (SRPS B.B6.032); in the paper industry; it is among A, B quality, while for the higher quality C and the highest quality D class its whiteness degree is not satisfying (SRPS B.B6.033); in rubber and PVC industry; it satisfies the highest quality standards and market requirements (SRPS B.B6.031); in the sugar industry, it is among the highest I class in accordance with market and standard requirements (6, SRPS B.B6.013); in the production of glass, due to the increased content of MgO (0.452%) and SiO_2 (0.23%) can be classified from II to V quality class, while due to the increased content of Al_2O_3 (0.026%) and Fe_2O_3 (0.053%) can be classified in IV and V class in accordance with the market requirements given by the standard (SRPS B.B6.020);in the production of cattle feed, it can be used in accordance with a defined standard ("Official Gazette of the Republic of Serbia 2/90, 20/00, 4/2010; 54/2017); it can be used for production of mineral fertilizers since its quality is in accordance with manufacturer's requirements (AzotaraPančevo).

Limestone from "Pješivački Do" – Danilovgrad deposit cannot be used:

- in the pharmaceutical and cosmetic industry due to the low degree of whiteness in relation to the market requirements defined by the standard(SRPS B.B6.034);for neutralization of acidic soils, because of the increased content of P_2O_5 (0,030%) as a biogenic element, the content of which is very strictly defined("Official Gazette of the Republic of Serbia"60/00, 41/09, 84/2017), due to the increased content of S (0,19%), it does not meet market requirements and standards in the foundry industry (SRPSB.B6.012) or in metallurgy(SRPSB.B6.011).

3.2 Evaluation of "Pješivački Do" –Danilovgrad limestonefiller quality based on users' requirements for the necessary raw material size (fineness)

Some industries require finely micronized limestone, while others require raw material of larger particle size, sometimes even coarse. Following industries use ground and micronized limestone:

- for paints and coatings industry; A quality 99.5% of - 20μm, B quality 97% of -20μm and 0.01% of + 44μm; for paper industry for both quality categories (A and B) the required fineness is 100% of -45μm, where for A quality 75% of -10μm, for B quality 80%;rubber and PVC industryrequires for A and B quality raw material to be 99.5% of -45μm, while for C and D quality upper limit limestone size is 45μm; for glass industry, since "Pješivački Do" limestone corresponds to quality IV and V according to its chemical composition, there is predefined granulometric composition for these quality classes, subdivided into six subclasses in size range from -1+0.1mm; for production of mineral fertilizers "Azotara"- Pančevo does not define size classes limestone should meet for this purpose.

Following industries demand larger sizes and coarse limestone:

- for sugar industry, limestone is to be classified into six subclasses in size range from -215+63mm, with maximum fine content in each subclass up to 8%.

4. CONCLUSION

Limestone from "Pješivački Do"- Danilovgrad deposit according to its physico-chemical properties belongs to high quality carbonate raw material with high content of $CaCO_3$of 98.65%, and low content of $MgCO_3$of 0.95% andsilicates (SiO_2 0.23%). It meets the requirements of standards for using calcium carbonates as fillers in industry of paints and coatings; paper industry; rubber and PVC industry; glass industry; production of mineral fertilizers; in the production of cattle feed; sugar industry. According to market demand and standards it belongs to high quality raw material in industry of paints and coatings, rubber and PVC, in the production of cattle feed, sugar industry, and for production of mineral fertilizers. However, for paper and glass production it does not comply with the standards for the highest quality classes. Due to the low degree of whiteness, and an increased content of: S (0.19%), heavy metal Cr (10 ppm), as well as the biogenic element P_2O_5 (0.03%), limestone "Pješivački Do" cannot be used in the pharmaceutical and cosmetic industry, for neutralization of acidic soils, in the foundry industry and in metallurgy. Obtaining of wide range of fillers for various industry branches would provide products which are more expensive per mass unit than products that have been used until now up to 10 times.

ACKNOWLEDGEMENTS

The research presented in this paper was done with financial support of the Ministry of Education, Science and Technological Development of the Republic of Serbia, within the funding of the scientific research work, according to the contracts with registration numbers 451-03-9/2021-14/200023.

REFERENCES

[1] D. Radulović, Terzić, A., Pezo, P., Lj. Andrić, Grigorova, I.Sci. Sinter., 49 (3) (2017) 247.
[2] D. S. Radulović, M. Petrov, G. Bogdanović, L. Andrić, D. Božović,J MIN METALL, 53 A (1) (2017) pp.43 -55.
[3] E. Yoğurtcuoğlu, M. Uçurum, Powder Technology 214 (2011) 47.
[4] http://minerals-n-more.com/Calcite_Info.html
[5] D. Saeid, S. Elnaz, International Journal of Mining Science and Technology 26 (2016) 577.
[6] K. De Weerdt, M. Haha, G. Saout, K.Kjellsen, H. Justnes, B. Lothenbach, Cement and Concrete Research 41 (2011) 279.
[7] E. Anastasiou, A. Liapis, I. Papayianni, ResourConservRecycl 101 (2015) 1.
[8] The report of the investigations of limestones from the area of Montenegro, for theirs application as a fillers in various branches of industry, ITNMS Archive, Belgrade, 2018. (In Serbian)

The 52nd International October Conference on Mining and Metallurgy
November 29th – 30th , 2021
www.ioc.tfbor.bg.ac.rs

ADVANTAGES OF MINING ENGINEERING CURRICULUM REALIZATION USING SOLUTIONS BASED ON FREE SOFTWARE

Predrag Stolić[1], Jelena Ivaz[1], Dejan Petrović[1], Zoran Stević[1]

[1]Technical Faculty in Bor, University of Belgrade, V.J. 12, 19210 Bor, Serbia

Abstract

Higher education institutions mainly use commercial software in the realization of their teaching process. The transition to the online teaching process revealed certain problems when using this type of software and it was necessary to find an adequate solution to overcome the problems related to online teaching environment. Certainly one of the solutions is to find appropriate software alternatives that are free from certain restrictions which are manifested during commercial software use. The paper shows how these problems are practically overcome by introducing free and open source software within the implementation of the teaching process in two subjects of the study program Mining Engineering at the Technical Faculty in Bor. The specific reasons and proper analysis for making such a transition are presented, as well as the analysis of the results achieved during the previous academic years when the mentioned software is used in a real environment during the teaching process.

***Keywords**: free software, freely redistributed software, higher education, open source software.*

1. INTRODUCTION

During the special circumstances of teaching in the past period in pandemic conditions caused by COVID-19 disease, certain problems related to the unavailability of school resources [1] were manifested, include computer classrooms. Computer classrooms are a key asset in the implementation of teaching that includes teaching units that cannot be mastered without adequate use of computers and appropriate software. By switching to the online teaching regime, the entire model of teaching, observed from the point of view of teaching in computer classrooms, moves from a homogeneous to a heterogeneous environment characterized by the use of students' own computers in the teaching process [2]. This heterogeneous environment entails in most cases the inability to use appropriate software used in the regular teaching process, as in most cases there is no possibility of transition of software related to use within computer classrooms in higher education institutions to students' personal computers mainly due to certain economic and legal restrictions that prevail in the field of use and distribution of software.

One of the potential solutions to overcome the above-mentioned problem was the possibility of replacing the existing software with related software that would not be proprietary and commercial, but that would be completely free to use in the given circumstances of the teaching process. The principles embedded in the way of using and distributing free software fully fit the academic community because they are based on freedom and free dissemination of knowledge [3] and accordingly such software is a perfect candidate for the implementation of teaching processes. Also, in the domain of well-known releases on the software scene, we have a situation that for years almost every well-known proprietary software has its equivalent in the FOSS (Free and Open Source Software) domain [4]. Efforts have been made for a long time to point out all the economic, legal and technical benefits that FOSS implementation at different levels of education brings [5]. The global tendency to migrate existing solutions to the FOSS world is becoming more represented in European countries, primarily due to the financial savings

achieved by implementing such solutions, but also gaining a certain degree of independence from software manufacturers [6].

2. ECONOMIC AND LEGAL ASPECTS

In the previous chapter, it was stated that the use of free software achieves significant economic benefits. This statement is completely true since free software not only implies freedom of use and distribution, but also implies the absence of any fee for its use.

Commercial software that would otherwise be used in teaching would realize three types of costs: software licensing costs per lecturer, software licensing costs per student and licensing costs of accompanying software (various types of OS and the like). For lecturer, the total cost of software licensing, with the realization of certain academic benefits during licensing, would be 458.73 euros per year (13.10 for OS, 227.18 for first software and 218.45 for second software) and for student, the total cost of software licensing, with the realization of certain student benefits during licensing, would be 110.93 euros per year (no cost for OS, 50.64 for first software and 60.29 for second software). Also, the basic minimum projections should include one license for the server operating system and the appropriate panel for administration, which amounts to around 843.24 euros per year. If the subject is attended by a group of, for example, five students, we come to a total projected cost of 1856.62 euros for the licensing of software for one academic year in the case of the implementation of exercises in the online domain.

Using FOSS these costs no longer exists regardless of the number of students who realize the exercises in the given subject. The use of the FOSS solution also eliminates the need to conduct special software procurement procedures for teaching purposes such as those in accordance with the Public Procurement Law of the Republic of Serbia, as FOSS is not covered by the provisions of this Law and similar legal procedures. It should be noted here that FOSS also relies on the use of appropriate licenses [7], but they are far different from those that can be encountered when licensing commercial software. One of the key differences is defining how the software is redistributed. In the case of commercial software, the rules of software redistribution are very restrictive and in most cases make it difficult or in some cases completely impossible to apply it in the implementation of the online teaching process that takes place outside the academic institutions. In the FOSS case, there is full applicability of this type of software in all forms of teaching, since the software can be freely redistributed and is not subject to any strict restrictions. This practically means that FOSS can be downloaded from official websites, but also that lecturers can freely copy software installations and give it to students.

3. EXAMPLE OF SOFTWARE REPLACEMENT AND ACHIEVED RESULTS

Due to COVID-19 restrictions, at the Technical Faculty in Bor, during the academic year 2019/2020, certain transitions were made from commercial to free software in certain subjects teaching process [2]. Due to the very short transition time due to the pandemic conditions that occurred, this was done for only one part of the semester and marked as a pilot program. After the success of the pilot program, during the academic year 2020/2021 in the regular online teaching process, exercises from the subjects given in Table 1 in undergraduate [8] and master [9] academic studies (study program Mining Engineering, Technical Faculty in Bor) were fully performed using FOSS. The subjects listed in Table 1 were suitable candidates for this realization, since more than 70% of the planned exercises were realized using computers and some appropriate software, since parts of laboratory and calculation exercises, in addition to computer, were done using appropriate software solutions.

Table 1 - Structure of exercises for analyzed courses

Course		Share in exercises		
Name	**Studies**	**Calculation**	**Computer**	**Lab**
Process Measurement Techniques	Undergraduate	26.67 %	60.00 %	13.33 %
Process Control in Mineral and Recycling Technologies	Master	40.00 %	60.00 %	/

For the realization of computer and laboratory exercises, the GNU Octave [10] software in version 5.x was used which working environment is shown in Figure 1. GNU PSPP [11] software in version 1.4.x was used for the realization of part of the calculation exercises which working environment is shown in Figure 2. Both of the aforementioned software were initially run on Linux Fedora Workstation 32 [12], and later, after regular system upgrades, on versions of Fedora Workstation 33 (from November 2020) and Fedora Workstation 34 (from May 2021). Additional teaching content in the online teaching process was provided using two servers that initially ran Linux Fedora Server 32 [13], and after regular system updates, the servers ran on Fedora Server 33 (from the end of October 2020) and Fedora Server 34 (from the end of April 2021), respectively.

The software configuration described above was used in two ways. First, it represented the software configuration used on real computers, but also the identical software configuration was used in the creation of virtual machines that were also used in the process of realizing online teaching. Virtual machines are fully realized using Oracle VM VirtualBox [14] version 6.1.x with providing full functionality of virtual machines using adequate Oracle VM VirtualBox Extension Packs and Oracle VM Guest Additions.

These are the key software solutions that were used during the teaching process. However, it must be mentioned that in addition to these software, many other software packages have been used in terms of the implementation of additional types of tasks that cover some other processes in the implementation of teaching, e.g. software for image manipulation, for creating presentations, text editors and the like. All of this software was part of the Linux Fedora Workstation, so no additional demanding installation procedures were required and it was easily available for further work.

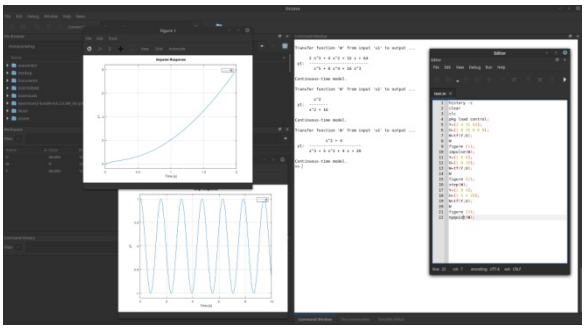

Figure 1 - GNU Octave working environment

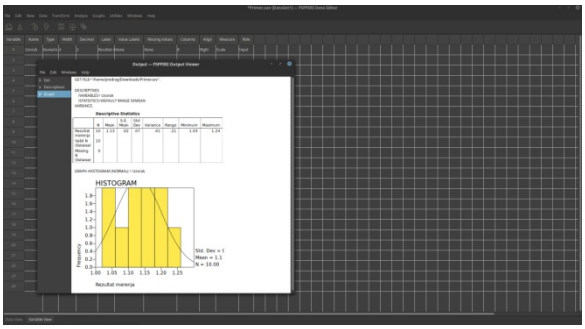

Figure 2 - GNU PSPP working environment

By using the mentioned software solutions, extremely positive effects were achieved on the teaching process itself, regardless of the development in rather difficult conditions. None of the students expressed any objections to the selection of the mentioned software, no problems were noted during the download of the software, their installation, or use. The work with the mentioned software went in accordance with the expectations observed from the side of the realization of the teaching process itself. None of the software required any additional registration during download, installation and use, so no personal data are additionally used during realization of teaching process which is in accordance with the Law on Personal Data Protection of the Republic of Serbia.

The realization of pre-examination activities in all cases is a maximum of 100 %, except in the case of subject in master academic studies in the academic year 2019/2020 where this realization is 80 % due to exceeding certain deadlines by one candidate. The success of candidates in taking the exams is also extremely high, which is shown by the average grades in the exams for the relevant subjects and academic years, which are shown in Table 2. As can be seen from Table 2, the lowest recorded average score is 8.75, while the other average scores are within the upper limits.

Table 2 - Achieved average exam grades for the appropriate academic year

Course		Average exam grade	
Name	**Studies**	**2019/2020**	**2020/2021**
Process Measurement Techniques	Undergraduate	10.00	9.50
Process Control in Mineral and Recycling Technologies	Master	8.75	10.00

4. CONCLUSION

From the previous analyzes it can be established that the transition from commercial software to FOSS in the implementation of the teaching process has been successfully completed. No indicators can be found that would call into question the participation of FOSS in various aspects of the implementation of the teaching process. On the contrary, the use of FOSS in the teaching process has achieved various benefits in economic, legal and technical terms.

In accordance with the obtained results, the use of FOSS is also planned for the implementation of the teaching process in the relevant subjects of Mining engineering at the Technical Faculty in Bor during the new accreditation cycle that started in the academic year 2021/2022.

REFERENCES

[1] [Decision on the suspension of teaching in higher education institutions, secondary and primary schools and the regular work of preschool education institutions (In Serbian), Službeni glasnik Republike Srbije broj 30/2020, Službeni glasnik, Belgrade, Serbia, 2020.
[2] P. Stolic, D. Milosevic, Proceedings of 8th International Scientific Conference Technics and Informatics in Education, Cacak, Serbia, 2020, p. 196-203
[3] M. Terbuc, Use of Free/Open Source Software in e-education, 2006 12th International Power Electronics and Motion Control Conference, 2006, pp. 1737-1742, doi: 10.1109/EPEPEMC.2006.4778656.
[4] A. Singh, R.K. Bansal, N. Jha, Open Source Software vs Proprietary Software, International Journal of Computer Applications, 114(18) (2015) 26-31
[5] S. Lakhan, K. Jhunjhunwala, Open Source Software in Education, EDUCAUSE Quarterly, 31(2) (2008) 32-40
[6] C. Mota and I. Seruca, Free/open source software vs. proprietary software in education, 10th Iberian Conference on Information Systems and Technologies (CISTI), 2015, pp. 1-6, doi: 10.1109/CISTI.2015.7170544.
[7] GNU General Public License, Version 3, Free Software Foundation, 2017. Available at https://www.gnu.org/licenses/gpl-3.0.en.html . Last accessed on November 9, 2021.
[8] Accreditation material, Book of courses, Study program: Mining engineering, Undergraduate studies, Technical faculty in Bor, Bor, Serbia, 2013, p. 59. Available at https://www.rudarstvo.tfbor.bg.ac.rs/Files/Curriculums/OAS_book.pdf . Last accessed on November 9, 2021.
[9] Accreditation material, Book of courses, Study program: Mining engineering, Master academic studies, Technical faculty in Bor, Bor, Serbia, 2013, p. 15. Available at https://www.rudarstvo.tfbor.bg.ac.rs/Files/Curriculums/MAS_book.pdf . Last accessed on November 9, 2021.
[10] https://www.gnu.org/software/octave/index . Last accessed on November 9, 2021.
[11] https://www.gnu.org/software/pspp/ . Last accessed on November 9, 2021.
[12] https://getfedora.org/en/workstation/ . Last accessed on November 9, 2021.
[13] https://getfedora.org/en/server/ . Last accessed on November 9, 2021.
[14] https://www.virtualbox.org/ . Last accessed on November 9, 2021.

The 52nd International October Conference on Mining and Metallurgy
November 29th – 30th , 2021
www.ioc.tfbor.bg.ac.rs

QUALITY INVESTIGATION OF SAND FOR THE PRODUCTION OF AGGREGATES ON VINOGRADI LOCALITY (DELIBLATSKA PEŠČARA)

Slađana Krstić[1], Emina Požega[1], Sanja Petrović[1], Srđana Magdalinović[1], Daniela Urošević[1], Slavica Miletić[1], Zdenka Stojanović Šimšić[1]

[1]Mining and Metallurgy Institute Bor, Zeleni bulevar 35, 19210 Bor, Serbia

Abstract

This paper represents a study which was made to evaluate and interpret the variations in the quality of sand as potential raw materials for the production of adregate on Vinogradi locality (Deliblatska peščara). Since deposits of sand constitute a valuable resource for a region it is desirable that extent and quality variations of these deposits are known. It was hoped that an evaluation of certain properties of the sands would assist in determining the value of the Vinogradi locality (Deliblatska peščara) as an undeveloped aggregate source by indicating the relative quality of the sand from alternate sites of the Deliblatska peščara.

Keywords: *raw material, quality investigation, sand, Deliblatska peščara, the production of agregates.*

1. INTRODUCTION

The largest European continental sandy terrain is located in the south-east part of the Pannonia Plain, i.e. in Banat, covering the area of nearly 35,000 ha. It is of elliptical shape and extends from south-east to north-west. It was formed during the Ice Age from the vast layers of silica-carbon sand. In the Modern Age, the east wind called "Košava" formed a clear dune relief, rising between 70 and 200 meters above sea level[1,2,3]. Locality Vinogradi it is spatially located on the territory of the municipality of Alibunar[4] (Figure 1). Samples submitted for partial tests, in addition to the existing field markings that contain the place (locality) of geological research, the mark of the exploration work and the testing interval, also received laboratory markings of analyzes. The weight of the individual samples was about 20 kg. Table 1 shows the laboratory markings of composite tests and the method of their formation (four individual tests in the manner required by the customer).

Table 1. General data on individual samples on location Vinogradi

Serial number	Well mark	Field rehearsal mark	Trial interval (m)	Composite (m)
1.	K-1/19	P-1/19	2,00-7,00	20,00
		P-3/19	1,00-6,00	
		P-5/19	2,00-7,00	
		P-7/19	3,00-8,00	
2.	K-2/19	P-2/19	7,00-12,00	20,00
		P-4/19	6,00-12,00	
		P-6/19	7,00-12,00	
		P-8/19	8,00-13,00	

2. EXPERIMENTAL

Examination of the quality of natural aggregate (sand) of Vinogradi locality, Banatski Karlovac was performed in accordance with Article 202 of the Rulebook on classification and categorization of reserves of solid mineral raw materials and keeping records on them (Official Gazette of SFRJ, No. 53/79), ie in accordance with the standards prescribing the quality of mineral raw materials for a given application:

Figure 1. Sand on the locality Vinogradi (the territory of the municipality of Alibunar); by https:// geografijazasve, 04.04.2020

• SRPS B.B2.009: 1982 (withdrawn) - Natural aggregate and stone for the production of concrete aggregates. Technical conditions,
• SRPS B.B2.009: 1982 (withdrawn) - Natural aggregate and stone for the production of concrete aggregates. Technical conditions, SRPS B.B3.100: 1982 (withdrawn) - Fractionated stone aggregate for concrete and asphalt. Technical conditions,
• SRPS B.B2.010: 1986 (withdrawn) - Fractionated stone aggregate (granulate) for concrete. Technical conditions, and
• Rule book on technical requirements for fractional aggregate for concrete and asphalt ("Official Gazette of RS", No. 78/2020).

3. RESULTS AND DISCUSSION

The methods used in the scope of testing partial and complete sample analyzes are presented by the following standards.

Individual samples were tested by the methods: granulometric composition, content of fine particles, content of clay lumps, water absorption, bulk density in loose and compacted state and bulk density (Table 2).

Table 2. Test results of individual samples

	Bulk density in loose state	Bulk density in compacted state	Bulk density (pycnometric method)	Water absorption < 4 mm [%]
standard deviation	48,85	62,25	41,06	1,80
coefficient of variation	0,05	0,05	0,01	0,34
coefficient of variation [%]	5,47	4,98	1,46	33,60
Minimum	824	1192	2780	3,39
Maximum	988	1390	2880	7,86
Range	164	198	100	2
Mean	894	1251	2815	5,35
Median	884	1237	2800	4,87
Varianse	2385.93	3875,27	1685,71	3,23

The complete sample analyzes test results of are shown in the Table 3, Figure 2 and Figure 3.

Table 3. Methods used in the scope of testing of complete sample analyzes and presents of the results

Ordinal no.	Characteristic		Test method	Results (Mean)	Technical requirements
1.	Mineralogical-petrographic composition		Annex III-Z	Fine grains quartz sand	1)
2.	Ingredients that prevent hydration of cement		Annex III-Z	not contain	Must not contain
3.	Bulk density γρ [kg/m^3] (pycnometric method)		SRPS ISO 7033	2815	2000-3000 kg/m^3
4.	Water absorption		SRPS ISO 7033	5,35	Max 1.5%
5.	Resistance to frost		Annex III-O	2.5	Loss max 12%
6.	Total sulfur as SO_3		Annex III-NJ	0.002	Max 1.0%
7.	Chloride content		Annex III-NJ	≤0.001	Max 0.10% Max 0.02% 2)
8.	Content of organic matter		Annex III-M	Color lighter than standard	Color lighter than standard
9.	Grain shape		Annex III-S	0	Min 0.18
10.	Granulometric composition, passage through a sieve,%	2.00 mm	Annex III-I	100	1)
		1.00 mm		99.9	
		0.5 mm		99.7	
		0.25 mm		99.3	
		0.125 mm		92.9	
11.	Content of fine particles [%]	0,09 mm	Annex III-K	44.4	1)
		0.063 mm		14.2	
12.	Content of clay lumps [%]		Annex III-E	0	1)
13.	Grain moduls			0,20	1)
14.	Content of crumbly grains [%]		Annex III-LJ	0	1)
15.	Content of light particles[%]		Annex III-J	14.17	1)
16.	Grain surface coverage[%]		Annex III-Z	0	1)
17.	Resistance to crushing and wear [%]		Annex III-P	5.0	Max 35%
18	Bulk density in loose and compacted state[kg / m^3]		SRPS ISO 6782	893 1251	1)

1) Technical requirements are not determined, but the test results are stated in the Test Report
2) If the aggregate is used for the production of prestressed concrete

Figure 3. Microscopic appearance of fraction 0.250 / 0.125 mm, binocular magnification 40X

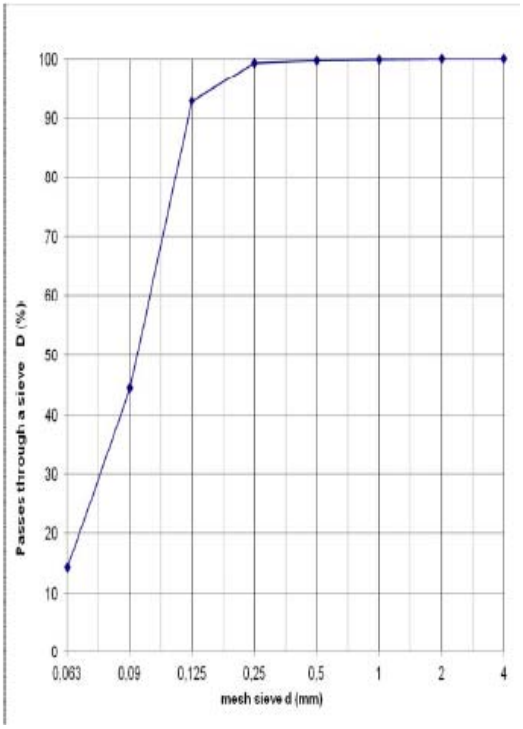

Figure 4. Granulometric composition of raw material

The analysis of the results of raw material quality testing was performed on the basis of the above the results of the examination and in accordance with the requirements quality for stone aggregate of Rule book on technical requirements for fractional aggregate for concrete and asphalt ("Official Gazette of RS", No. 78/2020).

In accordance with the requirements quality for stone aggregate of Rule book on technical requirements for fractional aggregate for concrete and asphalt ("Official Gazette of RS", No. 78/2020) raw material not satisfying, but,

Fine-grained quartz sand from the locality "Vinogradi", can be used for the production of lower bearing mechanically stabilized (tampon) layers of pavement structures according to the technical specification of ЈП ПУТЕВИ СРБИЈЕ from 29.12.2009. for the lower base layer:
• A layer of unbound stone material - sand.

ACKNOWLEDGEMENTS

This work was financially supported by the Ministry of Education, Science and Technological Development of the Republic of Serbia, Grant No. 451-03-9/2021-14/ 200052.

REFERENCES

[1] Bukurov, B., Geomorfološke prilike banatskog Podunavlja. Srpska akademija nauka, Beograd (1954) p.55-88.
[2] Butorac, B., Habijan-Mikeš, V., Vider, V., Opstanak peščara u Vojvodini. Grafoprodukt Subotica (2002).
[3] Marković, S., Ivanišević, P., Jovanović, M., Molnar, B., Galić, Z., Gaudenji. T., Savić, S., Bojanić, D., Paleopedološka i paleoekološka svojstva holocenih eolskih peskova Deliblatske peščare. Specijalni rezervat prirode Deliblatska peščara. Zbornik radova VII. JP Vojvodina šume, Novi Sad (2004) p.279-288.
[4] https:// geografijazasve, 04.04.2020.

The 52nd International October Conference on Mining and Metallurgy
November 29th – 30th , 2021
www.ioc.tfbor.bg.ac.rs

INFLUENCE OF COLD ROLLING AND ANNEALING ON HARDNESS OF BIMETALLIC STRIP Cu– Al

Saša Marjanović[1],Dragoslav Gusković[1],Milijana Mitrović[1],Emina Požega[2],Biserka Trumić[2], Uroš Stamenković[1]

[1]Technical Faculty Bor, University of Belgrade, V.J. 12, 19210 Bor, Serbia

[2]Mining and Metallurgy Institute Bor, Zelenibulevar 35, 19210 Bor, Serbia

Abstract

Samples of bimetallic strip Cu-Al were cold rolled with different reduction degrees, and the ones deformed with the highest reduction degrees were annealed afterwards at different temperatures for a period of one hour. The values of the hardness of the layers of the bimetallic strip were obtained as a function of the degree of deformation, and the annealing temperature. Global flow of curves hardness - total deformation, increases, where the increase in the hardness of aluminum with increasing degree of deformation is approximately linear. A decrease in hardness was observed with an increase in the annealing temperature, in both the aluminum layer and the copper layer.

Keywords: *bimetallic strip, hardness, deformation degree, annealing temperature*

1. INTRODUCTION

Thanks to combination of different properties in one material, bimetals are widely used in industry, because of saving expensive scarce metals, and for their specific properties which separate metals-components doesn't have.

In a bimetal, expensive metals and alloys are used as plating materials, with thickness of up to 25% of the bimetal's thickness. Thanks to that it is possible to get relatively cheap materials with required properties where performing layer keeps the properties it's got before joining into bimetal, while cheaper, basic material acts as carrying material that provides required mechanical properties.

Corrosion-proof bimetals with cooper as a plating layer are used more and more.

Cold rolling of a plated strip is a final operation in plastic processing in all cases when enhanced strength and deformation resistance are required [1, 2, 3, 4, 5].

2. EXPERIMENTAL

The samples cut from trilayer sheet Cu - Al – Cu, 10,4 mm thick, obtained by plating by explosion, were used for examination. One Cu layer was removed, so bimetal strips, 8,4 mm thick, were obtained. The initial thickness of Al, in those strips, were 6,4 mm, and2 mm for Cu.

Prior to rolling of the bimetal strip, the gap between the working rolls was set to 8,4 mm, and then the strip was let between for a few times till the total deformation of 10% was reached.

In order to simplify it, it was accepted that the deformation for a single pass was 2,5%. After the deformation of 10% the total thickness and layers thicknesses were measured on various spots.

The same procedure was repeated for the total deformations of 20%, 30%, 40%, 50%, 60%, 70%, and 80%.

The samples deformed with maximum deformation degree, ε_{max}=80%, were subjected to annealing.

The annealing was done in a protective atmosphere of nitrogen, for a period of one hour, at temperatures of 200, 250, 300, and 400 ^{o}C.

Hardness measurements were performed after all degrees of deformation and after the annealing.

The experimental flow is shown schematically in figure 1.

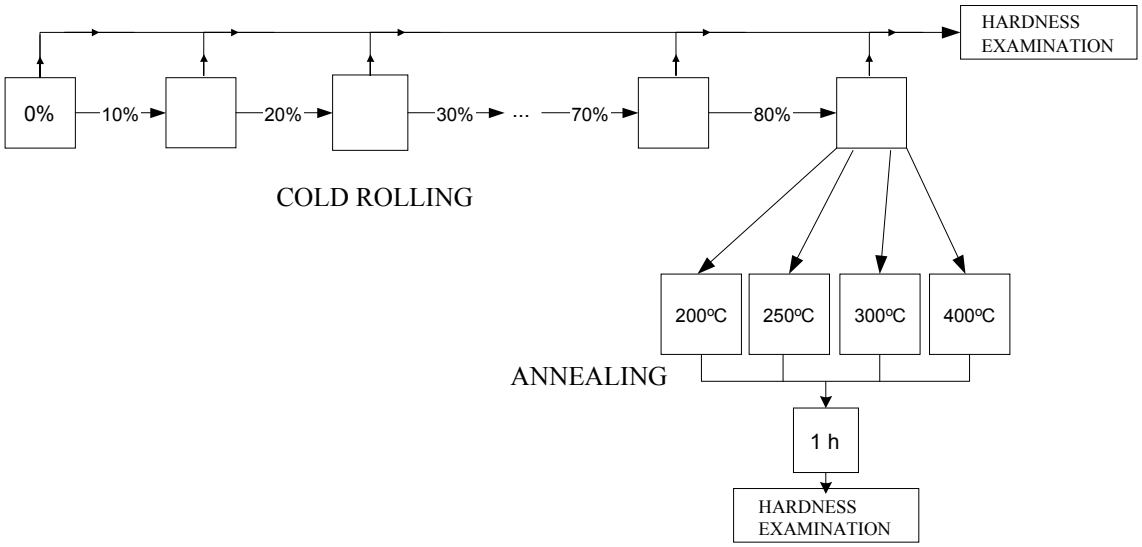

Figure 1. Schematic diagram of the experimental flow

3.RESULTS AND DISCUSSION

The obtained data for the hardness measurements, depending on the total deformation degree are given in Table 1. and Figure 2.

Table1. Dependence of the hardness of bimetallic strip layers on the degree of deformation

ε (%)	HV (daN/mm^2)	
	Al	Cu
0	43.83	106.00
10	44.20	115.75
20	46.33	117.00
30	47.27	120.40
40	48.04	121.67
50	48.44	125.50
60	49.20	131.80
70	49.80	136.00
80	51.05	146.75

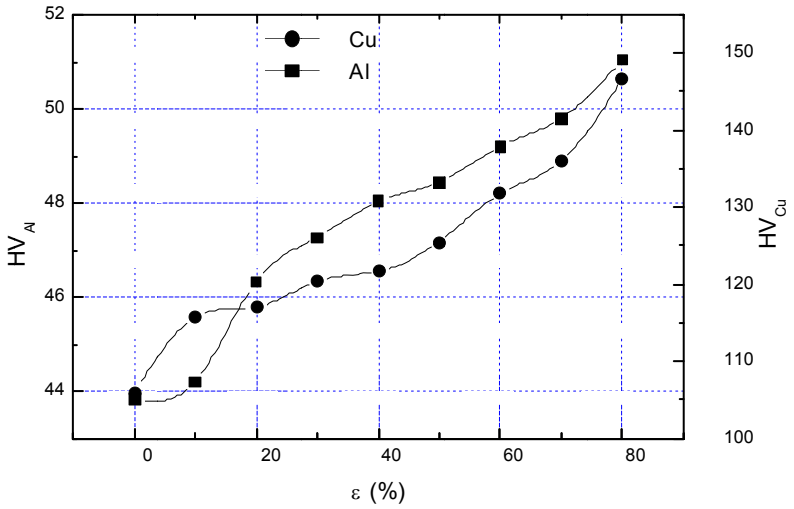

Figure 2.Diagram of the dependence of the hardness of the bimetallic strip layers on the degree of deformation

Global flow of curves hardness - total deformation, increases, where the increase in the hardness of aluminum with increasing degree of deformation is approximately linear.

The curve that represents dependence of the hardness of the copper layer on the degree of deformation, can be divided into three parts.In the first part of the curve, up to a deformation of 10%, the hardness of the copper layer increases sharply, in the second part of the curve, up to a deformation of 50%, slightly, and then increases rapidly again to a maximum value of 146.75 daN/mm^2, at a total deformation of the bimetallic strip of 80%.

The obtained test results, dependence of hardness (HV) from the annealing temperature are shown in Table 2 and the diagram in Figure 3.

Table2. Dependence of the hardness of bimetallic strip layers on the annealing temperature

t(°C)	HV (daN/mm^2)	
	Al	Cu
200	42.30	137.00
250	40.12	130.50
300	28.86	63.52
400	25.57	55.72

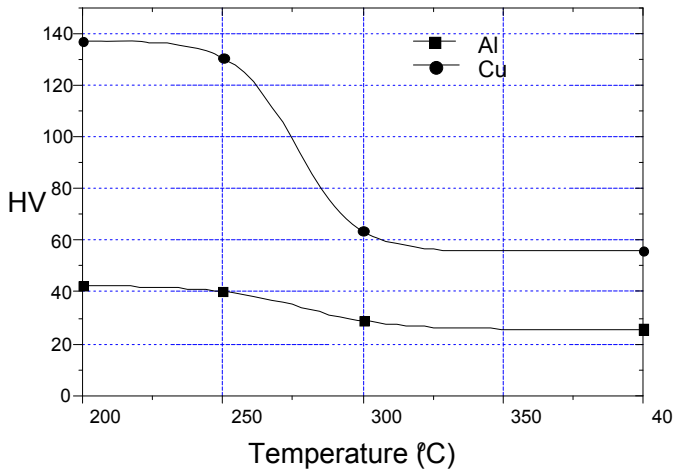

Figure 3. Diagram of the dependence of the hardness of the bimetallic strip layers on the annealing temperature

A decrease in hardness is observed with an increase in the annealing temperature, both in the aluminum layer and in the copper layer.
The hardness decreases slightly to T = 250 ^{o}C, and then decreases sharply in both layers in the temperature range of 250 - 300 ^{o}C, when recrystallization of both layers occurs.
Further increase of the annealing temperature, up to 400 ^{o}C, does not significantly affect the reduction of the hardness values of the layers.

4. CONCLUSION

The maximum hardness values characterize the samples obtained with the maximum single reductions.
Global flow of curves hardness - total deformation, increases, where the hardness curve for aluminum is approximately linear and is always lower than the hardness curve for copper, whose flow can be divided into three parts.
As the annealing temperature of the cold deformed bimetal strip (ε = 80%) increases, the hardness decreases in both the aluminum layer and the copper layer, slightly up to 250^{o}C, and then sharply in the interval from 250 ^{o}C to 300 ^{o}C, when both layers recrystallize.

ACKNOWLEDGEMENTS

This work was financially supported by the Ministry of Education, Science and Technological Development of the Republic of Serbia, Grant No. 451-03-9/2021-14/ 200131.

REFERENCES

[1] Grinberg. B. G., Knišev Y. B., Mnogoslojnijemetally v tehnike, Znanije, Moskva 1969.
[2] Vaccori J. A., The Manu Roles of clad Metals Design Engineering, January (1980) 55.
[3] Wright J. C., New Materials For sheet Metal working – Part 3. Sheet Metalindustries, March (1976) 126.
[4] Kubeta A., Present and Future of Explosive Clading, Chemical Economy and Engineering Review, 7, dec. (1975) 1.
[5] Konon A., Redorov V. H., Pervulin L. B., Bikov A. A., Korrozionostojkij bimetal – Mašinostroenie, Moskva, (1984)

ORGANIZER:

UNIVERSITY OF BELGRADE – TECHNICAL FACULTY IN BOR

Co-ORGANIZER:

INSTITUTE FOR MINING AND METALLURGY BOR

Under the Auspice of:

The Ministry of Education, Science and Technological Development of the Republic of Serbia

CONFERENCE SPONSORS

ISBN 978-86-6305-119-5